GDAŃSK UNIVERSITY OF TECHNOLOGY
FACULTY OF ELECTRONICS, TELECOMMUNICATIONS AND INFORMATICS

FACULTY OF ELECTRONICS, TELECOMMUNICATIONS AND INFORMATICS

The author of the PhD dissertation: Arkadiusz Zięba
Scientific discipline: Information and communication technology

DOCTORAL DISSERTATION

Title of PhD dissertation: Evaluation method of IP Scheduled Throughput for Inter-eNB Carrier Aggregation and Cloud based environment

Title of PhD dissertation (in Polish): Metoda szacowania przepływności IP dla Agregacji Nośnych pomiędzy różnymi eNB i w środowisku opartym na chmurze

Supervisor *signature*
dr hab. inż. Jarosław Sadowski, prof. PG

Gdańsk, year 2025

ABSTRACT

Summary of PhD dissertation in English: This dissertation investigates the challenges of accurately measuring IP scheduled throughput, a key metric for end-user Quality of Service (QoS) in the Evolved Universal Terrestrial Radio Access Network (E-UTRAN), within the context of modern distributed network architectures. The study analyzes the limitations of applying the 3GPP TS 36.314 definition of IP scheduled throughput in traditional Long Term Evolution (LTE) networks compared to Dual Connectivity (DC) topologies. A novel method is proposed for calculating IP scheduled throughput in an edge computing environment, addressing the complexities arising from distributed network architectures. Furthermore, the dissertation extends this approach to propose a solution for 5G networks utilizing the DC architecture. Through rigorous experimentation, the proposed methods are validated, demonstrating a strong correlation with the real-world user perception across diverse network configurations, including variations in protocol, radio channel quality, component carrier count, and user density. The findings contribute to a deeper understanding of IP scheduled throughput measurement in modern wireless networks and provide practical solutions for enhancing QoS in edge computing and 5G environments. The novel method has been developed and evaluated, exhibiting substantial enhancements in the precision of IP scheduled throughput measurement across a wide range of testing scenarios. This method has been successfully integrated into cellular networks within Nokia hardware devices deployed globally.

Summary of PhD dissertation in Polish: Niniejsza rozprawa bada wyzwania związane z dokładnym pomiarem przepływności IP, kluczowej miary jakości usług QoS dla użytkownika końcowego w radiowej sieci dostępowej E-UTRAN, w kontekście nowoczesnych rozproszonych architektur sieciowych. Badanie analizuje ograniczenia stosowania przepływności IP zdefiniowanej w 3GPP TS 36.314 w tradycyjnych sieciach LTE w porównaniu z topologiami DC. Zaproponowano nową metodę obliczania przepływności IP w środowisku rozproszonym, rozwiązując złożoność wynikającą z rozproszonych architektur sieciowych. Ponadto rozprawa rozszerza to podejście, proponując rozwiązanie dla sieci 5G wykorzystujących architekturę DC. Poprzez rygorystyczne eksperymenty, zaproponowana metoda została zweryfikowana w kontekści metody dostępnej w standardzie 3GPP, wykazując silną korelację w szacowaniu pomiaru przepływności IP z perspektywą użytkownika końcowego dla różnych konfiguracji sieci, typów protokołów, jakości kanału radiowego, liczby nośnych i gęstości użytkowników. Otrzymane wyniki przyczyniają się do głębszego zrozumienia pomiaru przepływności IP w nowoczesnych sieciach bezprzewodowych i dostarczają praktyczne rozwiązania w celu zwiększenia jakości usług w środowiskach rozproszonych z wykorzystaniem DC. Nowa metoda została opracowana i oceniona, wykazując znaczące ulepszenia w precyzji pomiaru przepływności IP w szerokim zakresie scenariuszy testowych. Metoda ta została z powodzeniem zintegrowana z sieciami komórkowymi w urządzeniach sprzętowych firmy Nokia wdrożonych na całym świecie.

Keywords: LTE, NR, 4G, 5G, IP scheduled throughput, QoS, QoE, user throughput, Dual Connectivity, Carrier Aggregation

Field of science and technology in accordance with OECD requirements: Engineering and technology, Information Engineering

TABLE OF CONTENTS

LIST OF IMPORTANT SYMBOLS AND ABBREVIATIONS

3GPP	–	3rd Generation Partnership Project
ACK/NACK	–	Acknowledgement/Negative Acknowledgement
App RE	–	Application layer throughput Relative Error
BBU	–	Baseband Unit
BLER	–	Block Error Rate
BTS	–	Base Transceiver Station
CA	–	Carrier Aggregation
Cat-M1	–	Category M1 devices
Cell RE	–	Cell throughput Relative Error
CN	–	Core Network
CPU	–	Central Processing Unit
CQI	–	Channel Quality Indicator
C-RAN	–	Cloud RAN
CU	–	Centralized Unit
DC	–	Dual Connectivity
DDDS	–	Downlink Data Delivery Status
DL	–	Downlink
DU	–	Distributed Unit
eNB	–	Evolved Node B
EN-DC	–	Evolved Non-standalone Dual Connectivity
eTh	–	expected throughput
eTputInitMcs	–	initial MCS value for expected throughput
eTputFilterConfig	–	exponential moving average filter with two variables
FR1	–	Frequency Range 1
FR2	–	Frequency Range 2
GTP-U	–	GPRS Tunneling Protocol in User plane
HARQ	–	Hybrid Automatic Repeat Request
IIR	–	Infinite Impulse Response
IoT	–	Internet of Things
IP	–	Internet Protocol
KPI	–	Key Performance Indicator
L1	–	Layer 1
LTE	–	Long Term Evolution
LTE-A	–	Long Term Evolution Advanced
M2M	–	Machine to Machine
MAC	–	Medium Access Control
MeNB	–	Master eNB
MR-DC	–	Multi-Radio Dual Connectivity
NB-IoT	–	Narrow Band Internet of Things

NFV	–	Network Function Virtualization
NMS	–	Network Management System
non-GBR	–	Non-Guaranteed Bit Rate
NR	–	New Radio
O-RAN	–	Open RAN
PCell	–	Primary Cell
PDCP	–	Packet Data Convergence Protocol
PDU	–	Protocol Data Unit
PHY	–	Physical layer
PM	–	Performance Management
QCI	–	Quality of Service Class Identifier
QoE	–	Quality of Experience
QoS	–	Quality of Service
RAN	–	Radio Access Network
RAT	–	Radio Access Technology
RLC	–	Radio Link Control
RRC	–	Radio Resource Control
RRH	–	Remote Radio Head
RU	–	Radio Unit
SA NR	–	Standalone NR
SCell	–	Secondary Cell
SDAP	–	Service Data Adaptation Protocol
SDU	–	Service Data Unit
SeNB	–	Secondary eNB
TB	–	Transport Block
TCP	–	Transmission Control Protocol
ThpTimeDl	–	IP scheduled throughput time in downlink direction
ThpTimeUl	–	IP scheduled throughput time in uplink direction
ThpVolDl	–	IP scheduled throughput data volume in downlink direction
ThpVolUl	–	IP scheduled throughput data volume in uplink direction
transferDelayMax	–	*eTh* exchange rate
tRlcPduDiscard	–	watchdog timer to discard RLC PDUs
TSN	–	Transport Service Network
TTI	–	Transmission Time Interval
UDP	–	User Datagram Protocol
UE	–	User Equipment
UL	–	Uplink

1. INTRODUCTION AND OBJECTIVES OF THESIS

1.1. Motivation

The proliferation of modern technologies and services, including video streaming, personalized television platforms, and mobile gaming, is driving an exponential increase in cellular network data traffic demand. To address this escalating demand, advanced Access Networks (AN) such as Long Term Evolution Advanced (LTE-A), LTE-A Pro, and New Radio (NR) have been introduced, aiming to achieve higher peak data rates through carrier aggregation and enlarged bandwidth sizes [1, 2, 3].

However, the further exponential growth of data traffic poses a significant challenge to traditional LTE architectures. The centralized control and fixed bandwidth allocation inherent in LTE struggle to accommodate the surge in data demand. This demand is driven by the proliferation of high-bandwidth applications, such as 8K video streaming, mobile banking and entertainment applications, high-volume file transfers, mobile application updates, and online gaming. The simultaneous access requirements of numerous users within a bandwidth-constrained cellular network exacerbate this challenge, leading to network capacity limitations. Furthermore, the traditional LTE architecture is ill-suited for the dynamic and unpredictable nature of modern data traffic patterns. The fixed bandwidth size of up to 20 MHz per cell limits network flexibility and scalability. To address these limitations, 5G technology has been introduced, offering revolutionary features that extend bandwidth capacity, deliver higher multi-Gbps peak data speeds, minimize latency, enhance network reliability, support a significantly larger number of connected devices, improve network availability, and provide a more consistent and equitable user experience across diverse network conditions. These advancements in 5G technology aim to address the limitations of LTE and provide a more robust and scalable network infrastructure to meet the evolving demands of modern data traffic [1].

In summary, the LTE architecture, while successful in its time, faces bottlenecks in handling the increasing data traffic and the shift towards distributed cellular networks. The centralized control, cell-based structure, and limitations in mobility management hinder its ability to adapt to the evolving demands of modern mobile communication. The transition to 5G with its distributed architecture, edge computing, and dynamic resource allocation is crucial for addressing these challenges and enabling a more efficient and scalable mobile network infrastructure. However, LTE can be adapted to a simplified DC system by leveraging inter-site Carrier Aggregation (CA) functionality.

The emergence of next-generation radio networks, exemplified by 5G, necessitates the adoption of distributed architectural paradigms. This transition introduces significant challenges in accurately measuring IP-scheduled throughput, as illustrated in Figure 1.1. In this scenario, data transmitted from the core network to a dual connectivity (DC)-capable user is dispersed across two physically distinct Radio Access Network (RAN) nodes. These nodes operate independently, lacking real-time communication regarding their internal scheduling cycles. Furthermore, the deployment of distributed and virtualized components within these architectures can lead to inconsistencies in data flow, hindering the precise tracking of end-to-end packet

trajectories. The pursuit of enhanced throughput and reduced latency in future 6G networks will necessitate the development of novel performance measurement methodologies. The anticipated extreme performance targets of 6G will challenge the accuracy and reliability of traditional measurement techniques, requiring advancements in measurement technology to ensure accurate and reliable performance assessment. The inherent distributed nature of these networks poses challenges in synchronizing measurements across diverse network elements, impeding the acquisition of a holistic understanding of network and user performance.

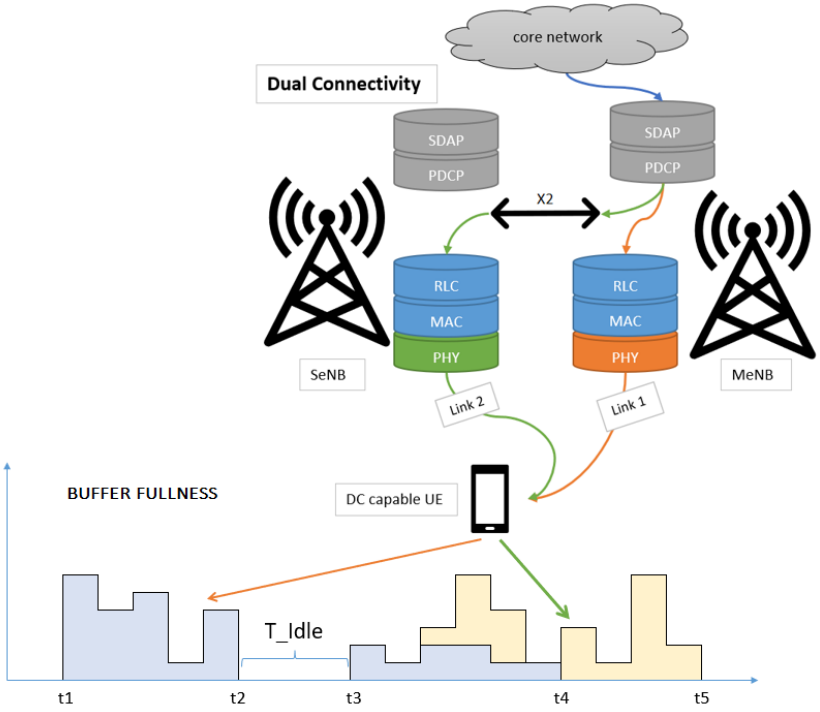

Figure 1.1: DC system measurement synchronization issues [1, 3].

In a single-cell, single-link connection scenario, IP-scheduled measurement computation is simplified, by the centralized control of a single scheduler. This facilitates straightforward calculations of data volume and time components. This is because the single scheduler possesses complete knowledge of transmission separation and delay associated with user communication. The system relies on a dedicated acknowledgment mechanism to confirm successful data transmission. However, when Carrier Aggregation (CA) is employed, where a user concurrently utilizes two distinct carriers originating from physically separated nodes, real-time synchronization between the serving and master nodes becomes computationally intensive and complex. The master node, responsible for overseeing the transmission process, faces challenges in maintaining accurate synchronization due to the distributed nature of CA architecture.

In cellular networks, the shared nature of system frequency bands necessitates a collective utilization model, rendering individual user-specific IP scheduled throughput measurement infeasible. Consequently, an average value is employed as a comparative benchmark. Real-time storage of individual user data poses significant computational and memory resource constraints for specific Base Transceiver Station (BTS) components,

particularly when considering the subsequent transmission to a centralized database for user-specific data management.

To address the challenges of data collection and storage of performance metrics, a Performance Management (PM) framework, adhering to 3GPP principles, has been established. This framework acts as a centralized database within each individual Evolved Node B (eNB), prioritizing system-level performance assessment over individual user performance. Individual user performance can be monitored through alternative on-demand tracing mechanisms. The comparative average value of IP scheduled throughput provides a relative measure of average user performance within a specific BTS cluster area. This metric is particularly valuable for understanding performance variations across different clusters, which can be influenced by factors such as selective interference, signal fading, system capacity, suboptimal configurations, and other environmental or network-related challenges.

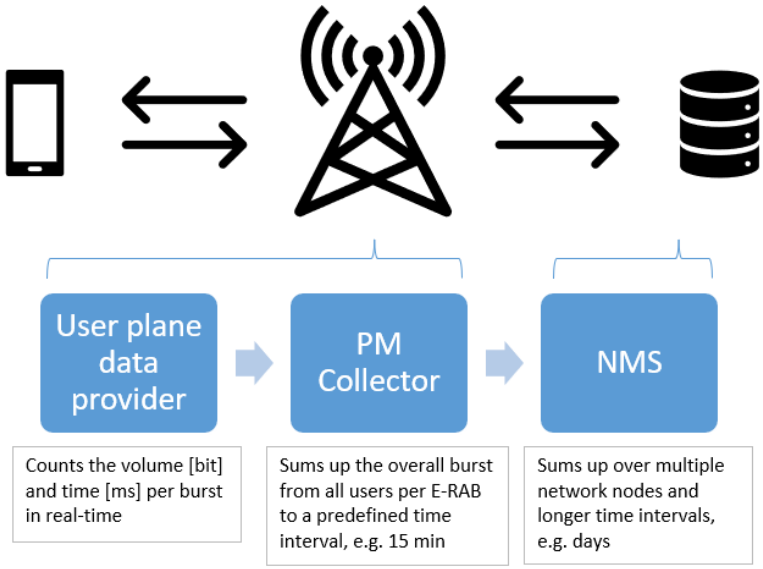

Figure 1.2: Performance monitoring in cellular networks based on 3GPP concept via PM counters with an example of IP scheduled throughput measurement.

Figure 1.2 illustrates the typical concept of Performance Monitoring framework in cellular networks, which is based on real-time measurements performed at specific system components. For example, the IP scheduled throughput measurement is calculated at specific user plane data provider which is responsible for measuring both the data volume (*ThpVolDl*) and time (*ThpTimeDl*) components described in 3GPP specification [12, 20]. Each data volume and time sample is captured by a counter provider component responsible for Packet Data Convergence Protocol (PDCP) level measurements. Subsequently, both internal counters containing instantaneous values are sent from counter provider to PM Collector, which shall perform the time aggregation over longer time interval from all the received samples, for example 5, 10 or 15 minutes. At the conclusion of each measurement interval, the aggregated value of a single counter (*ThpVolDl* or *ThpTimeDl*) is reported to an external data file with an .xml extension, as depicted in Figure 1.3. This data is subsequently transmitted to a centralized database, the

Network Management System (NMS), responsible for managing the performance data collection of network nodes.

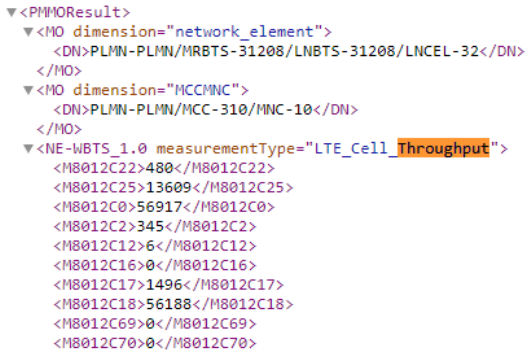

Figure 1.3: Content of PM counter report sent from eNB to NMS.

The provision of high-quality mobile network services is paramount for operator success, as user satisfaction is directly correlated with network performance. Subpar network conditions, characterized by insufficient data transmission rates and frequent connection disruptions, can lead to user churn, as subscribers seek alternative providers with superior service. Maintaining a high level of network integrity is crucial for all operators, as it directly impacts the end-user experience. Network integrity is a multifaceted concept, encompassing various aspects of network performance, and can be assessed through a suite of Key Performance Indicators (KPIs). These KPIs, collectively known as Quality of Service (QoS) indicators, provide a quantitative measure of network performance and include [21]:

- Latency: The time delay between the transmission of a data packet and its reception.
- Delay: The overall time taken for a data packet to traverse the network from source to destination.
- Throughput: The rate at which data is successfully transmitted over the network.
- Block Error Rate (BLER): The percentage of data blocks that are received with errors.
- Packet Loss/Drop Ratio: The percentage of data packets that are lost or discarded during transmission.

Comprehensive manual system testing and quality assurance procedures conducted on novel, complex LTE functionalities, exemplified by CA, have unequivocally demonstrated the paramount importance of network integrity metric measurement. These measurements provide invaluable insights into the performance enhancements afforded by these new features. KPIs, with particular emphasis on Integrity, play a critical role in evaluating these metrics and ensuring the preservation of a positive user experience, thereby contributing to the maintenance of network competitiveness. Conclusions from the conducted quality tests underscore the imperative of integrating precise performance monitoring mechanisms within the design of novel system architectures.

The evolution of data traffic patterns and the emergence of new network architectures necessitate a reevaluation of traditional performance metrics, such as IP scheduled throughput. In this thesis, a novel approach is proposed to address the challenges of measuring IP scheduled

throughput in edge computing environments, providing a more accurate representation of the real-world user experience.

The objective of IP scheduled throughput measurement is to quantify the average user's capacity for transmitting substantial data volumes in both downlink and uplink directions. This metric, as defined in [12, 20], provides insights into the user's ability to handle large file transfers, thus characterizing their network performance, and is given as follows:

$$If \sum \mathrm{ThpTimeDl} > 0 , \frac{\sum ThpVolDl}{\sum ThpTimeDl} \times 1000 \left[\frac{kbit}{s}\right]$$

$$If \sum \mathrm{ThpTimeDl} = 0 , 0 \left[\frac{kbit}{s}\right] \quad (1.1)$$

$$If \sum \mathrm{ThpTimeUl} > 0 , \frac{\sum ThpVolUl}{\sum ThpTimeUl} \times 1000 \left[\frac{kbit}{s}\right]$$

$$If \sum \mathrm{ThpTimeUl} = 0 , 0 \left[\frac{kbit}{s}\right] \quad (1.2)$$

Equations 1.1 and 1.2, along with their associated data volume and time components (*ThpVolDl, ThpVolUl, ThpTimeDl, and ThpTimeUl*), constitute the IP scheduled throughput measurement within a performance monitoring framework. *ThpVolDl* quantifies the volume of a data burst, excluding data transmitted during the Transmission Time Interval (TTI) when the buffer is emptied. This measurement is conducted at the PDCP Service Data Unit (SDU) level, representing the number of kilobits successfully transmitted (acknowledged by the User Equipment, UE) in the downlink for a single E-UTRAN Radio Access Bearer (E-RAB) during a sampling period defined by *ThpTimeDl*. The time component similarly excludes the TTI when the buffer is emptied. These parameters are aggregated over time, incorporating values collected from every E-RAB of each user connected to the primary cell, resulting in a consolidated value representing the average user throughput [12, 20].

Accurate IP scheduled throughput measurement provides significant benefits across various aspects of network operation and business strategy. It allows for precise quantification of the network's capacity to handle data traffic, enabling informed decision-making and optimization.

- [Business] Competitiveness, based on standard:

Accurate IP scheduled throughput measurement enables network operators to demonstrate compliance with industry standards and service level agreements (SLAs). This compliance is crucial for maintaining a competitive edge in the telecommunications market. Standards like 3GPP and ETSI define specific performance metrics for IP networks, including scheduled throughput. Meeting these standards ensures interoperability with other networks and devices, enhancing network reliability and user experience. This compliance also allows operators to participate in competitive bidding processes and secure contracts based on their network's performance capabilities.

- [Technical] Scalability awareness / end-user service demands:

Accurate IP scheduled throughput measurement provides insights into the network's capacity to handle increasing data traffic demands. This information is essential for planning network upgrades and ensuring scalability to meet future user needs. As data consumption

continues to grow exponentially, network operators need to understand the limits of their infrastructure. Accurate throughput measurements allow them to predict potential bottlenecks and proactively address them. This proactive approach ensures smooth network operation and prevents service degradation during peak usage periods, enhancing user satisfaction and loyalty.

- [Technical] Call quality status (integrity indicator):

IP scheduled throughput measurement serves as a crucial indicator of network health and call quality. Consistent and reliable throughput ensures smooth voice and video communication, minimizing dropped calls, latency, and jitter. Accurate throughput measurements provide a real-time assessment of network performance, enabling operators to identify and address issues that might impact call quality. This proactive approach ensures a positive user experience and reduces customer complaints.

- [Technical] Traffic model for testing purposes:

Accurate IP scheduled throughput measurements provide valuable data for developing realistic traffic models used in network simulations and testing. These models allow for accurate assessment of network performance under various load conditions, facilitating optimization and troubleshooting. By simulating real-world traffic scenarios, network operators can identify potential performance issues and optimize network configurations before deployment. This approach minimizes the risk of network failures and ensures a robust and reliable network infrastructure.

- [Business] Costs reduction / reduction of drive-tests amount:

Accurate IP scheduled throughput measurement reduces the need for costly and time-consuming drive tests, leading to significant cost savings for network operators. Drive tests involve physically driving around a network area to measure signal power level and data throughput. This method is expensive and time-consuming, especially for large networks. Accurate IP scheduled throughput measurements provide a more efficient and cost-effective alternative, allowing operators to monitor network performance remotely and identify potential issues without the need for physical testing.

Summarizing, the accurate IP scheduled throughput measurement is a critical tool for network operators, enabling them to optimize network performance, ensure compliance with industry standards, and meet evolving user demands. By providing a comprehensive understanding of network capacity and performance, it contributes to improved network efficiency, reduced costs, and enhanced user experience.

The IP scheduled throughput metric, encompassing both cellular and user performance aspects, necessitates a rigorous examination of its measurement accuracy. This dissertation will delve into the definition of evaluation points to assess the fidelity of this metric.

1.2. Aim and Scope

The aim of this dissertation is to prove the validity of the following thesis:

- T1. The development of a novel method enables more precise throughput estimation in LTE/5G cellular networks compared to existing methods described in technical documentation and recommended for use in these networks.

Additionally, in the research part of this work, the validity of above hypothesis will be demonstrated by designing and implementing a novel algorithm, characterized by the following properties:

- T2. The innovative method demonstrates improved accuracy in estimating the amount of data volume and transmission duration from the base station's perspective.
- T3. The presented method effectively estimates IP scheduled throughput for conventional connection types, including single cell or intra-site CA connections without DC, or in mixed network environments with DC and non-DC configurations under a single user connection type, regardless of transmission duration for transmission types meeting 3GPP requirements.
- T4. The novel method accurately estimates IP scheduled throughput under challenging radio channel quality conditions, regardless of the cell participating in specific user connection which experiences diminished signal quality.
- T5. The novel method yields accurate estimations of IP scheduled throughput for varying quantity of SCells from different SeNBs.
- T6. The enhanced method effectively estimates IP scheduled throughput for varying number of users under a specific MeNB cell.

Moreover, the study shall define and analyse major influential network phenomena in both IP and cellular domains that have a direct influence on the accuracy of IP scheduled throughput, for both the standard and the novel methods.

The enhanced estimation capability is critical for network performance analysis, providing valuable insights into the robustness, reliability, and accuracy of the estimation techniques under realistic network conditions. This evaluation is conducted through laboratory test cases designed to simulate end-user behavior, thereby ensuring the practical relevance and applicability of the findings.

This dissertation introduces a novel method for capturing traffic parameters exchanged between multiple base stations and user terminals within 4G and 5G cellular networks utilizing DC functionality. This modified approach significantly improves the accuracy of throughput estimation, enabling comprehensive network performance monitoring and evaluation of data transmission service quality. Notably, the proposed method maintains a high level of accuracy in non-DC environments, providing a robust and reliable indicator of network performance. Due to the inherent ambiguity in selecting a suitable reference point for comparison in DC systems (the standard method is demonstrably unsuitable for application within DC systems), two distinct reference points for relative error calculation are defined for the designed test cases, with further details provided in Chapter 3.6.

1.3. Structure of the Thesis

This dissertation is divided into two main sections and is organized as follows:

- Section 1: Problem and State of the Art: This section provides an in-depth overview of the research problem and similar research solutions for managing the synchronization of real-time data in DC systems.
    - Chapter 2 delves into the theoretical basics of the research problem, highlighting the architectural distinctions between non-DC and DC systems. It emphasizes the advantages and disadvantages of each architecture, providing a comprehensive understanding of their respective strengths and limitations. Furthermore, the chapter underscores the critical role of QoS parameters in network performance analysis, emphasizing their importance for network operators in optimizing network parameters to enhance end-user experience.
- Section 2: Contributions: This section presents the research contributions of the thesis in each chapter:
    - Chapter 3 investigates the challenges of accurately measuring IP scheduled throughput in DC systems. It begins by outlining the principles of the standard method defined in 3GPP, highlighting its limitations in the context of DC systems. Through practical examples, the chapter demonstrates the discrepancy between the standard method's perception of throughput and the actual throughput in a DC environment. To address this, two novel solutions are proposed: a computationally intensive approach and a novel method with approximation. The chapter delves into the principles of the novel method, presenting postulates and a buffer-centric perspective to elucidate its mechanisms. Finally, it defines reference points for verifying the accuracy of both proposed methods, providing a framework for evaluating their effectiveness in addressing the challenges of IP scheduled throughput measurement in DC systems.
    - Chapter 4 delves into the practical implementation of the novel method, highlighting the necessary modifications and supplementary mechanisms for successful integration into real devices. The chapter provides a detailed analysis of the algorithms governing traffic management and throughput estimation, emphasizing the need for a revised approach to IP scheduled throughput calculation in the context of DC-type system configurations. It explores the limitations of legacy flow control mechanisms and the need for a novel method, integrated with an extended flow control algorithm, to ensure efficient data scheduling. The chapter also introduces the approximation concept, grounded in flow control modifications, and presents the implementation principles of the novel method, emphasizing its robustness in maintaining throughput accuracy. Finally, it examines the implementation modification introduced in the time component calculation, highlighting its contribution to enhance the accuracy of measurement, more closely to user perception.
    - Chapter 5 presents a comprehensive evaluation of the standard and novel throughput estimation methods. The chapter utilizes a laboratory test line design based on real

devices, incorporating a detailed explanation of traffic generation principles and test constraints. It examines the accuracy and stability of the novel method within the context of the various network phenomena such as TCP slow start mechanism and various network configurations, comparing its performance to the standard method. The chapter further investigates the impact of radio channel quality fluctuations on the accuracy of both methods, conducting specific tests on the *eTh function* and presenting test cases illustrating the differences in burst time calculation. Finally, it examines the influence of increased component carrier allocation and user density on the accuracy of the novel method.

- Chapter 6 presents a comprehensive evaluation of the novel IP scheduled throughput measurement method, demonstrating its accuracy and adaptability across diverse network configurations, encompassing both DC and non-DC systems. The evaluation meticulously examines the influence of key parameters, time component calculation, and the impact of network phenomena such as TCP slow start, protocol types, packet sizes, and radio channel quality. The chapter also identifies key challenges that impede accurate throughput measurement. It summarizes the research presented in Chapter 5, validating the hypothesis proposed in Chapter 1.2, and demonstrating the significant contribution of the novel throughput estimation method to the advancement of cellular network design and operation, particularly in the context of supporting user traffic through multiple base stations simultaneously.

2. THEORETHICAL BACKGROUND OF THE PROBLEM

Chapter 2.1 presents a comparative analysis of non-DC and DC cellular network architectures, exemplified by LTE and NR respectively. The chapter explores the advantages and disadvantages of each architecture, ultimately highlighting the trend towards decentralized systems, such as cloud-based architectures, as the future of cellular networks. Chapter 2.2 delves into the transformation of LTE networks into distributed systems, identifying challenges in accurately measuring IP-scheduled throughput due to the distributed nature of the network components. Subsequently, the NR topology is analyzed, emphasizing the inherent challenges in QoS measurement posed by its decentralized nature. The last chapter concludes by emphasizing the paramount importance of QoS measurements in distributed architectures. This emphasis is grounded in a comprehensive review of relevant research papers that propose potential solutions to mitigate the challenges inherent in such architectures. The study further investigates the efficacy of these proposed solutions in addressing the specific problem presented within the dissertation.

2.1. LTE and NR architecture introduction

The exponential increase in data traffic presents a significant challenge for traditional LTE architectures. The LTE system, depicted in Figure 2.1, consists of a Radio Access Network (RAN), also known as E-UTRAN, an Evolved Packet Core (EPC), and a User Equipment (UE). Communication between the RAN and the core is facilitated through the S1-C and S1-U interfaces [3]. Communication between different base stations (BTS), referred to as evolved NodeB (eNB), occurs via the X2 interface within the RAN.

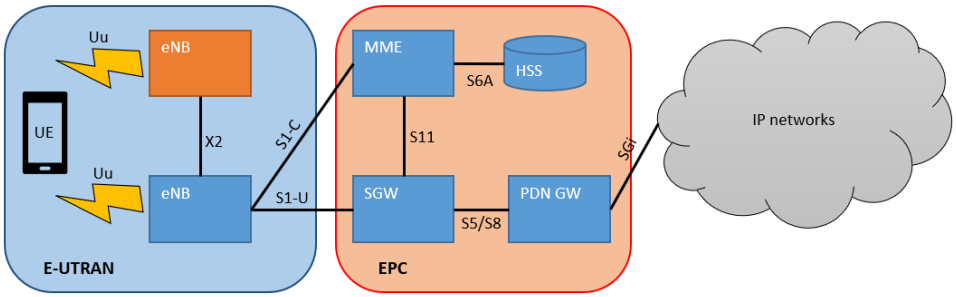

Figure 2.1: LTE basic system architecture [3].

The LTE architecture, with its centralized control and fixed bandwidth allocation, struggles to cope with the surge in data traffic. The increasing demand for high-bandwidth applications, such as heavy file size transfers, video streaming [43] or online gaming, overwhelms the capacity of LTE networks. Furthermore, the traditional LTE architecture is not optimized for the dynamic and unpredictable nature of modern data traffic patterns.

This resulted in the introduction of the 5G technology with some revolutionary features to deliver higher multi-Gbps peak data speeds, ultra-low latency, more reliability, massive network capacity, increased availability, and a more uniform user experience to a greater number of users. The 5G System (5GS) consists of 5G Radio Access Network (5GR), 5G Core Network (5GC) and UE where RAN communicates with core based on N2 and N3 interfaces and UE based on N1

interface [1]. For the purpose of this dissertation only RAN shall be discussed where division of control and user plane in gNB is done, as shown on Figure 2.2.

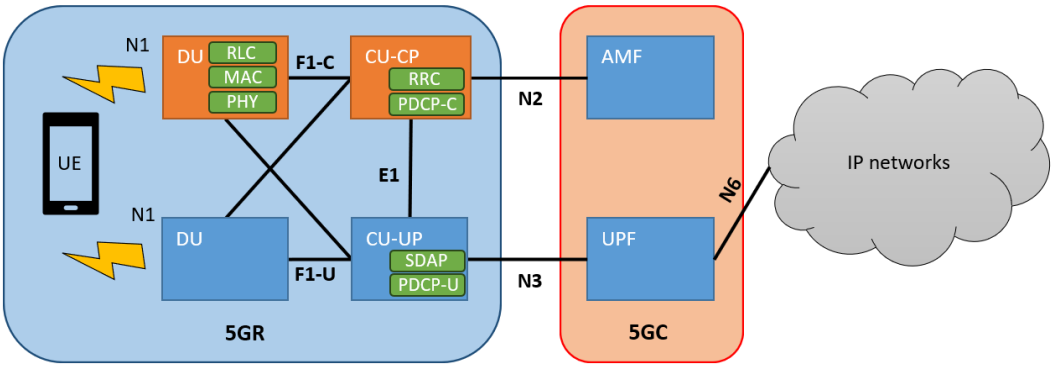

Figure 2.2: 5G system architecture [1].

In contemporary cellular network architectures, a centralized Control Unit (CU) is interconnected with decentralized Distribution Units (DUs) via F1 interfaces. The CU is functionally partitioned into control and user plane modules, enhancing performance, scalability, and resilience. A single CU can manage multiple DUs. The CU encompasses the Service Data Adaptation Protocol (SDAP) and PDCP protocol layers, while the DU comprises the Radio Link Control (RLC), Medium Access Control (MAC), and Physical (PHY) layers. This architectural division aims to enhance communication efficiency by bringing scheduler decisions closer to radio units, which can be located several kilometers away from the base station in legacy networks. Consequently, communication for lower protocol layers is optimized. However, this configuration introduces challenges in real-time measurement aggregation and synchronization between the CU and DU, particularly for centralized entities responsible for accumulating network data over extended periods. This challenge is analogous to the inter-site carrier aggregation (CA) scenario in LTE [3].

The LTE architecture, while a notable advancement in its era, encounters limitations in accommodating the exponential growth of data traffic and the evolving landscape of distributed cellular networks. LTE architecture relies heavily on a centralized control plane, where a single eNB manages user sessions, resource allocation, and mobility. This centralized approach becomes a bottleneck as data traffic surges, potentially leading to increased latency. The eNB, tasked with processing a massive number of requests, may experience delays in user connection establishment, data transmission, or handover. For instance, users in high-density areas, such as urban centers, may encounter congestion as the eNB becomes overloaded. Additionally, handovers between cells, particularly when users traverse cells in different geographical locations, can result in dropped calls and data interruptions. Furthermore, scalability challenges arise as the eNB becomes a single point of failure, limiting the overall network throughput. The centralized architecture also exhibits limited flexibility in adapting to the dynamic and heterogeneous nature of distributed networks. For example, the cell-based structure of LTE struggles to provide seamless coverage in areas with complex terrain or dense urban environments.

To address the limitations of centralized architectures, cellular networks are transitioning towards a distributed architecture characterized by decentralized control, edge computing, small cell deployment, and dynamic resource allocation [55, 56]. Decentralized control involves distributing control functions away from the centralized eNB across the network, while edge computing deploys computing resources closer to users, reducing latency and improving responsiveness. Small cells, such as picocells and femtocells, enhance coverage and capacity in specific areas. Dynamic resource allocation adapts resource allocation based on real-time traffic conditions and user demands. In distributed networks, user connections are no longer confined to a single cell but can be established and maintained across multiple cells in different geographical locations. This enables load balancing, distributing traffic across multiple cells to reduce congestion and improve overall network performance. Improved mobility facilitates seamless handovers between cells, even when users move between geographically dispersed areas. Enhanced coverage provides ubiquitous coverage in challenging environments.

The LTE architecture, while demonstrably effective in its initial deployment, encounters limitations in accommodating the escalating data traffic demands and the paradigm shift towards distributed cellular networks. The centralized control mechanism, together with inherently cell-based structure, and constraints in mobility management impede its adaptability to the evolving requirements of contemporary mobile communication. However, LTE can be adapted to a simplified DC system by leveraging inter-site CA functionality to mitigate some of these limitations. This transition introduces a novel challenge in performance monitoring, previously absent in LTE networks, which cannot be disregarded. Nonetheless, the transition to 5G, characterized by its distributed architecture, edge computing capabilities, and dynamic resource allocation, is essential for addressing these challenges faced by LTE and facilitating a more efficient and scalable mobile network infrastructure.

2.2. E-UTRAN DC Transition: Measurement Synchronization Challenges

In LTE systems, the eNB serves as a network element responsible for radio communication and it is typically situated within the coverage area of antennas. The eNB facilitates the translation of information received from the core network, utilizing the IP layer, to the MAC layer. This translation is necessary due to the distinct nature of radio transmission compared to standard IP-based transmission in fixed networks [3].

Figure 2.3 illustrates the layer stack employed within an eNB, revealing the specific layers involved in downlink transmission. Upon receiving IP traffic, the eNB translates it from the transport layer (GTP-U) to the PDCP layer. The PDCP layer ensures data integrity, performs encryption, and implements header compression. Subsequently, the RLC layer segments concatenates, and corrects errors in the data stream. The MAC layer maps logical and transport channels, generating Transport Blocks (TBs). Finally, the PHY layer transmits this information via the antenna [3].

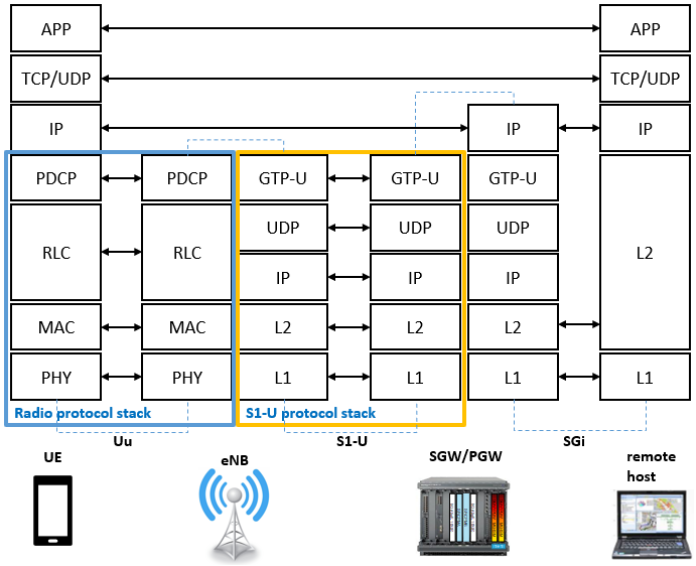

Figure 2.3: E-UTRAN layer stack for S1-U [3].

To address the escalating data traffic demands on mobile networks, network operators are implementing DC technology [54, 55]. In a DC configuration, a UE simultaneously connects to two eNBs: a Master eNB (MeNB) and a Secondary eNB (SeNB). When the MeNB and SeNB operate on distinct frequencies, the concept bears resemblance to CA [3].

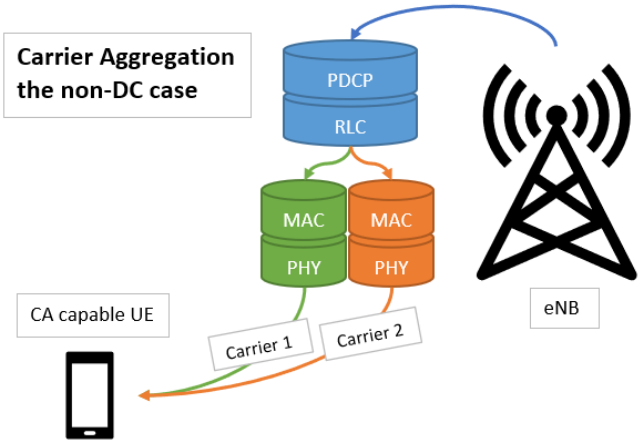

Figure 2.4: Classical CA functionality [3].

Figure 2.4 depicts conventional CA functionality, also referred to as non-DC, where distinct LTE cells are physically co-located within a single eNB. This eNB manages the entire protocol stack and possesses knowledge of the scheduling process across these cells. Downlink packets are transmitted to the eNB, where data splitting occurs at the RLC layer. Packets are either routed exclusively to the Primary Cell (PCell) or, following the split, to both the PCell and Secondary Cells (SCells). As the cells reside within the same BTS, the eNB is privy to the precise outcome of the radio transmission process. Leveraging this information, the eNB can ascertain whether the entire PDCP SDU packet was successfully transmitted for both the master and the secondary cells. If not, a retransmission process is initiated across the lower layers until all scheduled packets within the PDCP layer buffer are successfully delivered.

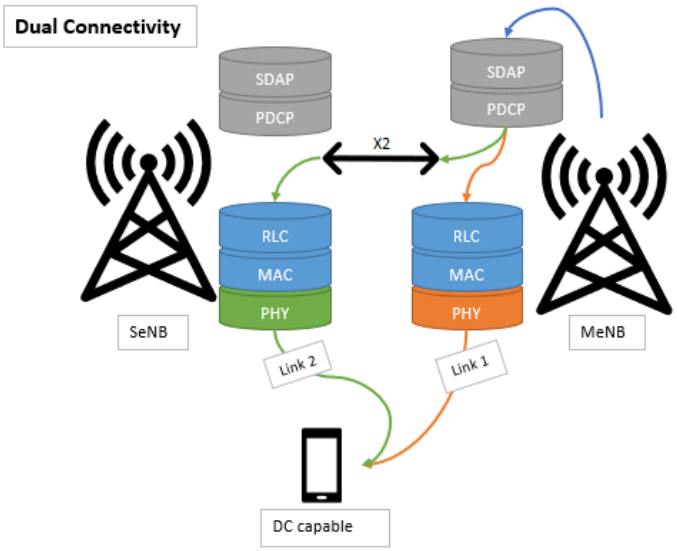

Figure 2.5. The concept of DC based CA [3].

Figure 2.5 illustrates the concept of DC based CA, where cells are associated with distinct eNBs interconnected via the X2 interface. These eNBs lack awareness of internal communication within their neighboring cells. A similar concept can be applied to multi-RAT DC, utilizing CA between NR and LTE cells. Data exchange occurs over the X2 link. IP packets are transmitted to the MeNB, where they are segmented at the PDCP layer and, based on data distribution, routed to both the PCell on the same MeNB and SCells on different SeNBs via the X2 interface. While the PDCP SDU packet size is known to the MeNB, the BTS lacks knowledge of the transmission success of lower layers on the SeNB for the given packet. A straightforward feedback mechanism could address this potential issue, but it would impose a significant message load on the X2 interface and the processing load on MeNB, potentially compromising the overall performance of the MeNB [3].

2.3. NR topology as a natural DC system encompassing multiple radio layer stacks

Figure 2.6 illustrates the architectural mapping of functional split options within the CU/DU/RU framework of the Open Radio Access Network (O-RAN) standard. To accommodate compatibility with existing 4G deployments, the conventional terminology of BBU (Baseband Unit) and RRH (Remote Radio Head) has been replaced with CU (Centralized Unit), DU (Distributed Unit), and RU (Radio Unit), respectively. This standardization process has resulted in the definition of five distinct CU/DU/RU functional block splitting configurations [26]:

- High-Layer Split for NR (A): This configuration segregates the CU functions from the combined DU/RU functions.
- Low-Layer Split for NR (B): This configuration isolates the RU functions from the combined CU/DU functions.
- Cascaded Layer Split for NR (C): This configuration implements a hierarchical separation, where each functional block is isolated from the others. This approach enables a more modular and flexible architecture.

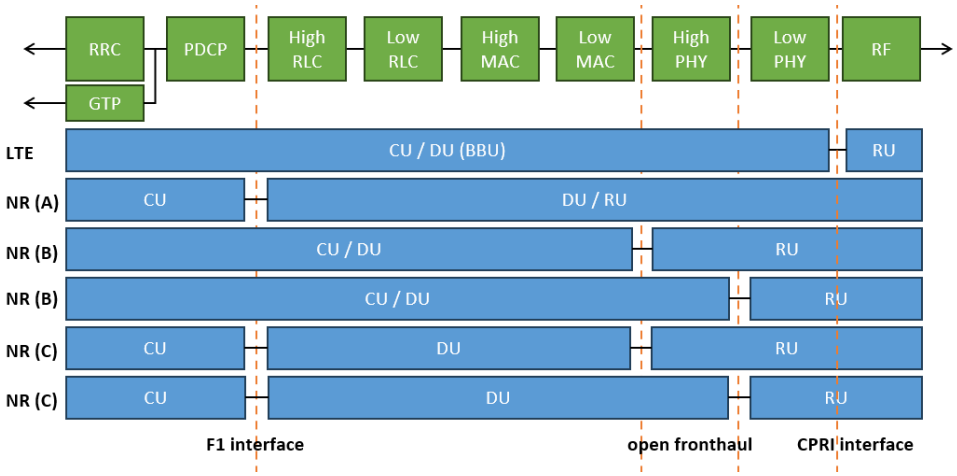

Figure 2.6: 5G radio access network architecture split between CU/DU/RU with different radio protocol stack division [26].

The aforementioned architectural split configurations present a challenge in accurately assessing real-time information, as such information is often localized to specific radio protocol layers. For instance, precise IP-scheduled throughput estimation necessitates data volume calculation at the PDCP layer, which resides within the CU. Conversely, the time duration for such throughput is typically available at lower layers, encompassing components distributed across both the CU and DU.

Irrespective of the specific split type employed in each network configuration, accurate measurement assessment becomes problematic when multiple components from both the CU and DU are required to calculate a specific metric. This arises from the distributed nature of the information required for the calculation, necessitating synchronization and coordination between the CU and DU, similarly as for inter-site CA in LTE network.

2.4. Advantages of nonDC and DC system and future growth

In general, the DC concept allows a group of network nodes to co-operate but appear as one for the end-user to maximize the user experience metrics, such as: throughput, latency, loss ratio and other [53]. However, such nodes are not typically aware of the processes happening over their counterparts. The DC logic is especially useful when the resources in the network are not utilized highly enough or when non-DC solution experiences a bottleneck for which a form of load balancing is needed [9, 54].

The adoption of a decentralized 5G network architecture with a CU/DU split was driven by the need to address evolving 5G and user demands. This architecture enables scalability by allowing multiple DUs to connect to a single CU, facilitating the handling of massive data volumes and user connections. The separation of CU and DU functions allows for flexible deployment, enabling DUs to be placed closer to user equipment, thereby reducing latency and enhancing network performance, which is particularly crucial for supporting emerging applications like cloud gaming and virtual reality. This decentralized approach also leads to improved throughput thanks to optimized resource allocation, reduced hardware costs due to less complex processing tasks handled by DUs, and simplified network management by distributing tasks across multiple units

[52, 55, 56]. Furthermore, the CU/DU split enhances network resilience by mitigating the impact of single DU failures and improves security through granular control mechanisms. Notably, this architecture is a key enabler for Open RAN [26], promoting open and interoperable radio access networks, fostering competition and innovation.

Despite the advancements in speed, capacity, and latency offered by 5G networks [53], LTE networks retain certain advantages in specific scenarios and use cases. LTE networks exhibit global coverage due to their widespread deployment and mature ecosystem, making them cost-effective for operators, particularly in areas with lower population density or where 5G deployment is nascent. LTE devices consume less power than 5G devices, which is crucial for applications with limited battery life, such as Internet of Things (IoT) devices and wearables. LTE networks possess a simpler architecture compared to 5G, facilitating management and maintenance, especially for smaller operators with limited technical resources. For applications that do not require the high speeds and low latency of 5G, such as basic data transfer or voice calls, LTE remains a cost-effective option. LTE Narrowband Internet of Things (NB-IoT) and Category-M1 (Cat-M1) are optimized for IoT applications, offering a balance of performance and power efficiency. Furthermore, more advanced LTE-A and LTE-A Pro networks, utilizing such functionalities as Evolved Non-standalone Dual Connectivity (EN-DC), seamlessly integrate with new 5G infrastructure, enabling a gradual transition to Standalone New Radio (SA NR) without significant disruptions.

The following article [39] explores the advantages and disadvantages of DC systems with traditional backhaul. DC significantly enhances user throughput by leveraging access to both macro and small cells, resulting in a larger transmission bandwidth. This is demonstrated by a 60% capacity gain for a target 5‰ outage throughput of 4 Mbps with bursty traffic compared to a non-DC system. DC also improves overall system performance by leveraging multi-user diversity and enabling faster load balancing between macro and small cells, ensuring efficient resource utilization and preventing congestion. The proposed flow control algorithm in [39] exhibits robustness and adaptability to various conditions, including different X2 latency, flow control periodicity, and traffic load, performing comparably to inter-site CA with fiber-based fronthaul connections. However, DC introduces a trade-off between throughput and SeNB buffering latency, requiring careful configuration of the target buffering time and flow control periodicity. Implementing DC with traditional backhaul necessitates a more complex flow control algorithm and careful management of RRM functionalities, potentially increasing system complexity. While DC with traditional backhaul offers significant improvements, its performance remains limited compared to inter-site CA with fiber-based fronthaul connections, suggesting that fiber-based fronthaul remains the ideal solution for achieving optimal performance.

Another research paper [40] investigates the potential of DC in 5G NR for IoT network deployment, specifically focusing on the Non-Standalone (NSA) NR architecture. The study analyzes the new DC features introduced in Release 15 and compares them to DC in LTE systems, outlining their features and operation procedures. Through system-level simulations, the paper demonstrates that the performance of DC in 5G NR deployment is significantly improved

compared to DC in LTE, particularly in scenarios with unbalanced bandwidth between macro and micro layers. The analysis focuses on optimizing key parameters for different scenarios and evaluating the UE throughput of EN-DC compared to E-UTRA DC to assess its potential for supporting the growing demand of IoT devices in a spectrum-constrained environment. The study reveals a significant gain in user throughput when utilizing EN-DC Option 3X in contrast to E-UTRA DC.

Non-DC and DC network architectures exhibit distinct advantages and disadvantages in resource management. Non-DC systems offer centralized control, enabling comprehensive monitoring across multiple protocol layers, but suffer from performance overhead and latency due to increased processing. Conversely, DC systems prioritize localized decision-making, delegating bandwidth allocation to the transmitting node, resulting in efficient and rapid responses to dynamic channel quality variations. This decentralized approach leads to improved user experience through reduced latency and enhanced responsiveness, as supported by [9]. However, current research lacks emphasis on maintaining adequate performance monitoring and consolidated information exchange between CU and DU components in DC systems, despite their performance advantages.

2.5. The importance of QoE and QoS measurements in distributed environment

To accommodate the escalating demand for high-throughput services, next-generation radio networks necessitate the adoption of a novel paradigm that incorporates an efficient resource allocation strategy. This mechanism should ideally operate in close proximity to the antenna, enabling real-time adaptation to dynamic channel conditions. The rapid fluctuations in radio channel quality demand instantaneous decision-making to maintain optimal performance. Furthermore, the system must provide an expanded bandwidth to satisfy the evolving needs of end users.

DC architecture inherently fulfills these requirements by delegating bandwidth resource allocation to individual network nodes. Each node manages its portion of data transmission, and the overall bandwidth is augmented through the simultaneous utilization of multiple radio signals originating from distinct nodes. Conversely, persisting with non-DC approaches would likely result in radio resource bottlenecks, as offloading mechanisms may prove not efficient enough. Alternatively, packet delays would increase to fully exploit the limited resources controlled by a single network node.

Subsequent sections will delve into existing research and concepts to demonstrate that DC architectures, such as cloud radio access and cloud core networks, represent a promising path towards enhancing end-user experience. Notably, cloud radio access serves as a representative example of inter-site CA in LTE or DC in the New Radio (NR) standard.

The significance of throughput measurement for network operators is evident when examining the research domain of QoS [1, 50, 57], Quality of Experience (QoE), and KPIs [21, 22, 48] for cellular networks. However, existing research lacks a comprehensive solution for addressing the challenges associated with real-time throughput measurement calculations. Specifically, the need to gather data from multiple network nodes across different protocol layers,

each contributing distinct information to the overall metric, necessitates a robust synchronization mechanism for both data volume and temporal alignment. The following paragraphs present a selection of publications that explore innovative techniques designed to enhance the end-user experience within this specific field. Some approaches propose the introduction of a novel network function entity, responsible for managing other nodes within the network across various protocol stack layers. This entity, irrespective of its location within the RAN or EPC transport stack, seeks to optimize end-user perception and network performance evaluation.

The solution proposed in the publications [13] and [17] for quantifying data volume traffic associated with PCell and SCell cells in a CA scenario involved establishing neighbor relation counters between cells belonging to distinct eNBs. This approach aimed at determining the proportion of traffic originating from each cell within a given neighbor relation. However, this solution presented significant practical challenges. Firstly, it necessitated the creation of a substantial number of counter instances, with up to 12 potential relations per cell. This requirement imposed a considerable implementation burden at lower protocol layers, potentially impacting system complexity and resource utilization. Secondly, the need to perform 12 separate calculations for each neighbor relation per cell would result in a substantial volume of data. This could lead to an overload in centralized databases, such as NMS, responsible for data aggregation and KPI analysis. Given that a network sector can comprise several thousand cells or more, the total number of counter instances could easily reach hundreds of thousands, further exacerbating the data management burden. These challenges highlight the potential limitations of this approach, suggesting the need for alternative solutions that address the scalability and complexity concerns associated with extensive counter instance creation and data processing. A comprehensive elaboration of the concept's practical implementation is presented in Chapter 4.1.

The solution proposed in the publication [5] investigates the performance of 5G networks and its impact on end-user experience. It employs a range of metrics, including fairness index, average cell throughput, spectral efficiency, cell-edge user throughput, and average user throughput, to assess network performance under varying user densities. The analysis demonstrates that mm-wave spectrum offers significantly enhanced overall performance due to its increased bandwidth and resource availability. However, it also acknowledges the inherent disadvantages of mm-wave, such as increased fading compared to lower frequency bands. The study further highlights the importance of selecting an appropriate propagation path-loss model for the specific environment, as this can significantly improve the accuracy of system KPIs. The impact of active users on average cell throughput is also investigated, revealing an exponential degradation with increasing user capacity. Notably, inactive users, who do not actively schedule resources, are excluded from these calculations. Furthermore, the study concludes that the high-frequency bands (FR2) exhibit superior efficiency in low-interference environments compared to the lower frequency bands (FR1). This paper concludes that optimization of signal power quality level and selection of appropriate propagation models are prerequisites for achieving optimal performance, specifically throughput and other system KPIs, thereby fulfilling customer expectations. This research demonstrates the critical role of accurate throughput measurement

in ensuring the performance and efficacy of 5G systems. The absence of reliable throughput measurement methods poses a significant threat to the scalability, competitiveness, and call quality of 5G networks [5].

For the next article, [6] the advent of 5G networks necessitates the adaptation of network and traffic parameters to accommodate the increasing demand for high-definition (HD) video streaming and massive machine-to-machine (M2M) communication. The integration of network function virtualization (NFV), including cloud radio access and cloud core networks, further complicates the process of measurement data acquisition and analysis. This article proposes the utilization of function blocks, namely Cloud QoS Management Function (CQMF) and Cloud QoS Control Function (CQCF), for the control and monitoring of QoS within a cloud environment. The paper analyzes traffic patterns in 4G networks, revealing that approximately one-third of data volume is attributed to YouTube services, while another third is dedicated to clear video and surveillance video. This observation underscores the significant role of streaming services in contemporary internet usage. As video resolution technology advances, providing enhanced user experiences, cellular networks must evolve to meet these burgeoning demands. Throughput capabilities become paramount for ensuring seamless streaming without stuttering or buffering delays, which has direct impact on the perceived QoE. The emergence of 8K Ultra HD video in 5G networks involves throughput requirements of up to 240 Mbps per user. However, the realization of such high-resolution video experiences is contingent upon the user's device possessing the capability to render 8K content, as not all mobile displays are equipped to handle such high resolutions. Beyond throughput, other QoS indicators, such as packet error loss rate, play a crucial role in network performance. The PDCP Loss Ratio, a commonly used metric in LTE networks, exemplifies the interconnectedness of various QoS indicators. The article further explores the application of Cloud QoS management and control functions, which enable traffic profiling, planning, and management of data flows. This approach involves a dedicated network node acting as a supervisor between the 5G RAN and 5G CN entities. While this concept proves beneficial for network slicing functionality, it does not offer direct improvements at lower layers of the base station, including throughput calculation. This limitation stems from the requirement for continuous confirmation of the specific interactions between the Distributed Unit (DU) and Centralized Unit (CU) for each end-user [6].

The solution in the research paper [7] proposes a novel framework to address the multifaceted challenges of QoS measurement in 5G networks. The framework aims to bridge the gap between high-level business requirements and the technical parameters used for resource monitoring. In the context of 5G, the increasing complexity of network functionalities, coupled with the stringent requirements of Service Level Agreements (SLAs) and Service Level Objectives (SLOs), calls for a dynamic and adaptive approach to QoS monitoring. The proposed framework leverages a dynamically adaptive monitoring algorithm, eliminating static time intervals and thresholds, thereby enhancing measurement accuracy without compromising network performance. Furthermore, the framework incorporates a mechanism for prioritizing QoS parameters based on enriched metadata derived from the Network Function Virtualization (NFV)

Catalogue. This enables the system to dynamically adjust its focus based on the specific requirements of different services and network conditions. The paper identifies the key QoS requirements for 5G, including high throughput, reliability, low latency, increased capacity, availability, connectivity, and dynamic resource sharing. However, the proposed framework's placement on top of the 5G Core network presents a potential limitation. While the Core network possesses significant computational resources, it may not be suitable for performing time-critical measurements for large data bursts due to the inherent latency associated with core network operations. The feasibility of the proposed framework hinges on the existence of a dedicated interface connecting each DU to the CU path with the CN. However, such an interface could impose an excessive load on the Layer 1 (L1) protocol stack, potentially impacting overall gNB performance. Moreover, relying on the CN for QoS measurements could compromise reliability, as the CN is not directly responsible for transmission redundancy mechanisms like HARQ ACK/NACK. In conclusion, while the proposed framework offers a promising approach to QoS measurement in 5G, further investigation is required to address the potential limitations associated with its placement and the impact on network performance and reliability [7].

Another research [8] explores the potential of Cloud RAN (C-RAN) as a transformative technology for base station functionality splitting. C-RAN architecture decouples the base station into remote radio heads (RRHs) and baseband units (BBUs) located in the network backbone. This separation enables centralized resource management, interference mitigation, and radio access technology (RAT) selection, leading to enhanced system throughput and reduced energy consumption. The paper focuses on a C-RAN system-level simulator that incorporates centralized user scheduling, edge-user joint transmission (JT), and global per-antenna CA. The simulator demonstrates its ability to identify fronthaul-link capacity bottlenecks from various QoS perspectives. Furthermore, the simulation results highlight significant throughput improvements compared to traditional RANs, achieved through efficient spectrum utilization. The proposed C-RAN architecture significantly impacts the base station's layer stack, offering greater flexibility in resource sharing and utilization. This flexibility is crucial for achieving enhanced reliability and improved QoS indicators compared to systems without such functionality. However, the analysis relies on theoretical assumptions, employing maximum resource utilization for system throughput estimation. The research, while implicitly emphasizing the role of accurate QoS monitoring via system-level metrics (throughput, channel capacity, outage probability) for performance benchmarking, neglects the complexities inherent in computing user-centric and multi-component QoS metrics within distributed architectures. Specifically, the computation of IP-scheduled throughput (performed between CU and DU and their constituent components), a crucial design parameter and a mandated 3GPP requirement, remains unaddressed [8].

Subsequent research [9] investigates the potential of Multi-Connectivity (MC) in the New Radio (NR) system, focusing on the separation of control plane (CP) and user plane (UP) transmissions over the air interface. The study compares the performance of MC in NR with E-UTRAN New Radio dual connectivity (EN-DC), a similar concept. Simulation results demonstrate a significant increase in average UE throughput when data demand is offloaded to

NR. The observed throughput enhancement is attributed to the potential for bandwidth disproportion between LTE and NR. While the UE establishes split bearers from both layers, LTE transmission can significantly hinder data reception on the NR bearer due to the faster data processing capabilities of NR. This leads to an underutilized NR channel and degraded UE throughput. Although the paper does not propose an improved method for calculating IP scheduled throughput, it highlights the potential for inaccurate throughput measurements, particularly in the context of Multi-Radio Dual Connectivity (MR-DC) functionality. The study suggests that increasing bandwidth, either through multiple CCs or wider bandwidth, increases the likelihood of measurement inaccuracies. In conclusion, the research demonstrates the potential benefits of MC in NR for enhancing UE throughput. However, it acknowledges the challenges associated with bandwidth disproportion and the need for further investigation into accurate throughput measurement techniques, particularly in MR-DC scenarios [9].

Other research paper [10] proposes an enhanced method for Dual Subscriber-identity-module Dual Standby (DSDS) capable devices, leveraging L1 mechanisms to optimize UE network admission and minimize Physical Channel Resource (PCR) wastage. The study compares the performance of different network admission mechanisms across various protocol layers: Radio Resource Control (RRC), Medium Access Control (MAC), and L1. The results demonstrate that L1, with its inherent HARQ process confirmation, exhibits the most favorable performance. This finding aligns with the principle that measurements conducted closer to the end-user perception generally yield more accurate and relevant results. The paper's approach, by operating closer to the physical layer, enables the achievement of optimal efficiency in network admission and PCR utilization for DSDS devices. The research highlights the significance of leveraging L1 mechanisms for optimizing DSDS device performance, emphasizing the importance of considering the proximity of measurement points to end-user perception for accurate performance evaluation [10]. Similarly, the novel method, detailed in Chapter 3, relies on communication and verification mechanisms implemented in the lower layers of the base station.

Another research paper [16] focuses on the problem of efficient bandwidth resource allocation in cloud computing environments. It highlights the limitations of existing approaches like NETSHARE, which lack a centralized management framework and fail to dynamically distribute bandwidth fairly based on QoS attributes. The paper proposes a novel Dynamic Virtualized Bandwidth Allocation (DVBA) scheme to address these shortcomings. DVBA leverages the SDN/OpenFlow architecture for centralized control of bandwidth resources, dynamically adjusting bandwidth allocation based on factors like loading status, QoS requirements, packet size, and bandwidth queue usage. The paper aims to demonstrate the effectiveness of DVBA through simulations, comparing its performance against the NETSHARE method using KPIs like throughput and average response time. While the research paper does not explicitly address the challenge of accurate throughput assessment in distributed networks, it tackles the issue of inefficient bandwidth allocation, aiming to enhance resource allocation accuracy and network performance with better utilization ratio. This implies that the distributed

nature of cloud networks exacerbates performance assessment challenges when multiple network nodes are involved in a single user's transmission. Consequently, network operators face difficulties in accurately evaluating QoS metrics, hindering their ability to optimize network configuration [16].

Alternative research [14, 15] presents a novel Distributed-to-Cloud Data Management (D2C-DM) architecture, leveraging a hierarchical structure encompassing Fog, cloudlet, and Cloud technologies. The architecture aims to optimize data management within the context of a smart city's coverage area, capitalizing on the benefits of both distributed and centralized approaches. D2C-DM aims to reduce network traffic and user latencies by strategically distributing data processing and storage across different layers. The framework facilitates the aggregation and organization of data from the entire network, enabling tailored data management strategies for diverse service types and their associated KPIs. Evaluation results demonstrate the high scalability of D2C-DM, accommodating cross-layer requirements and diverse data types. The architecture effectively reduces network load by leveraging real-time data processing at distributed layers. Furthermore, D2C-DM enhances security and communication reliability by minimizing data transmission distances. The research contributes to the advancement of data management in smart city environments by proposing a hybrid architecture that combines the advantages of distributed and centralized approaches. D2C-DM's ability to optimize data flow, enhance scalability, and improve security and reliability makes it a promising solution for managing the increasing volume and complexity of data generated in smart cities [14, 15]. However, the paper lacks a clear exposition of the synchronization method for real-time data received by a specific user from network entities that hold the disparate components required for throughput metric calculation.

Research paper [42] addresses the critical requirement for high throughput and low latency in real-time video streaming to optimize user QoE. While multi-path transmission holds promise for achieving these goals, ensuring timely delivery of prioritized video frames within resource-constrained environments remains a significant challenge. The proposed solution, vStreamPth, is a novel framework that leverages multi-path transmission in conjunction with key requirement indicators to guide frame transmission decisions. This framework employs a robust decision-making process that integrates application-oriented and network-oriented data scheduling, guaranteeing uninterrupted frame delivery and dynamically adapting to fluctuating network conditions. Empirical results demonstrate that vStreamPth significantly enhances QoE and deadline satisfaction ratio compared to existing solutions, achieving up to a 24% improvement in deadline satisfaction ratio and a 152% improvement in QoE performance. While the proposed solution introduces a novel framework for achieving reliable QoE metrics in real-time video streaming, it falls short of addressing the dissertation's focus on the issue of real-time network entity synchronization to achieve accurate results. Nevertheless, it underscores the importance of not only the accuracy of measurement calculations (i.e., the availability of complete information) but also the effectiveness of packet scheduling within multipath transmission scenarios utilizing

aggregated bandwidths. This emphasizes the crucial role of both data integrity and efficient resource allocation in optimizing throughput and ultimately enhancing QoE.

The previously mentioned articles [5-10, 14-16] strongly suggest that future access networks will necessitate a hybrid architecture, seamlessly integrating cloud and edge computing paradigms. This convergence of distributed and centralized systems holds the potential to unlock significant advantages, including:

- Reduced Network Traffic: By distributing processing and storage closer to users, edge computing minimizes the need for data to travel long distances to centralized cloud infrastructure, thereby reducing network congestion [6, 10].
- Enhanced Security: Edge computing allows for localized data processing and storage, reducing the attack area and enhancing data security by minimizing the need to transmit sensitive information over potentially vulnerable networks [28].
- Efficient Resource Allocation: The hybrid architecture enables dynamic resource allocation, optimizing bandwidth, CPU, memory, and disk utilization based on real-time demand. This optimizes performance and minimizes resource waste [5, 7, 8, 10, 16, 49, 52].

This hybrid approach, combining the strengths of both distributed and centralized systems, represents a promising path towards building robust, efficient, and secure access networks for the future. The mentioned research papers [5-10, 14-16] highlight the necessity of a dual approach to optimizing user experience through measurement:

- Developing Novel Measurement Coordination Strategies: The study advocates exploring innovative methods to coordinate measurement management across diverse network nodes and evaluation processes. This coordination should be tailored to specific traffic profiles and user needs, ultimately leading to a more refined and personalized user experience [6, 7, 14, 15].
- Optimizing Existing Measurement Techniques: Alongside the pursuit of novel coordination strategies, the research emphasizes the importance of refining existing measurement techniques to enhance their accuracy and reliability. This optimization is crucial for ensuring the validity and relevance of measurement data, particularly in the context of evolving network technologies and user demands [10].

The implementation of novel measurement coordination methods alongside the refinement of existing techniques will facilitate a more holistic comprehension of user experience. This enhanced understanding will, in turn, empower the development of more robust and efficient network performance management strategies.

The focus on optimizing known methods is particularly relevant in the light of emerging challenges associated with new system generations. While significant advancements have been made in user experience research, particularly regarding the critical role of network throughput in performance management, the transition towards DC systems presents unique challenges. The absence of standardized solutions within the 3GPP specification necessitates further investigation and development of robust measurement techniques for DC environments.

The subsequent chapter will delve into the optimization of the standard method for IP scheduled throughput measurement, aiming to address the evolving needs of next-generation systems and ensure accurate and reliable performance evaluation in the context of DC deployments. This research contributes to the ongoing effort to improve not only the user experience, but more importantly the whole performance monitoring aspect in evolving network architectures by highlighting the need for both innovation and optimization in measurement methods.

3. IP SCHEDULED THROUGHPUT

Chapter 3.1 introduces the principles of the standard method, defined in 3GPP standard and implemented in devices used in real cellular networks, for measuring IP scheduled throughput, outlining the calculation method for data volume and time components on a per-user basis. Chapter 3.2 elaborates on the challenge of accurately calculating this measurement within a DC system, as previously discussed in Chapter 2.2, and highlights the absence of a readily available solution. A practical example is provided to illustrate the limitations of the standard method. Chapter 3.3 extends the analysis to a more complex scenario, demonstrating with practical example values the discrepancy between the standard method's perception of throughput and its inadequacy in accurately reflecting the actual throughput in a DC system. Chapter 3.4 proposes two novel solutions to address the accuracy of IP scheduled throughput measurement in DC systems: a straightforward but computationally intensive approach and a novel method with an approximation. Chapter 3.5 delves deeper into the principles of the novel method, presenting postulates and a buffer-centric perspective to further elucidate its underlying mechanisms. Finally, Chapter 3.6 defines two reference points for verifying the accuracy of both proposed methods, providing a framework for evaluating their effectiveness in addressing the challenges of IP scheduled throughput measurement in DC systems.

3.1. Standard method for IP scheduled throughput formula discussion

Subscriber departure, characterized by users switching wireless providers due to perceived service quality degradation, poses a significant financial risk to network operators. Consequently, ensuring high service integrity is paramount from a business perspective. Throughput, a key metric for evaluating non-GBR services, is defined by 3GPP TS 32.451 [22] as an IP-level volume measurement. Notably, the measurement method must account for data flow burstiness by excluding periods of inactivity, represented by T_Idle in Figure 3.1, from the calculation [12, 22].

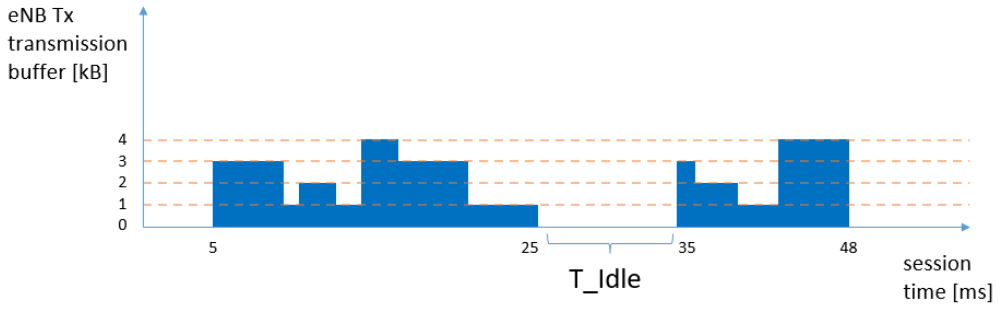

Figure 3.1: Principle of the burst measuring in a session with idle time exclusion [12].

3GPP TS 36.314 [12] defines the relevant throughput measurement as "IP Scheduled Throughput." Figure 3.2 provides a conceptual illustration of the DL IP Scheduled Throughput calculation for a single data burst.

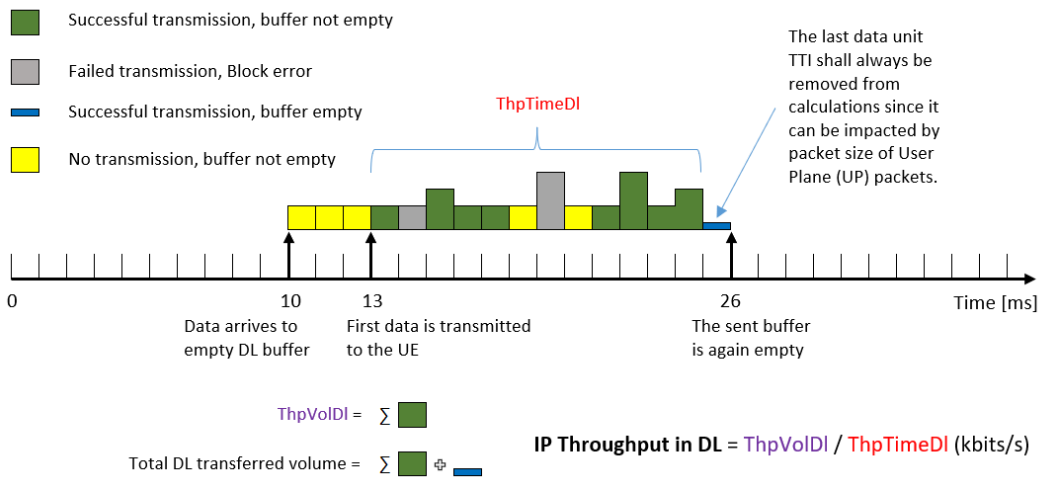

Figure 3.2: Principle of IP scheduled throughput measurement in DL [12].

ThpVolDl denotes the IP volume transmitted successfully to the UE, while *ThpTimeDl* represents the burst duration. Notably, subsequent investigations within the 3GPP SA5 group led to the definition of a dedicated IP latency measurement in 3GPP TS 32.450 [21]. This measurement quantifies the average initial latency of each new burst, spanning from the arrival of new burst data to an empty eNB buffer until the initial transmission via the air interface to the UE. Consequently, the initial latency of each new burst is excluded from *ThpTimeDl*. Additionally, the final TTIs that empty the eNB buffer, including bursts lasting a single TTI, are also excluded. This exclusion is attributed to the potential for insufficient user data to fill the entire TTI, leading to the addition of padding volume at the MAC layer or the use of more robust coding, which are unnecessary and may artificially influence the measured throughput [12, 20, 21].

3.2. IP Scheduled Throughput Measurement Challanges in DC Systems

Figure 3.3 depicts an example of a DC implementation within the Nokia environment. This implementation pertains to CA scenarios where the SeNB may cover the SCell while the MeNB covers the PCell.

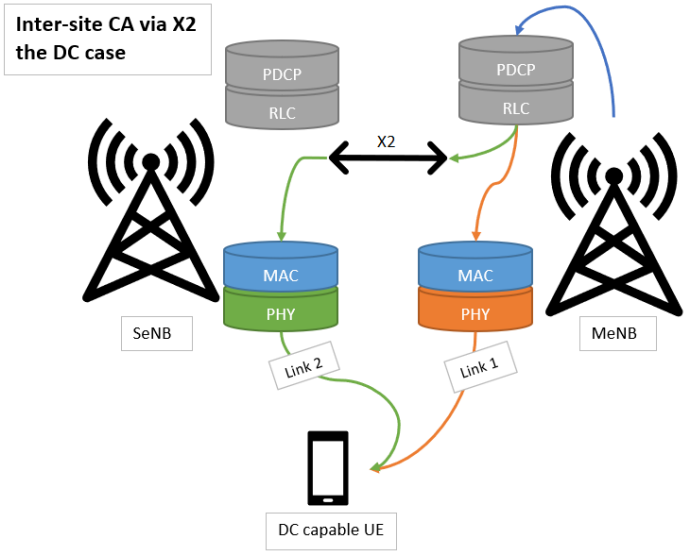

Figure 3.3: The concept of DC based Inter-site CA via X2 [3, 9].

This solution presents a potential advantage when extending CA to encompass carriers provided by eNBs situated in geographically distinct locations, commonly referred to as inter-site CA. In contrast to the DC concept outlined in Section 1 and 2, the data splitting occurs at the RLC PDU level, rather than the PDCP PDU level, which is characteristic of the standard CA concept, designated as intra-site CA in the remainder of this dissertation.

The IP scheduled throughput for a DC system adheres to the principles summarized in Section 2. However, due to the separation of the layer stack, each scheduler operates independently. The PCell's PDCP layer lacks awareness of the transmission outcome for portions of PDCP SDUs transmitted as RLC PDUs to the SCell. Consequently, the global buffer status encompassing both PCell and SCell remains unknown to the MeNB [3, 9]. Figure 3.4 illustrates an example of the global buffer status for a DC inter-site CA system comprising a PCell MeNB, represented by a teal-colored graph, and an SCell SeNB, represented by a yellow-colored graph.

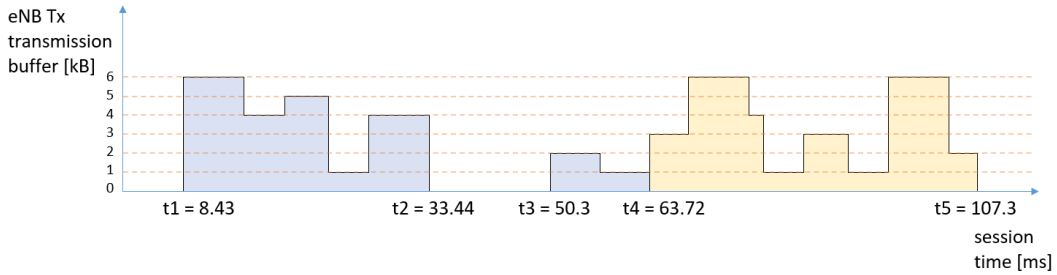

Figure 3.4: Example of buffer fullness in case of inter-site CA system.

This scenario presents a challenge in accurately calculating throughput due to incomplete data availability. While data exists in the buffer from time t1 to t2 and t3 to t5, the PCell MeNB only possesses knowledge of the intervals t1 to t2 and t3 to t4. Consequently, employing the standard IP scheduled throughput method outlined in 3GPP TS 36.314 would yield inaccurate results.

Several alternative approaches can be considered to address this issue. The first approach utilizes *ThpTimeDl*, defined as the time interval encompassing data within the PCell MeNB buffer (t1 to t2 and t3 to t4) and the total transmitted PDCP SDU volume, including portions transmitted via the SCell SeNB. This method, however, leads to an overestimation of throughput due to the exclusion of time intervals associated with data residing in the SCell SeNB buffer.

The second approach defines *ThpTimeDl* as the time interval encompassing data within the buffer from t1 to t5, along with the total transmitted PDCP SDU volume. This approach results in an underestimation of throughput as the interval t2 to t3 is erroneously included in the calculation.

Additional viable options involve considering only the time with data in the PCell MeNB buffer while excluding the portion of PDCP SDU volume transmitted via the SCell. However, none of these proposed methods achieve accurate throughput monitoring, as highlighted in [12].

The application of IP scheduled throughput calculation principles within DC systems remains undefined by both the 3GPP standard and existing scientific literature. To the authors' knowledge, no prior research has been conducted or published on this specific topic.

3.3. Limitations of Standard IP Scheduled Throughput Measurement in DC Systems with Inter-site CA

This chapter discusses the challenges of accurately measuring IP scheduled throughput in DC systems using the standard method. It presents three scenarios where the standard method leads to inaccurate throughput measurements.

Figure 3.5 presents an example of considerations regarding the measurement error of throughput for a DC system using the standard method. IP data packets have been divided between three cells: the main PCell in MeNB and two auxiliary SCell 1 and SCell 2 located in SeNB. Successful data transmissions to the user are marked in green, erroneous transmissions requiring retransmission in red, repeated transmissions in gray, transmissions in the last time slot in blue, buffer occupancy in yellow, and an empty buffer in white. For the x-axis, a single time unit is 1 ms, for the y-axis, the amount of data is from 1 kB to 3 kB, depending on the size of the data packet. At timestamp t9, a data volume transfer from the MeNB to the SeNB was initiated. However, upon arrival at the SeNB, the PDCP buffer was already occupied by another user's data, resulting in a buffer contention scenario.

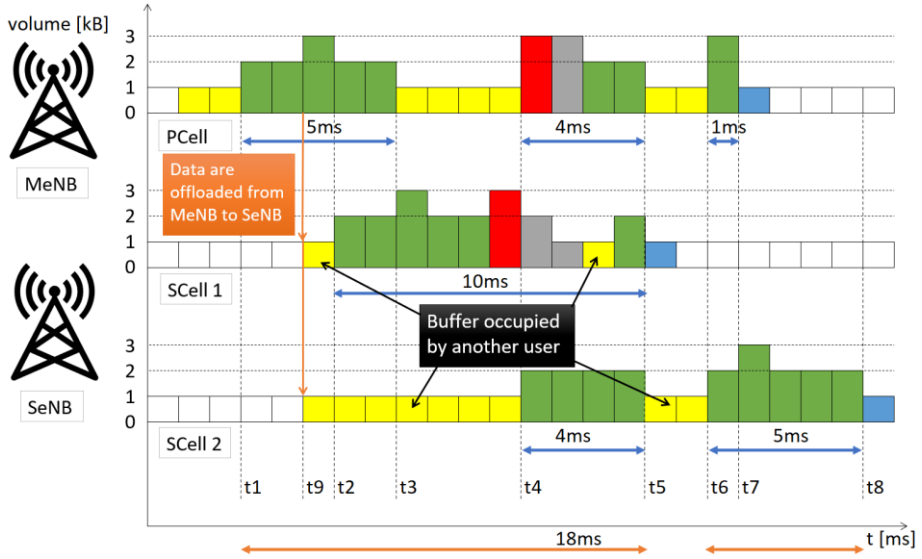

Figure 3.5: Problems with the accuracy of IP throughput measurement in the direction to the user in DC systems.

To understand the problem, consider the following events, keeping in mind that MeNB does not have any information about the transmission time in SeNB, nor the delay on the X2 interface.

The first event concerns the situation where the amount of PDCP data is equal to the sum of data packets directed to the main and auxiliary cells, while the time is counted only from the perspective of PCell and is based on timestamps from t1 to t3, from t4 to t5, and from t6 to t7. This type of solution significantly overestimates the throughput (Option 1 in Table 3.1).

The second event concerns the situation where the amount of data is equal to the sum of data packets directed to the main and auxiliary cells, while the time is measured from the perspective of PCell and SCell 1 and is based on timestamps from t1 to t5 and from t6 to t7. Although the time of the transmission interruption in PCell is counted, transmission is taking place

on SCell 1 at the same time, which MeNB is aware of due to the data previously sent to SeNB. Unfortunately, the time from t7 to t8, where transmission takes place on SCell 2, is not counted. This type of solution can both overestimate the throughput (Option 2 in Table 3.1) and underestimate it if the transmission interruptions are longer than the duration of the transmission in both cells.

The third scenario involves the situation where the amount of data is counted only in PCell, while the time measurement also includes the additional time of the data transmission interruption in both base stations at the same time, from t1 to t7. This solution underestimates the throughput (Option 3 in Table 3.1).

Table 3.1: Measurement results of the standard method for the DC system.

Reference point	*Data volume [kB]*	*Transmission time [ms]*	*Throughput [Mbps]*
PCell	21	10	16.80
SCell 1	16	10	12.80
SCell 2	19	9	16.89
Option 1	56	10	44.80
Option 2	56	14	32.00
Option 3	21	16	10.50
User	56	18	24.89

Table 3.1 summarizes the previously discussed results. From the user's perspective, for the given example, the throughput was 24.89 Mbps. None of the above considerations would allow for the calculation of the correct IP throughput from the user's perspective for the standard method in DC systems.

3.4. Potential Remediation Strategies for the Identified Problem

This chapter explores two approaches to address the measurement precision issue inherent in the standard method for evaluating IP throughput in Dual Connectivity (DC) systems.

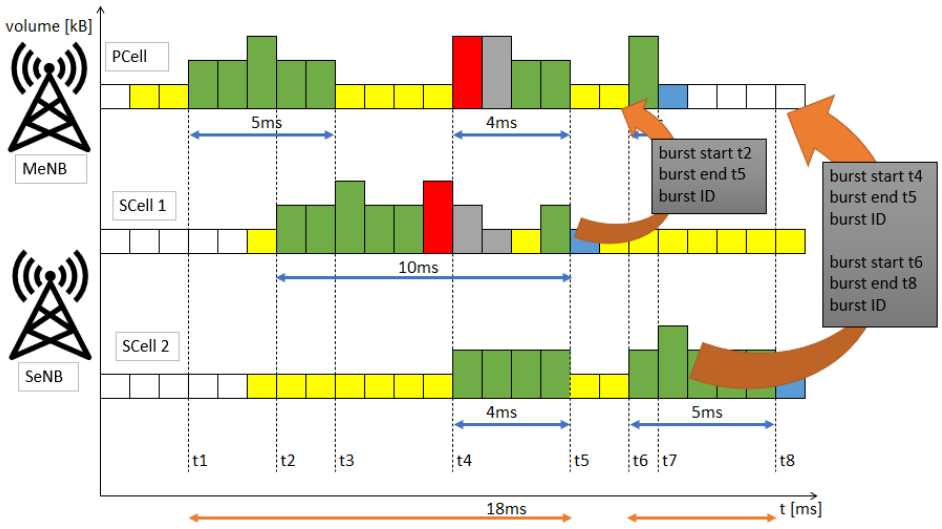

Figure 3.6: Straightforward solution with a timestamp-based acknowledgment mechanism for each packet.

First and a straightforward approach [27], as shown in Figure 3.6, leverages a timestamp-based acknowledgment mechanism, requiring each SCell of SeNB to transmit timestamps for the start and end of each PDCP packet. While this method provides detailed information about packet transmission, it imposes a significant burden on the X2 interface and MeNB control unit. The X2 interface, responsible for communication between the PCell of MeNB and the SeNB, is tasked with transmitting data irrelevant to the actual transmission correctness. Furthermore, the SeNB must report packet transmission correctness information for each individual user utilizing carrier aggregation. This results in a trade-off, where the X2 interface allocates bandwidth for informational data essential for the operator, at the expense of user data transmission. The load on the X2 interface is directly proportional to the amount of user data transmitted. Moreover, a more critical concern arises from the need to store this transmission correctness information in the MeNB from each SeNB and associate it with each burst and user. This process significantly impacts the overall base station performance, potentially leading to performance degradation. Moreover, the proposed solution implicitly assumes perfect time synchronization among network nodes, a condition that is not achievable in practice [27].

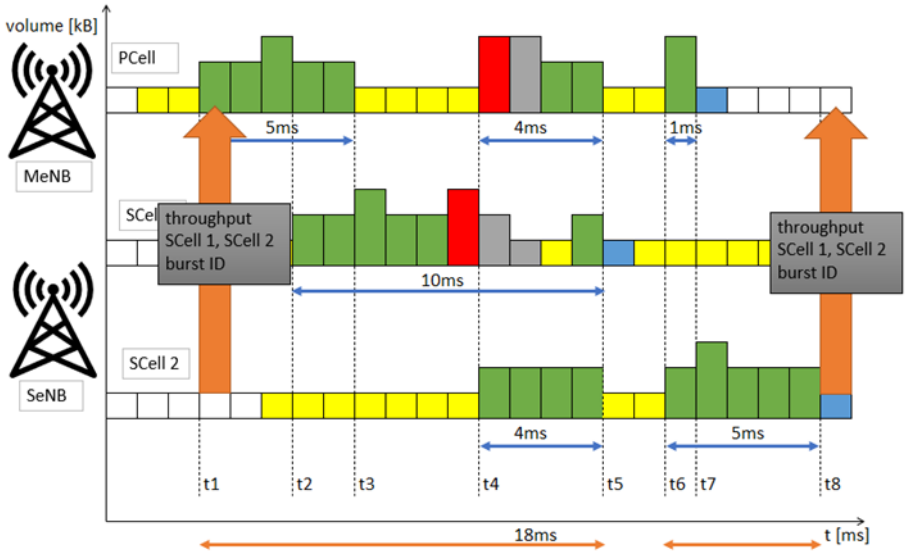

Figure 3.7: Alternative solution with an approximation mechanism.

An alternative solution, as shown in Figure 3.7, designed to mitigate the performance impact of the first approach, involves approximating the throughput [51] in each SCell and transmitting this information to the PCell at specific time intervals. This method ensures a constant and defined load on the X2 interface, unlike the timestamp-based approach. Moreover, the traffic control unit in the MeNB is relieved from associating information regarding the start and end of transmission on different carriers for a given user. The SeNB directly reports its current throughput capability for each user individually, simplifying the process. The SeNB dynamically estimates its current throughput capability, defined as the maximum data volume that can be transmitted in a single TB, using a specific expected throughput (eTh) function. This function employs an Infinite Impulse Response (IIR) filter to perform time averaging of the expected throughput, effectively mitigating the impact of short-duration, high-intensity interference fluctuations. The *eTh* value,

expressed in kbps, is then transmitted to the MeNB via the Downlink Data Delivery Status (DDDS) mechanism [58, 59] at a frequency determined by the parameter transferDelayMax, which can be configured with various values, such as 50ms by default. This approach further benefits from utilizing an existing mechanism, the DDDS defined in 3GPP TS 36.425 [24, 58, 59], which provides the capability for periodic reporting of values between base stations.

While the timestamp-based acknowledgment mechanism offers detailed information about packet transmission and thus a high measurement precision, it significantly impacts the X2 interface performance and overall base station efficiency [27]. The throughput approximation approach, coupled with the DDDS mechanism, presents a more efficient alternative, ensuring a constant and defined interface load while simplifying the data reporting process.

3.5. A Novel Approach to IP Scheduled Throughput Measurement in DC Systems with Inter-site CA

Accurate IP scheduled throughput calculation in inter-site CA system, as outlined in 3GPP TS 36.314 [12], enforces comprehensive knowledge of the global buffer status encompassing both the PCell and SCell.

A straightforward approach to informing the MeNB about the global buffer status involves transmitting the relevant information from the SeNB to the MeNB. This necessitates establishing a dedicated message flow between MeNB and SeNB for each data packet scheduled for processing at SeNB. Each message would convey the SCell buffer status, which, upon reception by MeNB, would be temporarily stored in memory.

Simultaneously, MeNB must maintain a record of its local buffer status, also stored in memory. This is crucial because SeNB reports can experience delays, requiring post-processing for global buffer status calculation.

The global buffer status is constructed using reported burst transmission timestamps. Consequently, MeNB and SeNB must be perfectly synchronized in terms of their system clocks. Asynchronous clocks would lead to an inaccurate global buffer status, ultimately resulting in errors in the IP scheduled throughput calculation.

Furthermore, MeNB would require substantial memory to store both MeNB and SeNB timestamp reports, along with sufficient processing power to effectively combine them. While this approach provides the necessary data for IP scheduled throughput calculation, it imposes unrealistic demands on MeNB and SeNB.

Therefore, to achieve a method for precise and efficient estimation of IP throughput for the end user, for both traditional and DC systems, it is necessary to define fundamental assumptions. These assumptions, referred to as postulates within the context of this dissertation, serve as the foundation for the proposed estimation method [13, 17, 60]:

- Postulate I: the initiation of burst transmission time counting is solely dependent on the buffer at the MeNB side. This aligns with the user experience, as the user is connected to the primary cell, which decides on the activation of secondary cells based on traffic volume demands and the terminal's capabilities for specific transmission functions. Consequently, the timestamp of the first RLC PDU packet reception at the SeNB side is considered insignificant.

- Postulate II: a master buffer needs to be defined in relation to the individual buffers of the MeNB and SeNB base stations. The master buffer will be considered occupied if either the MeNB or SeNB buffer is occupied.
- Postulate III: the buffer occupancy time in the SeNB for each $RLC\ PDU_{\mathrm{i}}$ packet should be defined as, where the subscript 'i' denotes the packet sequence number:

$$T'_{RLC\ PDU_i} = T_{X2\_RLC\ PDU_i} + T_{RLC\ PDU_i} \tag{3.1}$$

where $T_{X2\_RLC\ PDU_i}$ represents the transmission time of the packet through the X2 interface, and $T_{RLC\ PDU_i}$ represents the time the $RLC\ PDU_i$ packet resides in the SeNB buffer, calculated as:

$$T_{RLC\ PDU_i} = \frac{Data\ volume\ for\ RLC\ PDU_i}{SeNB\ IP\ Throughput} \tag{3.2}$$

The SeNB IP throughput is measured using the standard method (3GPP TS 36.314) solely within the SeNB for received $RLC\ PDU_i$ packets from the MeNB.

- Postulate IV: the averaged values of the X2 interface transmission delay and SeNB IP throughput will be used for calculations in equations (3.1) and (3.2). A parameter controlling the frequency of their transmission from the SeNB to the MeNB will also be defined. Based on the traffic intensity between the two base stations, this parameter can be adjusted to a value that prevents overloading the X2 interface, which would result in a decrease in throughput gain due to traffic splitting between different base stations, as shown in Figure 3.8.

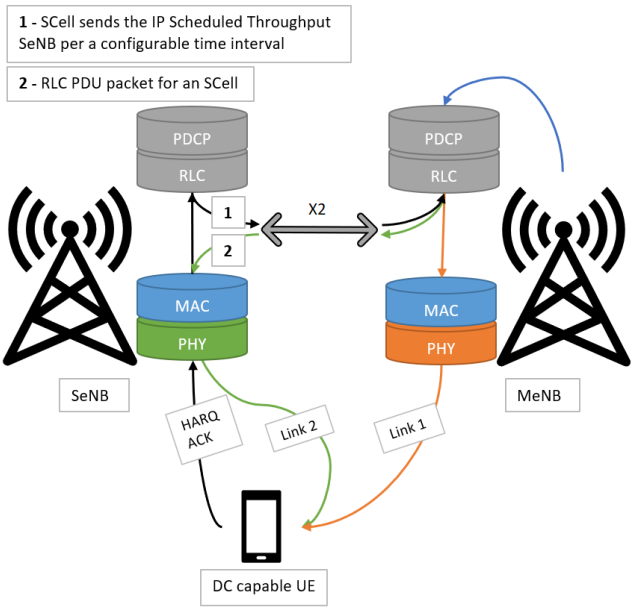

Figure 3.8: Message exchange between MeNB and SeNB according to the new method.

Figure 3.9 illustrates a scenario involving a single CA UE and a single SCell located within the SeNB. The proposed method's operation, as illustrated in Figure 3.9, can be described as follows:

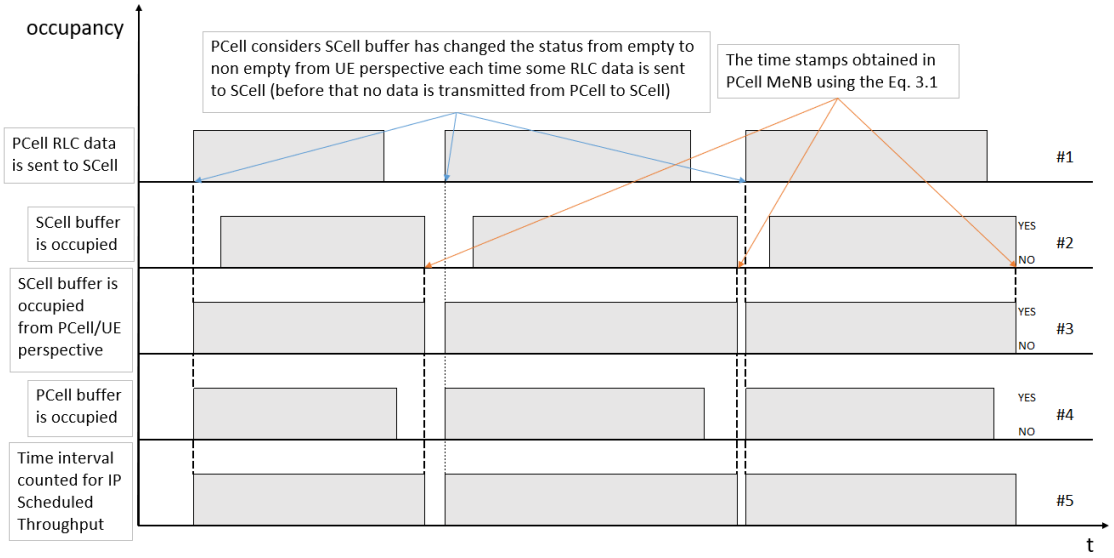

Figure 3.9: The principle of the method in example.

1. Upon arrival of IP packets at the MeNB, the PDCP buffer occupancy is initiated if immediate scheduling is possible. If not, the data is queued and the waiting period is excluded from the buffer occupancy calculation, as per 3GPP [12]. Once scheduled, the buffer occupancy time for the specific user is recorded in the PCell, marking the start of a data burst.
2. The PCell scheduler then determines whether the received data should be split between the PCell and SCells, triggering Carrier Aggregation (CA) activation in lower layers. The PCell assumes the SCell's current throughput capability is equal to the *eTh* value reported by the SeNB. In the absence of *eTh* information for a given user during transmission initialization, the first expected throughput is calculated using an initial MCS parameter value.
3. According to Postulate I, the PCell in the MeNB considers the SCell buffer occupied when RLC data is transmitted to the SCell, as depicted in Graph #1. This occurs when the PCell offloads a portion of received IP data to the SCell, assuming the SCell's PDCP buffer is occupied based on the eTh-indicated throughput capabilities, but before the impact of X2 interface transmission delay.
4. The exact time of data reception at the SCell is irrelevant (Figure 3.9, Graph #2). The PCell MeNB considers the SCell buffer empty at the timestamp calculated using Equation 3.1, which is noted in Graph #2. Conversely, the SeNB views the SCell buffer as occupied from the moment data is received via the X2 interface until successful transmission acknowledgement from the user, which is not depicted in the mentioned Figure 3.9 as it is an ambiguous detail unknown at the PCell MeNB and excluded from the novel method.
5. Figure 3.9, Graph #3, represents the SCell buffer status from the PCell/UE perspective, indicating its occupancy state. The PCell considers the SCell buffer occupied from the moment IP data arrives at the MeNB until the data volume is transmitted according to Equation 3.1, which includes the X2 transfer delay and *eTh* value.
6. Graph #4 represents the occupancy of the PCell's PDCP buffer with scheduling of data that are sent via PCell.

7. The time component depicted in Graph #5 for IP scheduled throughput measurement incorporates the previously described logic. As per Postulate II, it represents the transmission time from the PCell MeNB perspective, determined by buffer status checks. Transmission time is measured when data is present in either the PCell or SCell buffer, calculated using the logical OR function applied to Graphs #3 and #4 in Figure 3.9.

The proposed method leverages the principles outlined in 3GPP TS 36.314 for IP scheduled throughput measurement while simultaneously reducing implementation complexity. This approach does not compromise the accuracy of the obtained throughput values. The IP Scheduled Throughput at the SeNB is calculated over a configurable time interval, resulting in an average value consistent with the per-burst logic defined in 3GPP TS 36.314 [12]. The sampling periodicity of the *eTh* value may impact the precision of the averaged throughput during sudden changes in radio channel quality, such as fading or variations in the number of served users requiring resource allocation.

However, subsequent chapters that elaborate on the method's implementation, include a double protection mechanism that prevents SCell scheduling in the event of transmission issues at the SeNB. This mechanism serves to maintain transmission integrity and mitigate inaccuracies in the novel method which arise from SeNB transmission problems.

3.6. Defining relative error as a baseline for precision comparison

Precise reference point establishment for IP scheduled throughput assessment remains problematic. The 3GPP standard method inadequately represents application-layer throughput (UE perspective) and cell throughput (eNB perspective), instead of employing a hybrid approach. This approach, based on PDCP buffer occupancy and a burst calculation concept, provides an approximation of instantaneous throughput at both MeNB and SeNB. However, the SeNB approximation neglects lower-layer transmission success (HARQ ACK). The data volume component seeks to correlate with perceived user throughput, given the PDCP SDU composition (including IP header)..

An alternative approach for establishing a useful reference point would involve deriving buffer occupancy values for each individual user. However, this approach is not feasible as the PDCP buffer is maintained on a per-cell basis, rather than for specific users connected to that cell. Furthermore, if only the cell-level PDCP buffer occupancy were obtained, the exact number of scheduled users would need to be determined at each TTI. This metric is an internal, critical parameter that is not readily disclosed for external observation and is maintained as confidential information.

Given the aforementioned challenges, the following reference points assess the efficacy of both the standard and the novel data transmission methods in terms of accuracy. A two-pronged approach is necessary to establish a consistent and precise measurement framework.

The first approach involves comparing the calculated method throughput, defined as:

$$IP\ scheduled\ throughput\ [Mbps] = \frac{ThpVolDl}{ThpTimeDl}, \tag{3.3}$$

with the Cell's Throughput. Equation 3.4 provides the calculation for Cell Relative Error, derived from the preceding comparison, valid only for single-user eNB connections within a defined test set. This approach allows for the assessment of the eNB's efficient scheduling capabilities, as the Cell's Throughput is derived from the eNB based on the total PDCP SDU data volume received and the total number of TTIs scheduled with user data on the PDSCH.

Furthermore, this comparison provides insights into how individual TTI transmissions influence the transfer of a specific file size. It helps to determine whether the transmission exhibits a constant data volume exchange between the transfer initiator and the last IP network node prior to radio transmission. In essence, it quantifies the rate of data inflow between the server and the eNB.

However, this reference point has inherent limitations when compared to both methods and their respective logic of accounting for both data volume and time components per burst, particularly during retransmission scenarios. In such scenarios, characterized by poor radio channel quality, link adaptation mechanisms are required to correct the signal sent to the user which may overestimate the time component length for the burst calculation in comparison to total number of TTIs scheduled.

$$Cell\ Relative\ Error\ [\%] = \frac{100\times(IP\ scheduled\ throughput - Cell\ Throughput)}{Cell\ Throughput} \quad (3.4)$$

A second approach involves comparing the calculated method throughput with the application layer throughput to directly assess end-user experience. Equation 3.5 provides the calculation for App Relative Error, derived from the preceding comparison. App throughput can be obtained from the iperf application installed on the UE, which simulates data download behavior for the end-user. The iperf receiver value serves as a reference point for this measurement.

$$App\ Relative\ Error\ [\%] = \frac{100\times(IP\ scheduled\ throughput - App\ Throughput)}{App\ Throughput} \quad (3.5)$$

While acknowledging the inherent differences in the ISO/OSI layer model and the eNB intermediary position between the server and receiver, it is important to understand the alignment between the calculated method throughput and the user's perceived QoE. The eNB cannot directly measure the UE's application layer throughput. However, comparing these values provides valuable insights into the effectiveness of the methods employed. Figure 3.10 below depicts a screenshot from the application used to determine user throughput on the UE.

It is important to note that IP scheduled throughput measurements do not solely reflect the eNB's scheduling efficiency per user or the user's actual data download/upload rates. Instead, they represent a composite metric influenced by both factors. Consequently, a comprehensive evaluation necessitates the consideration of both reference points, namely eNB scheduling performance and user data throughput, to obtain a holistic understanding of network performance.

To streamline nomenclature and enhance brevity, the following conventions will be adopted:

- **App RE**: will represent the relative error in estimation of application layer throughput.
- **Cell RE**: will represent the relative error in estimation of cell throughput.

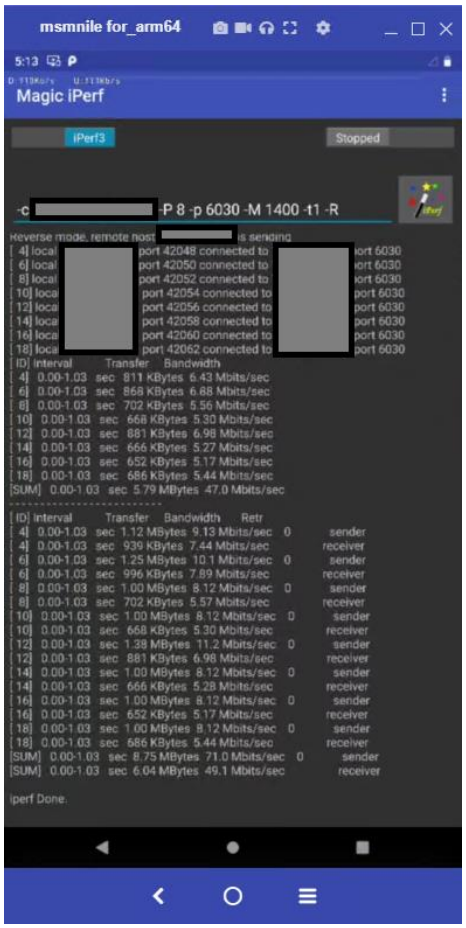

Figure 3.10. Example of UE Throughput measurement read from the iperf application installed on the UE.

This standardization facilitates concise communication and improves readability within this dissertation in Chapter 5.

Subsequent chapters will delve into the implementation of the novel method. This will encompass a detailed description of the method's *eTh* function and specific parameters that influence its effectiveness in calculating precise measurements. These parameters describe the following phenomena:

- The frequency at which *eTh* values are exchanged between SeNB and MeNB.
- The initial MCS value used when the first *eTh* value is unknown at the start of transmission.
- A mechanism to discard RLC PDUs in the event of transmission issues at the SeNB.
- Exponential moving average function which defines the rate at which the current measured *eTh* value converges to the actual SeNB SCell scheduler capability.

Understanding these constraints is crucial for assessing the accuracy of the novel method. It allows for the identification of conditions where the precision falls below acceptable levels and when the method achieves its highest precision.

4. IMPLEMENTATION OF THE NOVEL METHOD

The method described in Chapter 3 has been implemented in real devices [47]. However, for this implementation, it was necessary to add certain mechanisms, such as a "running average" filter and counters for the maximum time the packets spent in the eNB buffers. This section presents a detailed analysis of the implementation specifics and supplementary parameters employed within the algorithms governing traffic management and throughput estimation. These details are essential for understanding the description of the tests conducted and correctly interpreting the results.

Chapter 4.1 provides a comparative analysis of an alternative preliminary solution that was evaluated prior to the implementation of the novel method.

Chapter 4.2 examines the implications of integrating a novel DC-type system configuration into a conventional LTE system equipped with legacy flow control mechanisms. The chapter demonstrates the inadequacy of these legacy mechanisms in ensuring efficient data scheduling within the RAN under the new configuration. It highlights the need for a revised approach to IP scheduled throughput calculation due to the limitations of the standard method in this context. The standard method's inability to provide meaningful results necessitates the development of the novel method, integrated with an extended flow control algorithm.

Chapter 4.3 describes a formal introduction to the approximation concept, grounded in flow control modifications. This chapter provides a comprehensive overview of the flow control process during inter-site CA connections, specifically focusing on the application of the novel method, with a rainy-day scenario example.

Chapter 4.4 details the novel method's implementation, highlighting its robustness in ensuring throughput accuracy. Critical parameters for IP scheduled throughput calculation are defined. Subsequent sections analyze the SeNB's expected throughput function, its approximation of expected throughput, and its resilience to radio channel variations. MeNB PM counter analysis, accounting for burst data volume and time, is also presented for IP scheduled throughput estimation.

Chapter 4.5 examines the implementation modifications introduced in the time component calculation, distinguishing between the standard and novel methods. This analysis highlights the rationale behind these adjustments, emphasizing their contribution to enhancing user experience.

4.1. Preliminary Solution Concept Prior to the Novel Method Definition

As detailed in Chapter 2.5, an initial solution concept based on precise data volume quantification for each neighbor relationship using CA was investigated, as proposed in publications [13, 17, 60]. However, concerns regarding potential performance degradation of the eNB emerged, prompting the exploration of alternative solutions. The underlying concept, centered on neighbor relationships, is visually represented in Figure 4.1.

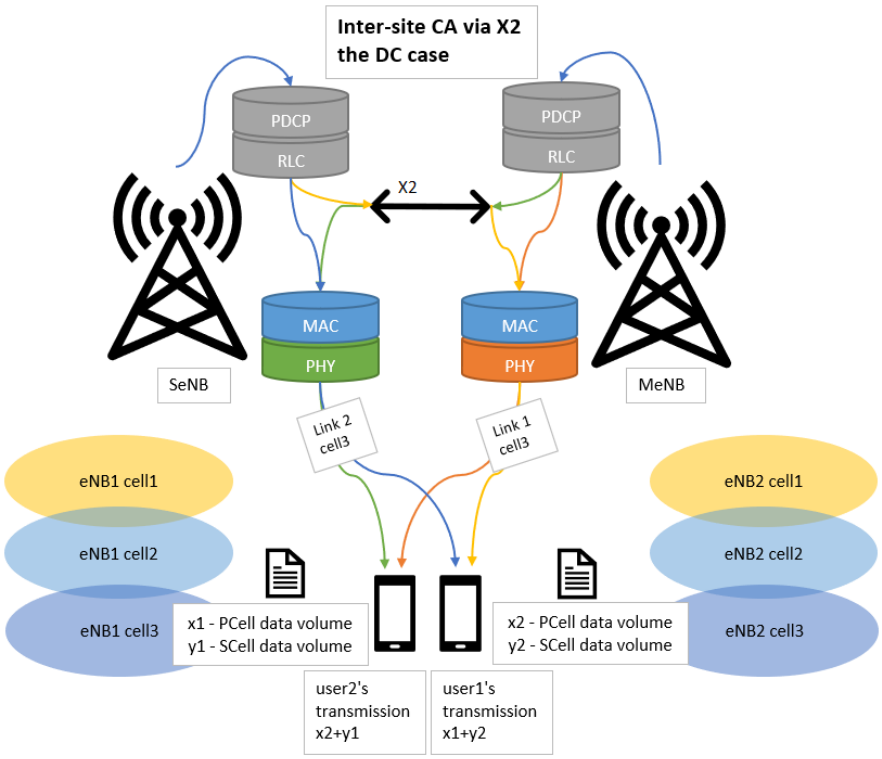

Figure 4.1 – Preliminary, Cell based IP throughput calculation example based on neighbor relation association.

This scenario involves two eNBs, each comprising three distinct cells, operating concurrently as both MeNB and SeNB based on user demands. One user is connected to eNB1 acting as MeNB and its third cell (Cell3) and simultaneously utilizes eNB2 acting as SeNB and its third cell (Cell3). Conversely, the second user is connected to eNB2 acting as MeNB and its Cell3, while also utilizing eNB1 acting as SeNB and its Cell3. This approach leverages exclusively the single neighbor relationship. The data volume transmitted via eNB1 Cell3 when acting as the PCell is denoted as x1, while the data volume when acting as the SCell is denoted as y1. Similarly, for eNB2 Cell3, the PCell data volume is represented as x2, and the SCell data volume as y2. To illustrate the diverse neighbor relationship combinations possible during any CA connection type, regardless of whether there are two Component Carriers (2CC) or up to 8CC used, other cells from both eNBs are included. In this specific example, a total of nine distinct neighbor relationships can be formed.

The IP scheduled throughput associated with the specific neighbor relationship between eNB1's Cell 3 and eNB2's Cell 3 can be directly determined by dividing the sum of x1, x2, y1, and y2 by the total time during which CA data is transmitted from PCell perspective. This method adheres to the specifications outlined in 3GPP TS 36.314 [12]. Extending this concept, it is possible to calculate the CA IP scheduled throughput from the perspective of a specific cell, but not from the user's perspective. For example, x1 + y2 represents the CA data volume for eNB1's Cell 3, and dividing this by the time during which CA data is transmitted on PCell yields the corresponding throughput value. However, a limitation exists in the absence of information regarding the transmission process on the SeNB. Only the time when CA is established from the

perspective of eNB1 is considered for the time calculation, neglecting the SeNB's transmission activity.

Post-processing data analysis within the NMS presents an additional layer of complexity. Every PM counter data for each neighbor relationship would be stored, necessitating NMS functions to connect two distinct counters from different eNBs. This process must be repeated for every neighbor relationship combination within the network. In networks comprising thousands of eNBs and hundreds of thousands of cells, post-processing every 5 or 15 minutes could significantly increase the processing load. Furthermore, NMS constraints on the maximum number of PM counter data from eNBs would preclude the implementation of this approach during the initial design phase.

While promising, the initial approach was hindered by high computational demands for real-time measurements and imprecise time accounting due to potential buffer emptying discrepancies between the MeNB and SeNB. This proposed solution exhibits limitations in its ability to provide a comprehensive network-wide throughput assessment. The requirement for operators to manually identify and aggregate results from diverse neighbor relations poses a significant challenge, particularly considering the variability in the number of SCells employed by different UEs. Consequently, the obtained results primarily reflect individual cell contributions to UE throughput, making it difficult to derive a meaningful average IP scheduled throughput across the entire network, where a multitude of UE configurations coexist. This led to its abandonment in favor of a more robust and efficient solution which is presented in Chapter 3.5 and in the subsequent chapters [13, 17].

4.2. New inter-site CA architecture impact on the flow control algorithm

The novel method presented in Chapter 3.5 is contingent upon the architectural modifications introduced in the network. These modifications encompass the introduction of novel logical network elements, the interplay between legacy and newly deployed nodes, and the communication protocols governing message exchange between these entities. The successful implementation of this novel method entails coordination and synchronization of these architectural changes. Only upon achieving configuration synchronization can the novel method proceed to calculate IP scheduled throughput based on the enhanced flow control mechanism, which has been adapted to function within the context of the newly established network architecture.

The introduction of the novel inter-site CA architecture concept into existing LTE systems necessitated significant modifications to the flow control mechanism. A primary concern was the lack of a unified solution for both intra-site and inter-site network environments. Existing flow control algorithms were unable to handle the transmission of inter-site CA configuration without substantial modifications and extensions to the system's core functionality.

The use of two separate solutions for both intra-site and inter-site CA, simultaneously available across the network, while potentially feasible, would introduce significant inefficiencies and complexities. This approach would not only be inefficient but also prone to potential defects,

increasing the complexity of the system by introducing more dependencies and greater configuration complexity.

The maintenance of distinct flow control algorithms for intra-site and inter-site CA scenarios hindered compliance with industry standards, which generally advocate for a single, unified approach to ensure interoperability and consistency. The presence of two distinct flow control algorithms required the use of two separate measurement methods for data flow performance assessment, introducing unnecessary complexity and ambiguity. This complexity made system performance monitoring and troubleshooting challenging. The requirement to select the appropriate measurement method based on the specific environment imposed operational constraints and limitations. Furthermore, in a mixed environment where a single user simultaneously utilizes both intra-site and inter-site CA, obtaining meaningful and precise results would be impossible, as each measurement method would only calculate a portion of the transmission of a single file. This lack of a unified approach hindered accurate performance evaluation and analysis. The need for a unified flow control mechanism with a single measurement method is crucial for achieving interoperability, consistency, and efficiency of the system management in LTE networks.

Therefore, a new and unified flow control solution was deemed necessary to address the inherent limitations of the existing system in handling the complexities introduced by inter-site CA. The development of a novel flow control algorithm aimed to address these limitations and ensure a seamless and efficient flow control mechanism across any network configuration type, ensuring support for both intra-site and inter-site environments. This unification was achieved through the implementation of a consistent logic, utilizing identical parameters and message exchanges across both scenarios, despite architectural differences. A key innovation was the incorporation of a mechanism to transmit the expected throughput value from the SCell back to the PCell scheduler. This mechanism effectively treated each SCell as if it originated from a different eNB than the PCell. By providing this information, the PCell scheduler could accurately assess the SCell's throughput capabilities and optimize resource allocation accordingly, regardless of the network configuration. This part of the novel flow control algorithm is inextricably linked to the novel measurement method detailed in Chapter 3.5. Both the methods rely on the *eTh* value obtained from the SeNB as a fundamental input for CA traffic split processes, governed by MeNB. This interdependence underscores the crucial role of the *eTh* value in both the measurement and flow control algorithms.

Moreover, the standard measurement method for throughput calculation, which was based on legacy flow control algorithm, employed by the eNB exhibited a limitation in its burst time estimation, resulting in reduced accuracy. This inaccuracy arose from the stochastic nature of IP packet arrival patterns, characterized by unpredictable inter-arrival times. Consequently, new packets could arrive before the buffer was fully emptied, leading to inconsistencies in the calculated burst duration.

To address this limitation, the novel measurement method, based on the new flow control algorithm, was developed to enhance burst time calculation. This algorithm incorporates a more

sophisticated model that explicitly accounts for the dynamic nature of packet arrivals during the lower layer activity associated with the relevant burst. By considering the temporal variability of packet arrivals, the algorithm aims to improve the accuracy of burst time estimation, thereby enhancing the precision of flow control decisions.

In conclusion, the development of the novel flow control algorithm, accompanied by the novel method for throughput assessment, was motivated by the need to address a few key limitations in existing flow control mechanisms. Both the novel flow control and measurement algorithms aimed to address these limitations by:

- Improving burst time accuracy: The novel measurement method incorporated a more sophisticated calculation method that accounted for the dynamic nature of packet arrivals, leading to more accurate burst time estimation.
- Unifying the flow control mechanism: The novel flow control algorithm established a standardized solution capable of operating seamlessly across both intra-site and inter-site environments, ensuring consistent performance across different network domains.
- Ensuring consistent logic and parameterization: The novel flow control algorithm implemented a consistent logical framework, utilizing identical parameters and message exchanges across all scenarios, regardless of network configuration.

These enhancements resulted in a more efficient, reliable, and standardized flow control system, ultimately leading to a more robust and predictable network performance. The unification of the flow control mechanism across different network configurations improved network scalability and facilitated the deployment of advanced features such as inter-site CA.

This chapter has discussed the rationale behind the necessity for modifications to the flow control algorithm and underscored the critical importance of unifying these changes. As outlined, the novel approximation concept is intrinsically linked to the flow control process, which governs the entire CA transmission. Moreover, the chapter highlighted the inevitability of modifications in the time component calculation, coordinated concurrently with the flow control enhancements, and provided the underlying motivations for these changes. In the subsequent Chapter 4.3, a high-level conceptualization of the CA transmission process incorporating the novel method approximation concept will be presented.

4.3. Formal introduction to approximation concept based on flow control changes

As established in Chapter 4.2, the novel measurement method employing an approximation concept for throughput measurement is inseparable with the novel flow control algorithm. The primary rationale for this interdependence lies in the shared reliance on functional components and their parameters. This inherent connection provides a foundation for a more in-depth analysis of the novel measurement method, specifically in the context of CA transmission process and its key parameters, which shall be discussed in this chapter.

As outlined in Chapter 3.5, the SeNB calculates its buffer occupancy time for each received $RLC\ PDU_{\mathrm{i}}$. This calculation incorporates the transmission time of the $RLC\ PDU_{\mathrm{i}}$ through the X2 interface and the time the $RLC\ PDU_{\mathrm{i}}$ resides in the SeNB buffer. The SeNB IP throughput

is then determined as the ratio of the data volume of the $RLC\ PDU_{\mathrm{i}}$ to the time spent in the SeNB buffer, according to the logic from Eq. 3.2.

The SeNB IP throughput is further defined, in system's implementation, as the expected throughput (*eTh*) parameter. This parameter is periodically transmitted from the SeNB to the MeNB at a frequency controlled by the transferDelayMax parameter. The *eTh* parameter represents the desired data volume to be transmitted from the master node to the secondary node per time interval between two consecutive DDDSs or per TTI, depending on the traffic load.

The *eTh* parameter serves as a starting point for the PCell scheduler to determine the amount of data volume to offload to a specific SCell in the SeNB. This offloading decision is based on the previously reported *eTh* value, which reflects the user's throughput capability.

However, during the initial phase of CA, the *eTh* value is unknown. To address this, the *eTputInitMcs* parameter is introduced. This parameter assumes the maximum achievable MCS value from the user's perspective, as if it were reporting its Channel Quality Indicator (CQI) value. The *eTputInitMcs* parameter effectively simulates the user's CQI-based MCS calculation. The *eTputInitMcs* parameter value is proportional to the radio channel quality. In challenging radio channel conditions, a lower *eTputInitMcs* value is chosen, leading to higher performance. Conversely, in excellent radio channel conditions, a higher *eTputInitMcs* value is preferred. More details about initial MCS parameter calculation are present in Chapter 4.4.

The concept of approximating user throughput using the *eTh* parameter involves a two-step process.

Firstly, the SeNB calculates the *eTh* value based on its local measurements and transmits it to the MeNB. The *eTh* function must be robust against rapid changes in radio channel quality caused by factors such as fading. To mitigate the impact of temporary extreme values and prevent overestimation or underestimation of user throughput, an Infinite Impulse Response (IIR) filter and a forgetfulness factor is proposed. These mechanisms effectively smooth out the *eTh* curve over time by minimizing the influence of transient channel fluctuations, which are widespread in real-world network environments, particularly in densely populated uban areas.

Secondly, the MeNB utilizes this *eTh* value to make informed decisions regarding data scheduling and offloading. A crucial aspect of this process is the implementation of a mechanism that prevents the division of CA data volume between the PCell and SCell. Instead, the data should be scheduled exclusively on the PCell. The *eTh* function provides an initial estimate of user throughput, serving as a starting point for data offloading decisions. However, the DDDS mechanism plays a crucial role in dynamically controlling the amount of data offloaded from the PCell to the SCells. This is because it conveys to the MeNB the specific transmission resolution, based on HARQ ACK mechanism on SeNB side, required for each individual $RLC\ PDU_{\mathrm{i}}$ packet that was sent from MeNB to SeNB.

To prevent data accumulation and ensure timely transmission, the *tRlcPduDiscard* parameter is introduced on MeNB. This parameter acts as a timer, discarding any $RLC\ PDU_{\mathrm{i}}$ sent to SeNB that remains in the RLC' buffer for longer than a predefined threshold. This watchdog mechanism effectively prevents further data transmission from the MeNB to the SeNB if the

previous PDU has not been successfully transmitted and acknowledged within DDDS. This ensures that the network resources are not wasted on data that is unlikely to be delivered successfully. However, such occurrences prolong the transmission duration, consequently diminishing the achieved throughput from both a flow control perspective and the perspective of the novel method's throughput measurement. Nevertheless, performance degradation is unavoidable when a user encounters adverse conditions that hinder cellular network connectivity.

This phenomenon arises due to the interruption of data transmission, leading to a probable retransmission process via the PCell in the MeNB. This retransmission is related to data previously split and routed to the SeNB, consequently extending the overall transmission duration. However, the data volume is accounted for only once, as the PDCP layer and its associated PDCP SDUs are not subject to retransmission processes, which are managed by lower layers. Furthermore, this mechanism does not compromise the accuracy of the novel method. Instead, it maintains the method's performance at a satisfactory level by preventing the further data split by MeNB to SeNB (the underlying assumption in this example is that the SeNB is incapable of providing service to the designated user due to severe radio channel conditions), which could negatively impact the overall throughput and efficiency of the system. In essence, it is unproductive to transmit additional data volume from the MeNB to the SeNB if the secondary cell lacks the capacity to handle the traffic load.

Figure 4.2 illustrates the CA transmission process with usage of the novel method's approximation concept, where the *eTh* value is sent from SeNB to MeNB.

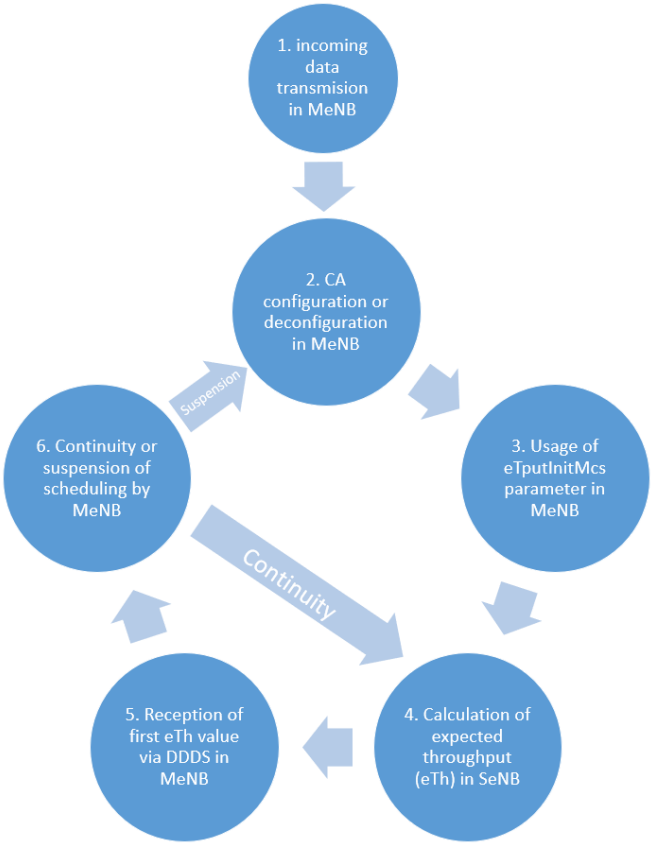

Figure 4.2: High-level concept of the CA transmission process with usage of the novel method approximation concept.

The following points summarize CA transmission process for a new user, which is CA capable, with usage of the novel method algorithm principles with commented details:

1. Incoming data transmission in MeNB
    - An RRC-connected user or a user transitioning from RRC Idle state initiates an uplink (UL) transmission or
    - A downlink (DL) transmission is initiated, either by waking up an RRC Idle user via a paging message or by an RRC-connected user requesting data download from a server.
2. CA configuration or deconfiguration performed for a particular user.
    - The CA initialization commences, involving verification of permissible band combinations. Subsequently, the user is configured with selected SCells, culminating in their activation by the MAC layer of the radio protocol stack.
3. Addressing unknown *eTh* values during initial configuration of CA with eTputInitMcs parameter in MeNB.
    - It simulates the user's CQI-based MCS calculation by assuming the maximum achievable MCS for the SCell on SeNB.
4. Buffer occupancy time and expected throughput (*eTh*) parameters calculation in SeNB.
    - The robustness of the *eTh* function against radio channel quality fluctuations is crucial for maintaining accurate data scheduling and in consequence precise measurement of throughput metric. As the *eTh* value is periodically transmitted from the SeNB to the MeNB, rapid changes in channel quality can lead to extreme *eTh* values between consecutive DDDS messages. This can result in either excessive or insufficient data being sent to the SeNB by the MeNB, potentially disrupting the overall data flow and performance, given by a maximum possible throughput that can be achieved by the user.
    - To mitigate the impact of transient extreme radio channel quality conditions, the *eTh* calculation principles require an averaging and convergence process. This process effectively filters out short-lived extreme values, which have minimal impact on overall performance and can lead to inaccurate data scheduling decisions.
5. The first *eTh* value, received by the MeNB via a DDDS message, serves as an initial estimate for precise CA transmission offloading.
    - The DDDS message also conveys information regarding the successful transmission of previously sent offloading data, based on the value of the eTputInitMcs parameter.
    - Subsequently, the scheduling of the offloading data volume to the SeNB is continued based on *eTh* value received.
6. Reception of DDDS messages containing information about the previously successfully transmitted data volume, determined by RLC ACK, and a new *eTh* value.

- In the event of unsuccessful transmission of the previously sent data volume, the MeNB will cease further CA data splitting between the PCell and SCell.
- Furthermore, if consecutive DDDS messages fail to acknowledge the successful transmission of the preceding data volume, the absence of confirmation will activate the tRlcPduDiscard parameter. This parameter serves as a watchdog mechanism, indicating a potential disruption in data transmission on SeNB and prompting necessary corrective actions. Consequently, the MeNB will retransmit the previously sent data volume to the SeNB, potentially impacting overall transmission performance by extending the burst length. However, this retransmission does not compromise the method's precision, as the data integrity remains unaffected.

Figure 4.3 illustrates a simulated scenario, referred to as the "rainy day" scenario, where data transmission via the SCell is intentionally disrupted. This disruption leads to the failure of previously transmitted RLC PDUs, denoted as $RLC\ PDU_{\mathrm{i}}$, during their transfer from the MeNB to the SeNB. Despite this interruption, the overall throughput metric remains minimally affected, preserving the validity of the proposed method's results. This is attributed to the negligible number of $RLC\ PDU_{\mathrm{i}}$ that fail to reach the user destination. Furthermore, any lost data is subsequently retransmitted via the PCell, which extends the duration of the current transmission burst by an additional TB in subsequent TTIs.

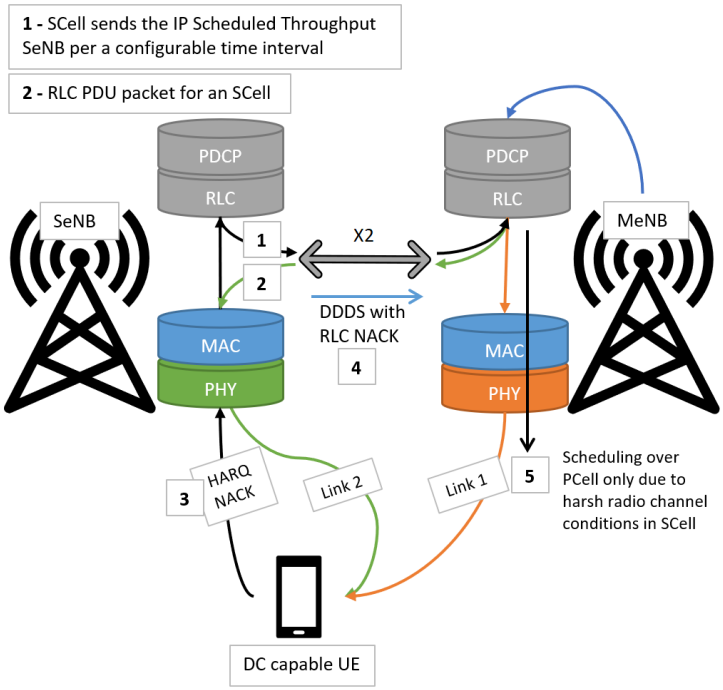

Figure 4.3: Rainy day scenario example of the transmission cycle for the novel method utilizing its watchdog mechanisms.

This formal introduction to the approximation concept serves as a foundational step in comprehending the holistic operation of the flow control and its associated novel measurement method. Subsequent chapters will delve into further details, encompassing the *eTh* calculation

method, as well as the final outputs of the novel approach, namely *ThpVolDl* and *ThpTimeDl* which are used to derive IP scheduled throughput value. Subsequent discussions will provide a comprehensive understanding of the intricate relationship between the *eTh* function parameters and their impact on both throughput measurement precision and flow control performance. The novel method is intrinsically linked to the newly developed flow control algorithm, underscoring the crucial role of these parameters in optimizing the overall system efficiency.

4.4. Novel Measurement Method, its Products and Internal Parameters

Building upon the foundation established in Chapter 4.3, the novel approximation concept yields new PM counters, adhering to the PM framework and adhering to 3GPP principles as promptly outlined in Chapter 1.1.

This chapter presents a comprehensive analysis of the novel method's products, focusing on two key aspects:

1. $\overline{eTh}(t)$ *Function* in SeNB: This function facilitates the estimation of expected throughput in the SeNB. The chapter will delve into its operational principles and how it contributes to the overall throughput estimation process.
2. PM Counter Calculation Principles in the MeNB: The chapter will explore the principles behind PM counter calculations in the MeNB, particularly focusing on how the boundaries for burst calculations are performed in the MeNB. The resulting burst calculations yield new PM counters within the PM framework, representing the sum of the downlink IP scheduled throughput data volume (*ThpVolDl*) and downlink IP scheduled throughput time (*ThpTimeDl*).

Furthermore, the chapter will examine the parameters of the $\overline{eTh}(t)$ function, highlighting their influence on the output value transmitted from the SeNB to the MeNB. Additionally, it will analyze the key parameters involved in the novel flow control algorithm within the MeNB, emphasizing their direct impact on the RLC PDU split between the MeNB and SeNB.

Finally, the chapter will delve into the concept of PM counter calculations, providing detailed scenario explanations and calculation logic. This analysis will focus on identifying the burst start and stop times, providing a comprehensive understanding of the PM counter calculation process.

4.4.1. $\overline{eTh}(t)$ Function and its Parameters

The accuracy of the IP scheduled throughput measurement is intrinsically linked to various network parameters. These parameters can significantly influence the precision of the measurement and may have impact on useability of the measurement for network planning. This analysis will first delve into the core functionality of the $\overline{eTh}(t)$ function, logically linked to Equation 3.2, followed by an examination of its associated parameters. Finally, the parameters involved in the novel flow control mechanism will be discussed and an example of $\overline{eTh}(t)$ shall be presented based on a simulated value.

1. $\overline{eTh}(t)$ function to calculate the SCell throughput capability for a particular user.

The SeNB downlink scheduler employs an Infinite Impulse Response (IIR) filter with a time-varying time constant to estimate the $\overline{eTh}(t)$ value, given by Equation 4.1. This value is then transmitted to the MeNB via the DDDS mechanism. The IIR filter performs time averaging of the expected throughput, effectively attenuating the effects of extreme temporal fluctuations induced by high-intensity, short-duration interference or fading. This averaging process utilizes a function that considers the current $eTh(t)$ value, the previously averaged $\overline{eTh}\,(t_{previous})$, and a forgetfulness factor $T_{eTh}(t)$.

$$\overline{eTh}(t) = \frac{1}{T_{eTh}(t)}\, eTh(t) + \left(1 - \frac{1}{T_{eTh}(t)}\right) \times \overline{eTh}\,(t_{previous}) \tag{4.1}$$

The $\overline{eTh}(t)$ is calculated as a historical throughput value based on the number of bytes transmitted for non-GBR data during TTIs where the SeNB buffer cannot be fully emptied. In TTIs where the user is not allocated downlink resources, the computation of the $\overline{eTh}(t)$ is suspended.

However, a potential for underestimation of the actual throughput $eTh(t)$ exists when traffic is sufficiently low and the buffer is drained in every TTI. In such scenarios, the historical throughput $\overline{eTh}(t)$ calculation fails to capture the full potential throughput. To address this underestimation, a solution is proposed to derive an estimated Transport Block Size (TBS) based on the assumption of unlimited data availability. This approach allows for a more accurate estimation of the potential throughput, even in low-traffic scenarios where the buffer is consistently emptied.

The function can be configured with two extreme scenarios. In the first scenario, the temporal $eTh(t)$ value holds the highest significance. In the second scenario, the significance of the previous averaged $\overline{eTh}\,(t_{previous})$ is maximized. The forgetfulness factor $T_{eTh}(t)$ facilitates a smoother curve as its value increases. The parameter *eTputFilterConfig* determines the rate at which the value is forgotten, exhibiting an initial rapid decay followed by a slower, logarithmic decline over time.

2. eTputFilterConfig – parameter configures two values *V* and *F* of an exponential moving average filter for expected throughput calculation.

The time constant, denoted as $T_{eTh}(t)$ in Equation 4.2, is a time-dependent function characterized by a linear increase at varying rates. This function is parameterized by *eTputFilterConfig*, which utilizes a two-variable configuration, *V* and *F*, to enable dynamic filtering behavior. The co-component variables *V* and *F* serve to optimize the representation of the input function by minimizing the impact of the forgetfulness function. This dynamic filtering approach aims to enhance the accuracy and responsiveness of the system by adaptively adjusting the time constant based on the specific characteristics of the input signal. The variable *t* in Equation 4.2 represents the scheduling time, which is equivalent to one TTI duration, namely 1 millisecond.

$$T_{eTh}(t) = \begin{cases} \left|\frac{t}{F}\right| + 1, \ if \ \left|\frac{t}{F}\right| < V \\ V, \ if \ \left|\frac{t}{F}\right| \geq V \end{cases} \tag{4.2}$$

Variable *V* represents the final $T_{eTh}(t)$ value, rounded down to the nearest multiple of 10. It is calculated as *V* = *eTputFilterConfig* - *F*. Variable *F* represents the least significant digit of

eTputFilterConfig, acting as a reduction factor that determines the rate of increase in $T_{eTh}(t)$. The parameter *F* represents a rate of change for the variable $T_{eTh}(t)$. When *F* = 0, T_{eTh} remains constant over time. As *F* increases, $T_{eTh}(t)$ experiences a gradual growth until it reaches a maximum value defined by the variable *V.* This maximum value is determined by the configuration parameter *eTputFilterConfig*. For instance, when *eTputFilterConfig* = 51, *V* is set to 50 and *F* to 1. Consequently, $T_{eTh}(t)$ will linearly increase from an initial value of 1 to a final value of 50, with the rate of increase determined by *F*. Upon reaching its predefined saturation point, variable *V* remains constant throughout the duration of the transmission process. Subsequent new transmissions will trigger a repetition of this saturation cycle. However, once saturated, *V* cannot return to its initial zero state until the transmission process is completed.

The configuration parameter *eTputFilterConfig* governs the behavior of the $T_{eTh}(t)$. The minimum value of *eTputFilterConfig*, 10, corresponds to a scenario where *V* = 10 and *F* = 0. Conversely, the maximum value of *eTputFilterConfig*, 999, results in *V* = 990 and *F* = 9.

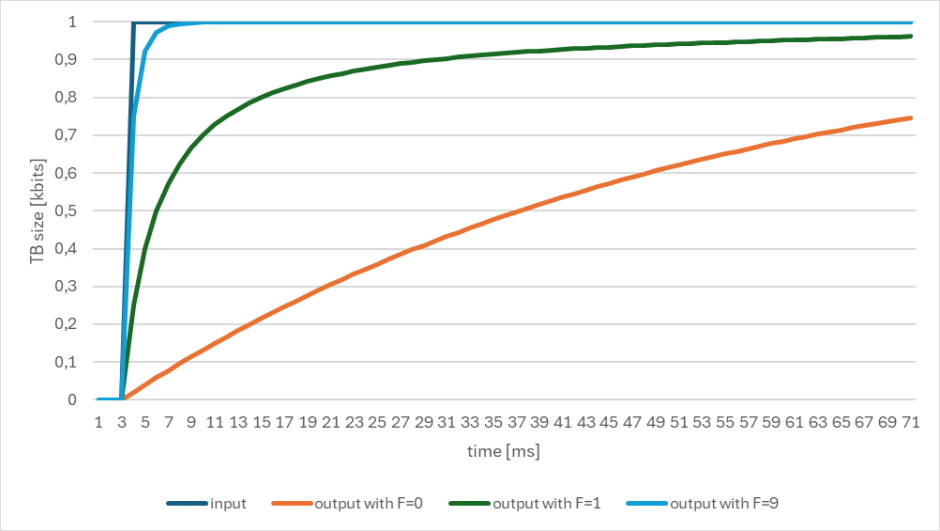

Figure 4.4: Impact on $\overline{eTh}(t)$ output function value with a change in variable *F* value of $T_{eTh}(t)$ function in comparison to $eTh(t)$ input function.

Figure 4.4 provides a visual representation of how $T_{eTh}(t)$ function evolves over time in $\overline{eTh}(t)$ function to help reach a target input value, given by current $eTh(t)$ calculated by SCell scheduler. This input value is determined by the SeNB SCell scheduler's allocation of resources to the user. The Figure 4.4 showcases different scenarios with varying values of *F*, while maintaining *V* at a constant value of 50. The parameter *F* directly influences the rate of change of $T_{eTh}(t)$, thereby affecting the time required for $T_{eTh}(t)$ to attain the target value of *V*. Higher values of *F* result in a faster rate of change for $T_{eTh}(t)$, leading to a shorter time for $\overline{eTh}(t)$ to reach the input value of $eTh(t)$. Conversely, lower values of *F* result in a slower rate of change, extending the time required to reach the input value.

3. eTputInitMcs – initial MCS value before reporting first $\overline{eTh}(t)$

The RLC entity dynamically manages its queue length, aiming to maintain it at the *transferDelayMax* threshold. This queue length is determined based on the volume of data in

transit and the $\overline{eTh}(t)$ provided by the RLC to the higher layer. At the initiation of a bearer, the radio channel quality is uncertain. When a user is selected for a CA connection, the throughput capacity of the SeNB remains unknown until the first $\overline{eTh}(t)$ value is received, which occurs only after successful configuration and activation of the SCell.

To address this issue, an additional parameter has been introduced to assume in advance the radio channel quality and throughput capabilities of the SeNB during the CA configuration initialization phase. Upon activation of the SCell, the $\overline{eTh}(t)$ is initialized to its default value, $eTh_{default}$. Subsequent updates to $\overline{eTh}(t)$ occur upon transmission of the DDDS message. In the absence of data transmission between DDDS messages, $\overline{eTh}(t)$ remains constant. The initial MCS value, *eTputInitMcs*, within the range of 0 to 28, is employed to calculate $eTh_{default}$ at the commencement of transmission, given by Equation 4.3.

$$\overline{eTh}(0) = eTh_{default} \tag{4.3}$$

The $eTh_{default}$ parameter is calculated based on the Transport Block Size (TBS) values specified in 3GPP 36.213 [46] Tables 7.1.7.2.1-1 and 7.1.7.2.2-1, subject to the following assumptions:

- The MCS Index is set to the value of eTputInitMcs.
- 256 Quadrature Amplitude Modulation (QAM) is not configured.
- The number of Physical Resource Blocks (PRBs) is known and determined by the channel bandwidth parameter.
- The TB is mapped to two spatial layers according to the specifications outlined in 3GPP 36.213 [46] Table 7.1.7.2.2-1.

For instance, in a 20 MHz cell with *eTputInitMcs* = 28, the resulting $eTh_{default}$ value is 149776 kbps and when *eTputInitMcs* = 10 the resulting $eTh_{default}$ value is 78704 kbps.

Favorable radio conditions, characterized by a high *eTputInitMcs* value, facilitate a rapid initiation of data flow. Conversely, in scenarios with suboptimal radio conditions, the RLC queue may not be fully drained within the reordering window (t-Reordering). This results in the retransmission of excess RLC PDUs. In essence, the RLC dynamically adjusts its queue length to optimize data flow based on the estimated throughput and radio channel quality. This mechanism ensures efficient data transmission even in the presence of varying radio conditions.

A comparative analysis of the *eTputInitMcs* parameter was conducted within a specific cluster of eNBs. The impact of different *eTputInitMcs* values on data flow and network performance was investigated. For *eTputInitMcs* = 20 the high value resulted in an excessive data load for the MAC scheduler, exceeding its capacity. Consequently, the RLC buffer was not drained at a sufficient rate, leading to packet discarding and retransmission. For *eTputInitMcs* = 2 the low value resulted in a buffer underrun scenario, where the RLC buffer became depleted due to insufficient data transmission. This led to a slow transmission rate, as the buffer's full potential was not utilized to match the actual radio conditions. For *eTputInitMcs* = 10 the value represented a balanced approach, effectively aligning the MAC scheduler's capacity with the

user's data requests. It achieved a compromise between efficient data flow and preventing buffer underrun or overload. The balanced approach demonstrates enhanced efficacy when utilizing an initial MCS value of 10 in urban environments situated within city suburbs. These environments characteristically exhibit a heterogeneous distribution of open and obstructed areas, leading to a diverse spectrum of signal propagation characteristics. The presence of buildings, trees, and other obstacles can induce signal attenuation, fading, and multipath propagation, consequently resulting in variable levels of channel quality.

An inappropriate initial MCS selection, based on the environment type of the SeNB, can lead to suboptimal flow control performance. If the initial MCS value is set too low (e.g., 5) and the radio channel quality of the SCell is perceived with a high SINR ratio (e.g., 25 dB), the throughput capabilities are not fully utilized, resulting in reduced user throughput for the time being the throughput is normalized over lapsed time, as shown in example in Figure 4.5 with *eTputFilterConfig* parameter configured to 51. Figure 4.5 illustrates the input value $eTh(t)$ and the corresponding output value, denoted as $\overline{eTh}(t)$. The output value, expressed as a volume, represents throughput, specifically the volume per TTI. For instance, a value of 100 kbits on the y-axis corresponds to an $\overline{eTh}(t)$ of 100kbps.

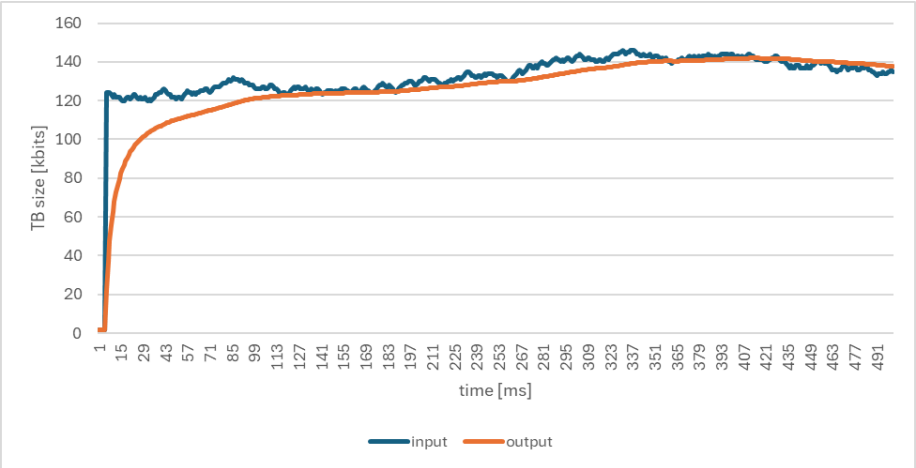

Figure 4.5: $\overline{eTh}(t)$ output function example with low initial MCS but high SINR conditions for $eTh(t)$ input function.

Conversely, if the initial MCS value is set too high (e.g., 25) but the radio channel quality of the SCell is perceived with a low SINR (e.g., 5 dB), transmission failure may occur due to improper signal decoding by the user, necessitating retransmission and consequently increasing the burst length. In Figure 4.6 it is illustrated how $\overline{eTh}(t)$ function value depicted as output reacts to the input value given by $eTh(t)$. Initial MCS value influences not only the first TTI, but also subsequent TTIs, until the $\overline{eTh}(t)$ function converges its throughput value to the current throughput capabilities represented by $eTh(t)$.

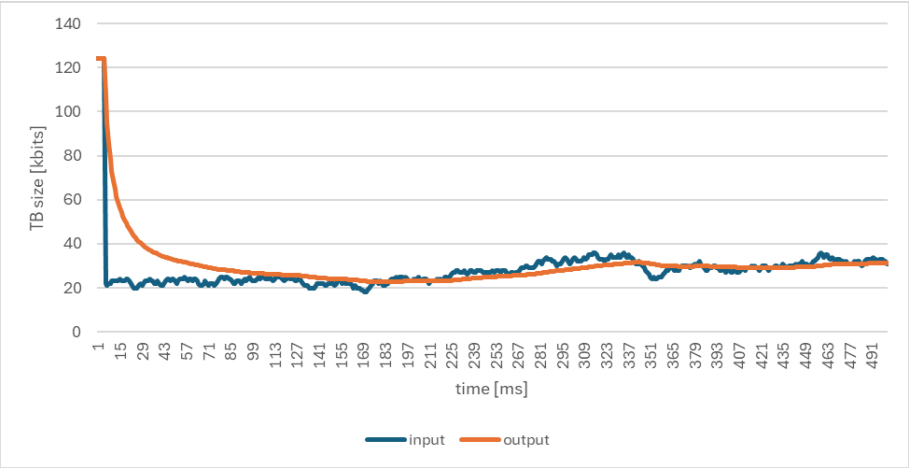

Figure 4.6: $\overline{eTh}(t)$ output function example with high initial MCS but low SINR conditions for $eTh(t)$ input function.

These findings highlight the importance of selecting an appropriate *eTputInitMcs* value to optimize data transmission and network performance. The optimal value depends on the specific radio conditions and the data load experienced by the network.

4. transferDelayMax – $\overline{eTh}(t)$ exchange rate

The *transferDelayMax* parameter specifies the maximum permissible delay for RLC PDUs after the splitting process. Consequently, the applied splitting algorithm also determines the buffer depths required for the RLC layer. This parameter is configurable with specific values ranging from 10 milliseconds to 200 milliseconds. It defines how often the $\overline{eTh}(t)$ function value is passed from SeNB over X2 to MeNB.

Traffic splitting algorithm prioritizes packet transmission on the path exhibiting the shortest delay. However, if the calculated delay exceeds the predefined threshold, transferDelayMax, the algorithm suspends transmission and awaits the depletion of the RLC buffers. This delay-based decision mechanism aims to minimize packet arrival time discrepancies at the UE. The total buffer capacity shown on Figure 4.7 is defined by Equation 3.1 in Chapter 3.5.

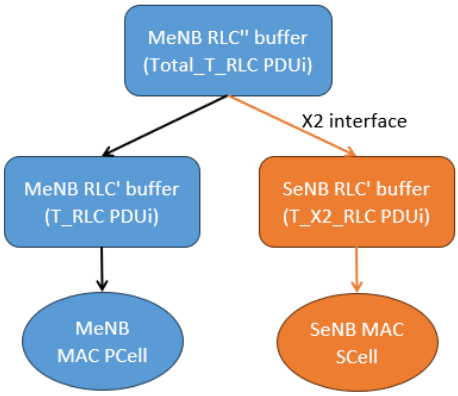

Figure 4.7: Splitting of RLC PDUs from main buffer to MeNB and SeNB buffers.

A smaller *transferDelayMax* value increases the likelihood of simultaneous packet arrival from both paths at the UE. However, excessively small values can lead to RLC buffer underrun or emptiness, potentially disrupting data flow.

In scenarios with large RLC buffers and unfavorable radio conditions, the buffer drain rate may be significantly reduced. This can result in the UE failing to receive the buffer tail within the reordering window (t-Reordering), leading to its discard by the RLC. Consequently, the overall efficiency of CA is compromised.

A comparative analysis of the *transferDelayMax* parameter was conducted based on specific cluster of eNBs, exploring its impact on RLC PDU packet discard rates and subsequent network performance. For *transferDelayMax* = 50ms the configuration, with a *tRlcPduDiscard* threshold of 100ms, exhibited a high discard ratio of RLC PDU packets. This resulted in a significant increase in retransmission attempts and a corresponding decrease in throughput. For *transferDelayMax* = 20ms setting led to a buffer underrun scenario, where the RLC buffers became depleted, resulting in a reduction in throughput. For *transferDelayMax* = 40ms a notable reduction in RLC PDU discard rate was observed with this intermediate value. The number of discarded packets decreased by order of magnitude, from approximately 1000 to 100, during experiments of the same duration time.

These findings highlight the importance of selecting an appropriate *transferDelayMax* value to optimize data transmission and network performance. The optimal value helps in minimizing packet discard rates while mitigating the risk of buffer underrun scenarios.

5. tRlcPduDiscard – a watchdog mechanism for RLC PDU discarding

The *tRlcPduDiscard* parameter is implemented on the MeNB to prevent data accumulation and ensure timely transmission. The parameter *tRlcPduDiscard* functions as a watchdog timer within the RLC layer, designed to discard $RLC\ PDU_{\mathrm{i}}$ that remain in the RLC' buffer beyond a predetermined threshold. This threshold can be configured to one of the following values: 20ms, 50ms, 100ms, 200ms, or 500ms. Increasing the value of *tRlcPduDiscard* enhances the likelihood of successful retransmission at the SeNB if the radio channel quality for a given user improves. However, it also increases the risk of transmission failure if the radio channel quality remains unsatisfactory.

This mechanism effectively prevents further data transmission from the MeNB to the SeNB if the previous PDU has not been successfully transmitted and acknowledged within the DDDS. This ensures that network resources are not wasted on data that is unlikely to be delivered successfully in SeNB. Moreover, this mechanism operates independently of the $\overline{eTh}(t)$ function calculation performed on the SeNB. It serves as a secondary layer of protection, primarily overseen by the MeNB, to ensure data transmission integrity in the event of SeNB failure to handle data transmission, irrespective of the underlying cause.

6. $\overline{eTh}(t)$ example comparison based on rapid changes in radio channel

Figure 4.8 illustrates the result of the calculation of the $\overline{eTh}(t)$ output function in scenarios characterized by rapid fluctuations in radio channel quality, such as those induced by fading

phenomena. The input function is the $eTh(t)$. This algorithm, employing an $\overline{eTh}(t)$ output function (with a low initial MCS in this example), mitigates the influence of transient extreme values of radio channel quality. The truncation process, managed by the forgetfulness factor of the IIR filter, effectively attenuates the impact of short-lived channel quality variations, promoting a more stable and representative estimation of $\overline{eTh}(t)$.

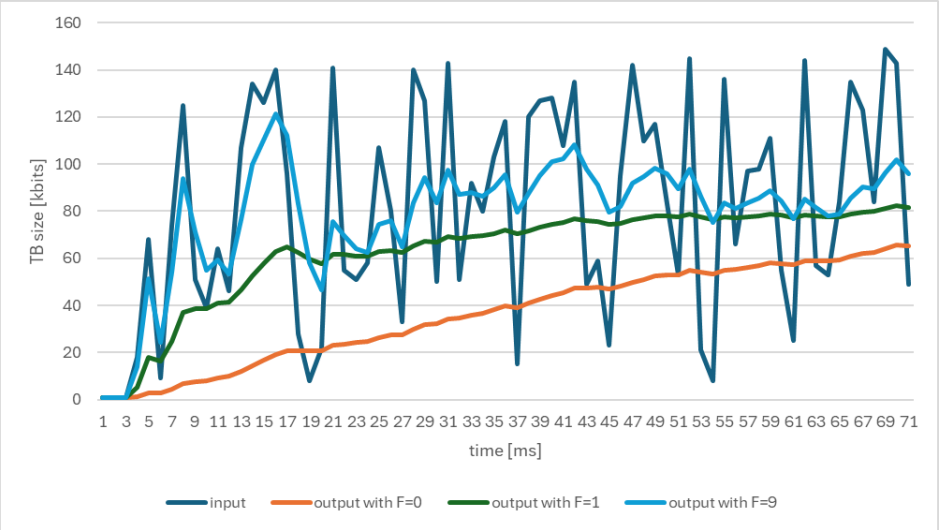

Figure 4.8: $\overline{eTh}(t)$ output function example with low initial MCS but with fading conditions for $eTh(t)$ input function.

Moreover, Figure 4.8 illustrates the behavior of the $\overline{eTh}(t)$ function as a function of the configurable IIR filter component, represented by the change in variable *F* of the time constant $T_{eTh}(t)$. Increasing the value of *F* reduces the impact of the forgetfulness factor, leading to a faster adaptation of the output value to the input value. However, this increase in *F* also elevates the likelihood of sudden fading events, which may disappear momentarily, subsequently increasing the throughput capacity of the SCell. This phenomenon can impact the accuracy of the $\overline{eTh}(t)$ value.

To mitigate this potential negative impact, a dual-layer protection mechanism is implemented. In the event of fading, the RLC PDU discard timer is activated within the MeNB for data that could not be successfully transmitted over the SeNB. This mechanism effectively reduces the negative impact of fading on the radio channel by preventing the accumulation of data that is unlikely to be successfully delivered. The unsuccessful data is then retransmitted over the PCell or another SCell from a different SeNB, leading to a throughput performance degradation.

4.4.2. PM counters for throughput measurement

As per Equation 3.3 and Figure 3.2, *ThpVolDl* represents the IP layer data volume, encompassing PDCP SDUs, while *ThpTimeDl* denotes the elapsed time on the Uu interface between the radio unit and the end-user during the transmission of the data volume encompassed by *ThpVolDl* [12, 20]. This measurement aims to quantify the IP throughput over the Uu interface, independent of traffic patterns and packet sizes. It is primarily intended for data bursts exceeding

a threshold that requires transmission across multiple TTIs. The measurement is conducted per Quality of Service Class Identifier (QCI) per UE, excluding initial buffering time at the eNB.

The measurement captures the throughput of PDCP SDU bits in the downlink for packet sizes or data bursts requiring transmission across multiple TTIs, excluding the transmission of the single TTI data and the last TTI within a burst. Only the data transmission time is considered, encompassing the period from the initiation of data transmission over Uu until its completion.

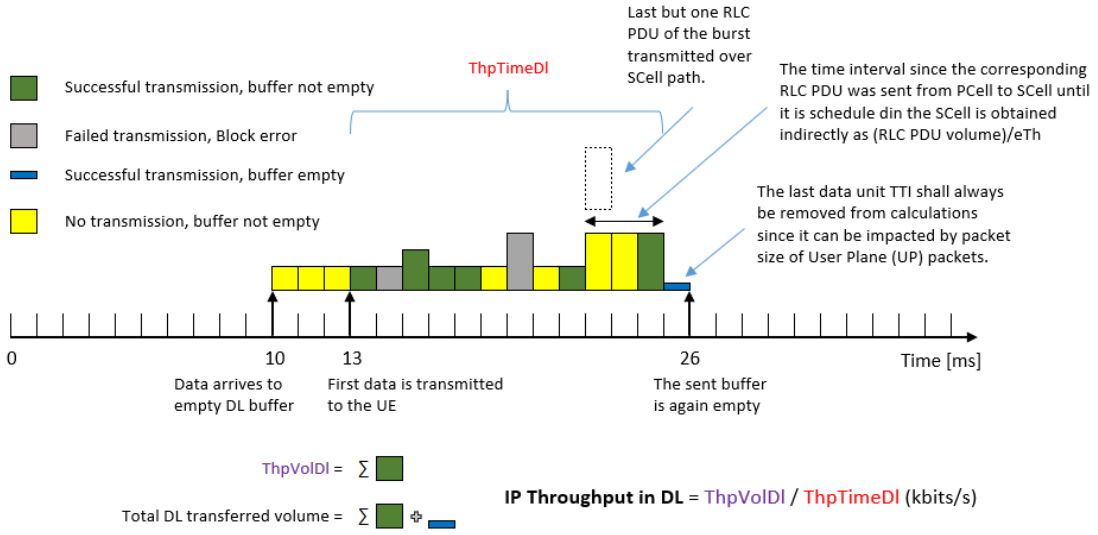

Figure 4.9: Example of the novel method for IP scheduled throughput measurement in DL for inter-site CA scenario.

Figure 4.9 illustrates an example of the novel method for the burst accounting where the penultimate RLC PDU of a specific PDCP SDU belonging to a particular burst is transmitted over the SCell path. The time required for the SCell to schedule the received $RLC\ PDU_i$ data volume is estimated using Equation 4.4. This represents a significant departure from the standard method, which lacked information from the SCell regarding its throughput capabilities or acknowledgment of the transmission status for the respective $RLC\ PDU_i$.

$$T_{RLC\ PDU_i} = \frac{Data\ volume\ for\ RLC\ PDU_i}{SeNB\ IP\ Throughput} = \frac{RLC\ PDU\ Volume_i}{\overline{eTh}(t)} \tag{4.4}$$

4.4.2.1. Data volume component ThpVolDl

The first group of PM counters calculate *ThpVolDl* [4, 20] based on the E-RAB type associated with a specific QCI value. This calculation involves summing the PDCP SDUs for each non-GBR QCI (6 to 9) within a burst meeting 3GPP criteria across all users engaged in downlink data traffic. PDCP SDUs transmitted within a single TTI or those comprising the last TTI segment of a burst spanning two or more consecutive TTIs are excluded from the measurement. Consequently, the total PDCP SDU volume received at the eNB for the respective QCI exceeds the sum of PDCP SDU volumes per burst logic. Summarizing, *ThpVolDl* represents the data volume of a burst during IP throughput measurement, excluding the data transmitted in the single TTI or those comprising the last TTI segment of a burst when the downlink buffer is emptied. Equation 4.5 presents a simplified formula for the data volume accounting of *ThpVolDl*. The formula quantifies the cumulative accounting mechanism embedded within the PM framework. It aggregates the burst data volume from all users for a specific QCI over a predefined time interval,

typically 15 minutes. The aggregated *ThpVolDl* and *ThpTimeDl* values collected at the MeNB are subsequently transmitted to the NMS from each eNB within the network. These values can be further aggregated within the NMS over extended time periods and across all eNBs and their respective PCells to derive an averaged IP scheduled throughput value. However, for optimal analysis of QoS metrics, it is generally more effective to focus on specific geographical areas, clusters of cells, or even individual cells.

$$ThpVolDl_{QCI_x} = \sum_{n=1}^{N} \sum_{i=1}^{I} \sum_{b=1}^{B} \left((V_{QCI_x})_{n,i,b} - (L_{QCI_x})_{n,b} \right) \quad (4.5)$$

The variables within the equation define its boundaries and are as follows:

- *N* – number of users, n=1 represents specific UE-id.
- B – number of bursts, b=1 represents specific burst-id of a specific UE-id.
- I – number of PDCP SDU packets received for a specific UE-id within a specific burst-id.
- QCIx – the PDCP SDU data volume is filtered per specific non-GBR E-RAB QCI value, x is ranging from 6 to 9.
- $(L_{QCI_x})_{n,b}$ – is the amount of PDCP SDU data in the last TTI of a certain burst emptying the buffer, which also includes the single TTI transmissions.
- $(V_{QCI_x})_{n,i,b}$ – is the amount of PDCP SDU data for a specific user and burst.

The interworking mechanism of inter-site CA, in relation to data volume component, is described as follows. The data volume of PDCP SDUs, excluding those transmitted in the single TTI and the last TTI within a burst when the buffer is emptied, is counted upon sending the corresponding RLC PDU to the SCell. The RLC PDU is considered successfully transmitted to the UE without HARQ consideration, unlike in PCell or SCell for intra-site CA scenarios. This is due to the potential delay in delivering HARQ ACKs from PCell to SCell via the X2 interface in inter-site CA. Consequently, instead of HARQ retransmissions, new RLC PDUs are sent, acting as ARQ from the user perspective and as new transmissions from the network perspective. This inclusion of new transmissions may artificially inflate the counter values, leading to potential inaccuracies in throughput measurement. To mitigate these inaccuracies, the *tRlcPduDiscard* parameter has been introduced in the MeNB. This parameter prevents data from being scheduled via the SCell in the SeNB in the event of continuous transmission failures. Subsequently, the MeNB scheduler allocates new resources for the data that failed to be transmitted in the PCell or other SCells. While this process can negatively impact throughput performance by extending the time to transmit unsuccessfully sent data, it maintains the integrity of the procedure within acceptable limits.

The following describes the standard method's mechanism within a non-DC system scenario, focusing on the data component to facilitate a direct comparison of implementation details. For each data burst, LTE Layer 2 maintains and updates the complete RLC SDU data volume per QCI per UE within the MAC PDU for each HARQ. A HARQ ACK for a complete RLC SDU triggers an update to the data volume count per QCI per UE for the corresponding PDCP PDU/SDU, reflecting the RLC SDU data volume in bits. Additionally, HARQ feedback information and the data volume of segmented RLC SDUs is retained until all HARQs containing segments

of the same RLC SDU are successfully completed. Upon successful completion of an RLC SDU (no lost segments), the data volume counter per QCI is updated for the corresponding PDCP PDU/SDU, reflecting the RLC SDU data volume in bits. The data volume of the last RLC SDU transmission that empties the RLC buffer is excluded from the data volume count. Similarly, if an RLC SDU transmission is segmented across multiple TB transmissions, the last TB data volume transmission for the last segment that empties the DL RLC buffer is excluded from the data volume count. LTE Layer 2 counts the PDCP SDU new data volume at the RLC layer, excluding the PDCP PDU header volume from the count. The PDCP SDU data volume is calculated as the RLC SDU data volume minus the PDCP header volume. The PDCP header volume is determined by the Transport Service Network (TSN) field length, which is 1 byte for a value of 5 and 2 bytes for a value of 10.

4.4.2.2. Time component ThpTimeDl

The second group of PM counters determine the time component, *ThpTimeDl*, of a burst based on the specific non-GBR E-RAB type associated with a particular QCI value. This calculation is more intricate, employing a dedicated $\overline{eTh}(t)$, as given in Eq. 4.1, to anticipate the SeNB throughput capability. The time required to transmit a data burst, excluding the last data segment transmitted in the TTI when the buffer is emptied, is measured for each specific non-GBR QCI value ranging from 6 to 9. Upon burst completion, depicted in Figure 4.9, the time spent by the last data burst segment (excluding the last TTI emptying the buffer) within the eNB buffer is measured. This measurement considers the data path (PCell or SCell) for this segment. The measurement commences when the corresponding RLC PDU is transmitted from the PCell to the MeNB/SeNB (in case of PCell as data path it is the same eNB) and concludes when the RLC PDU is scheduled for transmission within the MeNB/SeNB. This duration, as given by Equation 4.6, is calculated as the sum of the X2 delay (applicable for remote X2 SCell), the estimated RLC buffer queue delay for the utilized data path, and the quotient of the RLC PDU volume and the $\overline{eTh}(t)$ reported from MeNB/SeNB of the associated data path to the PCell. The $\overline{eTh}(t)$ is available on a per UE and E-RAB basis.

$$T_{RLC''} = T_{X2} + T_{buffer} + T_{RLC\ PDU_i} \quad (4.6)$$

The interworking mechanism of inter-site CA concerning time component calculation, specifically the quotient derived from Equation 4.6, is described as follows. The delay over X2 interface (T_{X2}) is calculated as half of the Round-Trip Time (RTT), while the estimated RLC buffer queue delay (T_{buffer}) is aligned with *transferDelayMax* parameter value. In case the last segment of the burst (excluding the buffer-emptying segment) is transmitted over the SCell, the end time point of the burst is determined by estimating the time interval between the $RLC\ PDU_i$ being sent from the PCell to the SCell and its scheduling for transmission in the SCell. This estimation is indirectly calculated using Equation 4.4. This calculation utilizes the $RLC\ PDU_i$ volume and the $\overline{eTh}(t)$ reported from the SCell to the PCell on a per UE and E-RAB basis. The corresponding $RLC\ PDU_i$ is considered successfully transmitted to the UE without HARQ considerations, as in the PCell or SCell for intra-site CA scenarios. This is because the HARQ process is not employed

between SCell and PCell for inter-site CA due to potential delays in delivering HARQ ACKs from the SCell to the PCell over the X2 interface. Consequently, a new $RLC\ PDU_i$ is transmitted instead of retransmitting via HARQ, effectively acting as ARQ from the user perspective and a new transmission from the network perspective. This approach, which excludes the time interval between the original and new $RLC\ PDU_i$ transmissions, may slightly decrease the reported counter values and introduce inaccuracies in the throughput measurement.

Measuring the time interval the final burst segment resides within the selected data path buffer enhances burst duration accuracy compared to the standard measurement method. In low throughput scenarios, a single burst can be artificially fragmented into multiple bursts, leading to an artificial reduction in measured throughput time and an overestimation of the IP scheduled throughput value.

Summarizing, *ThpTimeDl* represents the time duration required to transmit a data burst, excluding the single TTI or those comprising the last TTI segment of a burst transmitted when the downlink buffer is emptied. Equation 4.7 presents a simplified formula for the time accounting of *ThpTimeDl*. The formula quantifies the cumulative accounting mechanism embedded within the PM framework. It aggregates the burst data volume from all users for a specific QCI over a predefined time interval, typically 15 minutes.

$$ThpTimeDl_{QCI_x} = \sum_{n=1}^{N} \sum_{i=1}^{I} \sum_{b=1}^{B} ((e_{QCI_x})_{n,i,b} - (s_{QCI_x})_{n,i,b}) \quad (4.7)$$

The variables within the equation define its boundaries and are as follows:

- *N* – number of users, n=1 represents specific UE-id.
- B – number of bursts, b=1 represents specific burst-id of a specific UE-id.
- I – number of PDCP SDU packets received for a specific UE-id within a specific burst-id.
- QCIx – the PDCP SDU data volume is filtered per specific non-GBR E-RAB QCI value, x is ranging from 6 to 9.
- e_{QCI_x} – end of a burst of a certain burst per specific QCI.
- s_{QCI_x} – start of a burst of a certain burst per specific QCI.

The mechanism of the standard method for non-DC system scenario, in relation to time component, is described as follows to have a direct comparison of implementation specifics. LTE Layer 2 maintains and updates information regarding the transmission time used for data burst transmissions. The data burst time is counted when new data arrives in an empty RLC buffer, initiating data transmission for a new data burst spanning multiple TTIs. The transmission time for a data burst encompasses TTIs used for both successful and failed transmissions, including those subjected to retransmission. The last TTI that empties the RLC buffer is excluded, unless the entire transmission is unsuccessful, in which case the entire burst is disregarded from the count.

In contrast to the standard method, the novel approach introduces a novel guard time period mechanism for incoming IP packets, intrinsically linked to the modified time component calculation detailed in Chapter 4.5. This mechanism extends the eNB buffer occupancy at the PDCP layer after a transport block (TB) is scheduled on the physical layer until a Buffer Status Report (BSR) is received from the user. If new IP packets arrive before the guard time period

elapses, they are accounted for as belonging to the same burst ID, effectively extending the burst duration and consequently increasing the *ThpTimeDl* value. This effect is particularly evident in the test cases outlined in Chapters 5.3.4 and 5.4.2.1.

4.4.2.3. Diagram Examples

This subchapter presents diagrams illustrating TTIs accounted for by the standard and the novel method. These diagrams, incorporating precise data, depict various scenario examples to enhance understanding of the data volume and time accounting processes.

Figure 4.10 depicts a simplified sunny-day scenario for the standard method, featuring a single, continuous burst of four data packets arriving at the eNB. The transmission process utilizes a non-DC scenario type. *ThpVolDl* calculates the data volume of these packets at the PDCP SDU level, excluding the PDCP layer header. *ThpTimeDl* initiates accounting when the first TTI is scheduled and concludes when the penultimate packet is scheduled. While the exclusion of the last scheduled TTI is a predefined requirement, it is also necessary to monitor whether a HARQ ACK is received for its data. Only upon receiving the HARQ ACK can the measurement report be transmitted from the L2 layer performing the measurements to the PM Collector for the corresponding burst-id.

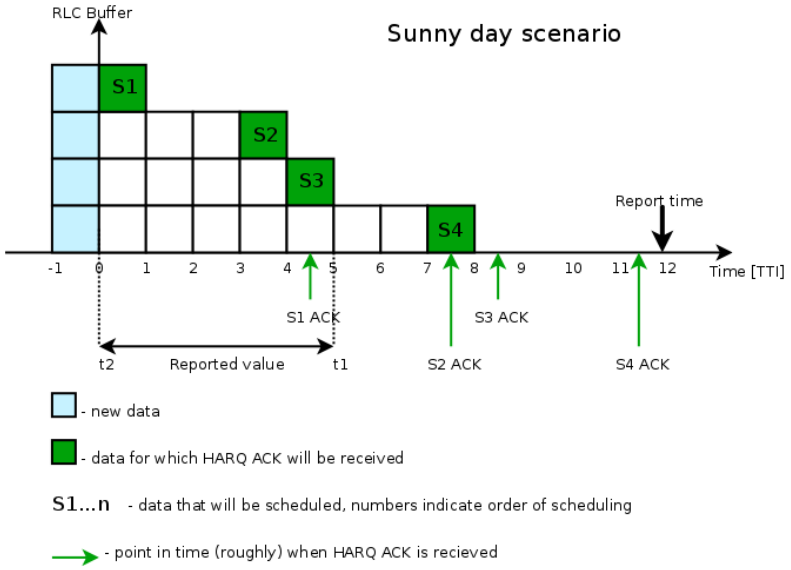

Figure 4.10: Sunny day scenario without new data after burst is started for the standard method.

Figure 4.11 presents a comparative scenario to Figure 4.10, incorporating the use of an X2 SCell data path in the SeNB. The time for the penultimate RLC PDU of the burst is calculated based on Equation 4.6, where no waiting time for HARQ ACK is considered, as in intra-site CA transmission. However, the total scheduling time (Eq. 4.6) in the SCell is estimated. *ThpTimeDl* is calculated identically in both examples, as the estimated scheduling time in the SCell is sufficiently small for the respective data volume to rapidly drain the RLC buffer on the SCell. The last TTI with S4 data scheduled in the PCell is excluded based on 3GPP requirements.

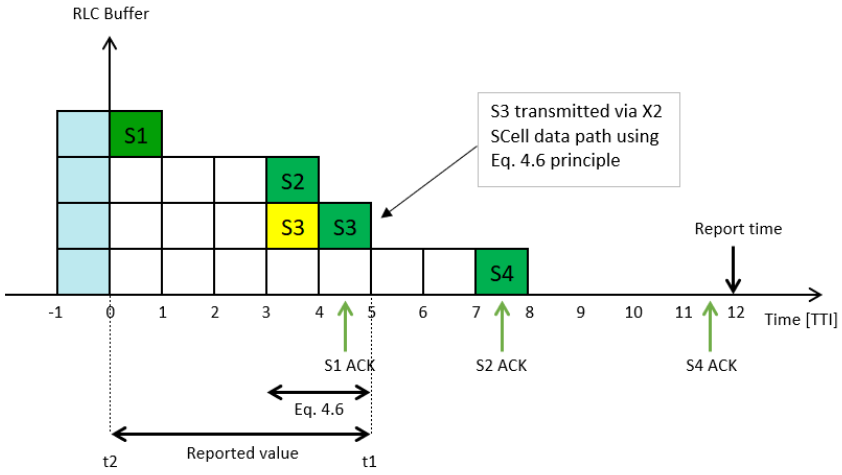

Figure 4.11: Sunny day scenario without new data after burst is started for the novel method.

Figure 4.12 depicts a successful retransmission scenario where an $RLC\ PDU_i$, denoted as S3, experiences initial transmission failure but is successfully retransmitted at the next available opportunity. The counting principle for retransmission time varies depending on whether S3 is retransmitted via the PCell or SCell. In the case of SCell retransmission, the novel method excludes the time interval between the initial S3 transmission and its retransmission, represented as X. Conversely, the standard method continues to count this time interval. For PCell retransmission, both the standard and novel methods consistently count the time between consecutive transmission attempts for the same $RLC\ PDU_i$.

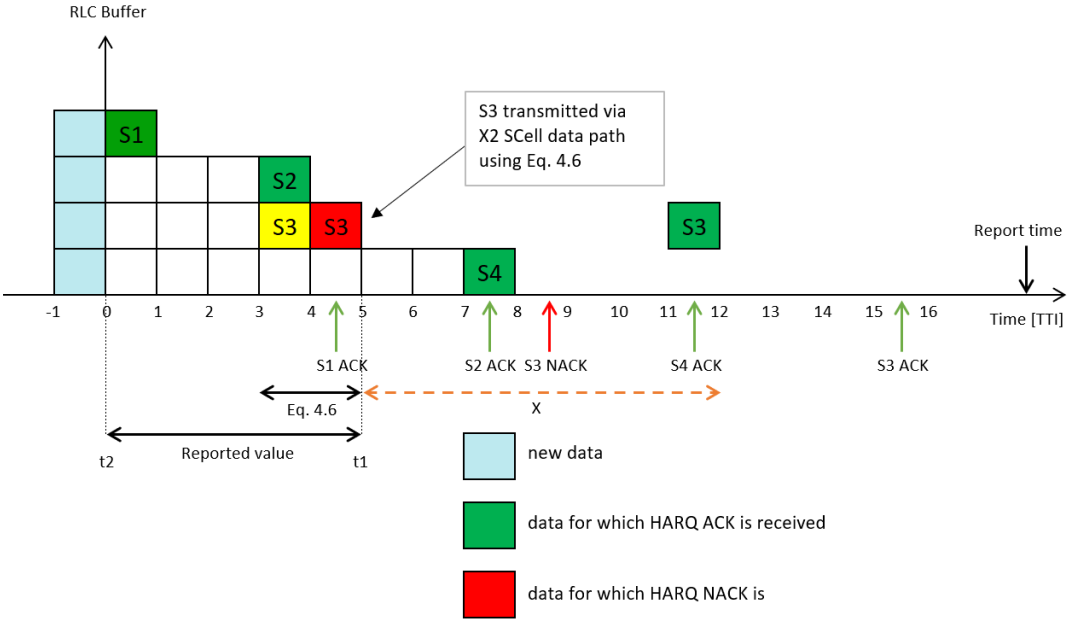

Figure 4.12: Rainy day scenario with ReTx before last TTI is scheduled.

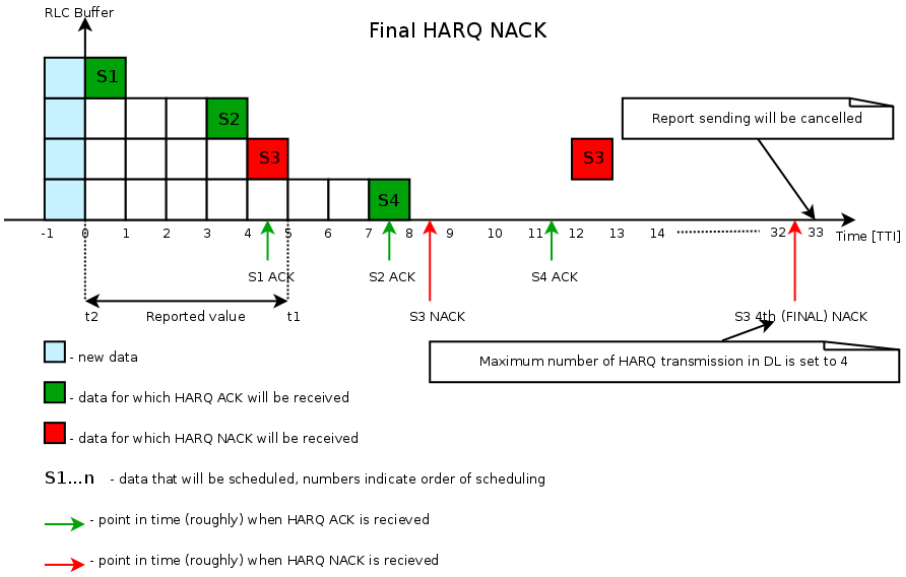

Figure 4.13: Rainy day scenario with Final HARQ NACK.

Figure 4.13 illustrates an unsuccessful retransmission scenario where an RLC PDU, denoted as S3, experiences initial transmission failure followed by subsequent unsuccessful retransmissions, the number of maximum retransmissions is controlled by a specific parameter, at the next available opportunity. Both methods employ the same counting principle, excluding such burst occurrences from the calculation. Consequently, neither the data volume nor the time components are included in the $ThpVolDl_{QCI_x}$ or $ThpTimeDl_{QCI_x}$ PM counters. This implies that if a HARQ NACK is received for the final retransmission, the burst is not counted.

4.5. Time component calculation change

The prior time component calculation method, designed for non-DC systems such as intra-site CA connections or single-cell connections, was specifically tailored for standard method implementation based on 3GPP specification [12], which provides flexibility in the implementation of the method, allowing for interpretation and variation in its execution.

The standard method's time component calculation relied on the interpretation that the time of a given burst concluded upon the indication of an empty PDCP buffer, even if the MAC buffer was still processing user data for the accounted burst. More specifically, upon reception of a new IP packet (#2) while the PDCP buffer was empty, but the MAC buffer remained occupied due to the scheduling of a previous IP packet (#1), the two IP packets were treated as belonging to separate bursts. This resulted in the time component failing to account for the time elapsed between the scheduling of two TBs for which the IP packets were received at different absolute times, despite a negligible reception time difference, specifically when the subsequent IP packet arrived during an empty PDCP buffer, but MAC buffer was still occupied. This resulted in a significant underestimation of the time component value compared to user perception due to the irregular nature of incoming IP packet flows from the server.

The introduction of a new method requires not only a revision of the flow control algorithm previously presented in Chapters 4.2 and 4.4 but also presents an opportunity to enhance the prior implementation of the standard method, particularly its time component calculation

algorithm. The necessity for this implementation change stems from the potential for improvement in the previous algorithm, which resulted in inaccurate accounting of the burst time component during the reception of consecutive IP packets. These packets, while belonging to the same transmission cycle, exhibited varying arrival rates at the eNB.

In the revised implementation done for the novel method, the time component accurately reflects the time interval between the scheduling of two TBs for which the IP packets were received at distinct absolute times. This is achieved by ensuring that the PDCP buffer is not considered empty while the MAC buffer remains occupied for the ongoing burst. The novel implementation logic aligns the time component calculation more closely with both user perception of throughput and eNB perception. This alignment is crucial because, from the eNB perspective, flushing the PDCP buffer immediately after the RLC buffer but before the absolute time for TB transmission at the MAC layer (operating on a TTI basis) is inaccurate, as the transmission for a specific user and its E-RAB may still be in progress. The revised implementation is expected to result in an overall increase in the time component value, consequently leading to a reduction in the measured throughput. Notably, the magnitude of this impact is inversely proportional to the file size being transmitted to the user. This relationship arises from the fact that larger file sizes result in a greater proportion of data being transmitted via constant bursts, which occur when the IP packet inflow rate at the eNB exceeds or equals its capacity to handle the traffic. Smaller file sizes will exhibit a more pronounced difference in time component values when compared between the two methods.

For traffic models predominantly composed of user data traffic generated by applications employing frequent small file transfers, such as the transmission of 50 kB of data every few seconds, the revised implementation will lead to a substantial increase in the temporal component. Consequently, this will result in a significant decrease in the IP scheduled throughput metric measured in such network cluster. It is noteworthy that this reduction in throughput is solely attributed to the inaccurate interpretation of the temporal component by the legacy implementation.

This modification to the algorithm for calculating the temporal component is elaborated upon in the next chapter which includes an illustrative example, but the test cases are available in Chapter 5.3.3.1, with results validating the discrepancy in outcomes between the legacy and revised implementations.

4.5.1. Time component calculation example

This chapter focuses on the difference in data traffic splitting between a single eNB and a configuration involving two separate eNBs. The analysis aims to determine the accuracy of the time component calculation within the IP scheduled throughput measurement, considering the influence of non-adjacent TBs on user data scheduling. Specifically, it examines the differences in values arising from the division of a single transmission cycle into multiple bursts instead of a single burst.

Two distinct scenarios can lead to the division of a single transmission cycle into multiple bursts. The first one is related to the TCP slow start mechanism. In scenarios involving small data

file transfers (e.g., 500 kB), the TCP slow start mechanism can introduce irregular data arrival patterns from the server. This irregularity results in the scheduling of data volumes within a single TTI separated by random intervals. The duration of these intervals is determined by the rate at which the remaining data is received by the eNB from the server, leading to a gradual increase in the transmission rate. The second one is high user density and radio resource contention. In environments with high user density, simultaneous demands for radio resources within the same cell can lead to non-consecutive scheduling of a particular user's data transmission in the MAC layer. This occurs due to the allocation of intervening TBs to other users, effectively fragmenting the transmission cycle into multiple bursts. This can lead to a situation where the PDCP buffer is emptied before the next scheduled TB.

The proposed implementation, promptly described in Chapter 4.5, refines the calculation of the time component, resulting in a more accurate representation of end-user perceived throughput time. However, this refinement does not directly enhance the user experience itself. Instead, it improves the fidelity of the measurement, providing a more precise reflection of the actual QoE. While the 3GPP standardization [12] outlines general scheduling principles, it does not explicitly define the precise calculation method within the lower layers of radio protocols. This leaves implementation details to individual vendors. However, neglecting the time elapsed between two TBs for the same transmission file (when the transmission time has already started) requested by the user, is not a logically sound approach. Consequently, by incorporating the time elapsed between TBs, the proposed implementation provides a more accurate representation of the end-user's perceived latency compared to the previous method. This enhancement contributes to a more efficient and user-centric data transmission experience in high-density scenarios. The implementation aligns more closely with the 3GPP concept, which explicitly suggests accounting for the time during which data transmission over the Uu interface has commenced but not yet concluded.

Figure 4.14 illustrates a representative traffic pattern of TCP slow start or radio resource contention, where the legacy algorithm identifies the burst duration as separated, regardless of the ongoing buffer occupancy due to initial part of the received packet data for a given transmission. SM and NM represent the abbreviations for the standard and novel methods, respectively.

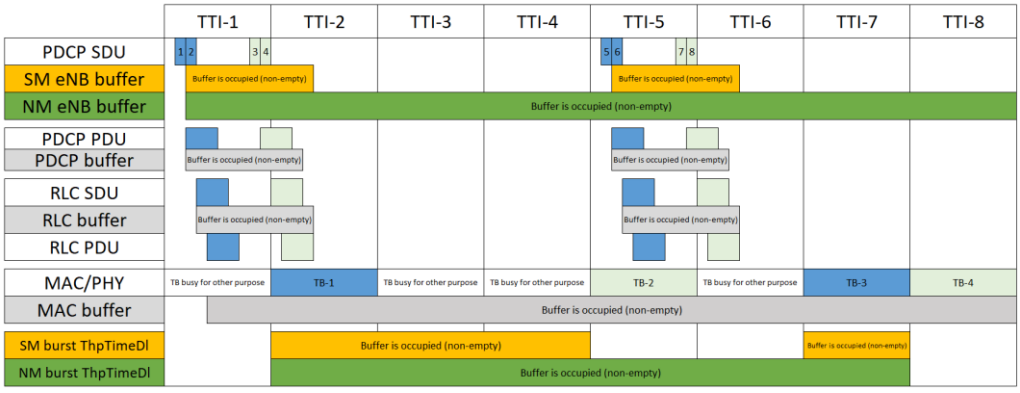

Figure 4.14: Example of time component calculation differences between the standard and the novel methods.

A user's transmission cycle involves the delivery of eight IP packets, which form a single transmission file. However, within this scenario, the immediate scheduling of received packets in consecutive TBs is constrained by the MAC buffer occupancy allocated for other purposes, including control messages and user data destined for other UEs. The first four packets are received by PDCP buffer during TTI-1, while the remaining four during TTI-5. The first two IP packets are grouped into a single TB-1, followed by another two packets grouped into TB-2. Due to high system load, the MAC scheduler was unable to allocate resources for these four packets in consecutive TBs. Consequently, TB-1 was scheduled during TTI-2 and TB-2 during TTI-5. Since the next four IP packets arrived during TTI-5, the entire transmission is considered a single transmission event. The subsequent two IP packets are grouped into TB-3, followed by the final two packets grouped into TB-4. Again, due to high system load, the MAC scheduler could not allocate resources for these last four packets immediately in TTI-6. However, free resources were available in TTI-7 and TTI-8, allowing the scheduling of the final two TBs in a consecutive manner.

The time component for the standard method was calculated by dividing it into two distinct bursts due to the PDCP buffer being empty during the reception of the last four IP packets, despite their association with a single file. The initiation of burst-1 coincided with the commencement of TTI-2 when TB-1 was scheduled, and its termination occurred at the start of TTI-5 when TB-2 was scheduled, resulting in a duration of 3ms. Burst-2 was equivalent to the duration of TTI-7 (1ms), as consecutive TB scheduling was employed for TB-3 and TB-4, having the last slot excluded from counting.

The time component calculation for the new method underwent a complete revision, incorporating the time interval between burst-1 and burst-2. The transmission of all eight IP packets was considered a single transmission due to the non-empty state of the MAC buffer during the reception of packets 5 through 8.

The standard method exhibits limitations in accurately determining burst duration from both the eNB and user perspective under high load conditions. This leads to an underestimation of the time component, resulting in overly optimistic throughput values. The implementation of the new method addresses this issue by aligning with the eNB and user perception of time, accurately accounting for the time interval between bursts when transmission cycles are stalled due to high load. The discrepancy between the standard and new method becomes more pronounced with increasingly bursty traffic models.

The example of new time calculation change for the burst (illustrated in Figure 4.14) shall be verified in Chapter 5.4.3 with specific test case scenarios.

The novel method introduces a modification to the HARQ confirmation mechanism, eliminating the waiting period for HARQ ACK confirmation from the user. Instead, it focuses on counting the number of TTIs until the buffer is emptied (excluding the final TTI), irrespective of HARQ confirmation for the penultimate TTI. Conversely, the standard method awaits confirmation for the penultimate TTI (as the final TTI is always excluded from the count) via UCI regarding the HARQ status. This implies that for a cell with a maximum HARQ confirmation limit of 8, the retransmission process can be repeated up to 7 times (with the initial transmission constituting

one attempt), extending the burst duration by an additional 8 ms for each retransmission, potentially reaching 56 ms if the final retransmission receives a HARQ ACK. Figure 4.15 provides a visual representation of this implementation change.

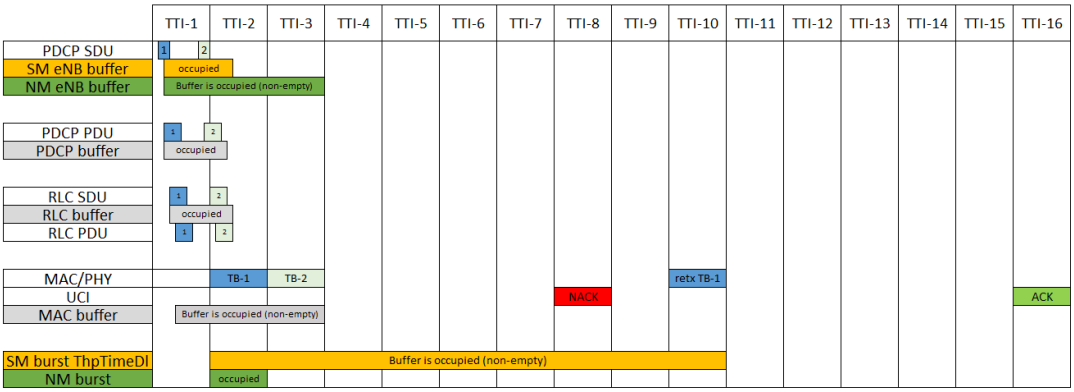

Figure 4.15: Comparative Analysis of Time Component Calculation Example: Impact of HARQ Mechanism Awaiting Time on Standard and Novel Methods.

5. TEST RESULTS

Chapter 5 will evaluate the implementation results of the standard and novel measurement methods in real devices, as described in Chapter 4. These tests will determine if the thesis and supplemental objectives established in Chapter 1.2 are achieved and if the calculation principles outlined in Chapter 4.4 produce expected results.

Chapters 5.1 and 5.2 present a laboratory test line design utilizing a cluster of eNBs, based on real devices employed by Nokia customers. The design incorporates a detailed explanation of traffic generation principles, including an example illustrating the variability of traffic flow through the BTS, along with an explanation of test constraints. Furthermore, a comprehensive list of acronyms is defined for the data presented in the tables and graphs, enhancing readability and comprehension.

Chapter 5.3 presents a comprehensive evaluation of the novel throughput estimation method, examining its accuracy and stability within the context of the TCP slow start mechanism and various network configurations employing different transmission protocols. The evaluation includes comparisons to the standard method.

Chapter 5.4 investigates the impact of radio channel quality fluctuations, a common occurrence in cellular networks, on the accuracy of both standard and novel throughput estimation methods. The chapter includes specific tests conducted on the *eTh* function, with results presented to determine optimal parameter values based on radio channel quality. Furthermore, the chapter presents test cases that illustrate the differences in burst time calculation changes previously discussed in Chapter 4.5.

Chapter 5.5 investigates the influence of increased component carrier allocation for individual users and increased user density on the accuracy of the novel throughput estimation method.

5.1. Test line design

To validate the gain, accuracy, stability and correctness of the proposed method, a series of experiments was conducted, as defined in Chapter 1.2. A schematic representation of the downlink (DL) throughput test design is depicted in Figure 5.1, based on a block diagram framework [23, 25, 19].

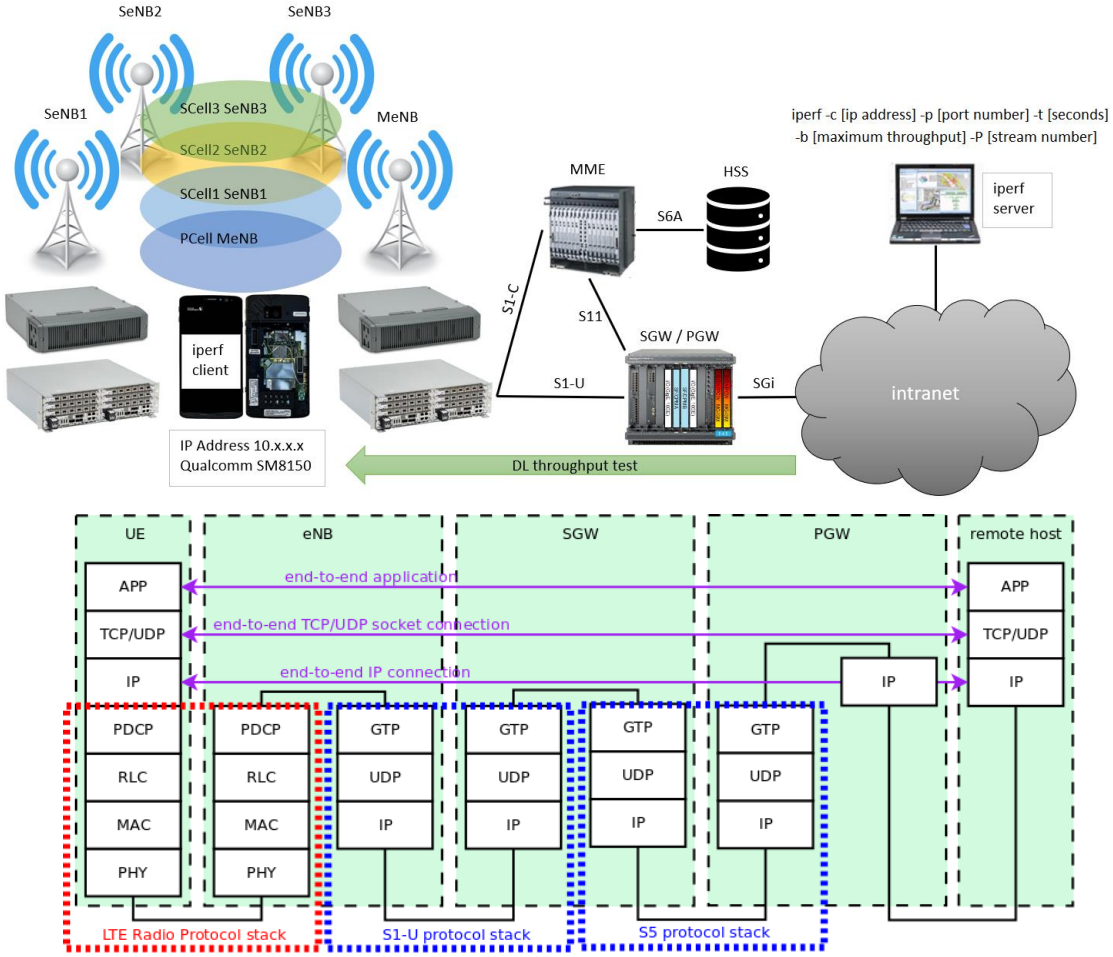

Figure 5.1: Test design architecture.

The laboratory test line setup comprises the following components:

- A Qualcomm SM8150 capable of supporting multiple carrier aggregation (CA) configurations and executing DL throughput tests.
- Four Nokia eNBs, 3 FDD, 1 TDD, responsible for radio communication, consisting of three 10 MHz cells, the specific configuration is shown in Table 5.1 and 5.2.
- Nokia Core Network: A set of Nokia core network components, including the Mobility Management Entity (MME), Home Subscriber Server (HSS), Serving Gateway (SGW), and Packet Data Network Gateway (PGW), responsible for managing IP communication between the client and server.
- Nokia Intranet: A Nokia intranet network providing connectivity between the PGW and the laboratory management area.
- Data Generator PC: A personal computer configured with an iperf-based application designed to generate transmissions utilizing the maximum achievable bandwidth on IP networks [18].
- Iperf Application on UE: An iperf application deployed on the UE to simulate the behavior of data download from the user's perspective.

Table 5.1: eNB cluster configuration part I.

BTS id	1111 (MeNB) FDD			1112 (SeNB) FDD		
PCI	31	32	33	41	42	43
EUTRAN cell id	284417	284417	284418	284673	284674	284675
EARFCN DL	3500	3500	3600	100	200	300
EARFCN UL	21500	21500	21600	18100	18200	18300
DL carrier freq	930 MHz	930 MHz	940 MHz	2120 MHz	2130 MHz	2140 MHz
UL carrier freq	885 MHz	885 MHz	895 MHz	1930 MHz	1940 MHz	1950 MHz
Intra-site CA	FDD PCell	FDD PCell	FDD SCell1	FDD PCell	FDD SCell1	FDD SCell2
BW	10MHz	10MHz	10MHz	10MHz	10MHz	10MHz
Band	8 (900 GSM)	8 (900 GSM)	8 (900 GSM)	1 (2100)	1 (2100)	1 (2100)
MIMO	2x2	2x2	2x2	2x2	2x2	2x2
PDCCH symbol	2	2	2	3	3	3
Highest modulation scheme	256QAM	256QAM	256QAM	256QAM	256QAM	256QAM
DL MIMO mode	DOL MIMO	DOL MIMO	DOL MIMO	DOL MIMO	DOL MIMO	DOL MIMO
Max cell throughput	94 Mbps	94 Mbps	94 Mbps	72 Mbps	72 Mbps	72 Mbps

Table 5.2: eNB cluster configuration part II.

BTS id	1109 (SeNB3) FDD			1110 (SeNB2) TDD		
PCI	11	12	13	21	22	23
EUTRAN cell id	283905	283906	283907	284161	284162	284163
EARFCN DL	1425	1425	1425	38700	38800	38800
EARFCN UL	19425	19425	19425			
DL carrier freq	1827.5 MHz	1827.5 MHz	1827.5 MHz	2305.0 MHz	2315.0 MHz	2315.0 MHz
UL carrier freq	1732.5 MHz	1732.5 MHz	1732.5 MHz			
Intra-site CA	FDD PCell	FDD PCell	FDD SCell1	TDD PCell	TDD SCell1	TDD SCell2
BW	10MHz	10MHz	10MHz	10MHz	10MHz	10MHz
Band	3 (1800+)	3 (1800+)	3 (1800+)	40 (TD 2300)	40 (TD 2300)	40 (TD 2300)
MIMO	2x2	2x2	2x2	2x2	2x2	2x2
PDCCH symbol	2	2	2	3	3	3
Highest modulation scheme	256QAM	256QAM	256QAM	256QAM	256QAM	256QAM
DL MIMO mode	DOL MIMO	DOL MIMO	DOL MIMO	DOL MIMO	DOL MIMO	DOL MIMO
Max cell throughput	94 Mbps	94 Mbps	94 Mbps	72 Mbps	72 Mbps	72 Mbps

Chapter 5 presents laboratory test cases designed to evaluate the accuracy and limitations of both the standard and novel methods. The standard method serves as a reference for non-DC system scenarios, while in DC systems, the two reference points defined in Chapter 3.6 are crucial for comparison. The novel method, however, is applicable to all traffic types, aiming to provide a solution for DC systems while maintaining comparable precision to the standard method in non-DC systems.

IP scheduled throughput calculation algorithm imposes specific post-processing conditions due to principles outlined in the 3GPP standard. This evaluation is conducted despite

the 3GPP specification requirement, which mandates that the usability of the method is only applicable to traffic characterized by bursts exceeding the single TTI duration and when the data transmission over the Uu interface has commenced but not yet concluded. The standard and the novel methods will be evaluated for transmission types that deviate from 3GPP counting criteria to determine their respective limits, for example by lowering down the file size to the lowest possible value.

The framework how Throughput (*ThpVolDl* / *ThpTimeDl*) [Mbps] is calculated is based on measurement principles described in 3GPP specification [12,20]. Each burst sample defined by the volume of *ThpVolDl* and the time length *ThpTimeDl* are captured by a counter provider component responsible for PDCP level measurements. Subsequently, both internal counters containing the instantaneous values are sent from counter provider to counter collector, which shall perform the time aggregation over longer time interval from all the received samples, for example 5, 10 or 15 minutes. The aggregated value of a single counter (*ThpVolDl* or *ThpTimeDl*) is reported to external data file at the end of measurement time interval.

The Qualcomm eXtensible Diagnostic Monitor (QXDM) provides a measurement of throughput, expressed in Mbps, which represents the average data rate experienced by the UE at the application layer during data transmission. This metric is calculated by averaging throughput values obtained from multiple samples collected throughout the data transfer process. QXDM, a software application developed by Qualcomm Technologies, serves as a tool for debugging and analyzing the performance of mobile devices in wireless communication systems. It enables the measurement of user-perceived wireless network metrics, including Received Signal Strength Indicator (RSSI), Signal-to-Interference-plus-Noise Ratio (SINR), user throughput, Block Error Rate (BLER), and control messaging during ongoing transmissions. This comprehensive analysis allows for a deeper understanding of the user experience in wireless communication, facilitating the identification of performance bottlenecks and optimization of network parameters for improved data transfer and overall communication quality.

The experimental outcomes exhibit independence from specific channel numbers, including E-UTRA Absolute Radio Frequency Channel Number (E-ARFCN). Variations observed between consecutive trials are attributed to the temporal availability of the designated equipment.

5.1.1. Important network parameters influencing accuracy of measurement

This thesis aims to address the challenge of designing and implementing the novel IP scheduled throughput measurement for distributed networks, known as DC systems. The novel method shall undergo comprehensive verification steps to carefully define its boundaries in cellular network and ensure its reliability and precision. This testing framework should encompass a wide range of network configurations, traffic conditions, and radio channel quality scenarios. This section outlines the key aspects of this testing framework and the rationale behind them.

The accuracy of the IP scheduled throughput measurement is intrinsically linked to various network parameters. These parameters can significantly influence the precision of the measurement and require careful consideration during testing.

- Network Architecture: The performance of the proposed method must be evaluated across diverse network architectures, including single-cell, intra-site CA, and inter-site CA configurations. Additionally, the method's behavior in mixed architectures, combining different configurations, should be investigated. This comprehensive evaluation will provide insights into the method's robustness and adaptability to different network topologies.
- Data Burst Length and Packet Size: The proposed method's response to different data burst lengths and packet sizes needs to be evaluated. Testing with small bursts consisting of lots of single TTIs, and other varying packet sizes will reveal how the method adapts to changing data traffic patterns.
    - Minimum TCP Packet Size: For a constant radio link quality level, it is essential to determine the minimum TCP/IP packet size that can be measured reliably. This test will identify the minimum data volume required for accurate measurement in laboratory settings, even though 3GPP specifications do not explicitly define this minimum.
    - Maximum TCP Packet Size: Conversely, it is crucial to determine the maximum TCP packet size that does not affect the measurement precision under constant radio link quality conditions. This test will establish the upper limit of data volume that can be accurately measured without compromising the method's accuracy.
    - Stability of Long Burst: The stability of the novel method under prolonged data transmission scenarios must be assessed. Specifically, it is crucial to verify that the accuracy of the method remains unaffected by extended data file transmissions, particularly during periods of high network traffic. Such periods may induce elevated processing loads, potentially leading to anomalous behavior.
- Radio Channel Quality variations and *eTh* Function: The radio channel quality, characterized by parameters like RSRP (Reference Signal Received Power) and SINR (Signal-to-Interference-plus-Noise Ratio), significantly impacts the measurement precision. Testing with varying channel quality conditions, including slow and fast changes, will reveal how the *eTh* function adapts to dynamic channel conditions and maintains measurement accuracy. The *eTh* function serves as an estimation mechanism for the achievable throughput of a secondary eNodeB (SeNB) for a specific user's active E-RAB. This calculated throughput value is transmitted to the master eNodeB (MeNB) to inform the transmission control unit about the SeNB's capacity. The MeNB subsequently utilizes this information to determine the optimal data volume that can be transmitted from the MeNB to the SeNB during Carrier Aggregation (CA) connection. In essence, the *eTh* function provides an approximation of the SeNB's throughput capabilities, facilitating efficient data transmission during CA operation.
    - Retransmissions: Harsh radio channel conditions can lead to signal reception errors, requiring retransmissions. These retransmissions can impact the measurement precision, for example by changing the length of a burst. Testing with different retransmission scenarios will quantify the impact of retransmissions on the measurement accuracy.

- Method-Specific Parameters: The effectiveness of the IP scheduled throughput method is influenced by parameters like the *eTh* exchange rate, initial Modulation and Coding Scheme (MCS), and the *eTh* calculation function. Testing with different combinations of these parameters will reveal their impact on the measurement accuracy.

- Number of Component Carriers: The number and distribution of secondary cells (SCells) and their interaction with the primary cell (PCell) scheduler play a crucial role in data distribution during transmission and measurement accuracy. An evaluation of the proposed method's adaptability to the PCell scheduler data distribution algorithm will be conducted using various SCell configurations. The accuracy of the resulting burst-based throughput will be assessed, particularly in comparison to the standard method.
- Number of Users: The number of active users in the network directly impacts the flow control algorithm's performance. This, in turn, affects the system's capacity and the precision of the throughput measurement. Testing with varying user densities will reveal how the flow control mechanism influences the measurement accuracy.
- Protocol type: The distinct characteristics of Transmission Control Protocol (TCP) and User Datagram Protocol (UDP) in the context of data transmission will be analyzed, with particular focus on the data transfer rate, packet arrival frequency, and data integrity. The study will further examine the influence of these protocol-specific characteristics on the accuracy of data transmission measurements.

To evaluate the accuracy of two measurement methods for assessing traffic patterns in a cellular network, a series of measurements under laboratory conditions were conducted to simulate the end-user behavior. The accuracy of the methods was quantified using relative error, and the simulations were performed across a range of transmission cycle variations.

5.1.2. List of acronyms and parameters used during test cases

To enhance readability and facilitate comprehension, a list of acronyms is provided in this Chapter. This glossary serves as a reference for interpreting all tabulated and graphical data presented in subsequent chapters. The decision to compile a dedicated glossary was driven by the extensive length of many abbreviations, which could otherwise hinder the clarity of the presented information. These abbreviations are as follows:

- RE - Relative Error.
- FC ON - Flow Control Enabled, indicating the implementation of the enhanced flow control algorithm described in Chapter 4.3, and the time component calculation change described in Chapter 4.5, applicable to both non-DC and DC systems.
- FC OFF - Flow Control Disabled, indicating the use of the legacy flow control algorithm, applicable only to non-DC systems.
- NM VL - Novel's Method Data Volume component.
- SM VL - Standard's Method Data Volume component.
- NM TM - Novel's Method Time component.

- SM TM - Standard's Method Time component.
- BDR - Burst Data Ratio - a metric representing the proportion of PDCP SDU data volume transmitted within a burst relative to the total PDCP SDU data volume received by the eNB within its specific cell.
- BTR - Burst Time Ratio - a metric representing the proportion of IP scheduled throughput time allocated to a burst relative to the total number of scheduled TTIs with user data by the eNB within its specific cell.
- NM TP - Novel's Method IP Scheduled Throughput.
- SM TP - Standard's Method IP Scheduled Throughput.
- App TP - Application Layer Throughput.
- Cell TP - Cell Throughput.
- No CA - Single Cell Transmission, indicating a transmission type without the use of Carrier Aggregation (CA), comparable to non-DC systems.
- Intra-site CA - Intra-site Carrier Aggregation, indicating multiple cell transmission under a single eNB, comparable to non-DC systems.
- Inter-site CA - Inter-site Carrier Aggregation, indicating multiple cell transmission under multiple eNBs, comparable to DC systems.
- SS - Single stream TCP traffic.
- nMS - n-multi stream TCP traffic.
- STTI BR - single TTI burst ratio – a metric representing the proportion of single TTI occurrences relative to the sum of single TTIs and IP scheduled throughput time allocated to a burst.
- ReTx Ratio - retransmission ratio – a metric defined as the quotient of the number of HARQ retransmissions for user data on the Downlink Shared Channel (DL-SCH) and the total number of user data TBs transmitted on the DL-SCH in the PCell.

5.2. Data Download Simulation concept in tests

This subchapter describes the implementation of an iperf framework in the test line design. The iperf application serves as a tool to simulate data download behavior from the user's perspective.

The iperf application on the UE acts as a client, initiating data download requests to an iperf server listening on a designated port. Upon receiving these requests, the server generates traffic according to the parameters specified by the UE client. This process effectively simulates a real-world data download scenario from the user's point of view.

The data initialization process acts as the following:

- Request Initiation: The iperf application on the UE sends a request to the iperf server, specifying the desired download parameters (e.g., data volume, transfer rate).
- Server Response: The iperf server, upon receiving the request, begins generating traffic according to the specified parameters.

- Data Transfer: The server transmits the generated data to the UE client, simulating the download process.
- Performance Measurement: The iperf application on the UE measures the download performance metrics (e.g., throughput, latency, packet loss).

The iperf application on the UE provides a valuable tool for evaluating and analyzing data download performance from the user's perspective. It allows for controlled simulations of various download scenarios, enabling researchers and engineers to assess the impact of different network configurations and parameters on user experience. The iperf application on the UE offers a practical and efficient method for simulating data download behavior. By acting as a client and interacting with a dedicated server, it provides a realistic representation of the user experience, facilitating performance analysis and optimization efforts.

5.2.1. Stochastic variation of generated traffic in the IP network

The inherent variability of a live system necessitates the consideration of potential performance fluctuations. These fluctuations are primarily attributed to variations in transmission patterns, specifically the inter-packet spacing, the packet arrival rate, and the scheduling decisions made by the BTS. The inter-packet spacing, or the time interval between consecutive packet arrivals, can vary significantly. Similarly, the packet arrival rate, or the frequency at which packets arrive at the receiver, can fluctuate. Furthermore, the BTS scheduler, responsible for prioritizing and scheduling packet transmission to the user, introduces another layer of variability. These factors collectively influence the overall data transmission performance, potentially leading to variations in latency, throughput, and packet loss.

To quantify these potential variations, a series of file transmission tests was conducted using 2 MB files. These variations were attributed to the UE processor's dual role as both server and receiver, simulating real-world user behavior where the user initiates downloads, and the server subsequently transmits data. This dual role, coupled with the TCP slow start mechanism, resulted in the division of data bursts from the PDCP buffer perspective. The QXDM application was employed to extract the throughput metric from the perspective of the user at the PDCP layer level.

Furthermore, the initial volume of IP packets transmitted to the eNB directly influenced the overall transmission time. Smaller initial packet volumes led to prolonged transmission durations as the eNB interpreted this as a low demand for high throughput capabilities. Consequently, substantial differences in transmission time were observed (exceeding a factor or two), leading to a decrease in throughput despite optimal radio channel conditions (SINR = 30 dB).

An initial evaluation, designated as Iteration 1 (Table 5.3), revealed that the new method accounted for only 68.21% of the transmission time, given as Burst Time Ratio (BTR), compared to 69.62% for the standard method. The unaccounted transmission time was attributed to single or last TTI transmissions, as defined by 3GPP standardization. A subsequent iteration, defined as Iteration 2, demonstrated a reduction in this unaccounted time to 29.30% and 31.66%, respectively, highlighting the significant impact of 3GPP requirements on overall performance. In

Iteration 2, the new method accounted for only 90.09% of the traffic volume, given as Burst Data Ratio (BDR). This discrepancy was attributed to a reduced traffic rate from the iperf server to the eNB at the transmission initiation. This reduced rate resulted in an increased number of bursts that could be transmitted to the user within a single TTI, due to the slow arrival rate of consecutive IP packets at the eNB. Consequently, the IP scheduled throughput counting method interpreted approximately 10% of the data volume during 70% of the total transmission time from the user's perspective as not meeting 3GPP requirements.

Figure 5.2 presents the throughput measurement from the end-user perspective, obtained using the QXDM application directly connected to the user device. While the chart does not illustrate the variation in IP packet arrival rate from the eNB perspective, it highlights the disparate routing of the same transmission file by the same system when utilizing an inefficient protocol in terms of throughput maximization. Figure 5.2 represents the aggregated throughput data volume and time derived from Table 5.3 for each iteration type. The throughput samples obtained by QXDM are acquired at intervals of approximately 50 milliseconds, with minor fluctuations influenced by variations in data reception by the user and QXDM's capacity to retrieve this information from the device.

Table 5.3: Stochastic variation of traffic due to slow TCP start.

	Verification point	Volume [bit]	BDR [%]	Time [ms]	BTR [%]	Throughput [Mbps]
Iteration 1	Standard method	23206992	96.90	346	69.62	67.07
	New method	23003688	96.05	339	68.21	67.86
	QXDM (app layer)	23948736		497		48.19
Iteration 2	Standard method	19220312	94.13	309	31.66	62.20
	New method	18395488	90.09	286	29.30	64.32
	QXDM (app layer)	20418720		976		20.92

The calculated throughput, using both methods, represents a fraction of the total transmission cycle duration due to the exclusion of bursts that do not meet 3GPP criteria. This discrepancy arises primarily from the sparse transmission of initial bursts with extended delays, leading to a misinterpretation of the transmission cycle from the eNB's perspective. Additionally, the traffic fragmentation determined by the RAN node, beyond the engineer's control, contributes to performance variations across iterations. As a result, the 3GPP design of exclusion of single TTI bursts and last TTIs, containing partial user data and padding bits, stabilizes throughput measurement by preventing artificially low values. Counting these bursts would inflate burst duration disproportionately to transmitted data, leading to inaccurate throughput. Consequently, the PM counter results obtained in Table 5.3, despite differences in transmission pattern, were similar, reflecting consistent time value interpretation from the eNB perspective rather than from the application layer.

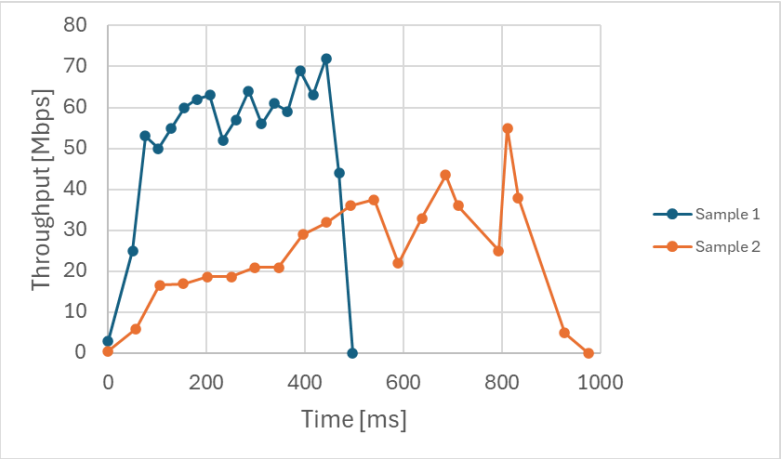

Figure 5.2: QXDM throughput on PDCP layer for two samples.

To mitigate the impact of non-uniform IP packet arrival patterns at the eNB and traffic fragmentation, which are influenced by scheduler-dependent factors, multiple test iterations are conducted to obtain statistically significant results. This approach aims to reduce the influence of extreme throughput measurements, including minimum and maximum values, which may be skewed by the presence of multiple traffic bursts. By averaging the results across multiple iterations, a more representative and reliable assessment of network performance can be achieved.

5.2.2. Explanation on the test constraints

The observed slow transmission rate between the iperf server and the eNB can be attributed to the lack of a defined maximum bandwidth constraint. This absence of a pre-established bandwidth limit necessitates a dynamic process of bandwidth estimation by the TCP server. The TCP server, adhering to the principles of congestion control, employs a gradual increase in the number of packets transmitted per sending period. This incremental approach allows the server to probe the network's capacity and determine the maximum sustainable data rate. The slow pace arises from the inherent latency associated with this probing mechanism. The TCP server must iteratively adjust its transmission rate based on feedback signals, such as packet loss or acknowledgments, received from the eNB. This feedback loop, while essential for ensuring reliable data delivery, introduces a delay in reaching the optimal transmission rate. In essence, the absence of a pre-defined bandwidth limit compels the TCP server to engage in a dynamic bandwidth discovery process, resulting in a slower initial transmission rate until the maximum sustainable data rate is established.

The command "iperf3 -c xxx.xxx.xxx.xxx -p xxxx -i1 -M1400 -P1 -n 50M -R" is employed to generate a high burst rate in a network environment. The "-c" flag designates the execution of iperf in client mode, establishing a connection to an iperf server residing at the specified IP address. The "-p" flag defines the port utilized for iperf traffic on the host. The "-i" parameter sets the reporting interval for user experience metrics, such as throughput, jitter, and packet loss, displayed within the iperf application at the UE. In this instance, "-i1" indicates a report generation every second. The “-M1400” flag sets the TCP maximum segment size. The "-P" flag specifies

the number of parallel connections from the server to the receiver, referred to as the stream number in this context. The "-P1" setting signifies the use of a single stream. The "-n" flag determines the size of the transmission file, which can be correlated with the data volume of the PDCP SDU. The "-n50M" parameter designates the use of a 50 MB file for transmission. Finally, the "-R" flag indicates that the whole command operates in reverse mode, where the UE initiates the command, but the iperf server acts as the initiator of the actual data traffic. This configuration effectively simulates real-world user behavior in a cellular network, where the user initiates a request for information, and the server subsequently grants access to the requested data.

To comprehensively assess the performance of a reference point, both cell-level throughput and application-layer throughput are presented for comparative analysis. Cell-level throughput, directly reflecting the scheduler's efficiency, is calculated as the total volume of PDCP SDU data received divided by the total number of active Transmission Time Intervals (TTIs) with scheduled user data. Application-layer throughput, representing the UE perspective, provides a measure of the data rate experienced by the application. By considering both metrics, a holistic understanding of the reference point's performance can be achieved, encompassing both the network's scheduling capabilities and the end-user's perceived data rate.

Moreover, recognizing the inherent stochastic nature of user-initiated data transmission, including the frequency, size, and duration of transmission cycles, the measurement scenarios were categorized based on distinct file size ranges: 100 kB, 200 kB, 500 kB, 1 MB, 2 MB, 5 MB, 10 MB, 20 MB, and 50 MB. Each file size was chosen to be at least twice as large as its predecessor, with the primary objective of demonstrating precision differences between distinct categories. The specific numerical value of each file size is inconsequential, as the primary focus is on verifying the stepwise change in inaccuracy across varying file sizes. Based on these criteria, a graphical representation can be generated depicting the relationship between file size and inaccuracy, demonstrating a decreasing trend in inaccuracy as file size increases. Additionally, two transmission durations were considered: 5 seconds and 10 seconds. Given the dominance of the TCP protocol in cellular network traffic volume, the majority of test cases were designed with TCP as the primary protocol under consideration [18].

5.3. Network Architecture, Burst Length, Packet Size and Protocol Type related tests

This chapter presents a comprehensive evaluation of the novel throughput estimation method, encompassing aspects of accuracy and stability, with comparison to the standard method. Due to the inherent interdependency of these factors, the investigation combines elements from several research objectives:

- Accuracy under varying network configurations: The method's accuracy is assessed in single-cell deployments and across different Carrier Aggregation (CA) configurations, including local SCells (intra-site CA), remote SCells (inter-site CA), and mixed environments.
- Stability under diverse traffic transmission types: The robustness of the proposed method is evaluated under a range of traffic transmission scenarios. This analysis encompasses variations in transmission durations and packet sizes, thereby encompassing diverse burst characteristics in terms of both number and length.

- Protocol type: The distinct characteristics of Transmission Control Protocol (TCP) and User Datagram Protocol (UDP) in the context of data transmission will be analyzed, with particular focus on the data transfer rate, packet arrival frequency, and data integrity. The study will further examine the influence of these protocol-specific characteristics on the accuracy of data transmission measurements.

5.3.1. Slow transmission using single TCP stream

This study aims to validate the accuracy of implementation of IP scheduled throughput measurement in a multi-burst scenario for TCP single-stream transmission across various UE-level connection types. A single TCP stream will be employed to simulate a scenario characterized by slow data transmission. Specifically, the investigation focuses on three connection configurations: single-cell, intra-site carrier aggregation (non-DC), and inter-site carrier aggregation (DC).

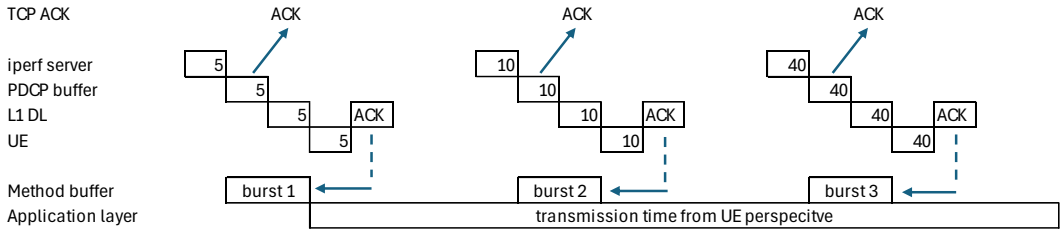

Figure 5.3: The effect of TCP acknowledgment mechanism from eNB perspective for a single TCP stream.

The effect of a single stream and TCP acknowledgment mechanism shall result in a segmentation and delay for the transmission over transport network between iperf server and PDCP buffer in eNB regardless of the file size to be sent. It is particularly pronounced at the initiation of transmission or upon resumption following fading events in the radio channel. From the perspective of the PDCP buffer, each segmented block is perceived as an individual data burst, resulting in multiple bursts for a single transmission. This means that from eNB perspective the type of traffic cannot be properly interpreted as a single transmission, which is only possible for the sender and receiver. This impact is especially noticeable in the beginning of TCP transmission where the receiver side (eNB) has not reached its full buffer capabilities yet. The transmission of IP packet data from an iperf server to an end-user, as illustrated in Figure 5.3, utilizes the TCP. The number of packets transmitted is represented by the rectangles within the figure. IP packets are initially delivered to the PDCP buffer via the S1-U interface, where they are acknowledged back to the sender upon successful reception, depicted with the diagonal arrow for TCP ACK. This successful delivery triggers an increase in the TCP congestion window size by one segment. However, it's important to note that this does not result in a doubling of the window size with each Round-Trip Time (RTT) of the transmission and acknowledgment cycle. The TCP slow start algorithm gradually increases the transmission rate until one of three conditions is met: packet loss, the receiver's window size limits the amount of data it can accept at a time, or the slow start threshold is reached. The TCP slow start algorithm aims to find the optimal transmission rate for a given network condition, balancing throughput with network

stability to avoid network congestion. A comprehensive description of the TCP slow start congestion control algorithm is provided in reference [35].

While other algorithms, such as congestion avoidance, fast retransmit, and fast recovery, can influence packet inflow at the eNB, this dissertation focuses on the general impact of slow packet inflow at the RAN side for IP scheduled throughput measurement accuracy. The TCP slow start algorithm serves as an illustrative example of slow packet inflow. Further details on these algorithms can be found in reference [36, 37, 38].

To facilitate analysis, the example of data transmission process is shown in Figure 5.4, where TCP is used to send 1 MB of payload (consisting of 685 IP packets with MTU 1460 plus additional 40 IP packets of the same MTU for TCP/IP overhead) of data from the iperf server to the end-user. The number of packets transmitted is represented by the rectangles within the figure, with various colors depending on the packet arrival time at eNB. TCP ACK denotes the acknowledgment of individual packets by the network, while HARQ ACK signifies the user's confirmation of successful reception of a specific TB. The time interval during which the eNB buffer is occupied by incoming data for a single user is denoted as "burst N." This represents the time the eNB is actively processing data for that particular user. *ThpTimeDl*, representing the temporal component of the IP scheduled throughput method, is determined by the summation of t1 and t2. This value accounts for the time taken to process and transmit data according to the IP scheduling algorithm. The active TTI represents the eNB's scheduling time, serving as a reference point for cell throughput. This interval defines the time frame within which the eNB schedules and transmits data to users. Finally, the application layer perspective describes the transmission time from the user's point of view. This perspective considers the time it takes for the user to perceive the data transmission, including factors such as network latency and application processing time.

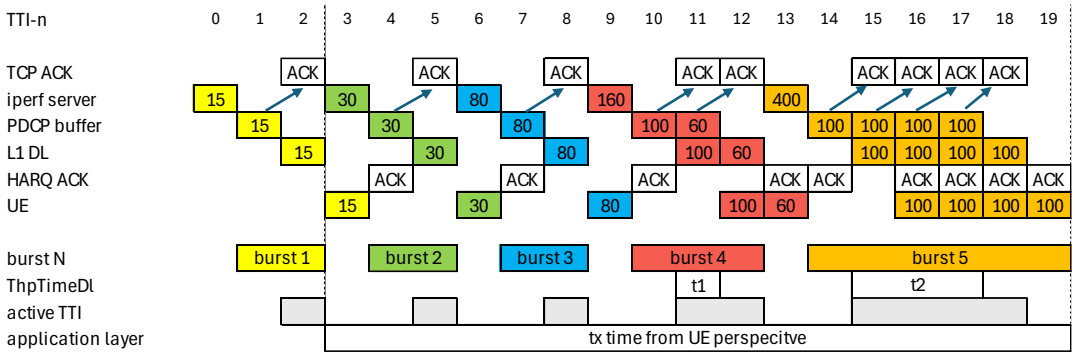

Figure 5.4: TCP/IP packet transmission process with single stream via single cell with burst transmission logic.

The initial IP packet transmission rate to the eNB was incrementally increased. Following the reception of the first five ACK messages, the rate was adjusted from 15 to 30 packets, subsequently from 30 to 80 packets, 80 to 160 packets, and finally from 160 to 400 packets. To induce saturation of the RAN throughput capacity and enable precise measurement using 3GPP method, the packet rate at Layer 1 was artificially constrained to 100 packets per TB. This limitation ensured that the eNB could accurately estimate burst length from an application-layer perspective only after reaching the saturation threshold, as data reception transitioned from irregular to a more consistent pattern. This constraint effectively extended the duration of bursts

in the PDCP layer, facilitating measurement by 3GPP methods, which are not designed to account for single TTIs occurring at the commencement of the transmission cycle or the final TTI within a burst.

Figure 5.4 highlights the disparity in the perceived transmission time and data volume between the UE, eNB, and iperf server. The BTS, acting as a proxy, encounters limitations in accurately measuring the transmission time due to the non-uniform arrival of IP packets. The BTS is unable to discern whether a specific group of IP packets constitutes a complete transmission cycle, as the inter-packet spacing may be irregular. This irregularity leads to the omission of single TTI transmissions, resulting in an incomplete representation of the actual transmission time from the user's perspective. Consequently, a comparative analysis of the IP scheduled throughput time (*ThpTimeDl*) should be conducted using two reference points: one representing the eNB perspective, defined by active TTIs, and the other representing the user perspective, defined by the application layer time.

The Figure 5.4 demonstrates that *ThpTimeDl* shall significantly deviate from the actual transmission time. In this example, *ThpTimeDl* covers 25% of transmission time from user perspective and 44% from eNB perspective. The 3GPP method mandates the exclusion of single TTIs and the last TTIs within each burst, defined as a sequence of at least two consecutive TTIs, from the calculation. Consequently, for bursts 1-3, where a single TTI transmission occurs, no contribution is considered for the time constituent as last TTIs are deducted. Conversely, bursts 4 and 5 require 2 and 4 TTIs respectively for transmission to the user, fulfilling the criteria for inclusion in the measurement. However, due to the deduction of the last TTI, burst 4 and 5 are accounted for 1 and 3 TTIs, respectively. The active TTIs constitute 53% of the total transmission time from application layer perspective.

The interpretation of test results solely based on application layer throughput is insufficient due to the presence of factors beyond the eNB's control, leading to potential misinterpretations. These factors include the inherent characteristics of the TCP/IP protocol, such as the TCP slow start mechanism, as well as radio link disruptions and fading phenomena caused by interference. To mitigate the impact of these factors, a carefully chosen reference point is crucial. The optimal approach involves designing test cases with a single user connected to a specific eNB, or multiple eNBs in the case of inter-site solutions. This ensures that resource allocation is dedicated to the designated user, enabling the accurate measurement of total PDCP SDU data volume received by the MeNB's PCell, which directly corresponds to the end user's received volume. Furthermore, the time required for user resource scheduling can be determined by counting the number of TTIs in the downlink (DL) where at least one UE is scheduled to receive user plane data. This approach allows for a comprehensive accounting of user volume and time resources from the eNB's perspective, according to its available performance, providing a reliable reference point for calculating user throughput. However, this approach has limitations when dealing with multiple users. In such scenarios, the reference point can only be utilized if the frequency and time matrix resources are allocated equally among all connected users, which may be challenging to achieve in practice.

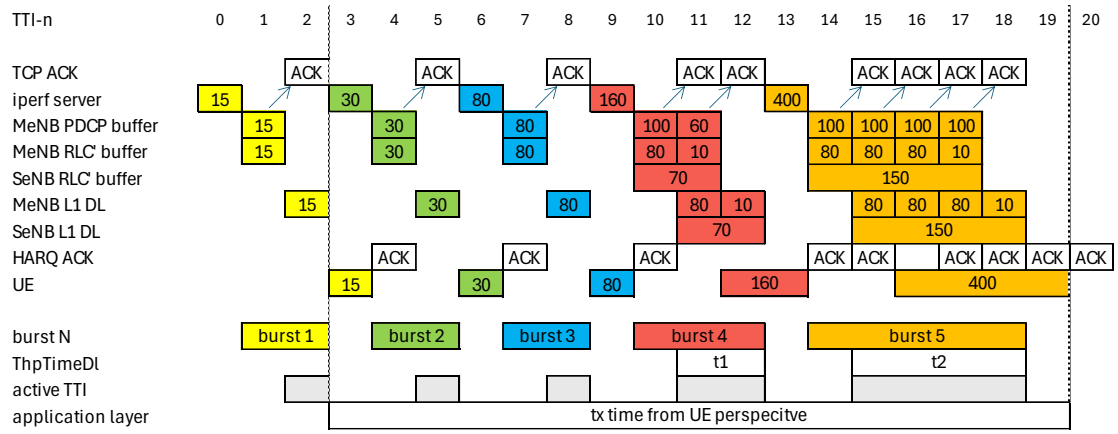

Figure 5.5: TCP/IP packet transmission process with single stream via inter-site CA with burst transmission logic of the novel method.

Figure 5.5 presents a comparative analysis of file transmission using an inter-site CA connection versus a single cell configuration, maintaining the same file size as in Figure 5.4. The data volume from the MeNB PDCP buffer is transferred to the RLC layer, where it is subsequently divided into two distinct sub-buffers: MeNB RLC and SeNB RLC, as detailed in Chapter 4.4.1 and Figure 4.7. Each of the MeNB and SeNB possesses a separate L1 DL instance, visually depicted within the graph. The time component calculation, based on the SeNB RLC buffer, is estimated using the T_{RLC},, parameter defined in Equation 4.6. In contrast to Figure 5.4, the *ThpTimeDl* value is determined with greater accuracy, a direct consequence of employing the estimation logic derived from the novel method. This enhanced precision facilitates a more accurate accounting of the time component during the transmission of very small files, which necessitate at least two Transmission Time Intervals (TTIs) for data transfer.

Figure 5.5 highlights a significant discrepancy between *ThpTimeDl* and the actual transmission time. In this scenario, *ThpTimeDl* accounts for 35% of the transmission time from the user's perspective and 67% from the eNB perspective. The 3GPP standard mandates the exclusion of single TTIs and the final TTIs within each burst, defined as a sequence of at least two consecutive TTIs, from the calculation. Consequently, bursts 1-3, characterized by single TTI transmission and no CA splitting due to small data volumes, do not contribute to the time constituent as the last TTIs are excluded. Conversely, bursts 4 and 5, requiring 2 and 4 TTIs respectively for user transmission, meet the inclusion criteria. This observed deviation represents an improvement compared to the previously analyzed single cell scenario where the last TTIs of burst 4 and 5 where subtracted, demonstrating the impact of inter-site CA on the accuracy of *ThpTimeDl* measurement.

The below subchapters present a comparative analysis of IP scheduled throughput measurement between the standard method, the novel approach and two comparative reference points, the cell throughput and application layer throughput. The primary objective of these tests evaluation is conducted within a multi-burst scenario for TCP single-stream transmission across various UE-level connection types and file sizes. The secondary objective of these tests is to analyze the impact of the TCP slow start phenomenon on the precision of IP scheduled

throughput measurement. To induce this effect, a single-stream TCP transmission is employed. This transmission type necessitates the division of a single file size into multiple TBs for transmission to the user, potentially violating 3GPP criteria for accurate measurement. As the transmitted file size increases, the influence of the TCP slow start mechanism diminishes. Comprehensive descriptions of each test case and their specific results for data volume and time component are presented in Appendix 1.

5.3.1.1. Summary – Cell's throughput as a reference point

Table 5.4 presents a comparative analysis of the relative error in estimation of cell throughput for various transmission file sizes, considering both the standard method and the new approach. The analysis encompasses three transmission types: single cell, intra-site CA, and inter-site CA, all utilizing a single stream TCP/IP protocol. The standard intra-site configuration was evaluated using the legacy flow control algorithm (FC OFF), distinct from all other configurations. This approach serves to isolate the impact of the novel measurement method and flow control algorithm by highlighting the modifications implemented between the standard and novel approaches. The results demonstrate the efficiency of the novel approach. However, it is important to note that intra-site configuration tests with FC OFF and FC ON were conducted independently. Consequently, the transmission of desired file sizes was processed uniquely, lacking a one-to-one mapping between test case results due to the scheduler's non-deterministic behavior.

Table 5.4: Cell's throughput relative error comparison between the two methods for all connection types.

File sizes	No CA		Intra-site CA		Inter-site CA	
	FC ON	FC ON	FC OFF	FC ON	FC ON	FC ON
	SM TP Cell RE [%]	NM TP Cell RE [%]	SM TP Cell RE [%]	NM TP Cell RE [%]	SM TP Cell RE [%]	NM TP Cell RE [%]
100 kB	105.26	126.88	103.93	65.83	82.35	59.10
200 kB	63.46	72.64	86.13	42.67	42.00	51.73
500 kB	43.11	51.88	37.19	28.10	-10.48	15.06
1 MB	20.51	28.55	15.31	18.39	-25.87	11.78
2 MB	14.14	17.53	19.10	11.92	-38.98	3.96
5 MB	10.27	12.45	11.72	9.09	-51.64	5.71
10 MB	5.39	6.55	9.28	7.15	-58.58	6.78
20 MB	2.32	2.88	3.18	4.34	-60.84	3.63
50 MB	1.05	1.24	3.11	1.70	-62.96	2.16
5s	1.28	1.51	1.18	0.87	-64.43	0.89
10s	0.57	0.69	0.75	0.43	-64.42	0.52

In single-cell transmission scenarios, the standard method consistently exhibits lower error values across all file sizes compared to the novel method when flow control is enabled. For example, the relative error difference for a 200 kB file size is 72.64% for the novel method and 63.46% for the standard method, while for a 2 MB file size, it is 17.53% and 14.14%, respectively. However, the difference in precision between the two methods becomes negligible for file sizes exceeding 10 MB, as it is less than 0.56%. Notably, the flow control enhancement significantly improves the performance of the standard method implementation in comparison to the novel method in single-cell transmission, demonstrating an improvement ranging from 0.12% to 21.62%.

For intra-site CA transmission scenarios, the novel method demonstrates enhanced performance in most instances when the novel flow control algorithm is enabled. For example, the relative error difference for a 200 kB file size is 42.67% for the novel method and 86.13% for the standard method, while for a 2 MB file size, it is 11.92% and 19.1%, respectively. Although the relative error measured for the standard method is comparable to the novel method for file sizes exceeding 10 MB across repeated tests and file sizes, demonstrating an improvement ranging from 0.31% to 1.41%, direct comparison is challenging due to the distinct approaches employed by the flow control algorithms in managing and distributing incoming traffic volume.

For Inter-site CA transmission scenarios with the flow control enhancement algorithm enabled by default, the novel method demonstrates favorable results in most cases. For example, the relative error difference for a 2 MB file size is 3.96% for the novel method and -38.98% for the standard method. However, for file sizes of 200 kB and 500 kB, the standard method achieves a lower relative error. For instance, for a 500 kB file size, the relative error is 15.1% for the novel method and -10% for the standard method, respectively. This discrepancy arises from the standard method's erroneous counting of only a portion of the PCell data and no SCell data volume, resulting in a quotient closer to the cell's throughput reference. Despite these exceptions, the standard method is unable to accurately measure the IP scheduled throughput value for larger file sizes (1 MB and above), where the relative error values range from -25.87% to -64.43%.

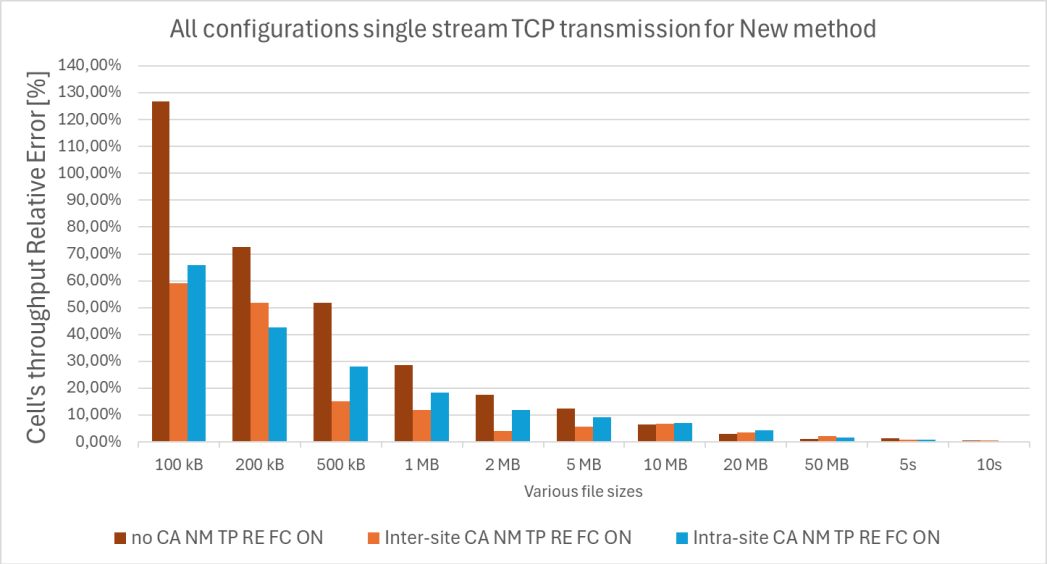

Figure 5.6: TCP/IP single stream transmission traffic across all network configurations with relative error for new method.

Figures 5.6 and 5.7 present a graphical comparison of performance metrics for all connection types, separately illustrating the results obtained using the new method and the standard method, in comparison to cell throughput as a reference point. These figures highlight the diminished accuracy of the standard method when applied to inter-site CA network configurations. For instance, during a 50 MB file size transmission, the standard method exhibits relative error of -62.96%. Conversely, the novel method demonstrates significantly improved accuracy, achieving relative error of 2.16% for the same transmission parameters. Furthermore, the results demonstrate that the novel method exhibits no significant performance degradation in

non-DC environment configurations compared to the standard method. For example, for 10 MB file size, the novel method achieves relative errors of 6.55% for a single-cell configuration and 7.15% for an intra-site CA configuration. In contrast, the standard method exhibits relative errors of 5.39% and 9.28% for the same transmission configurations, respectively.

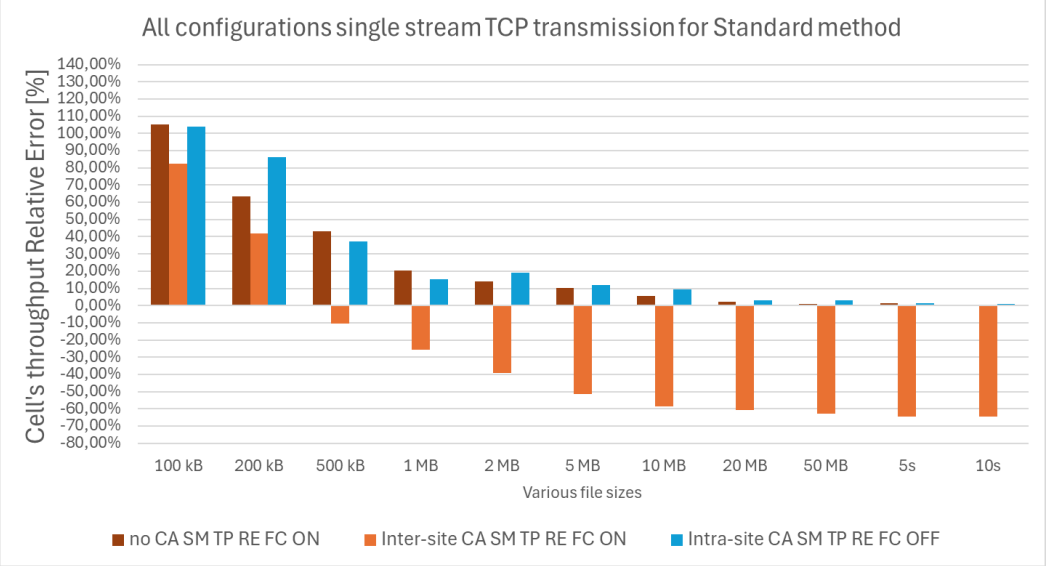

Figure 5.7: TCP/IP single stream transmission traffic across all network configurations with relative error for standard method.

The study evaluated the performance of the novel measurement method in different transmission scenarios using single stream TCP, comparing it to the standard method with usage of cell's throughput reference point. In single-cell transmission, the standard method outperformed the novel method for smaller file sizes, but the difference became negligible for larger files. In intra-site CA, the novel method generally exhibited better performance, particularly for smaller files, while the standard method showed comparable results for larger files. In inter-site CA, the novel method generally performed better, especially for larger files, while the standard method showed inaccuracies for majority of file transfers, larger than 1 MB, due to its incomplete data counting.

5.3.1.2. Summary – Application layer throughput as a reference point

Table 5.5 presents a comparative analysis of the relative error in estimation of application layer throughput for varying transmission file sizes. The analysis encompasses the standard and the new method, across three distinct transmission types: single cell, intra-site carrier aggregation (CA), and inter-site CA. All transmissions utilize a single stream TCP/IP protocol.

For single-cell transmission, the standard method consistently demonstrates lower relative error values across all file sizes compared to the novel method with flow control enabled. The improvement for relative error difference ranges from 0.13% to 30.51% between the standard and the novel methods. For example, the relative error difference for a 200 kB file size is 195.05% for the novel method and 179.37% for the standard method, while for a 2 MB file size, it is 98.43% and 92.71%, respectively. However, the precision difference between the two methods becomes negligible for file sizes exceeding 10 MB, as it is less than 0.63%.

Table 5.5: Application layer throughput relative error comparison between the two methods for all connection types.

File sizes	No CA		Intra-site CA		Inter-site CA	
	FC ON	FC ON	FC OFF	FC ON	FC ON	FC ON
	SM TP App RE [%]	NM TP App RE [%]	SM TP App RE [%]	NM TP App RE [%]	SM TP App RE [%]	NM TP App RE [%]
100 kB	189.59	220.10	201.45	176.82	169.94	135.52
200 kB	179.37	195.05	211.30	174.64	144.99	161.77
500 kB	183.10	200.46	237.17	228.04	102.91	160.81
1 MB	124.74	139.74	166.88	207.74	52.34	129.73
2 MB	92.71	98.43	181.20	198.81	22.57	108.85
5 MB	55.58	58.66	135.15	153.32	-10.44	95.76
10 MB	36.50	38.01	96.79	102.05	-29.84	80.89
20 MB	16.13	16.76	49.61	56.97	-45.48	44.28
50 MB	9.60	9.81	32.21	25.54	-54.97	24.20
5s	5.62	5.86	13.44	12.34	-60.08	13.24
10s	4.19	4.32	9.45	7.82	-62.00	7.36

For intra-site CA transmission scenarios, the novel measurement method demonstrates improved performance in approximately half of the test cases compared to the standard method. For instance, for file sizes between 100 kB and 500 kB, the improvement ranges from 9.13% to 36.66%, while for file sizes exceeding 20 MB, the improvement ranges from 1.1% to 6.67%. However, the standard method exhibits superior performance for file sizes ranging from 1 MB to 20 MB, with improvements ranging from 5.26% to 40.86%. Direct comparison of these test cases is challenging due to the distinct traffic management and distribution characteristics inherent to the two flow control algorithms. The relative error results are higher than for single-cell transmission scenarios for file sizes higher than 500 kB. For example, the relative error difference for a 2 MB file size is 198.81% for the novel method and 181.2% for the standard method.

In inter-site CA transmission scenarios, with the flow control enhancement algorithm enabled by default, the novel method demonstrates superior performance for file sizes exceeding 20 MB compared to the standard method. For example, for file sizes exceeding 20 MB, the improvement for relative error ranges from 30.77% to 54.64%. Conversely, for file sizes ranging from 200 kB to 10 MB, the standard method exhibits an advantage with lower relative error values, ranging from 16.78% to 86.28%. This discrepancy arises from the standard method's inaccurate data volume calculation, which only accounts for a portion of the PCell data and excludes SCell data. Consequently, the standard method's quotient of counted data volume and time components more closely approximates the application layer throughput reference. More details about data volume and time component values are present in Appendix 1. Despite these exceptions, the standard method is incapable of accurately measuring IP scheduled throughput for larger file sizes exceeding 20 MB, consistently showing relative error values ranging from -45.48% to -62%.

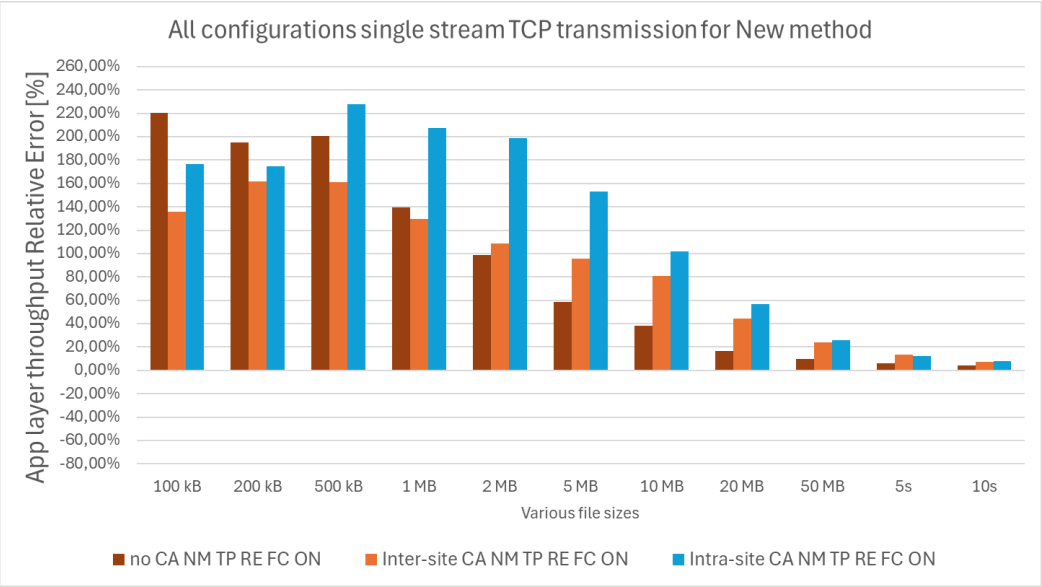

Figure 5.8: TCP/IP single stream transmission traffic across all network configurations with relative error for new method.

Figures 5.8 and 5.9 present graphical representations of the data for all connection types, comparing the performance of the new and standard methods. These figures highlight the diminished accuracy of the standard method in inter-site CA network configurations. For instance, during a 50 MB file size transmission, the standard method exhibits relative error of -54.97%. Conversely, the novel method demonstrates significantly improved accuracy, achieving relative error of 24.2% for the same transmission parameters. Furthermore, the results demonstrate that the novel method exhibits no significant performance degradation in non-DC environment configurations compared to the standard method. For example, for 10 MB file size, the novel method achieves relative errors of 38.01% for a single-cell configuration and 102.05% for an intra-site CA configuration. In contrast, the standard method exhibits relative errors of 36.5% and 96.79% for the same transmission configurations, respectively.

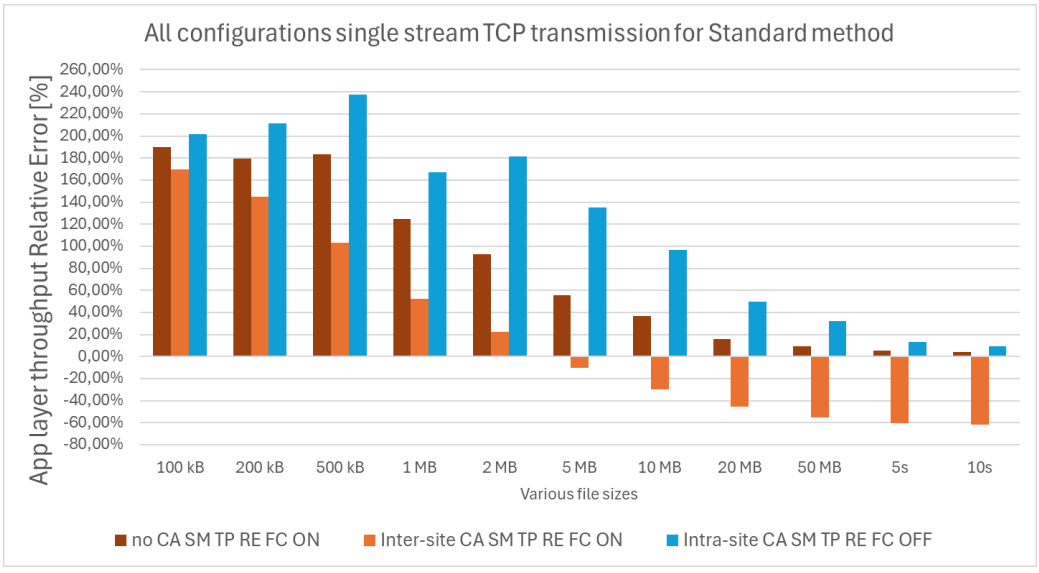

Figure 5.9: TCP/IP single stream transmission traffic across all network configurations with relative error for standard method.

This study investigated the performance of the novel measurement method in various transmission scenarios using single-stream TCP, comparing it to the standard method employing an application layer throughput reference point. In single-cell transmission scenarios, the standard method, consistent with findings in Chapter 5.3.1.1, outperformed the novel method for smaller file sizes, although the difference became negligible for larger files. In intra-site carrier aggregation (CA), the novel method generally exhibited superior performance, particularly for smaller files, while the standard method demonstrated comparable results for larger files. In inter-site CA, the novel method generally performed better, especially for larger files exceeding 20 MB. Interestingly, the standard method exhibited surprisingly accurate results for files between 500 kB and 10 MB, attributed to its fractional data counting methodology. However, the results indicate that for small file transmissions, the IP scheduled throughput measurement exhibits significant discrepancies compared to the application layer throughput, as perceived by the end-user. This discrepancy is particularly pronounced in intra-site CA scenarios, where the relative error for 1 MB file sizes reaches 207.74%. Consequently, the cell's throughput serves as a more reliable reference point, demonstrating a relative error of 18.39% in analogous scenario.

5.3.2. Fast transmission using multi-TCP streams

This study aims to validate the accuracy of IP scheduled throughput measurement in a multi-burst scenario for TCP multi-stream transmission across various UE-level connection types. A multiple TCP streams will be employed to simulate a scenario characterized by fast data transmission. Specifically, the investigation focuses on three connection configurations: single-cell, intra-site carrier aggregation (non-DC), and inter-site carrier aggregation (DC).

Despite the prevalence of single-stream TCP connections in contemporary network traffic, a notable shift towards multi-stream TCP is underway. This evolution is propelled by the increasing demands of high-bandwidth applications, such as video streaming, and the concurrent development of novel algorithms and techniques aimed at enhancing TCP efficiency [29, 30, 31, 32, 34, 44, 45]. Platforms such as Netflix and YouTube utilize predetermined multi-stream TCP connections during the initial handshake phase, where the server's application layer dictates the number of streams for optimal transmission based on device capabilities and network conditions. This dynamic approach allows for adaptive stream management, adjusting the number of streams over time to optimize performance [41]. Research indicates that the proportion of multi-stream TCP usage is projected to increase significantly in the future [29]. This shift is motivated by the limitations of single-stream TCP in keeping pace with the escalating throughput capabilities of modern devices, particularly mobile phones relying on radio connectivity. Single-stream TCP struggles to fully utilize the available bandwidth, leading to inefficient resource utilization, especially for small file transfers. Moreover, the challenges of TCP performance in mobile broadband networks like LTE are highlighted in [33], despite the significant growth in mobile internet usage. The study investigates the behavior of different TCP implementations under various network conditions, including varying network loads, flow types, start-up phases, and mobility scenarios. CUBIC, a specific TCP variant, exhibits a slower start-up phase due to its Hybrid Slow-Start mechanism, hindering efficient resource utilization in short transmission

sessions. The paper [33] concludes that further research is needed to optimize TCP performance in mobile networks, particularly in dynamic and challenging environments.

Emerging research focuses on enhancing the efficiency of TCP-based communication between servers and receivers by exploring the potential of multi-stream TCP based on different implementations:

- The increasing volume of TCP/IP traffic necessitates the development of faster network systems. Research [29] proposes the novel approach called simultaneous TCP multi-streaming, which combines multiple TCP streams across different IP domains to enhance data transfer rates. This system leverages a virtual network switch to manage packets from multiple network interface cards (NICs), aligning with the concept of software-defined networking (SDN), a key technology for future networks like 5G. Experimental validation on a local network demonstrates a significant improvement in communication rate, supporting the effectiveness of the proposed multi-streaming system.
- The benefits of per-packet multipath routing for maximizing network capacity are highlighted in [30], but its incompatibility with TCP is acknowledged. To bridge this gap, the authors propose Multi-Stream TCP (MSTCP), a protocol that enables TCP applications to leverage the performance advantages of per-packet multipath routing.
- Research [31] explores the feasibility and advantages of allowing a single TCP connection to support multiple streams through distinct sockets, focusing on enhancing the efficiency of concurrent web transactions.
- A proxy-based solution for adapting scalable video streams at the edge of a wireless network is presented in [32], capable of responding quickly to highly dynamic wireless links. The scheme supports differentiated services for different streams and competes fairly with TCP flows, demonstrating a connection to multi-stream concepts.
- The limitations of traditional TCP in high-speed networks, where its slow response to large bandwidth leads to inefficient utilization, are addressed in [34]. The paper proposes a new transport protocol called DMS-TCP, which utilizes multiple simultaneous streams to achieve scalability, fairness, and friendliness in high-speed environments. DMS-TCP dynamically adjusts the number of streams based on network conditions.

The collective findings of these studies strongly suggest that the future of network communication lies in the adoption of multi-stream TCP. Moreover, emerging research endeavors are exploring new approaches to enhance TCP/IP transfer speed over the internet. It is anticipated that wireless networks will eventually fully realize their inherent throughput potential, leveraging these advancements to achieve more efficient data transmission. This trend underscores the importance of providing multi-stream TCP test results for the accuracy of the novel method, as highlighted in this dissertation.

Multi-stream TCP transmissions, characterized by the simultaneous transmission of multiple data streams, exhibit segmentation and delay characteristics comparable to single-stream transmissions. However, this similarity is transient, persisting only for a brief period before the receiver's buffer reaches saturation at a significantly accelerated rate. This accelerated

saturation is attributed to the increased data influx from multiple streams, leading to a rapid depletion of buffer capacity. Consequently, the sender's transmission rate adapts to mitigate congestion, resulting in a divergence from the initial single-stream-like behavior. This adaptation, coupled with the accelerated saturation, brings the performance of multi-stream TCP closer to that of UDP.

The described logic is shown in Figure 5.10 below, where TCP is used to send 1 MB (consisting of 685 IP packets with MTU 1460) of data from the iperf server to the end-user, similarly as for single stream transmission. The number of packets transmitted is represented by the rectangles within the figure, with various colors depending on the packet arrival time at eNB. TCP ACK denotes the acknowledgment of individual packets by the network, while HARQ ACK signifies the user's confirmation of successful reception of a specific TB. The time interval during which the eNB buffer is occupied by incoming data for a single user is denoted as “burst”. This represents the time the eNB is actively processing data for that particular user. *ThpTimeDl* represents the time component value, given as t1, associated with the IP scheduled throughput method. This value accounts for the time taken to process and transmit data according to the IP scheduling algorithm. The active TTI represents the eNB's scheduling time, serving as a reference point for cell throughput. This interval defines the time frame within which the eNB schedules and transmits data to users. Finally, the application layer perspective describes the transmission time from the user's point of view. This perspective considers the time it takes for the user to perceive the data transmission, including factors such as network latency and application processing time.

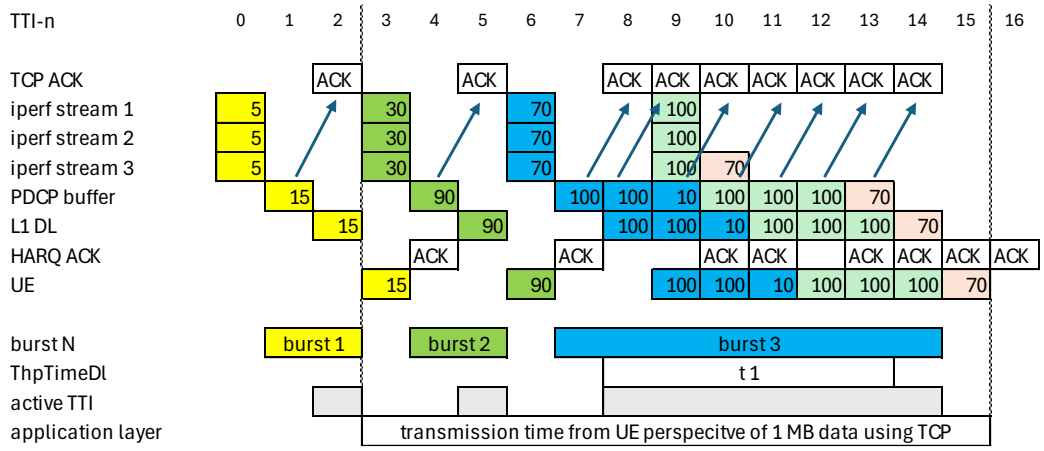

Figure 5.10: TCP/IP packet transmission process with multiple parallel streams via RAN with burst transmission logic.

To facilitate analysis, the initial IP packet transmission rate to the eNB was incrementally increased. Following the reception of the first 15 ACK messages, the rate was adjusted from 15 to 90 packets, subsequently from 90 to 210 packets, and finally from 210 to 370 remaining packets. To demonstrate the saturation effect of RAN throughput capabilities and facilitate accurate measurement by 3GPP methods, the packet rate at L1 was artificially limited to 100 packets per Transport Block. This constraint extended the duration of bursts in the PDCP layer, enabling measurement by 3GPP methods, which do not account for single TTIs or the final TTI within a burst. The example is also used to demonstrate that *ThpTimeDl* shall deviate from the actual transmission time. This difference is closer to the user's perception compared to single

stream transmission but still lags behind the rate achievable with UDP. This example, utilizing three parallel data streams (-P3 command in iperf3), reveals that the *ThpTimeDl* metric occupies 46% of the total transmission time from the user's perspective. This represents an 85% enhancement in accuracy compared to single-stream transmission for equivalent file sizes. Furthermore, from the eNB perspective, *ThpTimeDl* accounts for 67% of the transmission time, indicating a notable improvement of 50% in accuracy relative to single-stream transmission. The active TTIs constitute 69% of the total transmission time from application layer perspective.

Figure 5.11 presents a comparative analysis of file transmission using an inter-site CA connection versus a single cell configuration, maintaining the same file size as in Figure 5.10. The data volume from the MeNB PDCP buffer is transferred to the RLC layer, where it is subsequently divided into two distinct sub-buffers: MeNB RLC and SeNB RLC, as detailed in Chapter 4.4.1 and Figure 4.7. Each of the MeNB and SeNB possesses a separate L1 DL instance, visually depicted within the graph. The time component calculation, based on the SeNB RLC buffer, is estimated using the $T_{RLC'}$, parameter defined in Equation 4.6. In contrast to Figure 5.4, the *ThpTimeDl* value is determined with greater accuracy, a direct consequence of employing the estimation logic derived from the novel method and the burst time calculation change described in Chapter 4.5. This enhanced precision facilitates a more accurate accounting of the time component during the transmission of small file transfers that meet 3GPP requirements for IP scheduled throughput.

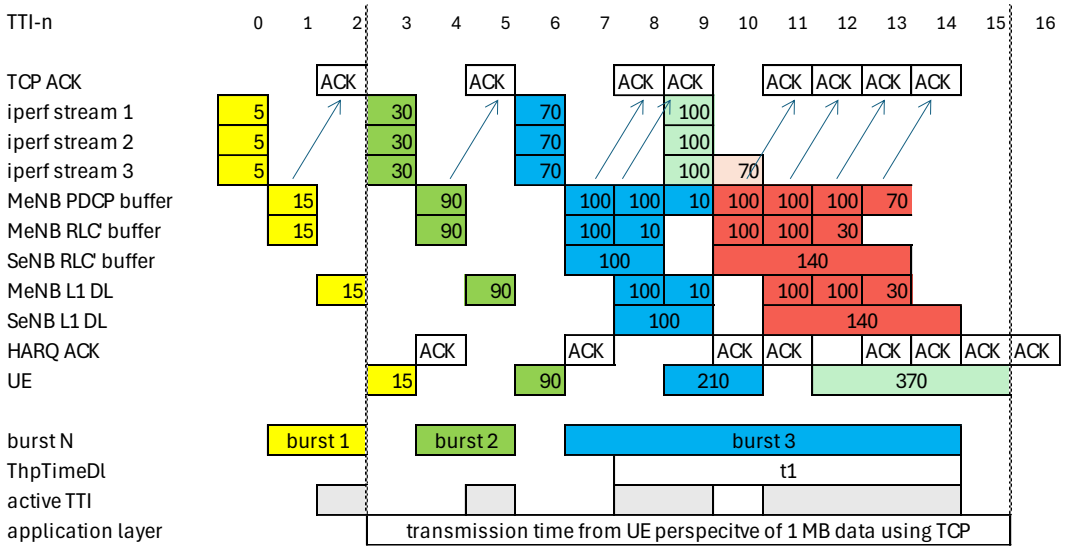

Figure 5.11: TCP/IP packet transmission process with 3 multi stream via inter-site CA with burst transmission logic of the novel method.

Figure 5.11 highlights a significant discrepancy between *ThpTimeDl* and the actual transmission time. In this scenario, *ThpTimeDl* accounts for 54% of the transmission time from the user's perspective and 88% from the eNB perspective. The 3GPP standard mandates the exclusion of single TTIs and the final TTIs within each burst, defined as a sequence of at least two consecutive TTIs, from the calculation. Consequently, bursts 1-2, characterized by single TTI transmission and no CA splitting due to small data volumes, do not contribute to the time constituent as the last TTIs are excluded. Conversely, burst 3, requiring 6 TTIs for user

transmission, meet the inclusion criteria. This observed deviation represents an improvement compared to the previously analyzed single cell scenario where the last TTI of burst 3 was subtracted, demonstrating the impact of inter-site CA on the accuracy of *ThpTimeDl* measurement.

The subchapters below present a comparative analysis of IP scheduled throughput measurement implementation, evaluating the novel approach against the standard method and two reference points: cell throughput and application layer throughput. The analysis is conducted within a multi-burst scenario using TCP multi-stream transmission across various UE-level connection types and file sizes. The primary objective is to assess the impact of the TCP slow start phenomenon on the precision of IP scheduled throughput measurement. Multi-stream TCP transmission is employed to mitigate the slow start effect, enabling a direct comparison with single-stream transmission. Multi-stream transmission type necessitates faster eNB buffer occupancy, reducing the number of small bursts at the transmission initiation and potentially enhancing measurement accuracy by increasing the likelihood of meeting 3GPP criteria. Furthermore, the influence of the TCP slow start mechanism diminishes as the transmitted file size increases. Comprehensive descriptions of each test case, including data volume and time component results, are presented in Appendix 2.

5.3.2.1. Summary - Cell's throughput as a reference point

Tables 5.6-5.8 present a comparative analysis of the relative error in estimation of cell throughput for various transmission file sizes, considering both the standard method and the new approach, for different multi-TCP streams. The analysis encompasses three transmission types: single cell, intra-site CA, and inter-site CA, all utilizing multi stream TCP/IP protocol. Table 5.6 utilizes 2 multi stream transmission, Table 5.7 utilizes 8 multi stream transmission and Table 5.8 utilizes 16 multi stream transmission.

Table 5.6: Cell's throughput relative error comparison between the two methods for all connection types for 2MS TCP.

File sizes	No CA		Intra-site CA		Inter-site CA	
	FC ON	FC ON	FC OFF	FC ON	FC ON	FC ON
	SM TP RE [%]	NM TP RE [%]	SM TP RE [%]	NM TP RE [%]	SM TP RE [%]	NM TP RE [%]
100 kB	134.76	151.03	44.72	57.64	10.20	60.50
200 kB	111.43	123.86	43.16	51.59	-0.06	18.90
500 kB	58.32	62.29	25.69	34.98	-21.95	22.60
1 MB	33.17	37.85	20.07	22.55	-29.65	17.34
2 MB	16.67	21.25	6.58	12.44	-44.13	11.29
5 MB	8.24	9.44	2.41	9.48	-50.16	8.39
10 MB	4.35	5.02	5.52	5.90	-56.91	5.16
20 MB	2.16	2.49	2.58	3.37	-59.49	4.78
50 MB	0.89	1.03	0.93	1.49	-63.38	1.48
5s	0.93	1.07	0.63	0.68	-63.80	0.76
10s	0.40	0.48	0.35	0.33	-63.93	0.52

Table 5.7: Cell's throughput relative error comparison between the two methods for all connection types for 8MS TCP.

File sizes	No CA		Intra-site CA		Inter-site CA	
	FC ON	FC ON	FC OFF	FC ON	FC ON	FC ON
	SM TP RE [%]	NM TP RE [%]	SM TP RE [%]	NM TP RE [%]	SM TP RE [%]	NM TP RE [%]
100 kB	N/A	N/A	N/A	N/A	N/A	N/A
200 kB	40.59	40.26	38.24	33.76	-24.64	25.47
500 kB	34.47	34.38	29.35	35.30	-32.77	20.60
1 MB	26.74	26.85	29.47	24.36	-40.98	23.76
2 MB	17.28	17.32	16.72	19.60	-48.30	18.26
5 MB	8.52	8.56	10.40	14.92	-55.01	10.38
10 MB	4.50	4.57	6.10	5.46	-60.25	4.51
20 MB	2.40	2.41	2.90	2.78	-61.99	2.25
50 MB	0.96	0.96	1.24	1.16	-63.33	1.14
5s	0.93	0.95	0.59	0.59	-63.20	0.62
10s	0.52	0.54	0.34	0.29	-64.16	0.31

Table 5.8: Cell's throughput relative error comparison between the two methods for all connection types for 16MS TCP.

File sizes	No CA		Intra-site CA		Inter-site CA	
	FC ON	FC ON	FC OFF	FC ON	FC ON	FC ON
	SM TP RE [%]	NM TP RE [%]	SM TP RE [%]	NM TP RE [%]	SM TP RE [%]	NM TP RE [%]
100 kB	N/A	N/A	N/A	N/A	N/A	N/A
200 kB	30.99	30.79	33.64	33.85	-37.06	27.42
500 kB	27.39	27.25	32.75	30.52	-38.65	21.85
1 MB	24.26	24.05	25.63	26.86	-43.18	24.47
2 MB	17.47	17.35	21.03	20.61	-47.06	19.04
5 MB	10.32	10.26	11.86	12.44	-54.21	10.05
10 MB	5.89	5.89	8.12	7.36	-58.35	7.13
20 MB	2.97	2.94	4.12	4.04	-61.16	3.26
50 MB	1.51	1.52	1.68	1.73	-62.93	1.53
5s	1.21	1.23	0.89	0.88	-63.90	0.78
10s	0.65	0.66	0.43	0.45	-63.80	0.34

In single-cell transmission with 2MS transmission, the standard method exhibits lower relative error values across all file sizes compared to the novel approach when flow control is enabled. However, the difference in precision between the two methods becomes negligible for file sizes exceeding 10 MB, as the relative error difference between the two methods is less than 0.33%. Notably, 2MS transmission demonstrates lower precision than SS transmission for files between 100 kB and 2 MB. For instance, the relative error difference for a 200 kB file size is 72.64% for SS and 123.86% for 2MS, while for a 2 MB file size, it is 17.53% for SS and 21.25% for 2MS. For 8MS and 16MS TCP transmission, the relative error results for small file sizes are significantly lower than for SS or 2MS, positively impacting burst length interpretation and consequently throughput assessment. For example, the relative error for a 200 kB file size is 40.26% for 8MS and 30.79% for 16MS. However, for file sizes exceeding 1 MB, no discernible difference exists between 8MS and 16MS transmission, suggesting that satisfactory buffer occupancy is achieved with 8MS for the majority of file sizes.

In intra-site CA transmission with 2MS transmission, the standard method demonstrates improved performance in comparison to the novel method. The difference in performance

between the standard and novel methods diminishes for 8MS and 16MS transmission, resulting in comparable outcomes. While the relative error measured for the standard method is comparable to the new method across repeated tests and file sizes, direct comparison is challenging due to the differing ways in which the flow control algorithms manage and distribute incoming traffic volume. However, faster and more efficient eNB buffer fulfillment leads to comparable results between the two methods. An enhancement in measurement precision is evident with an escalation in the quantity of TCP streams for file sizes inferior to 500 kB. For instance, the novel methods relative error for a 200 kB file size with 2MS transmission attains 51.59%, whereas with 8MS transmission, it reduces to 33.76%. Conversely, for file sizes exceeding 500 kB, no discernible improvement is observed when transitioning from 8MS to 16MS transmission. As an illustration, the novel method's relative error for a 2 MB file size with 8MS transmission achieves 19.6%, while with 16MS transmission, it marginally increases to 20.61%.

In inter-site CA transmission with the flow control enhancement algorithm enabled by default, the novel method consistently demonstrates favorable results in most cases. However, for 2MS transmission with file sizes of 100 kB and 200 kB, the standard method exhibits a lower relative error. This discrepancy arises from the standard method's erroneous counting of only a portion of the PCell data and no SCell data volume and portion of burst time component, resulting in a quotient closer to the cell's throughput reference. Despite these exceptions for 2MS, the standard method fails to accurately measure the IP scheduled throughput value for file sizes of 500 kB and above. For 8MS and 16MS transmission, the standard method is unable to provide meaningful results for any file size. The novel method not only surpasses the standard method in the same inter-site CA configuration but also exhibits comparable results to intra-site CA or single-cell configurations. For instance, during a 5-second transmission for inter-site CA, the novel method achieves relative errors of 0.76%, 0.62%, and 0.78% for 2MS, 8MS, and 16MS, respectively. In contrast, the standard method exhibits significantly higher relative errors of -63.93%, -64.16%, and -63.8% for the same transmission parameters. Notably, the novel method achieves relative errors of 1.07%, 0.95%, and 1.23% for a single-cell connection and 0.68%, 0.59%, and 0.88% for an intra-site CA connection, respectively.

Figures 5.10-5.15 present a graphical comparison of performance metrics for all connection types, separately illustrating the results obtained using the new method and the standard method, in comparison to cell throughput as a reference point. These figures highlight the diminished accuracy of the standard method when applied to inter-site CA network configurations. For instance, during a 50 MB file size transmission, the standard method exhibits relative errors of -62.96%, -63.33%, and -62.93% for 2MS, 8MS, and 16MS, respectively. Conversely, the novel method demonstrates significantly improved accuracy, achieving relative errors of 1.48%, 1.14%, and 1.53% for the same transmission parameters. Furthermore, the results demonstrate that the novel method exhibits no significant performance degradation in non-DC environment configurations compared to the standard method. For example, with a 16MS transmission and a 10 MB file size, the novel method achieves relative errors of 7.13% for a single-cell configuration and 7.36% for an intra-site CA configuration. In contrast, the standard

method exhibits relative errors of 5.89% and 8.12% for the same transmission configurations, respectively.

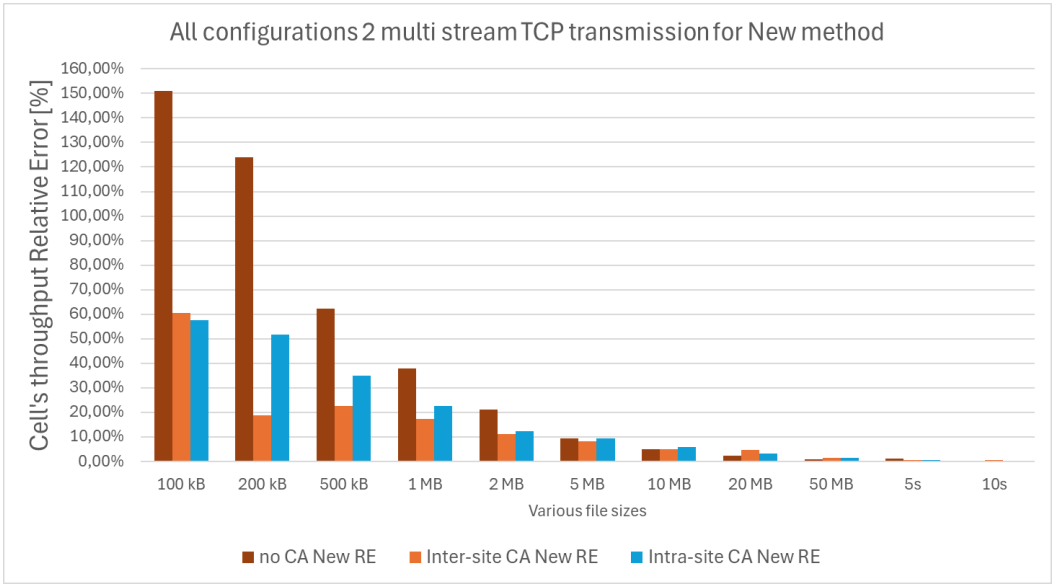

Figure 5.10: TCP/IP 2 stream transmission traffic across all network configurations with relative error for new method.

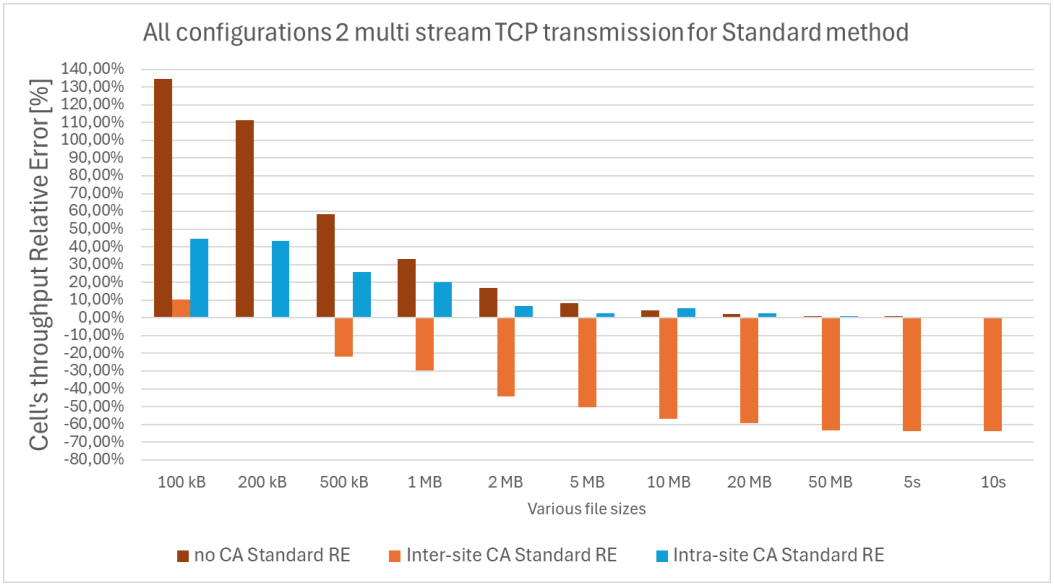

Figure 5.11: TCP/IP 2 stream transmission traffic across all network configurations with relative error for standard method.

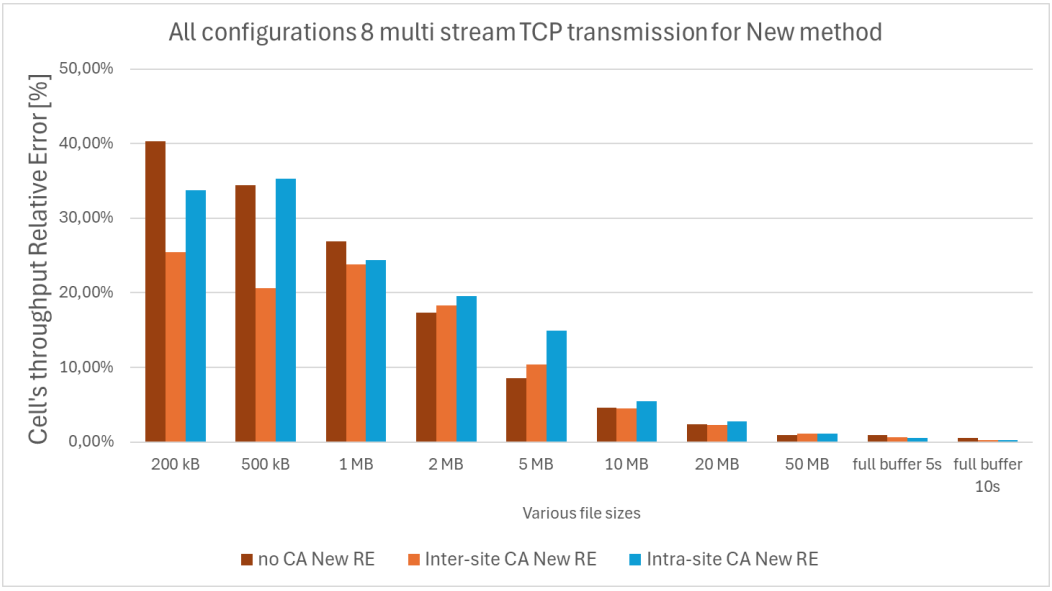

Figure 5.12: TCP/IP 8 stream transmission traffic across all network configurations with relative error for new method.

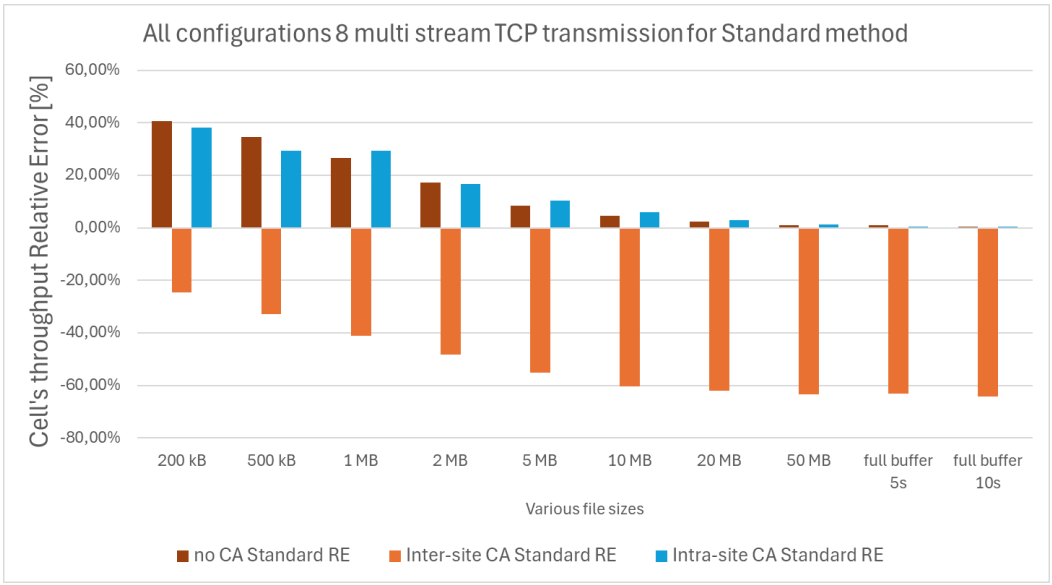

Figure 5.13: TCP/IP 8 stream transmission traffic across all network configurations with relative error for standard method.

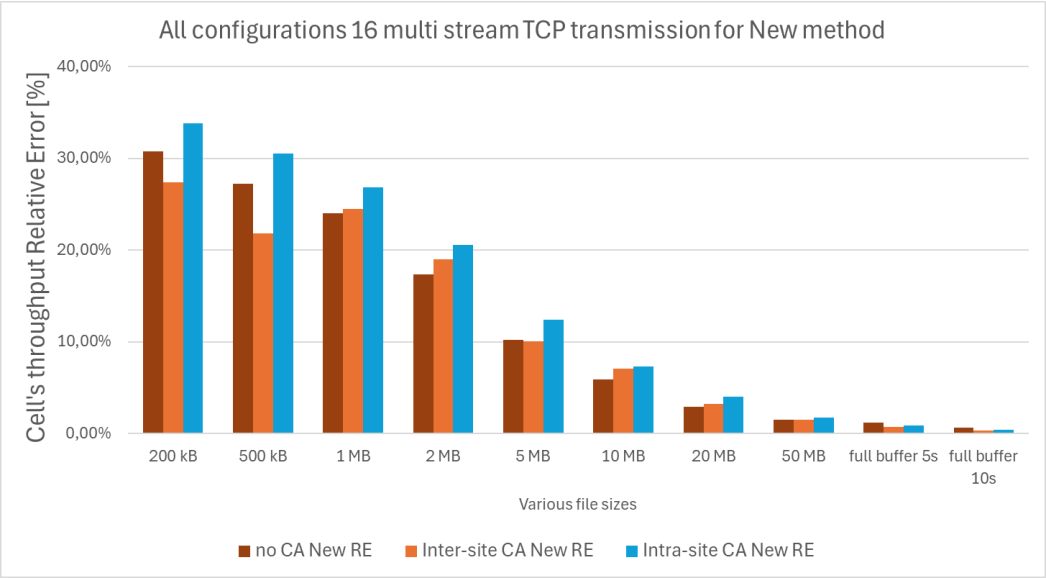

Figure 5.14: TCP/IP 16 stream transmission traffic across all network configurations with relative error for new method.

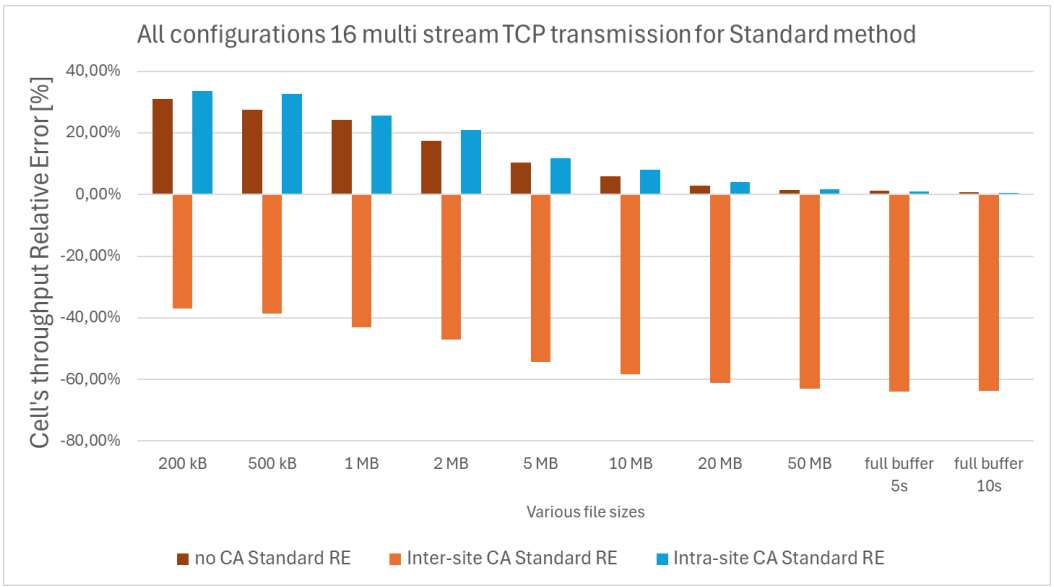

Figure 5.15: TCP/IP 16 stream transmission traffic across all network configurations with relative error for standard method.

5.3.2.2. Summary - Application layer throughput as a reference point

Tables 5.9-5.11 present a comparative analysis of the relative error in estimation of application layer throughput for varying transmission file sizes for different multi-TCP streams. The analysis encompasses the standard and the new method, across three distinct transmission types: single cell, intra-site CA, and inter-site CA. All transmissions utilize a single stream TCP/IP protocol. Table 5.9 utilizes 2 multi stream transmission, Table 5.10 utilizes 8 multi stream transmission and Table 5.11 utilizes 16 multi stream transmission. Due to unreasonable values exhibited by the iperf application on the UE, certain results could not be obtained and were marked as not applicable (N/A).

Table 5.9: Application layer throughput relative error comparison between the two methods for all connection types for 2MS TCP.

File sizes	No CA		Intra-site CA		Inter-site CA	
	FC ON	FC ON	FC OFF	FC ON	FC ON	FC ON
	SM TP RE [%]	NM TP RE [%]	SM TP RE [%]	NM TP RE [%]	SM TP RE [%]	NM TP RE [%]
100 kB	61.91	73.13	63.94	72.99	7.67	56.81
200 kB	82.69	93.43	78.07	109.38	23.02	46.35
500 kB	71.85	76.16	97.84	142.64	12.05	76
1 MB	66.83	72.69	111.6	132.65	15.94	93.39
2 MB	40.56	46.09	88.46	115.26	-10.42	78.45
5 MB	23.73	25.11	73.75	84.26	-28.14	56.28
10 MB	13.49	14.22	47.2	57.24	-39.05	48.73
20 MB	9.67	10.03	30.56	31.82	-50.96	26.85
50 MB	6.35	6.5	14.89	15.29	-59.42	12.46
5s	2.08	2.22	7.31	6.57	-61.85	6.18
10s	3.87	3.95	5.39	5.46	-61.86	6.3

Table 5.10: Application layer throughput relative error comparison between the two methods for all connection types for 8MS TCP.

File sizes	No CA		Intra-site CA		Inter-site CA	
	FC ON	FC ON	FC OFF	FC ON	FC ON	FC ON
	SM TP RE [%]	NM TP RE [%]	SM TP RE [%]	NM TP RE [%]	SM TP RE [%]	NM TP RE [%]
100 kB	N/A	N/A	N/A	N/A	N/A	N/A
200 kB	N/A	N/A	N/A	N/A	-33.44	10.81
500 kB	N/A	N/A	0.05	19.39	-41.05	5.76
1 MB	-10.09	-10.01	9.46	11.02	-51.02	2.72
2 MB	-11.07	-11.04	-0.87	14.66	-55.09	2.73
5 MB	-2.32	-2.27	4.68	6.36	-56.80	5.99
10 MB	0.27	0.33	5.91	9.74	-59.69	5.98
20 MB	2.66	2.67	4.73	3.97	-61.27	4.18
50 MB	3.20	3.20	4.08	4.22	-62.14	4.44
5s	-0.59	-0.56	1.04	0.85	-62.85	1.59
10s	2.00	2.01	2.98	3.12	-63.38	2.52

Table 5.11: Application layer throughput relative error comparison between the two methods for all connection types for 16MS TCP.

File sizes	No CA		Intra-site CA		Inter-site CA	
	FC ON	FC ON	FC OFF	FC ON	FC ON	FC ON
	SM TP RE [%]	NM TP RE [%]	SM TP RE [%]	NM TP RE [%]	SM TP RE [%]	NM TP RE [%]
100 kB	N/A	N/A	N/A	N/A	N/A	N/A
200 kB	N/A	N/A	N/A	N/A	-63,97	-27,05
500 kB	N/A	N/A	N/A	N/A	-59,06	-18,70
1 MB	-34,78	-34,89	N/A	N/A	-61,14	-14,86
2 MB	-28,99	-29,06	N/A	N/A	-59,85	-9,71
5 MB	-10,82	-10,87	N/A	N/A	-62,86	-10,74
10 MB	-3,79	-3,79	-2,60	1,65	-61,90	-1,98
20 MB	-0,27	-0,30	0,34	0,57	-62,02	0,97
50 MB	1,86	1,86	3,39	2,51	-62,82	1,83
5s	-2,37	-2,35	0,01	-0,11	-64,11	0,20
10s	2,52	2,53	2,79	2,64	-63,11	2,26

In single-cell transmission with a 2MS configuration, the standard method consistently demonstrates lower relative error values across all file sizes compared to the novel method with flow control enabled. However, the precision difference between the two methods becomes negligible for file sizes exceeding 5 MB, with a relative error difference of less than 0.73%. For 8MS and 16MS transmission, no significant difference exists between the results of both methods, with a relative error difference of less than 0.11%. A general improvement in measurement accuracy is observed with an increase in the number of TCP streams. However, for 16MS transmission, an increased underestimation of relative error is observed between 1 MB and 5 MB, almost three times higher than for 8MS. For instance, the relative error of the novel method for a 1 MB file size is 139.74% for SS, 72.69% for 2MS, -10.01% for 8MS, and -34.89% for 16MS. This discrepancy arises from the iperf application overestimating the achieved throughput value relative to the given cell's capacity to transmit at maximum throughput. Furthermore, for 8MS and 16MS TCP transmission, the relative error results for file sizes larger than 5 MB are also lower than for SS or 2MS, positively impacting burst length interpretation and consequently throughput assessment. For example, the relative error for a 10 MB file size is 38.01% for SS, 14.22% for 2MS, 0.33% for 8MS, and -3.79% for 16MS. Even for full buffer transmission duration of 10s, the relative error is still improved for 8MS and 16MS, resulting in 4.32% for SS, 3.95% for 2MS, 2.01% for 8MS, and 2.53% for 16MS.

In intra-site CA transmission scenarios employing 2MS and 8MS configurations, the standard method exhibits improved performance compared to the novel method for a majority of file sizes. Specifically, for file sizes ranging from 100 kB to 2 MB, the relative error difference between the standard and novel methods is between 9.05% and 44.8% for 2MS, and between 1.56% and 19.34% for 8MS. However, the precision difference between the two methods becomes negligible for file sizes exceeding 10 MB for both 2MS and 8MS, with a relative error difference of less than 1.26% and 0.76%, respectively. The slight advantage in relative error observed for the standard method diminishes for 16MS transmission, resulting in comparable outcomes with a slight advantage for the novel method. For instance, for a 10 MB file transfer, the relative error achieved for the standard method is -2.6%, while the novel method achieves 1.65%. While the relative error measured for the standard method is comparable to the novel method across repeated tests and file sizes, direct comparison is challenging due to the differing ways in which the flow control algorithms manage and distribute incoming traffic volume. However, faster and more efficient eNB buffer fulfillment leads to comparable results between the two methods. Additionally, a general improvement in measurement accuracy is observed with an increase in the number of TCP streams. For example, for the novel method, the relative error for a 10 MB file size is 102.05% for SS, 57.24% for 2MS, 9.74% for 8MS, and 1.65% for 16MS. Even for full buffer transmission durations of 10 seconds, the relative error is still improved for 8MS and 16MS, resulting in 7.82% for SS, 5.46% for 2MS, 3.12% for 8MS, and 2.64% for 16MS.

In inter-site CA transmission scenarios with the flow control enhancement algorithm enabled by default, the novel method consistently demonstrates favorable results for 8MS and 16MS configurations. The relative error difference between the novel and standard methods

ranges from 22.63% to 61.26% for 8MS and 36.92% to 63.91% for 16MS across all file sizes for the favor of the novel method. Furthermore, the relative error value for the novel method for 8MS is less than 6% for file sizes greater than 200 kB, while for 16MS it is less than 2.27% for file sizes greater than 5 MB. Interestingly, 16MS transmission exhibits reduced accuracy compared to 8MS, with an underestimation of throughput value for file sizes between 200 kB and 5 MB. However, for 2MS transmission with file sizes up to 20 MB, the standard method exhibits a lower relative error. For instance, for a 2 MB file size, the relative error for the standard method reaches -10.42%, while for the novel method it is 78.45%. This discrepancy arises from the standard method's erroneous counting of only a portion of the PCell data, no SCell data volume, and a portion of the burst time component, resulting in a quotient closer to the application layer throughput reference. Despite these exceptions for 2MS, the standard method fails to accurately measure the IP scheduled throughput value for larger file sizes (20 MB and above). For 8MS and 16MS transmission, the standard method is unable to provide meaningful results for any file size. For example, for a file size of 20 MB, the standard method relative error shows -50.96% for 2MS, -61.27% for 8MS, and -62.02% for 16MS. The novel method not only surpasses the standard method in the same inter-site CA configuration but also exhibits improved performance compared to intra-site CA or single-cell configurations. Additionally, a general improvement in measurement accuracy is observed with an increase in the number of TCP streams. For example, for the novel method, the relative error for a 10 MB file size is 80.89% for SS, 48.73% for 2MS, 5.98% for 8MS, and -1.98% for 16MS. Even for full buffer transmission durations of 10 seconds, the relative error is still improved for 8MS and 16MS, resulting in 7.36% for SS, 6.3% for 2MS, 2.52% for 8MS, and 2.26% for 16MS.

Figures 5.16-5.21 present graphical representations of the data for all connection types, comparing the performance of the new and standard methods for various multi-TCP streams. These figures highlight the diminished accuracy of the standard method when applied to inter-site CA network configurations. Furthermore, the results demonstrate that the novel method exhibits small performance degradation in non-DC environment configurations compared to the standard method for small file sizes.

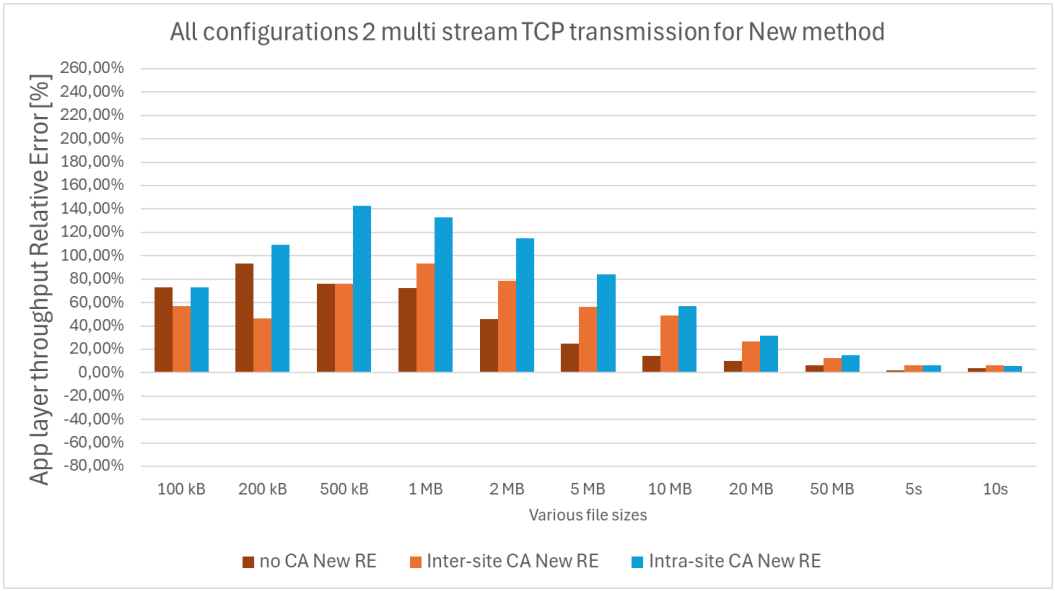

Figure 5.16: TCP/IP 2 stream transmission traffic across all network configurations with relative error for new method.

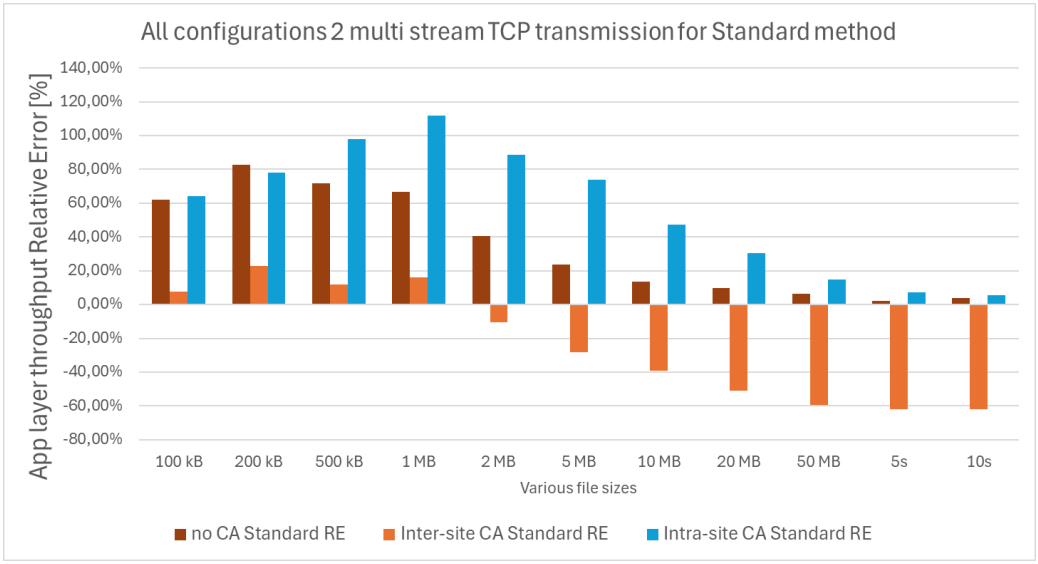

Figure 5.17: TCP/IP 2 stream transmission traffic across all network configurations with relative error for standard method.

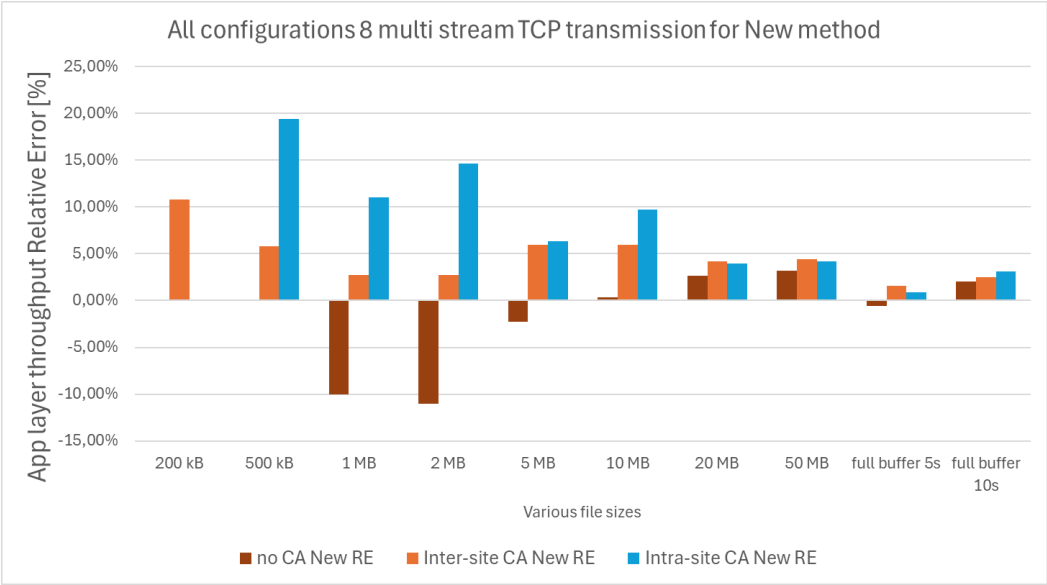

Figure 5.18: TCP/IP 8 stream transmission traffic across all network configurations with relative error for new method.

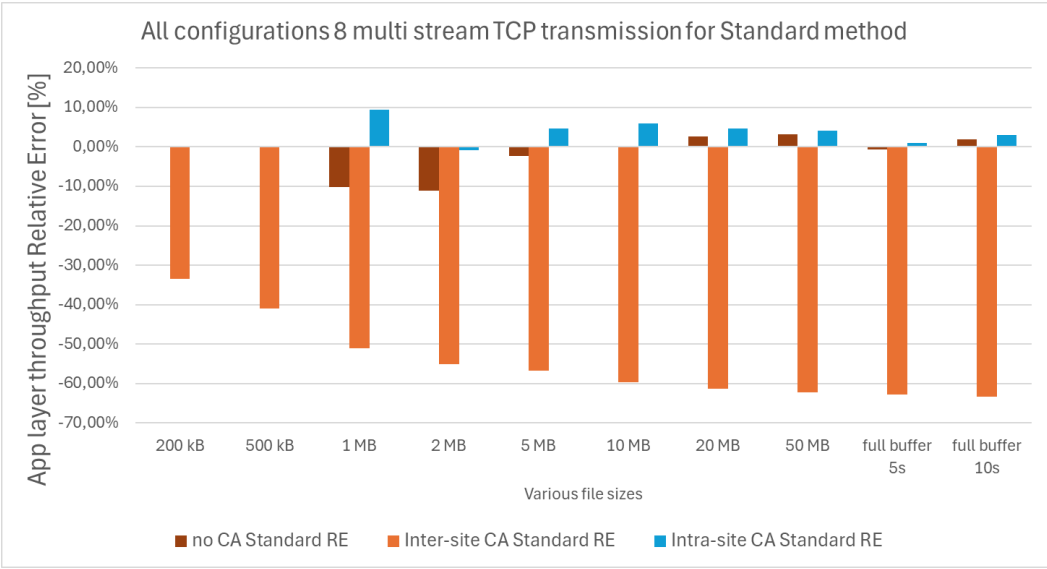

Figure 5.19: TCP/IP 8 stream transmission traffic across all network configurations with relative error for standard method.

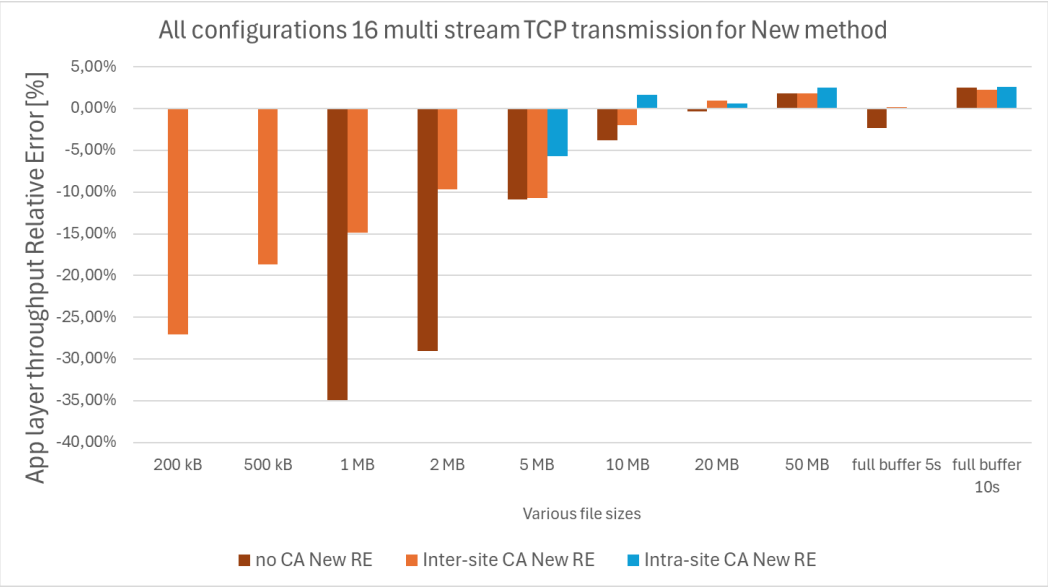

Figure 5.20: TCP/IP 16 stream transmission traffic across all network configurations with relative error for new method.

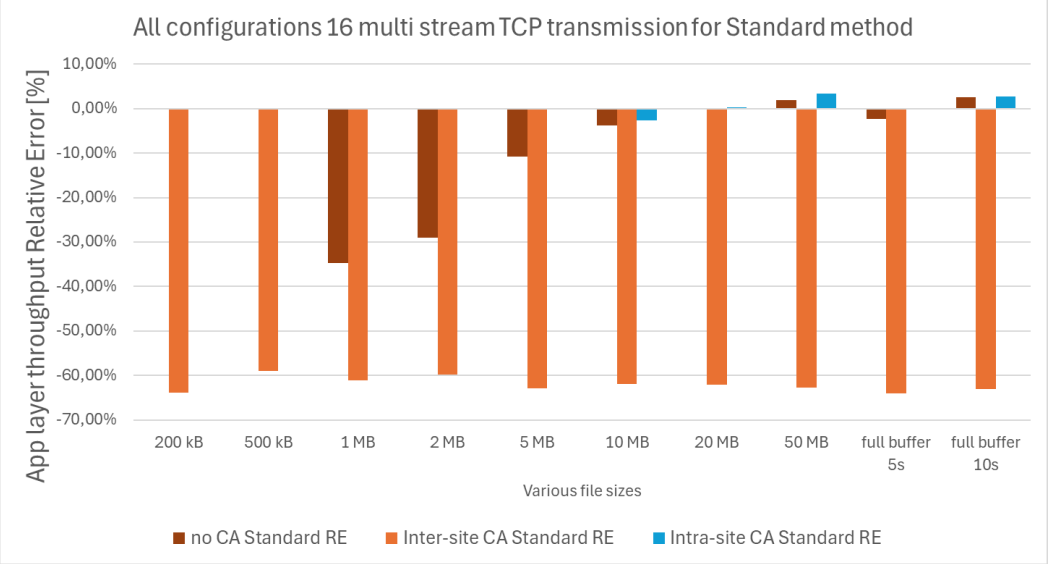

Figure 5.21: TCP/IP 16 stream transmission traffic across all network configurations with relative error for standard method.

5.3.3. Summary Evaluation of Novel Method in DC Environments

This chapter presents a comparative analysis of the novel method for measuring IP scheduled throughput in DC environments, juxtaposed against the conventional approach. The conventional method demonstrates substantial limitations in achieving accurate measurements, whereas the proposed methodology provides a resolution to these shortcomings, as evidenced by results obtained from real-world devices.

To evaluate the efficacy of the new method, a comparative analysis is conducted with the standard method. This analysis involves examining different TCP stream transmission types in a DC environment, focusing on:

- Correlation between file size and protocol characteristics: This analysis aims to identify the relationship between the transmitted file size and the specific characteristics of the TCP

protocol, specifically the number of TCP streams, which directly impact the measured precision of both methods.

- Maximum relative error: The study quantifies the maximum relative error experienced by the standard method and evaluates how effectively the novel method mitigates this error by comparing measured values.

The test results demonstrate that the standard method fails to provide meaningful throughput information in DC scenarios, in contrast to non-DC scenarios presented in Chapter 5.3.1 and 5.3.2 where the standard method provides reliable values. Specifically, for 2CC inter-site CA connections, as shown in Figures 5.22 and 5.23, the standard method exhibits a significant relative error of up to -64% for cell throughput and -62% for application layer throughput when operating at full capacity. The relative error in throughput estimation exhibits a positive correlation with the number of component carriers allocated to a user's bandwidth spectrum. This implies that as the bandwidth spectrum expands through the addition of more component carriers, the relative error in throughput estimation measurement increases proportionally. This relationship will be investigated in more detail in Chapter 5.5.1. However, the magnitude of this proportional increase depends primarily on the data volume split between different component carriers.

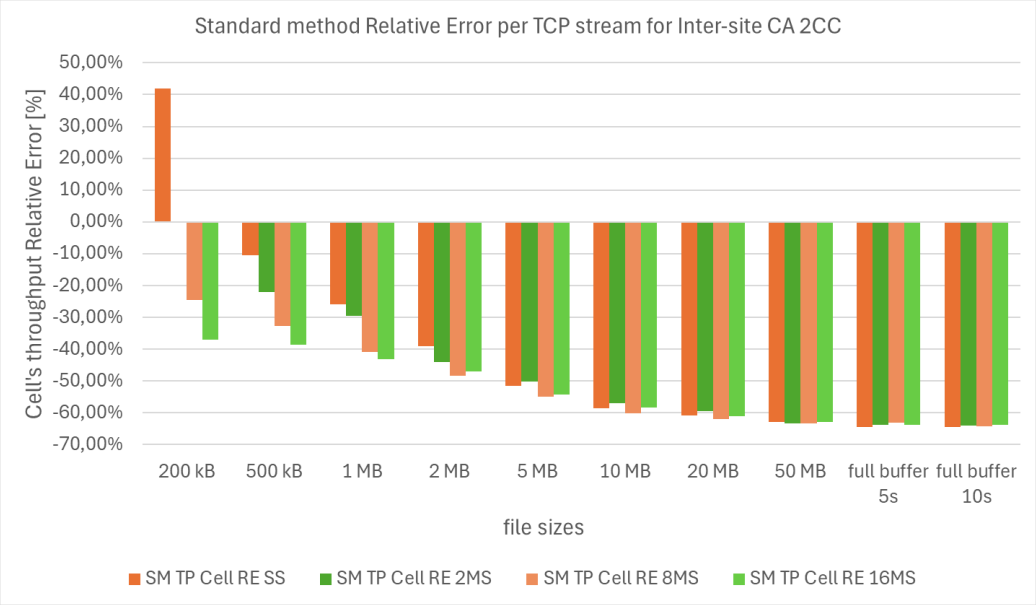

Figure 5.22: TCP/IP different stream transmission traffic type for inter-site CA with cell's relative error for the standard method.

Increasing the number of TCP streams during transmission generally maximizes the rate at which the PDCP buffer fills with new data. However, the standard method, as described in Chapter 3.3, suffers from a lack of a suitable architectural solution and implementation limitations, hindering its ability to accurately calculate the IP scheduled throughput value. The novel method, presented in Chapter 4.4, provides a robust solution for throughput measurement in DC environments, overcoming the limitations of the standard method, as illustrated in Figures 5.22-5.23. Test results, shown in Figures 5.24-5.25, highlight the significant improvement in

accuracy offered by the new method, particularly in scenarios involving multiple TCP streams and inter-site CA connections. For example, the new method exhibits promising performance for 8-stream TCP transmissions, demonstrating an application layer throughput relative error consistently within the range of 2-10% across varying file sizes. Similarly, in the case of cell throughput relative error, the results for 8MS show values lower than 5% for file size transfers of 10 MB and above. This contrasts with the standard method, which for App RE showed results between -30% and -62% and for Cell RE showed results for file sizes of 10 MB and above between -60% and -64%, respectively.

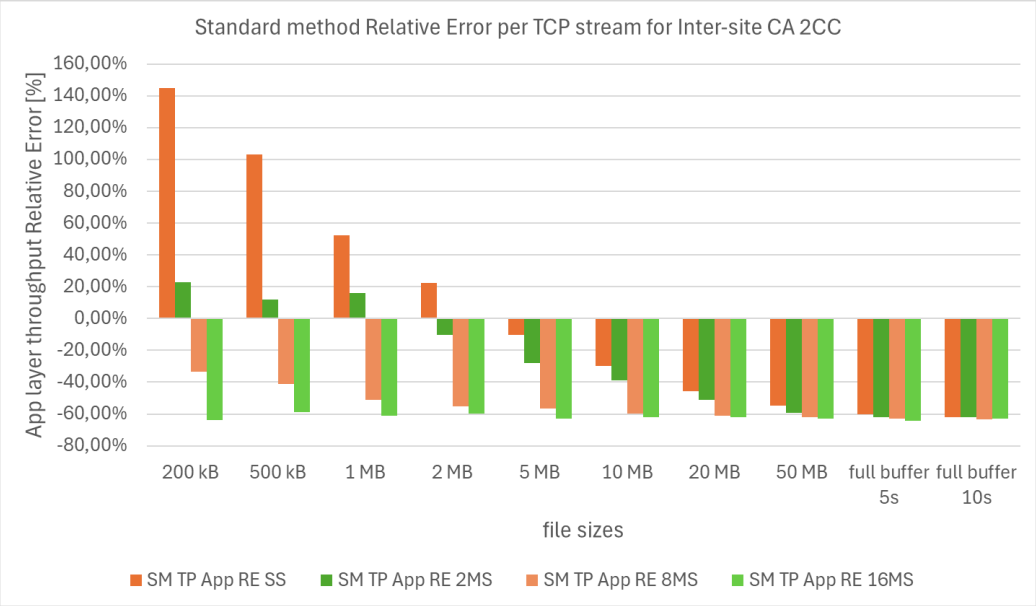

Figure 5.23: TCP/IP different stream transmission traffic type for inter-site CA with application layer relative error for the standard method.

However, utilizing the novel method with a stream count of 16 leads to a significant underestimation of end-user perceived throughput, exhibiting a relative error ranging from -27% to -10% for file sizes between 200 kB and 5 MB. This contrasts with the 8MS transmission where the App RE ranges from 2.72% to 10.81%. This observation suggests a potential limitation of the method when employed with a high number of streams, particularly within this specific file size range. Moreover, the tests concerning cell relative error reveal a contrasting trend between different stream counts. Within the small file size range, specifically between 500 kB and 5 MB, an increase in the number of streams results in a corresponding increase in cell relative error. This phenomenon is attributed to a disproportionate increase between the data volume and time components. For instance, during a 2 MB file transmission with 2 streams, the data volume component reaches 91.79% while the time component reaches 82.48%. In contrast, with 8 streams, these values become 97.50% and 82.45%, respectively, and with 16 streams, they reach 98.89% and 83.07%. This indicates that the measured data volume increases by 5.71% between 2 and 8 streams and by 7.09% between 2 and 16 streams, while the measured time component decreases by 0.04% between 2 and 8 streams and increases by 0.58% between 2 and 16 streams. This disproportionate growth between measured data volume and time components leads to the observed discrepancies in performance across different stream counts.

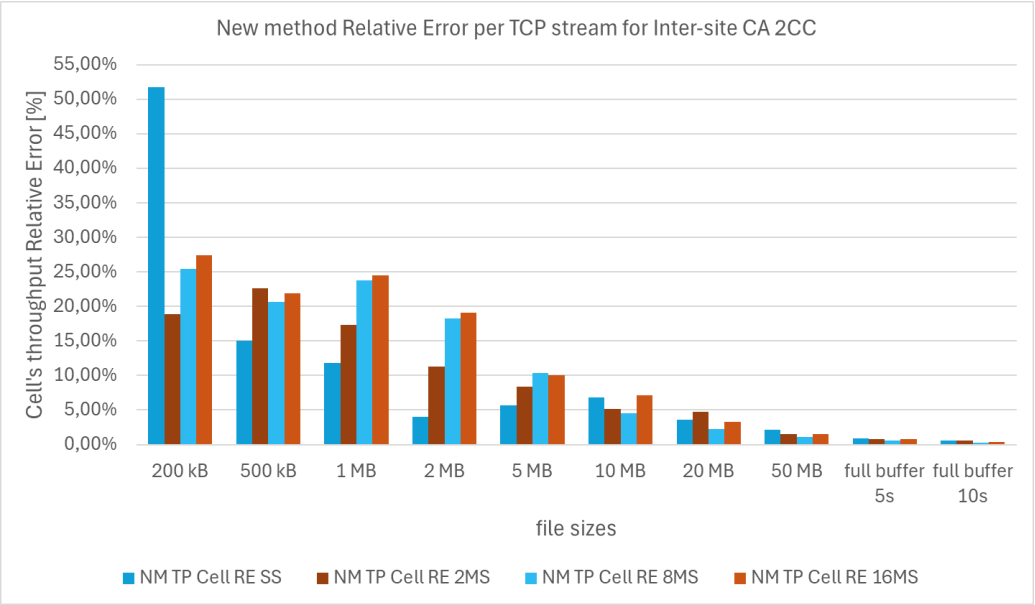

Figure 5.24: TCP/IP different stream transmission traffic type for inter-site CA with cell's relative error for the new method.

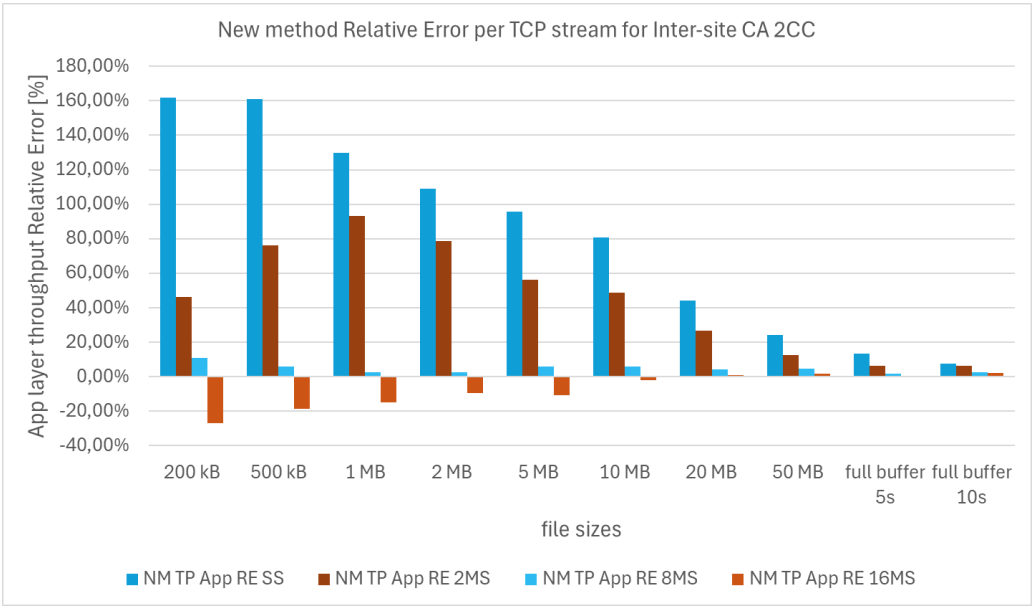

Figure 5.25: TCP/IP different stream transmission traffic type for inter-site CA with application layer relative error for the new method.

5.3.4. Mixed non-DC and DC environment tests with full buffer UDP traffic

This research study aims to evaluate the accuracy of both the standard and the novel method for mixed CA configurations, encompassing both non-DC and DC scenarios simultaneously. While the standard method is demonstrably ineffective for inter-site CA configurations due to its inherent limitations, it is crucial to quantify its level of inaccuracy for comparative purposes. This research will investigate the performance of a proposed method under diverse network traffic conditions. The study will employ diverse UDP transmission types with varying data inflow rates to the eNB, which will impact the time component calculation change detailed in Chapter 4.5.

This test case deviates from the test line design outlined in Chapter 5.1. It involves an eNB cluster configuration with up to 5CC, incorporating a mix of intra and inter-site cells. Each cell bandwidth is set to 20 MHz. Modulation is configured to 256QAM with up to 2x2 MIMO layers. The maximum achievable throughput per CC in this study is set to 195 Mbps, with a combined maximum throughput of almost 1 Gbps for a 5CC CA configuration. Throughout the test cases conducted, optimal radio channel quality conditions were consistently maintained.

This study aims to investigate the influence of varying UDP transmission rates on data volume and time component calculations, which are employed to determine IP scheduled throughput. The results will be compared to the maximum throughput achievable using iperf with UDP protocol, hereafter referred to as "Iperf set TP", to determine the accuracy level employed as relative error.

Three distinct traffic patterns are simulated using UDP protocol:

- Full buffer: Represents a scenario where the network buffer is fully utilized.
- Non-full buffer (moderate data inflow): Represents a scenario with moderate data inflow, resulting in a partially filled buffer.
- Low traffic: Represents a scenario with minimal data inflow.

These traffic patterns aim to simulate real-world network scenarios where user throughput can be constrained by core network limitations or resource allocation among multiple users. By analyzing the burst calculation under these varying conditions, this test case provides insights into the performance and behavior of the Intra-site CA configuration in a dynamic network environment.

5.3.4.1. Non-DC Intra-site CA connection, UDP protocol

This test case focuses solely on Intra-site CA configuration, as detailed in Tables 5.12-5.14. The test case presented in Table 5.12 utilizes a full buffer UDP traffic scenario, exceeding the maximum achievable throughput for each CA configuration. Specifically, the application layer throughput reaches 390 Mbps for 2CC, 585 Mbps for 3CC, and 975 Mbps for 5CC. These values serve as the reference for relative error calculations. However, in these test cases, the upper boundaries of throughput were deliberately set above the theoretically achievable maximum throughput for specific configurations, to induce a state of full buffer occupancy. For instance, in the 2CC configuration (Table 5.12), the observed application-layer throughput of 390 Mbps was below the iperf-defined threshold of 480 Mbps.

Both the standard and newly proposed methods demonstrate comparable performance in this scenario. This is attributed to the traffic pattern being dominated by a single data burst, allowing for precise estimations with relative errors below 1%. The results indicate that accurately estimating IP scheduled throughput in a full buffer scenario is relatively straightforward. However, further validation is necessary for the remaining two scenarios: medium and low traffic. These scenarios represent different traffic patterns and may require further analysis to assess the accuracy and effectiveness of the proposed methods.

Table 5.12: Intra-site CA configuration with full buffer UDP traffic.

CA type	intra-site SCells	inter-site SCells	NM VL FC ON [bits]	NM TM FC ON [ms]	SM VL FC OFF [bits]	SM TM FC OFF [ms]	Iperf set TP [Mbps]	NM TP App RE [%]	SM TP App RE [%]
2CC	1	0	480236816	1231	479746048	1230	480	0.03	0.01
3CC	2	0	640314120	1094	639616416	1093	640	0.05	0.03
5CC	4	0	1000568024	1035	999623280	1033	1000	-0.85	-0.75

Table 5.13 presents the results of a medium UDP traffic scenario. For the test case, the upper throughput threshold was established as 320 Mbps for both 2CC and 3CC configurations, while a threshold of 480 Mbps was set for the 5CC configuration. The NM TP RE was determined using ‘Iperf set TP’ value.

Table 5.13: Intra-site CA configuration with moderate amount of UDP traffic.

CA type	intra-site SCells	inter-site SCells	NM VL FC ON [bits]	NM TM FC ON [ms]	SM VL FC OFF [bits]	SM TM FC OFF [ms]	Iperf set TP [Mbps]	NM TP App RE [%]	SM TP App RE [%]
2CC	1	0	320160000	974	56904000	183	320	2.72	-2.83
3CC	2	0	320160000	967	45888000	147	320	3.46	-2.45
5CC	4	0	480184024	979	157466304	294	480	2.18	11.58

The standard method for estimating IP scheduled throughput exhibited limitations in accurately capturing the total data volume and time components. This was due to the high number of bursts with significant inter-packet spacing, resulting from an unknown UDP packet inflow rate from the iperf server to the eNB. Consequently, a majority of bursts were single TTI bursts, where the standard method only accounted for a small fraction of the total data volume and time. Despite this, the quotient of data volume and time yielded high accuracy for 2CC and 3CC scenarios. However, for the 5CC configuration, overestimation became more pronounced, reaching 11.58%.

The novel method, which introduced a guard period between consecutive IP packets received at the eNB, effectively addressed the issue of omitted time intervals, ensuring accurate counting of all data by treating all data within a burst as a single transmission. The novel method demonstrated superior resilience in non-full buffer scenarios, achieving more accurate IP scheduled throughput estimation compared to the standard method in a non-DC environment, where the UDP packet inflow rate is not at full-buffer levels. The novel method exhibited a significantly lower relative error of 2.18% compared to the standard method's 11.58% in the 5CC scenario. This improvement is particularly notable in the context of 5CC, highlighting the enhanced accuracy of the novel method in complex network configurations involving high amount of CCs.

Table 5.14 presents the performance characteristics of a low UDP traffic scenario, employing 2CC, 3CC, and 5CC configurations with an upper throughput threshold of 40 Mbps. A reduction in packet arrival rate at the eNB resulted in the fragmentation of UDP transmission into numerous, short-duration bursts, in contrast to the medium traffic scenario. This fragmentation further amplified the inherent limitations of the standard method for estimating IP scheduled throughput, as detailed in Chapter 4.5 and visually represented in Figure 4.14. The NM TP RE was determined using ‘Iperf set TP’ value.

Table 5.14: Intra-site CA configuration with low amount of UDP traffic.

CA type	intra-site SCells	inter-site SCells	NM VL FC ON [bits]	NM TM FC ON [ms]	SM VL FC OFF [bits]	SM TM FC OFF [ms]	Iperf set TP [Mbps]	NM TP App RE [%]	SM TP App RE [%]
2CC	1	0	40016000	1000	1552000	48	40	0.04	-19.17
3CC	2	0	40000000	1000	816000	25	40	0.00	-18.40
5CC	4	0	39984000	999	48000	6	40	0.06	-80.00

The relative error for the standard method in the 5CC configuration reached -80%, indicating a substantial underestimation. This highlights the increased inaccuracy of the standard method when data flow is distributed across a higher number of SCells, particularly in conjunction with a high number of short-duration bursts.

The novel method, incorporating the guard period concept, consistently demonstrated high accuracy in this low traffic scenario. It successfully counted all received data, achieving a relative error of only 0.06% for the 5CC configuration. This highlights the resilience of the novel method in accurately estimating IP scheduled throughput, even under conditions of low traffic and high burst frequency.

The test results underscore the robustness and effectiveness of the novel method to accurately account for data even under low throughput conditions for non-DC environment. The mechanism of a guard time interval introduced by the novel method effectively keeps MeNB buffer busy, as depicted in Figure 4.14, ensuring precise accounting of incoming data even at low predefined throughput thresholds, such as 40 Mbps. This demonstrates the superior accuracy of the novel method compared to the standard method, even in Intra-site CA scenarios where the issue of DC system is not apparent. The observed discrepancy arises from an imperfect implementation of the standard method, as the 3GPP standard for LTE lacks explicit guidance regarding the inclusion of a guard period concept in IP scheduled throughput measurement. This omission is perceived as a deficiency within the standard itself, as the absence of a guard time period solution leads to the fragmentation of irregular transmissions with low packet inflow at the eNB into multiple burst scenarios. This fragmentation undermines the effectiveness of the measurement method. Consequently, an improvement that ensures accurate accounting of data associated with a single transmission file is a necessary requirement to address this limitation.

5.3.4.2. Mixed CA connection, UDP protocol

This test case focuses on mixed CA configuration, including various combination of both intra-site and inter-site, as detailed in Tables 5.15-5.17. The test case presented in Table 5.15 utilizes a full buffer UDP traffic scenario, exceeding the maximum achievable throughput for each CA configuration. Specifically, the application layer throughput reaches 390 Mbps for 2CC, 585 Mbps for 3CC. These values serve as the reference for relative error calculations. However, in these test cases, the upper boundaries of throughput were deliberately set above the theoretically achievable maximum throughput for specific configurations, to induce a state of full buffer occupancy. For instance, in the 2CC configuration (Table 5.15), the observed application-layer throughput of 390 Mbps was below the iperf-defined threshold of 480 Mbps.

Table 5.15: Mixed CA configuration with full buffer UDP traffic.

CA type	intra-site SCells	inter-site SCells	NM VL FC ON [bits]	NM TM FC ON [ms]	SM VL FC OFF [bits]	SM TM FC OFF [ms]	Iperf set TP [Mbps]	NM TP App RE [%]	SM TP App RE [%]
2CC	0	1	480187168	1231	160883440	1025	480	0,02	-59,75
3CC	1	1	640316216	1088	343055168	1087	640	0,60	-46,05
3CC	0	2	640316216	1098	173420800	1097	640	-0,31	-72,98

The standard method, when utilizing inter-site SCells, exhibits a substantial accuracy degradation compared to the novel method. For a 2CC connection employing a single inter-site SCell, the degradation reaches -60.76%. In a 3CC connection with one intra-site SCell and one inter-site SCell, the relative error is -47.40%, while for two inter-site SCells, it reaches -73.65%. This discrepancy arises from the inadequate accounting of data volume allocated to inter-site SCells, where it is simply disregarded. The tests were conducted under ideal radio channel conditions, eliminating the need for retransmission mechanisms which simplified the time component calculation. However, the differences in burst time calculation outlined in Chapter 4.5 remain relevant.

The novel method exhibits exceptional performance in this scenario, with relative errors ranging from -2.81% to -1.91%. While employing solely inter-site SCells results in slightly lower accuracy compared to a mix of SCell types, the high accuracy is attributed to the traffic pattern being dominated by a single data burst, enabling precise estimations with relative errors below few percent. These findings suggest that accurately estimating IP scheduled throughput in a full buffer scenario is relatively straightforward. However, further validation is required for medium and low traffic scenarios, as these scenarios represent distinct traffic patterns and may necessitate additional analysis to evaluate the accuracy and effectiveness of the proposed methods.

Table 5.16 presents the results of a medium UDP traffic scenario. For the test case, the upper throughput threshold was established as 320 Mbps for both 2CC and 3CC configurations, while a threshold of 480 Mbps was set for the 5CC configuration. The NM TP RE was determined using ‘Iperf set TP’ value.

Table 5.16: Mixed CA configuration with moderate amount of UDP traffic.

CA type	intra-site SCells	inter-site SCells	NM VL FC ON [bits]	NM TM FC ON [ms]	SM VL FC OFF [bits]	SM TM FC OFF [ms]	Iperf set TP [Mbps]	NM TP App RE [%]	SM TP App RE [%]
2CC	0	1	320060216	1001	129762440	738	320	-0.08	-45.05
3CC	1	1	320160000	1000	30539304	157	320	0.05	-39.21
3CC	0	2	320060216	1000	68595464	381	320	0.02	-43.74
5CC	0	4	480240000	1003	88597120	572	480	-0.25	-67.73
5CC	1	3	480188232	1001	45006800	181	480	-0.06	-48.20
5CC	2	2	479952000	999	80457688	264	480	0.09	-36.51
5CC	3	1	479952000	999	89240048	224	480	0.09	-17.00

Analogous to the full buffer test, the standard method for estimating IP scheduled throughput demonstrated limitations in precisely capturing the total data volume and time components when employing inter-site SCells. For a 2CC connection employing a single inter-site SCell, the degradation reaches -45.05%. In a 3CC connection with one intra-site SCell and one inter-site SCell, the relative error is -39.21%, while for two inter-site SCells, it reaches

-43.74%. This was due to the high number of bursts with significant inter-packet spacing, resulting from an unknown UDP packet inflow rate from the iperf server to the eNB. Consequently, a majority of bursts were single TTI bursts, where the standard method only accounted for a small fraction of the total data volume and time. In 5CC test cases, the standard method demonstrated an improvement in accuracy as the number of intra-site SCells increased within the configuration. Notably, with a configuration of 3 local SCells and 1 remote SCell, the relative error decreased to -17%. This improvement is directly linked to an underestimation of the time component, with a value of 224 ms for a transmission duration of 1 s. Consequently, the quotient of data volume and time was accurately estimated by chance, in contrast to other test cases where remote SCells were more prevalent. The standard method, due to accounting for a reduced time component based on the example as depicted in Figure 4.15, exhibits a more accurate estimation of IP scheduled throughput in scenarios with lower packet data inflow rates. This can be interpreted as a fortuitous outcome, as the stochastic nature of packet arrival rates can readily transform favorable results into unfavorable ones.

The novel method, which introduced a guard period between consecutive IP packets received at the eNB, effectively addressed the issue of omitted time intervals, ensuring accurate counting of all data by treating all data within a burst as a single transmission. The novel method demonstrated superior resilience in non-full buffer scenarios, achieving superior IP scheduled throughput estimation compared to the standard method in a mixed environment, where the UDP packet inflow rate is not at full-buffer levels. The novel method exhibited relative error less than one percent.

Table 5.17 Mixed CA configuration with low amount of UDP traffic.

CA type	intra-site SCells	inter-site SCells	NM VL FC ON [bits]	NM TM FC ON [ms]	SM VL FC OFF [bits]	SM TM FC OFF [ms]	Iperf set TP [Mbps]	NM TP App RE [%]	SM TP App RE [%]
2CC	0	1	40000000	999	2056000	65	40	0.10	-20.92
3CC	1	1	40000000	999	1456000	46	40	0.10	-20.87
3CC	0	2	40000000	999	1856000	64	40	0.10	-27.50
5CC	0	4	39984000	999	1330032	47	40	0.06	-29.25
5CC	1	3	39984000	999	976000	30	40	0.06	-18.67
5CC	2	2	39984000	999	8000	1	40	0.06	-80.00
5CC	3	1	40016000	1000	8000	1	40	0.04	-80.00

Table 5.17 presents the results of a low UDP traffic scenario. For the test case, the upper throughput threshold was established as 40 Mbps for every CC combination. The NM TP RE was determined using ‘Iperf set TP’ value. Similar to the medium UDP traffic test, the standard method for estimating IP scheduled throughput exhibited limitations in accurately capturing the total data volume and time components when utilizing inter-site SCells. These limitations were less pronounced compared to tests in Table 5.16, as the IP scheduled throughput estimation and its precision, as indicated by relative error, achieved more accurate results. Notably, the further reduction in packet inflow, determined by the upper throughput threshold of 40 Mbps, resulted in a further decrease in time component values. However, for 2CC and 3CC configurations, the quotient of data volume and time components yielded improved results. Conversely, for 5CC configurations, the results deviated from those observed in the medium UDP traffic test. With the

number of local SCells increased, the relative error exhibited entirely erroneous values of -80%, with the time component registering only 1ms of transmission time out of a total transmission time of 1s. In summary, the standard method demonstrates an inability to accurately account for transmitted data in mixed environment scenarios as the packet inflow rate at the eNB decreases.

The novel method, incorporating a guard period between consecutive IP packets received at the eNB, effectively mitigated the issue of omitted time intervals. This approach ensured accurate data counting by treating all data within a burst as a single transmission. The novel method exhibited superior resilience in non-full buffer scenarios, achieving superior IP scheduled throughput estimation compared to the standard method in a mixed environment characterized by a low UDP packet inflow rate. Consistent with previous test cases, the novel method demonstrated a relative error below one percent.

5.3.5. Long stability test with UDP and TCP protocol

The main purpose of this test case is to verify the stability of precision in non-DC and DC environments of both the methods during long transmission durations with a particular interest whether the novel method does not experience any degradation in new accounting mechanism. To perform comprehensive analysis UDP and TCP protocols have been used, representing Acknowledgment Mode (AM) and Unacknowledgment Mode (UM) [61], where for UDP the full buffer configuration was configured and for TCP the 8 multi streams were chosen.

A test case configuration used two eNBs, eNB-1112 and eNB-1109, as described in Chapter 5.1, with distinct hardware configurations. eNB-1112 functioned as the MeNB with a 20 MHz PCell and a 15 MHz SCell for intra-site CA configuration. The PCell employed a maximum modulation scheme of 256 QAM, while the SCell utilized 64QAM. The second eNB, eNB-1109, acted as the SeNB with a 10 MHz SCell for inter-site CA configuration, utilizing a maximum modulation scheme of 256QAM. Both eNBs were configured with two MIMO layers. With these configurations, intra-site CA with two 2CC achieved a maximum application layer throughput of 287 Mbps, while inter-site CA attained 278 Mbps. For the test scenario, the radio channel quality exhibited a SINR of approximately 30 dB and a RSSI of -60 dBm for all cells.

Table 5.18 presents test results conducted with a 2CC configuration for a single UE in an LTE system. Full buffer UDP traffic was simulated using iperf commands with an upper throughput threshold of 600 Mbps, exceeding the RAN capability. The novel method exhibits a low Cell RE of -0.67% for DC scenarios and -2.25% for non-DC scenarios with FC ON for 800 seconds. Conversely, the standard method demonstrates Cell RE of -51.96% for DC scenarios and -2.0% for non-DC scenarios with FC OFF for 800 seconds. The BDR and BTR values for the standard method during the 800-second DC test case were measured at 47.97% and 99.87%, respectively. The new method exhibited values of 100% and 100.67% for the same test case.

Table 5.19 presents test results conducted with a 2CC configuration for a single UE in an LTE system using the iperf commands to simulate 8 multi stream TCP traffic. Transmission times differed depending on the test case and are as according to Table 5.19. The novel method exhibits a low Cell RE of -0.20% for DC scenarios and -1.97% for non-DC scenarios with FC ON for 800 seconds. Conversely, the standard method demonstrates Cell RE of -52.79% for DC scenarios

and -2.09% for non-DC scenarios with FC OFF for 800 seconds. The BDR and BTR values for the standard method during the 800-second DC test case were measured at 46.94% and 99.43%, respectively. Conversely, the new method exhibited values of 100% and 100.20% for the same test case.

Table 5.18: Test results for 2CC with full buffer UDP traffic in LTE.

CA configuration type	NM BDR [%]	NM BTR [%]	SM BDR [%]	SM BTR [%]	NM TP Cell RE [%]	NM TP App RE [%]	SM TP Cell RE [%]	SM TP App RE [%]	ReTx ratio [%]	Test duration
Intra-site CA (non-DC) FC OFF	99.73	97.41	98.59	95.82	2.38	17.17	2.89	17.75	0.524	10s
Intra-site CA (non-DC) FC OFF	99.99	102.06	99.18	101.30	-2.03	4.16	-2.10	4.09	1.624	200s
Intra-site CA (non-DC) FC OFF	100.00	102.00	99.18	101.21	-1.96	4.34	-2.00	4.30	1.485	800s
Intra-site CA (non-DC) FC ON	99.32	97.10	98.18	96.04	2.28	18.88	2.23	18.82	1.209	10s
Intra-site CA (non-DC) FC ON	99.97	102.39	98.74	101.18	-2.36	3.93	-2.41	3.88	1.862	200s
Intra-site CA (non-DC) FC ON	99.99	102.29	99.17	101.50	-2.25	5.17	-2.29	5.12	1.774	800s
Inter-site CA (DC)	100.00	98.16	48.05	97.47	1.88	6.12	-50.70	-48.65	1.203	10s
Inter-site CA (DC)	100.00	101.28	47.99	100.47	-1.27	2.73	-52.24	-50.30	1.415	200s
Inter-site CA (DC)	100.00	100.67	47.97	99.87	-0.67	3.31	-51.96	-50.04	0.697	800s

Table 5.19: Test results for 2CC with full buffer 8MS TCP traffic in LTE.

CA configuration type	NM BDR [%]	NM BTR [%]	SM BDR [%]	SM BTR [%]	NM TP Cell RE [%]	NM TP App RE [%]	SM TP Cell RE [%]	SM TP App RE [%]	ReTx ratio [%]	Test duration
Intra-site CA (non-DC) FC OFF	99.96	99.24	99.23	98.40	0.73	3.58	0.84	3.70	1.101	10s
Intra-site CA (non-DC) FC OFF	100.00	101.50	99.20	100.71	-1.48	3.59	-1.50	3.58	1.220	200s
Intra-site CA (non-DC) FC OFF	100.00	102.09	99.19	101.31	-2.05	3.58	-2.09	3.53	1.526	800s
Intra-site CA (non-DC) FC ON	99.82	100.80	95.44	96.36	-0.97	5.08	-0.96	5.09	2.613	10s
Intra-site CA (non-DC) FC ON	99.99	101.23	99.12	100.40	-1.22	3.65	-1.28	3.59	1.087	200s
Intra-site CA (non-DC) FC ON	100.00	102.01	99.17	101.22	-1.97	3.64	-2.03	3.59	1.474	800s
Inter-site CA (DC)	99.91	96.09	46.96	95.27	3.98	5.31	-50.71	-50.08	1.297	10s
Inter-site CA (DC)	99.99	100.93	46.75	100.14	-0.93	3.74	-53.32	-51.12	1.139	200s
Inter-site CA (DC)	100.00	100.20	46.94	99.43	-0.20	3.68	-52.79	-50.95	0.239	800s

The disparity in performance between DC and non-DC use cases for the novel method, observed for both UDP and TCP, is attributed to increased retransmissions during intra-site CA configuration. The ReTx ratio for UDP is 0.697% and for TCP is 0.239% for DC scenarios, while for non-DC scenarios, it increases to 1.774% for UDP and 1.474% for TCP.

The discrepancy in Cell RE between DC and non-DC scenarios for the standard method arises from the lack of a comprehensive solution, unlike the novel method. This discrepancy stems from differing interpretations of data bursts due to the division between PCell MeNB and

SCell SeNB over X2. This division results in the exclusion of not only the single and last TTIs emptying the buffer but also packets partially directed to the PCell MeNB and the supplementary carrier. Consequently, the standard method underestimates the total PDCP data volume transmitted solely over the PCell MeNB.

These findings highlight a limitation of the standard method in DC systems, exhibiting a Cell RE of -52.79%. The novel method effectively addresses this limitation, achieving accurate results with a Cell RE of -0.20%. Moreover, the novel method demonstrates its applicability in both non-DC and DC systems, exhibiting highly precise values during extended transmissions, thereby proving the stability of the proposed method.

Another stability test case with long transmission duration has been conducted. The experimental setup mirrored that employed in prior sections of this chapter. An upper throughput limit of 200 Mbps was enforced. This limit aimed to induce sparse SCell utilization during CA transmission, resulting in a transfer of only a fraction of the data volume from PCell to SCell. This behavior mimics a high-load scenario for the SCell, which is shared among multiple CA users, yet viewed from the perspective of a single user.

Table 5.20 presents test results conducted with a 2CC configuration for a single UE in an LTE system. Single stream TCP traffic was simulated using iperf commands with an upper throughput threshold of 200 Mbps. The novel method exhibits a low Cell RE of -1.17% for DC scenarios and -1.23% for non-DC scenarios with FC ON for 800 seconds. Conversely, the standard method demonstrates Cell RE of -17.65% for DC scenarios and -1.40% for non-DC scenarios with FC OFF for 800 seconds. The BDR and BTR values for the standard method during the 800-second DC test case were measured at 63.02% and 76.53%, respectively. The new method exhibited BDR and BTR values of 99.98% and 101.16% for the same test case.

Table 5.20: Test results for 2CC with TCP traffic with upper throughput limit (200 Mbps) in LTE.

CA configuration type	NM BDR [%]	NM BTR [%]	SM BDR [%]	SM BTR [%]	NM TP Cell RE [%]	NM TP App RE [%]	SM TP Cell RE [%]	SM TP App RE [%]	ReTx ratio [%]	Test duration
Intra-site CA (non-DC) FC OFF	99.99	101.27	99.08	100.49	-1.26	5.27	-1.40	5.12	1.277	800s
Intra-site CA (non-DC) FC ON	99.98	101.22	-	-	-1.23	5.80	-	-	0.947	800s
Inter-site CA (DC)	99.98	101.16	63.02	76.53	-1.17	5.58	-17.65	-12.03	1.322	800s

Table 5.21 presents test results conducted with a 2CC configuration for a single UE in an LTE system. An UDP traffic was simulated using iperf commands with an upper throughput threshold of 200 Mbps. The novel method exhibits a low Cell RE of -1.38% for DC scenarios and -2.03% for non-DC scenarios with FC ON for 800 seconds. Conversely, the standard method demonstrates Cell RE of -12.94% for DC scenarios and -3.05% for non-DC scenarios with FC OFF for 800 seconds. The BDR and BTR values for the standard method during the 800-second DC test case were measured at 62.14% and 71.38%, respectively. The new method exhibited BDR and BTR values of 100.00% and 101.40% for the same test case.

Analysis of Tables 5.20 and 5.21 indicates that for the DC system, employing the standard method, simultaneously low values of data volume and transmission time result in a throughput

value (given by Cell RE) that is more likely to exhibit random behavior rather than a deterministic guarantee. Discrepancies in data burst perception arise from the division of PCell MeNB and SCell SeNB over X2, excluding single and last TTIs. This leads to an underestimation of PDCP data volume transmitted solely over the PCell MeNB. The standard method cannot interpret these bursts as belonging to the same transmission cycle without a proper solution. The novel method provides a solution using the guard time period concept described in Chapter 4.5.

Table 5.21: Test results for 2CC with UDP traffic with upper throughput limit (200 Mbps) in LTE.

CA configuration type	NM BDR [%]	NM BTR [%]	SM BDR [%]	SM BTR [%]	NM TP Cell RE [%]	NM TP App RE [%]	SM TP Cell RE [%]	SM TP App RE [%]	ReTx ratio [%]	Test duration
Intra-site CA (non-DC) FC OFF	100.00	102.77	98.63	101.74	-2.70	2.01	-3.05	1.64	2.503	800s
Intra-site CA (non-DC) FC ON	100.00	102.07	-	-	-2.03	2.01	-	-	1.400	800s
Inter-site CA (DC)	100.00	101.40	62.14	71.38	-1.38	2.00	-12.94	-9.95	1.419	800s

The standard method exhibits limitations in DC systems, including inability to account for SCell SeNB traffic, underestimation of PCell MeNB traffic, and lack of a guard time period mechanism. This results in inaccurate network performance assessment, particularly in mixed CA networks, encompassing both non-DC and DC configurations. However, the new method exhibits applicability in both non-DC and DC systems and provides highly precise throughput values using the Cell RE metric as a reference point.

5.4. Radio Channel Quality variations

This chapter presents a comprehensive evaluation of the novel throughput estimation method, encompassing aspects of accuracy under various radio channel quality levels [62], with comparison to the standard method. Due to the inherent interdependency of these factors, the investigation combines elements from several research objectives:

- Accuracy of the novel measurement method under static, slow-paced and rapid-paced radio channel quality variations. The radio channel quality, characterized by parameters like RSRP (Reference Signal Received Power) and SINR (Signal-to-Interference-plus-Noise Ratio), significantly impacts the measurement precision [62].
- Retransmissions: Harsh radio channel conditions can lead to signal reception errors, requiring retransmissions [63]. These retransmissions can impact the measurement precision, for example by changing the length of a burst. Testing with different retransmission scenarios will quantify the impact of retransmissions on the measurement accuracy.
- Method-Specific Parameters: The effectiveness of the IP scheduled throughput method is influenced by parameters like the *eTh* exchange rate, initial Modulation and Coding Scheme (MCS), and the *eTh* calculation function. Testing with different combinations of these parameters will reveal their impact on the measurement accuracy.

5.4.1. Static RSRP and SINR

This study investigates the impact of increasing attenuation on the relative error of both the standard and the new method for measuring throughput in both PCell and SCell cells. The

analysis will examine the distribution of volume and time component ratios in relation to the relative error of cell throughput and application layer throughput. The study will also explore the relevance of cell throughput in high retransmission scenarios. In such scenarios, the increased burst time required for retransmissions diminishes the direct comparability of cell throughput to IP scheduled throughput measurement for a single user connection. To mitigate the influence of TCP slow start and minimize the number of single TTI transmissions, TCP 8 multi-stream transmission is employed. This approach allows for a direct assessment of the impact of challenging radio channel conditions that necessitate link adaptation mechanisms for signal decoding and successful data delivery to the user.

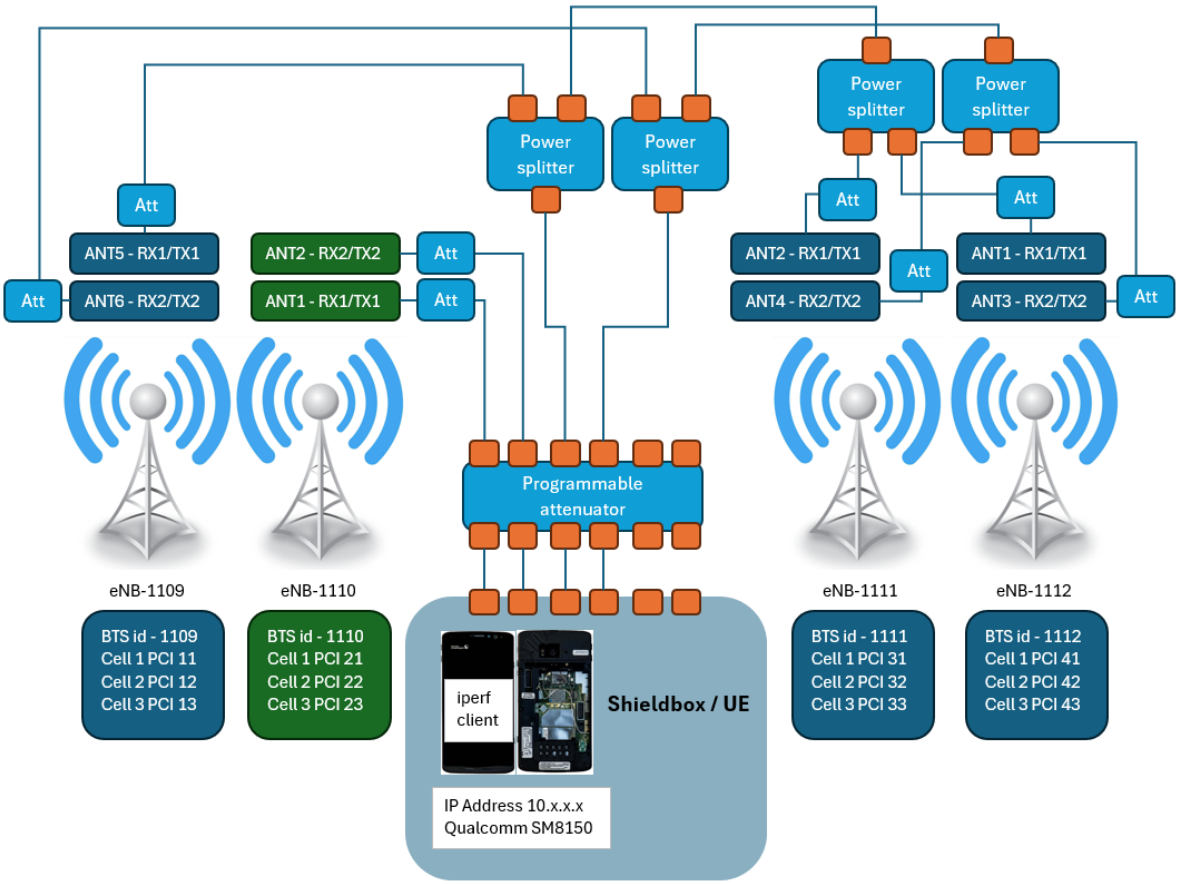

Figure 5.26: Lab test line schematic of RF connection between the four eNBs and the UE with usage of programmable attenuator.

The novel throughput measurement method was evaluated under realistic network conditions characterized by time-varying radio channel quality. To simulate degraded radio signal reception between the eNB RF ports and the UE ports, a JWF Industries model 50PA-574 programmable attenuator with a frequency range of 200-6000 MHz was employed (Figure 5.26). The attenuation was applied uniformly across the entire frequency spectrum, affecting both the PCell and SCell. Due to the separation of RF signals from each eNB, the attenuation level for the SCells of the SeNB-1110 could be independently adjusted compared to the MeNB. For inter-site CA configuration with 2CC, the PCI 41 cell served as the PCell and the PCI 21 cell as the SCell. For intra-site CA configuration with 2CC, the PCI 41 cell acted as the PCell and the PCI 42 cell as the SCell. Mini-Circuits ZN2PD2-63-S+ (350-6000 MHz) power splitters were used to combine

RF signals from different antenna ports of eNB-1112, eNB-1111, and eNB-1109, using FDD. For the purposes of test cases in Chapter 5.4, eNB-1111 and eNB-1109 were disabled.

Baseline tests conducted without a programmable attenuator yielded ideal radio conditions, exhibiting SINR of approximately 30 dB and RSSI of -60 dBm. However, these baseline tests also utilized Omnitek fixed attenuator (AT-RD-4G-50-50-NM-NF) devices (50dB/50W), depicted as “Att” in Figure 5.26, mounted at each RF port to reduce the output power value.

To assess the performance of both methods, the programmable attenuator was set to two levels: 30 dB (moderate) and 45 dB (high) across the entire test line. RSSI measurements, presented in Tables 5.22 and 5.24, reflect varying antenna signal power level, while SINR measurements, presented in Tables 5.23 and 5.25, show quality indicators. Simultaneous attenuation of both DL and UL channels can lead to a reduction in signal power level, potentially impeding the reception of HARQ ACKs. Consequently, the degradation necessitates retransmissions, thereby increasing the frequency of retransmission events and providing a more realistic representation of challenging radio channel conditions.

Table 5.22: Intra-site CA antenna signal attenuation details with RSSI values.

Attenuation	Cell type	RSSI Ant 0 [dBm]	RSSI Ant 1 [dBm]	RSSI Ant 2 [dBm]	RSSI Ant 3 [dBm]
0dB	PCell	-51 +/-2	-55 +/-2	-62 +/-2	-51 +/-2
	SCell	-40 +/-2	-38 +/-2	-70 +/-2	-40 +/-2
30dB (moderate)	PCell	-80 +/-2	-83 +/-2	-85 +/-2	-79 +/-2
	SCell	-80 +/-2	-83 +/-2	-87 +/-2	-81 +/-2
45dB (high)	PCell	-80 +/-2	-83 +/-2	-94 +/-2	-89 +/-2
	SCell	-82 +/-2	-84 +/-2	-96 +/-2	-90 +/-2

Table 5.23: Intra-site CA antenna signal attenuation details with SINR values.

Attenuation	Cell type	SINR Ant 0 [dB]	SINR Ant 1 [dB]	SINR Ant 2 [dB]	SINR Ant 3 [dB]
0dB	PCell	30	30	30	30
	SCell	30	30	22,7	17,3
30dB (moderate)	PCell	10,5 to 11	7 to 9	9,3 to 10,5	14 to 15,2
	SCell	9,3 to 10,9	8,2 to 8,9	6,6 to 7,6	14,6 to 15,6
45dB (high)	PCell	11,3 to 13,1	7,9 to 9	-1,5 to 3,2	4,7 to 5,3
	SCell	9,5 to 11	7,7 to 8,6	-5,6 to 0,1	4,2 to 5,4

Table 5.24: Inter-site CA antenna signal attenuation details with RSSI values.

Attenuation	Cell type	RSSI Ant 0 [dBm]	RSSI Ant 1 [dBm]	RSSI Ant 2 [dBm]	RSSI Ant 3 [dBm]
0dB	PCell	-51 +/-2	-55 +/-2	-62 +/-2	-51 +/-2
	SCell	-40 +/-2	-38 +/-2	-70 +/-2	-40 +/-2
30dB (moderate)	PCell	-84 +/-2	-88 +/-2	-88 +/-2	-84 +/-2
	SCell	-76 +/-2	-73 +/-2	-84 +/-2	-88 +/-2
45dB (high)	PCell	-80 +/-2	-83 +/-2	-94 +/-2	-89 +/-2
	SCell	-82 +/-2	-84 +/-2	-96 +/-2	-90 +/-2

Table 5.25: Inter-site CA antenna signal attenuation details with SINR values.

Attenuation	Cell type	SINR Ant 0 [dB]	SINR Ant 1 [dB]	SINR Ant 2 [dB]	SINR Ant 3 [dB]
0dB	PCell	30	30	30	30
	SCell	30	30	18,7 to 22,7	14,5 to 17,3
30dB (moderate)	PCell	10,5 to 11,7	6,9 to 8,1	10,1 to 10,8	13,4 to 14,7
	SCell	17,1 to 17,9	19,1 to 20,2	3,7 to 8,9	-12,7 to -6,4
45dB (high)	PCell	11,6 to 12,8	8,1 to 9,5	1,8 to 2,8	3,9 to 5
	SCell	1,5 to 3,1	4,9 to 6,1	-18,1 to -7,1	-18,3 to -9,5

While a direct comparison of two methods under identical test constraints is conducted, inherent variations exist between traffic simulations. Consequently, the processing of the same file size in the MeNB and SeNB, during transmission in DL direction, may exhibit differing patterns, leading to variations in throughput values and relative errors. To mitigate this variability, multiple test repetitions are performed to obtain an average value of throughput relative error, providing a reliable basis for comparison.

The below subchapters present a comparative analysis of IP scheduled throughput measurement implementation, evaluating the novel approach against the standard method and two reference points: cell throughput and application layer throughput. The analysis is conducted within a multi-burst scenario using 8 TCP streams for transmission across intra and inter-site CA connection types, different file sizes and attenuation levels. The primary objective is to assess the accuracy of the novel method under static but challenging radio channel quality. Multi-stream TCP transmission is employed to mitigate the slow start effect, based on the Chapter 5.3 results the best values are achieved for 8MS transmission type. Multi-stream transmission type necessitates faster eNB buffer occupancy, reducing the number of small bursts at the transmission initiation and potentially enhancing measurement accuracy by increasing the likelihood of meeting 3GPP criteria. Comprehensive descriptions of each test case, including data volume and time component results, are presented in Appendix 3.

5.4.1.1. Summary of Intra-site CA (non-DC) – Cell's throughput as a reference point

Table 5.26 presents a comparative analysis of the relative error in estimation of cell throughput for various transmission file sizes, considering both the standard method and the new approach. The analysis encompasses intra-site CA transmission type utilizing an 8 multi stream TCP/IP protocol.

Table 5.26: Cell's throughput relative error results for both the standard and new method for Intra-site CA with varying RF signal attenuation in radio channel.

File sizes	Attenuation of 0 dB		Attenuation of 30 dB		Attenuation of 45 dB	
	FC OFF	FC ON	FC OFF	FC ON	FC OFF	FC ON
	SM TP Cell RE [%]	NM TP Cell RE [%]	SM TP Cell RE [%]	NM TP Cell RE [%]	SM TP Cell RE [%]	NM TP Cell RE [%]
200 kB	38.24	33.76	15.09	10.11	4.29	-8.61
500 kB	29.35	35.30	2.21	7.68	-4.22	4.04
1 MB	29.47	24.36	3.82	9.29	0.61	0.37
2 MB	16.72	19.60	5.32	4.04	-4.41	-3.09
5 MB	10.40	14.92	-5.33	-1.15	-6.29	-4.90
10 MB	6.10	5.46	-4.21	-4.17	-8.20	-6.95
20 MB	2.90	2.78	-7.81	-5.90	-9.34	-6.83
50 MB	1.24	1.16	-7.59	-7.70	-9.16	-8.68
5s	0.59	0.59	-8.57	-8.10	-9.00	-9.90
10s	0.34	0.29	-8.50	-8.30	-9.32	-9.20

Under ideal radio channel conditions, the relative error consistently remains non-negative for both the standard and the novel method. This is attributed to the absence of re-transmission mechanisms, which typically occur during strong interference when user data cannot be

successfully decoded. For attenuation of 0 dB, the relative error for both methods demonstrates close proximity, rarely exceeding a 5% difference for small file sizes and remaining below 0.2% for files larger than 20 MB.

In moderate attenuation scenarios, the relative error for small file sizes exhibits a reduction to an acceptable level, typically below 10% for most tests. However, for larger file sizes, both methods exhibit underestimation exceeding -9%. Similarly, under 45 dB attenuation, underestimation is observed even for 200 kB file sizes. This phenomenon is attributed to re-transmission mechanisms, which extend the duration of the time component. Detailed information regarding data volume and time component ratio values is presented in Table 5.27.

Table 5.27: Data volume and time components ratios results for both the standard and new method for Intra-site CA with varying RF signal attenuation in radio channel.

File size	Attenuation - 0 dB				Attenuation - 30 dB				Attenuation - 45 dB			
	SM BDR [%]	SM BTR [%]	NM BDR [%]	NM BTR [%]	SM BDR [%]	SM BTR [%]	NM BDR [%]	NM BTR [%]	SM BDR [%]	SM BTR [%]	NM BDR [%]	NM BTR [%]
200 kB	89.00	64.38	93.95	70.24	96.43	83.78	96.10	87.27	99.06	94.98	99.88	109.29
500 kB	96.78	74.82	93.46	69.08	96.17	94.09	95.97	89.12	98.39	102.72	98.80	94.96
1 MB	97.71	75.47	95.89	77.11	97.66	94.06	96.58	88.37	99.18	98.58	99.25	98.89
2 MB	98.00	83.96	97.56	81.57	98.74	93.75	96.54	92.79	99.35	103.94	99.04	102.20
5 MB	99.32	89.96	98.77	85.95	99.53	105.13	99.04	100.19	99.83	106.53	99.85	105.00
10 MB	99.62	93.89	99.30	94.16	99.69	104.07	99.79	104.13	99.21	108.07	99.95	107.42
20 MB	99.21	96.41	99.72	97.03	99.24	107.65	99.86	106.12	98.79	108.97	99.97	107.29
50 MB	99.32	98.10	99.89	98.74	99.26	107.42	99.94	108.28	98.87	108.84	99.91	109.41
5s	99.24	98.65	99.95	99.36	99.05	108.34	99.95	108.76	99.09	108.89	99.89	110.88
10s	99.26	98.93	99.97	99.68	98.98	108.18	99.98	109.03	98.92	109.08	99.92	110.05

Furthermore, challenging radio channel conditions necessitate the scheduler to segment incoming PDCP SDU packets into smaller TB sizes. This segmentation results in burst extension with enhanced coding robustness, leading to a reduction in overall throughput and increasing the probability of a burst to be counted according to 3GPP requirements. Deterioration in radio channel quality leads to an increased frequency of retransmissions. Retransmissions within the PCell result in an extended burst length.

A comparative analysis of measurement accuracy between the standard and the new method reveals that for Intra-site CA scenarios involving file sizes exceeding 2 MB and utilizing 8-stream TCP transmission, both methods exhibit high accuracy from the eNB perspective, resulting in negligible differences. This proves that the new method doesn’t experience any degradation in comparison to the standard method.

5.4.1.2. Summary of Intra-site CA (non-DC) – Application layer throughput as a reference point

Table 5.28 presents a comparative analysis of the relative error in estimation of application layer throughput for varying transmission file sizes, considering both the standard method and the new approach. The analysis encompasses intra-site CA transmission type utilizing an 8 multi stream TCP/IP protocol.

Table 5.28: Application layer throughput relative error results for both the standard and new method for Intra-site CA with varying RF signal attenuation in radio channel.

File sizes	Attenuation of 0 dB		Attenuation of 30 dB		Attenuation of 45 dB	
	FC OFF	FC ON	FC OFF	FC ON	FC OFF	FC ON
	SM TP App RE [%]	NM TP App RE [%]	SM TP App RE [%]	NM TP App RE [%]	SM TP App RE [%]	NM TP App RE [%]
200 kB	N/A	N/A	N/A	N/A	N/A	N/A
500 kB	0.05	19.39	14.68	-10.28	-26.68	-28.16
1 MB	9.46	11.02	-32.02	-7.05	-9.55	-19.53
2 MB	-0.87	14.66	1.28	-0.97	-24.34	-4.99
5 MB	4.68	6.36	1.26	1.00	-11.29	-1.75
10 MB	5.91	9.74	5.57	0.41	-0.25	1.51
20 MB	4.73	3.97	1.62	3.94	0.40	0.99
50 MB	4.08	4.22	3.29	2.79	2.45	2.51
5s	1.04	0.85	2.32	-0.43	-2.27	0.30
10s	2.98	3.12	0.85	1.08	0.94	1.75

In intra-site CA transmission with 8MS transmission, the standard method exhibits slightly better performance compared to the novel method under ideal radio channel conditions. As attenuation increases, particularly for smaller file sizes, the time component duration is extended due to the increased likelihood of retransmission, resulting in significant underestimation of relative error for application layer throughput. For instance, for 45 dB attenuation both the standard and novel methods demonstrate approximately -28% underestimation for a 500 kB file size. However, with increasing file sizes, exceeding 10 MB, the obtained results closely align with end-user perception, exhibiting values below 10% for 0 dB and below 3% for 45 dB attenuation. While the relative error measured for the standard method is comparable to the novel method across repeated tests and file sizes higher than 5 MB, direct comparison is challenging due to the differing approaches employed by the flow control algorithms in managing and distributing incoming traffic volume. Nevertheless, faster and more efficient eNB buffer fulfillment leads to comparable outcomes between the two methods.

5.4.1.3. Summary of Inter-site CA (DC) – Cell's throughput as a reference point

Table 5.29 presents a comparative analysis of the relative error in estimation of cell throughput for various transmission file sizes, considering both the standard method and the new approach. The analysis encompasses inter-site CA transmission type utilizing an 8 multi stream TCP/IP protocol.

Under ideal radio channel conditions, the relative error consistently remains negative for the standard method. This underestimation of throughput is attributed to the lack of proper solution for accounting the data and time components accurately. Conversaly, the relative error for the novel method remains non-negative which is attributed to the absence of re-transmission mechanisms, which typically occur during strong interference when user data cannot be successfully decoded.

In moderate attenuation scenarios, the standard method demonstrates a further reduction in relative error. The novel method exhibits a decrease in relative error for small file sizes, reaching an acceptable level, typically below 16% for most tests. However, for larger file sizes,

underestimation exceeding -7% is observed. Similarly, under 45 dB attenuation, underestimation is observed even for 1 MB file sizes. This phenomenon can be attributed to the re-transmission mechanism, which extends the duration of the time component. Table 5.30 provides detailed information regarding data volume and time component ratio values for comparison purposes in relation to Table 5.29 relative error values. Despite an increase in attenuation, both methods exhibit a reduction in relative error estimation.

Table 5.29: Relative error results for both the standard and new method for Inter-site CA with varying RF signal attenuation in radio channel.

File sizes	Attenuation of 0 dB		Attenuation of 30 dB		Attenuation of 45 dB	
	FC ON	FC ON	FC ON	FC ON	FC ON	FC ON
	SM TP Cell RE [%]	NM TP Cell RE [%]	SM TP Cell RE [%]	NM TP Cell RE [%]	SM TP Cell RE [%]	NM TP Cell RE [%]
200 kB	-33.85	18.60	-40.54	10.17	-58.20	3.50
500 kB	-29.46	25.86	-45.17	10.20	-62.58	1.25
1 MB	-37.92	25.78	-47.59	15.24	-66.21	-0.39
2 MB	-45.20	22.31	-55.79	5.60	-71.86	-4.00
5 MB	-55.00	11.18	-51.29	-2.23	-75.30	-5.41
10 MB	-58.77	6.79	-66.30	-5.06	-78.59	-7.22
20 MB	-61.52	2.97	-64.80	-6.24	-79.22	-8.02
50 MB	-63.02	1.64	-66.92	-6.88	-78.25	-8.85
5s	-63.22	0.87	-69.52	-7.45	-79.61	-8.48
10s	-63.94	0.41	-69.64	-7.84	-80.05	-8.84

In high attenuation scenarios, the demanding radio channel conditions necessitate the scheduler to segment incoming PDCP SDU packets into smaller TB sizes. This segmentation results in burst extension, enhancing coding robustness, but leading to a reduction in overall throughput and increasing the probability of a burst being counted according to 3GPP requirements. Deterioration in radio channel quality leads to an increased frequency of retransmissions. Retransmissions within the PCell result in an extended burst length.

Table 5.30: Data volume and time components ratios results for both the standard and new method for Inter-site CA with varying RF signal attenuation in radio channel.

File size	Attenuation - 0 dB				Attenuation - 30 dB				Attenuation - 45 dB			
	SM BDR [%]	SM BTR [%]	NM BDR [%]	NM BTR [%]	SM BDR [%]	SM BTR [%]	NM BDR [%]	NM BTR [%]	SM BDR [%]	SM BTR [%]	NM BDR [%]	NM BTR [%]
200 kB	53.38	80.69	94.99	80.09	47.50	79.88	96.01	87.15	39.96	95.62	98.71	95.37
500 kB	53.35	75.63	94.99	75.47	47.48	86.59	96.73	87.78	36.08	96.42	98.83	97.60
1 MB	48.60	78.28	96.56	76.76	43.88	83.72	97.40	84.52	33.51	99.15	99.41	99.80
2 MB	44.63	81.44	97.63	79.82	41.32	93.44	98.44	93.22	28.84	102.48	99.55	103.70
5 MB	40.23	89.40	99.02	89.06	49.46	101.54	99.37	101.64	25.91	104.88	99.83	105.55
10 MB	38.38	93.10	99.46	93.14	35.30	104.75	99.55	104.85	22.91	107.04	99.90	107.68
20 MB	36.97	96.07	99.75	96.88	37.24	105.80	99.82	106.46	22.44	108.01	99.96	108.67
50 MB	36.17	97.82	99.89	98.27	35.32	106.78	99.92	107.30	23.69	108.93	99.98	109.69
5s	36.33	98.79	99.94	99.08	32.91	107.99	99.96	108.01	22.11	108.48	99.98	109.24
10s	35.67	98.91	99.96	99.55	32.70	107.71	99.97	108.47	21.72	108.86	99.99	109.69

A comparative analysis of measurement accuracy between the standard and the new method reveals significant discrepancies in the context of Inter-site CA scenarios. The new method demonstrates high accuracy from the eNB perspective, regardless of the file size. Conversely, the standard method exhibits extremely low accuracy due to its incompatibility with the new burst calculation logic employed in Inter-site CA scenarios. This incompatibility results in inaccurate measurement of transmission data volume component. These findings indicate that the new method effectively addresses the limitations of the standard method in Inter-site CA environments. Furthermore, the new method exhibits no degradation in accuracy compared to Intra-site CA configurations, suggesting its applicability across diverse CA scenarios. The superior accuracy of the new method stems from its adaptation to the specific requirements of Inter-site CA, particularly in terms of burst calculation. This adaptation ensures accurate measurement of transmission components, leading to a more reliable assessment of performance metrics.

The novel throughput estimation method demonstrates a substantial enhancement in measurement accuracy for inter-site CA scenarios across diverse radio channel quality levels. This improvement addresses the limitations of the standard method, showcasing the robustness of the novel approach across various CA configurations. For smaller file sizes, the novel method exhibits increased precision with increasing radio channel attenuation. Conversely, for larger file sizes, the highly accurate throughput assessment observed under ideal radio channel conditions undergoes a transition towards a more pronounced underestimation as attenuation increases.

5.4.1.4. Summary of Inter-site CA (DC) – Application layer throughput as a reference point

Table 5.31 presents a comparative analysis of the relative error in estimation of cell throughput for various transmission file sizes, considering both the standard method and the new approach. The analysis encompasses inter-site CA transmission type utilizing an 8 multi stream TCP/IP protocol.

Table 5.31: Application layer throughput relative error results for both the standard and new method for Inter-site CA with varying RF signal attenuation in radio channel.

File sizes	Attenuation of 0 dB		Attenuation of 30 dB		Attenuation of 45 dB	
	FC ON	FC ON	FC ON	FC ON	FC ON	FC ON
	SM TP App RE [%]	NM TP App RE [%]	SM TP App RE [%]	NM TP App RE [%]	SM TP App RE [%]	NM TP App RE [%]
200 kB	-46.30	-3.71	-49.43	-6.30	-74.30	-36.35
500 kB	-40.70	5.82	-46.98	6.56	-72.45	-25.47
1 MB	-48.71	3.91	-57.20	-5.90	-72.55	-19.08
2 MB	-53.50	3.78	-59.27	-2.71	-74.15	-11.81
5 MB	-57.04	6.15	-52.60	-4.86	-76.10	-8.47
10 MB	-58.24	8.17	-63.20	3.67	-76.89	0.18
20 MB	-61.24	3.70	-62.62	-0.44	-77.02	1.73
50 MB	-62.01	4.42	-64.98	-1.42	-77.08	-3.92
5s	-63.01	1.47	-66.91	0.50	-77.99	-1.18
10s	-63.06	2.86	-66.20	2.59	-77.63	2.21

In inter-site CA transmission with 8MS transmission, the novel method exhibits superior performance compared to the standard method under ideal radio channel conditions. As

attenuation increases, particularly for smaller file sizes, the time component duration is extended due to the increased likelihood of retransmission, resulting in significant underestimation of relative error for application layer throughput. For instance, for 45 dB attenuation the novel method demonstrates approximately -25% underestimation for a 500 kB file size. However, with increasing file sizes, exceeding 10 MB, the obtained results closely align with end-user perception, exhibiting values below 9% for 0 dB and below 4% for 45 dB attenuation. For 8MS transmission, the standard method is unable to provide meaningful results for any file size under any radio channel quality. The novel method not only surpasses the standard method in the same inter-site CA configuration but also exhibits slightly improved performance compared to intra-site CA configurations.

5.4.2. Evaluation of the eTh Function in SeNB

This chapter presents a dedicated evaluation of the *eTh* function mechanism and its associated parameters within the SeNB, focusing on the precise accounting of IP scheduled throughput measurements obtained from PM counters in the MeNB. Furthermore, the investigation delves into the impact of synchronization and timestamp exchange between scheduler modules on the accuracy of throughput estimation and the signaling traffic intensity within the network, particularly on the X2 interface. The research objectives are twofold:

- Demonstrate the high accuracy of the novel method in estimating throughput, even under dynamic and challenging radio channel conditions and without optimized parameter configurations tailored to specific network environments (e.g., rural or urban areas). This validation aims to establish the robustness of the novel method across diverse network scenarios by adapting radio channel quality.
- Determine the optimal parameter configuration for the eTh function, maximizing its effectiveness and minimizing potential overestimation. This optimization process seeks to identify the ideal balance between historical data and current measurements, ensuring both accuracy and efficiency in throughput estimation.

This chapter aims to provide a comprehensive assessment of the *eTh* function's performance, specifically focusing on its ability to accurately account for IP scheduled throughput. The primary objective is to evaluate the precision of the measurement mechanism, rather than directly address network efficiency or resource allocation optimization. By achieving a high level of precision in throughput measurement, the *eTh* function can serve as a reliable foundation for future research and development efforts aimed at enhancing network performance and resource management in diverse cellular environments.

5.4.2.1. Time component calculation changes

This chapter presents test case results and analyzes the accuracy of the time component calculation within IP scheduled throughput measurement, considering the impact of non-conforming Transport Blocks (TBs) on user data scheduling. The study specifically examines the discrepancies in values resulting from the division of a single transmission cycle into multiple bursts, rather than a single burst, as previously discussed in Chapter 4.5.

Table 5.32 presents the results of a comparative analysis of time calculation differences for Intra-site CA connections with activated flow control, where the communication between two different cells on the same eNB is supervised as it was Inter-site CA, utilizing single and multiple streams of TCP traffic. The comparison of relative time errors is conducted based on the number of scheduled TTIs containing user data. This metric provides a balanced approach by considering both the total number of individual TTIs (which are not accounted for by the methods) and the time intervals between TTIs containing sufficiently large data bursts to be counted by the 3GPP principle.

Table 5.32: Time component calculation differences between the standard and the new method with activated new flow control algorithm.

File size	Single stream TCP traffic		2 streams TCP traffic		8 streams TCP traffic		16 streams TCP traffic	
	SM BTR [%]	NM BTR [%]	SM BTR [%]	NM BTR [%]	SM BTR [%]	NM BTR [%]	SM BTR [%]	NM BTR [%]
200 kB	49.06	53.16	33.16	53.13	42.75	70.24	46.47	72.95
500 kB	38.56	62.26	38.18	56.13	40.72	69.08	32.15	74.79
1 MB	40.07	67.08	47.02	63.65	43.42	77.11	57.07	77.59
2 MB	55.45	75.97	44.36	72.03	49.87	81.57	58.30	81.85
5 MB	69.75	83.26	34.03	79.82	45.50	85.95	53.77	88.29
10 MB	76.38	88.11	61.06	85.40	75.85	94.16	64.77	92.78
20 MB	86.79	93.09	78.39	90.98	96.06	97.03	92.61	95.93

The new flow control algorithm demonstrates enhanced precision in scheduling user data during the reception of new data by the eNB from the iperf server. This improvement is attributed to the algorithm's ability to bundle a greater number of TTIs within its time component. Conversely, the standard method exhibits a less comprehensive accounting of bursts within the same transmission pattern. The traffic patterns employed in each test case, involving varying file sizes, were randomized. This implies that the transmission patterns differed for varying numbers of data streams. Analysis reveals that for single TCP stream transmission for 1 MB file size, the new method exhibits a positive BTR difference of up to 27.01% compared to the standard method. Notably, this difference escalates to 45.79% for 2 multiple stream transmission for 5MB file size. This phenomenon arises from the increased volume of IP packets received by the eNB when multiple parallel streams originate from the iperf server, before the PDCP buffer is emptied.

Table 5.33: Data volume component calculation differences between the standard and the new method with activated new flow control algorithm

File size	Single stream TCP traffic		2 streams TCP traffic		8 streams TCP traffic		16 streams TCP traffic	
	SM BDR [%]	NM BDR [%]	SM BDR [%]	NM BDR [%]	SM BDR [%]	NM BDR [%]	SM BDR [%]	NM BDR [%]
200 kB	63.89	75.85	46.29	85.08	50.64	93.95	61.10	97.64
500 kB	49.98	79.76	47.95	85.91	52.84	93.46	36.35	97.62
1 MB	49.81	79.42	51.09	88.28	49.90	95.89	71.02	98.44
2 MB	70.07	85.02	37.40	89.75	56.39	97.56	70.53	98.72
5 MB	81.99	90.82	70.32	93.49	51.03	98.77	59.85	99.27
10 MB	86.31	94.40	84.59	96.35	79.59	99.30	69.45	99.61
20 MB	92.75	97.12	93.91	97.89	98.97	99.72	96.49	99.80

The Table 5.33 presents the results of a comparative analysis of data volume calculation differences for Intra-site CA connections with activated flow control, similarly as for the previous time example. The comparison of relative volume errors is performed based on the total number

of PDCP SDU data volume received for the MeNB cell. This metric provides the ability to measure user data volume from IP packets with IP header volume received in the transport layer.

5.4.2.2. eTputInitMcs related tests

This study investigates the accuracy of IP scheduled throughput measurement in a 2CC environment for TCP 8 multi-stream transmission over an inter-site CA connection. The focus is on evaluating the optimal value of the eTputInitMcs parameter for small data file transfers (e.g., 1 MB). The significance of this parameter is considerably higher for small file transfers compared to large data volume transfers (e.g., 50 MB), where variations in the eTputInitMcs value may only result in minor, potentially insignificant, differences in throughput measurement.

The eTputInitMcs parameter is designed to estimate the initial transmission speed of the SCell on the SeNB at the start of the transmission cycle. Following the configuration and activation of inter-site CA, the MeNB lacks information about the current throughput capabilities of the SCell for a specific user. Therefore, the MeNB relies on an initial input value to estimate the data volume that can be transmitted from the MeNB to the SeNB. This initial value directly influences the shape and responsiveness of the *eTh(t)* function, which governs the adaptation to changing radio channel quality conditions. However, the relevance of the eTputInitMcs parameter diminishes with each subsequent *eTh* value received from the SeNB.

The eTputInitMcs parameter configures the MCS Index, which can range from 0 to 28 and is directly linked to a corresponding MCS table used by the SeNB's cell. Based on specific configuration parameters, including cell bandwidth, number of MIMO layers, and MCS, the MeNB determines the data volume distribution across different carrier components.

A series of tests were conducted with varying eTputInitMcs values, employing a single user in a network cluster. The relative error in throughput measurement was calculated based on the cell's throughput. Due to the inherent randomness of traffic scheduling for small file sizes (1 MB), each test was repeated multiple times to obtain an average throughput value.

To assess the performance under different radio channel conditions, three attenuation levels were applied across the entire test line: 0 dB (no attenuation), 30 dB (medium attenuation), and 45 dB (high attenuation). This resulted in varying antenna signal attenuation, as detailed in Table 5.22-5.25 of Chapter 5.4.1, using the metrics RSSI and SINR.

Figure 5.27 presents an analysis of the relative error associated with the novel method. The results indicate that an initial MCS value of 20 yields the most accurate outcomes. This configuration exhibits an approximate relative error of 18% under ideal radio conditions, 13% under moderate interference, and 8% under high interference levels.

While the relative error is slightly lower for an initial MCS of 28 (maximum Transport Block (TB) size) in the 0 dB test case, this is expected due to the high SINR (30 dB) facilitating optimal data volume rates. However, for the 30 dB and 45 dB test cases, the lower SINR values lead to increased BLER, resulting in retransmissions and a gradual decrease in TB size at the beginning of the transmission cycle. This can potentially lead to unsuccessful transmissions due to reaching the maximum HARQ retransmission limit, which are excluded from the throughput calculation.

Consequently, the throughput measurement is slightly overestimated for an initial MCS of 28 compared to 20, as the burst time is slightly shorter.

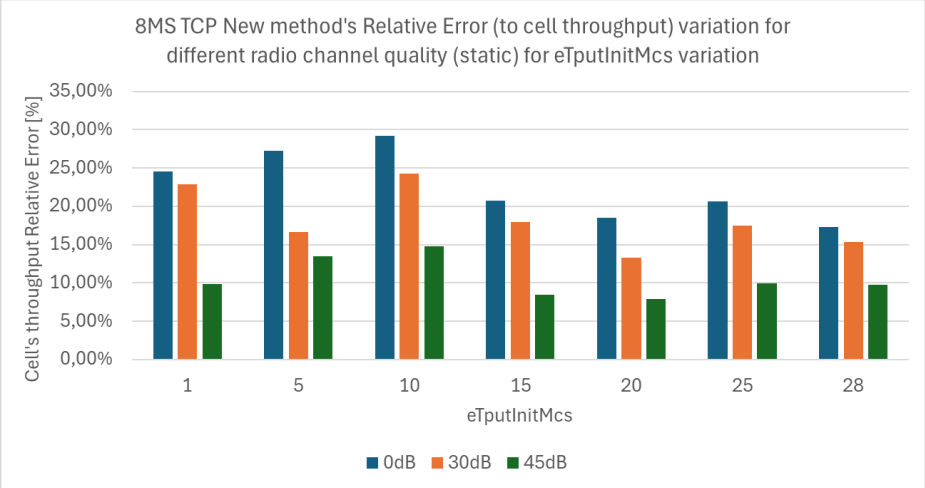

Figure 5.27: TCP/IP 8 multi stream transmission for Inter-site CA with Cell RE for New method with varying eTputInitMcs value and radio channel quality conditions.

Furthermore, for the 45 dB test case, an initial MCS of 1 yields more accurate results than MCS values of 5 and 10. This is attributed to the lower MCS value being more suitable for challenging radio channel quality conditions.

In summary, the optimal initial MCS value for the new method varies depending on the radio channel conditions. An initial MCS of 20 generally provides the most accurate results across different interference levels, while a lower MCS value (e.g., 1) may be more appropriate for extremely challenging conditions.

Figure 5.28 presents a detailed breakdown of data volume and time components for specific initial MCS values. As radio channel attenuation increases, the accuracy of both component measurements improves, approaching 100%. This phenomenon arises from the inability to transmit user data within a single TTI, particularly at the beginning of transmission when radio channel quality is poor. Consequently, the data must be segmented into multiple TBs distributed across different TTIs.

This segmentation strategy, necessitated by challenging radio conditions, leads to a more precise accounting of data volume and time components. As the data is spread across multiple TTIs, the measurement process captures a more accurate representation of the actual data transmission, resulting in values closer to 100%.

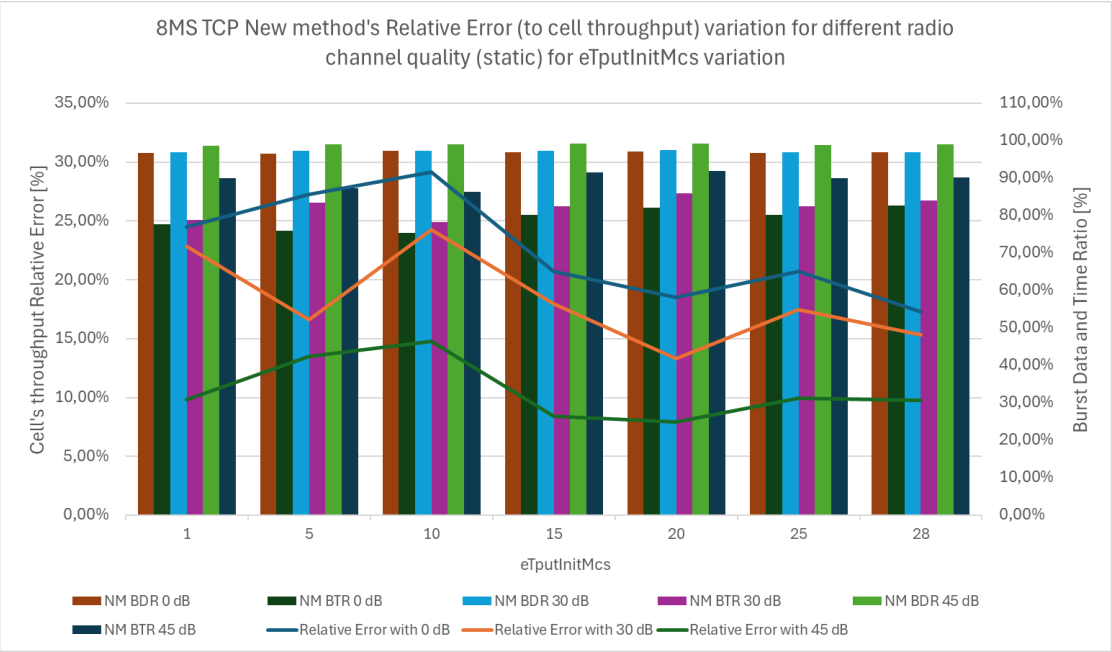

Figure 5.28: TCP/IP 8 multi stream transmission for Inter-site CA with Cell RE and burst components for New method with varying eTputInitMcs value and radio channel quality conditions.

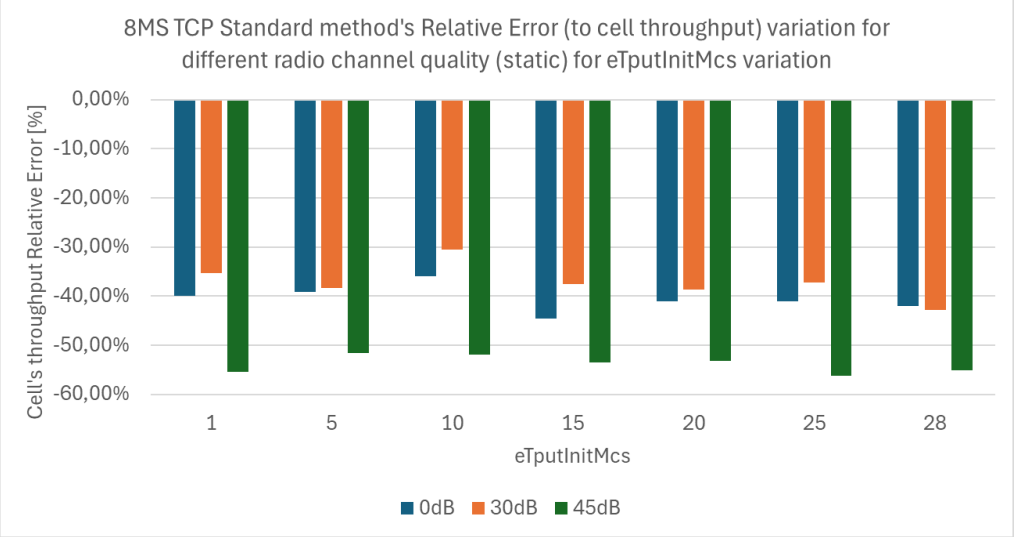

Figure 5.29: TCP/IP 8 multi stream transmission for Inter-site CA with Cell RE for Standard method with varying eTputInitMcs value and radio channel quality conditions.

Analysis of the standard method, as depicted in Figures 5.29 and 5.30, reveals that an eTputInitMcs parameter value of 10 yields the most accurate results. This observation is attributed to the fact that the initial MCS value of 10 exhibits the highest proportion of data volume and time components. Conversely, the new method demonstrates a contrasting trend, exhibiting the highest relative error for an initial MCS value of 10.

Further examination of the data volume and time component values for the standard method indicates that an initial MCS value of 20 produces the most precise results among all sampled values, allocating 42.39% to data volume and 90.63% to time. However, a

comprehensive analysis of this behavior remains inconclusive due to the standard method's inability to accurately account for inter-site CA connections.

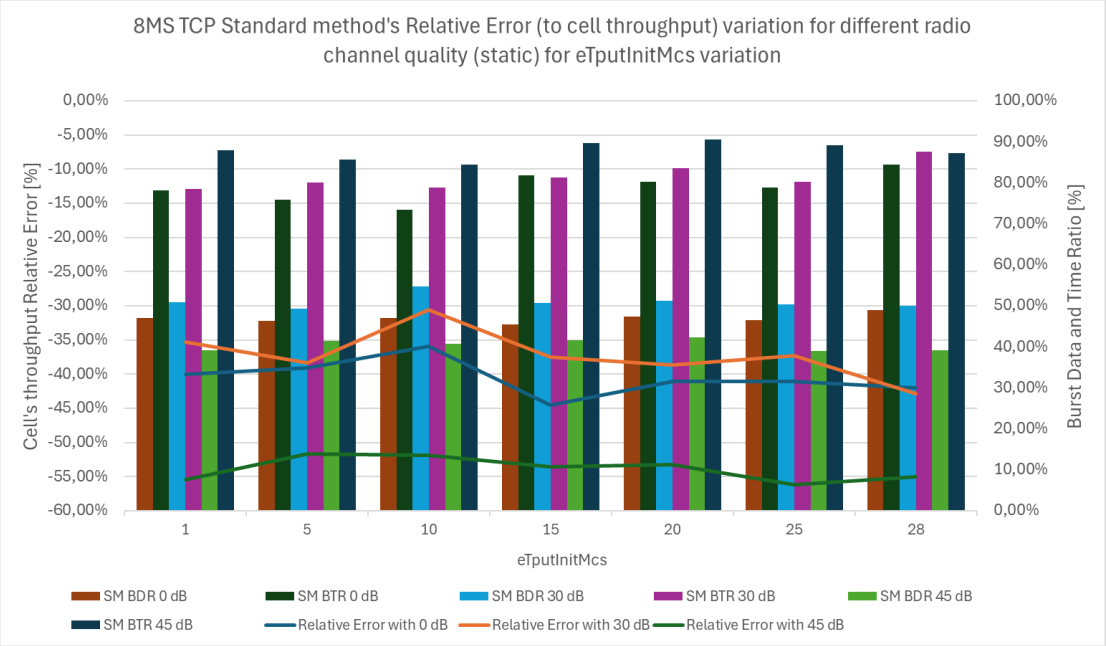

Figure 5.30: TCP/IP 8 multi stream transmission for Inter-site CA with Cell RE and burst components for Standard method with varying eTputInitMcs value and radio channel quality conditions.

5.4.2.3. transferDelayMax related tests

This study investigates the accuracy of IP scheduled throughput measurements in a 2CC environment for TCP 8 multi-stream transmission with inter-site CA connections. The focus is on the impact of the transferDelayMax parameter, which governs the frequency of exchanged *eTh* values between the SeNB and the MeNB. The study aims to evaluate the relative error of IP scheduled throughput measurements for various transferDelayMax values across different file sizes during 8MS TCP transmission, which was chosen to minimize the influence of the TCP slow start mechanism, particularly for smaller file sizes.

The transferDelayMax parameter facilitates the transmission of *eTh* values from the SeNB to the MeNB at a specific periodicity, providing insights into the current throughput capabilities of a user from the SCell perspective. This information is crucial for the MeNB, as it lacks direct access to the SeNB's radio channel quality information for the SCell. Without this parameter, the MeNB would have to estimate the traffic distribution between the master and secondary cells, leading to inefficiency and inaccuracies. The transferDelayMax parameter defines the maximum allowed RLC PDU delay after traffic splitting and can be configured with values ranging from 10ms to 200ms.

A series of tests were conducted for 2CC inter-site CA connections with varying transferDelayMax values. The relative error was measured based on the cell's throughput, with a single user in the network cluster. Due to the inherent randomness of traffic scheduling, particularly for smaller file sizes, the tests were repeated multiple times to obtain an average relative error. To assess the performance under different radio channel conditions, the attenuation from programmable attenuator was set to three levels: 0 dB (no attenuation), 30 dB (medium),

and 45 dB (high) across the test line. Moreover, a fixed attenuator device (50dB/50W) has been used at each RF port of the antenna line for all eNBs in the cluster. This resulted in varying antenna signal attenuation, as presented in as detailed in Table 5.22-5.25 of Chapter 5.4.1, using the metrics RSSI and SINR.

Figures 5.31-5.33 depict the relative error for the new method with different transferDelayMax values under none, medium, and high attenuation level, respectively. The most significant differences are observed for smaller file sizes, where the number of DDDS reports containing *eTh* from the SeNB during transmission is limited, leading to a greater impact on the calculated IP scheduled throughput. As the transmission time increases for larger file sizes, the number of *eTh* reports received also increases.

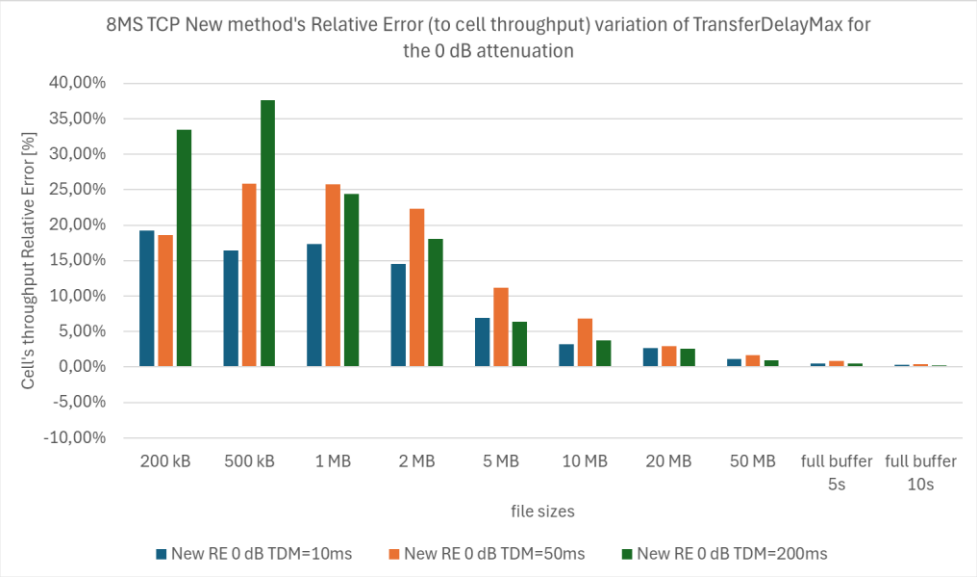

Figure 5.31: TCP/IP 8 multi stream transmission for Inter-site CA with Cell RE for New method with varying transferDelayMax and no attenuation.

Figure 5.31 demonstrates that under perfect conditions, a transferDelayMax value of 10ms achieves the lowest relative error across different file sizes, while 200ms results in the highest (worst) relative error. Figure 5.32 shows that the precision of the IP scheduled throughput measurement improves under medium radio channel quality compared to perfect conditions. For larger file sizes, the disparity in performance between different transferDelayMax values diminishes due to the predominance of stable bursts, which consistently fill the PDCP buffer. This results in a more consistent and predictable data flow, reducing the impact of variations in the transferDelayMax parameter. Moderate interference compromises transmission integrity, necessitating retransmissions. Each retransmission increases the overall burst time, leading to an increment in the time component counter. In certain scenarios, the overall burst time can exceed the total number of scheduled Transmission Time Intervals (TTIs) with user data, as the time between TTIs is counted by the new method but not by the reference statistic. Consequently, the relative error for file sizes exceeding 5 MB exhibits underestimated values, where the data volume component accurately calculates the value near 100%, while the time component reaches approximately 110%.

Figure 5.33 reveals that this phenomenon is more prevalent even for smaller file sizes, with overestimation rarely exceeding 5%. Under high interference, single TTI transmission becomes infrequent, as the data received at the MeNB from the iperf server is divided into consecutive and more robust TBs. This results in the counting of a majority of TBs, leading to a high precision of the measurement.

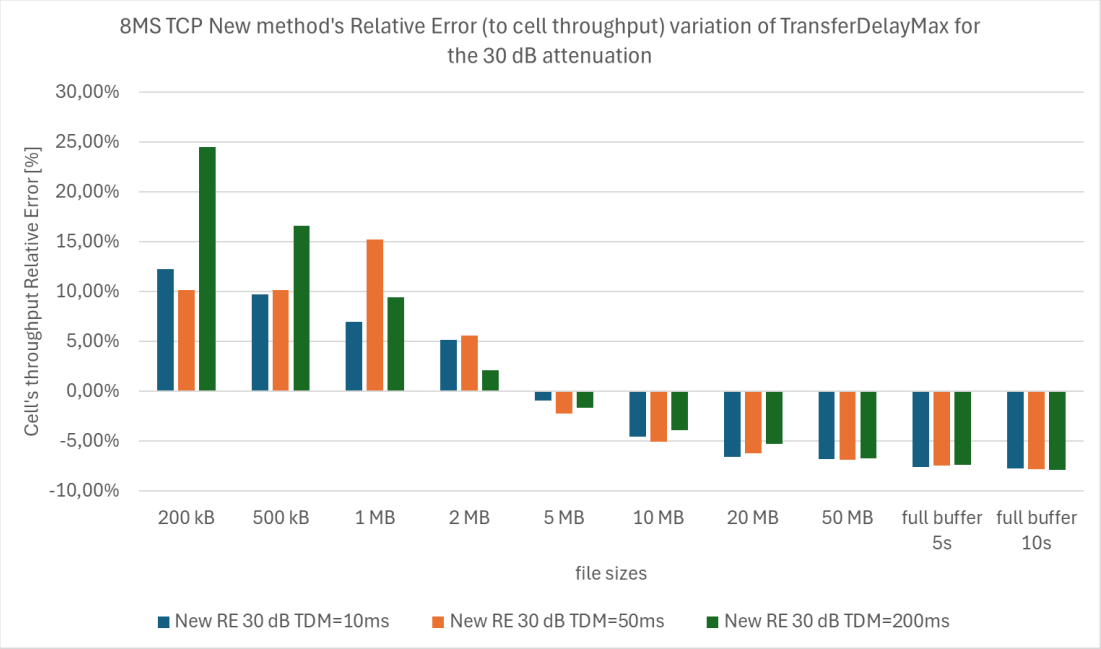

Figure 5.32: TCP/IP 8 multi stream transmission for Inter-site CA with Cell RE for New method with varying transferDelayMax and 30 dB attenuation.

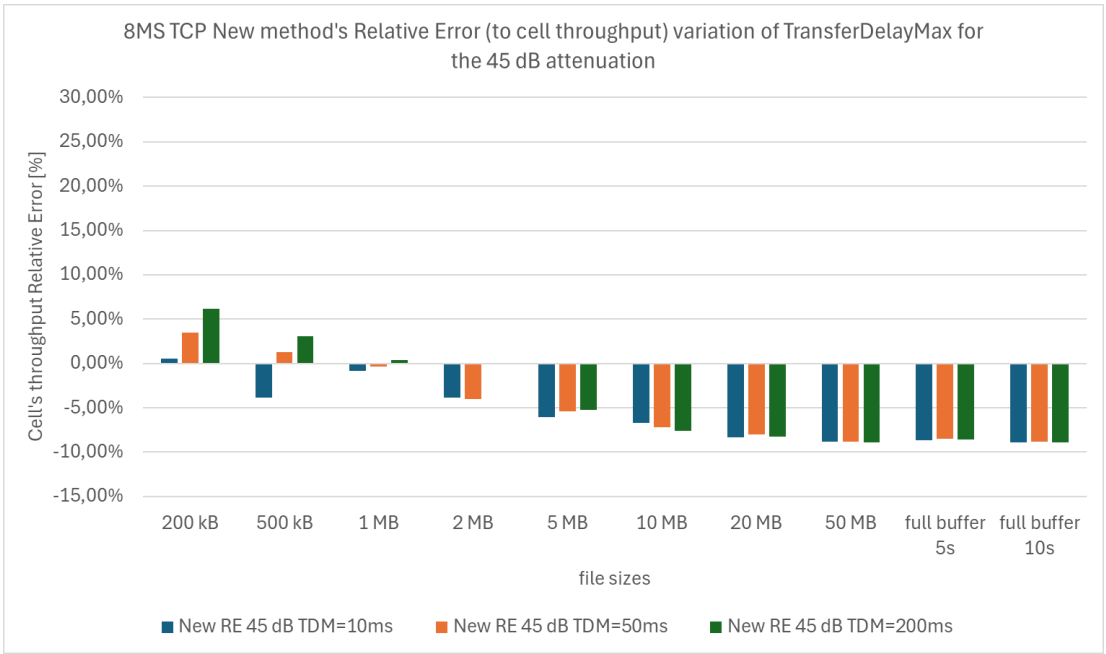

Figure 5.33: TCP/IP 8 multi stream transmission for Inter-site CA with Cell RE for New method with varying transferDelayMax and 45 dB attenuation.

While setting the transferDelayMax parameter to the lowest possible value can be beneficial, it can also pose challenges for the network, as it necessitates the exchange of

numerous reports over the X2 interface. This can lead to network overload during peak hours with a high number of connected CA users.

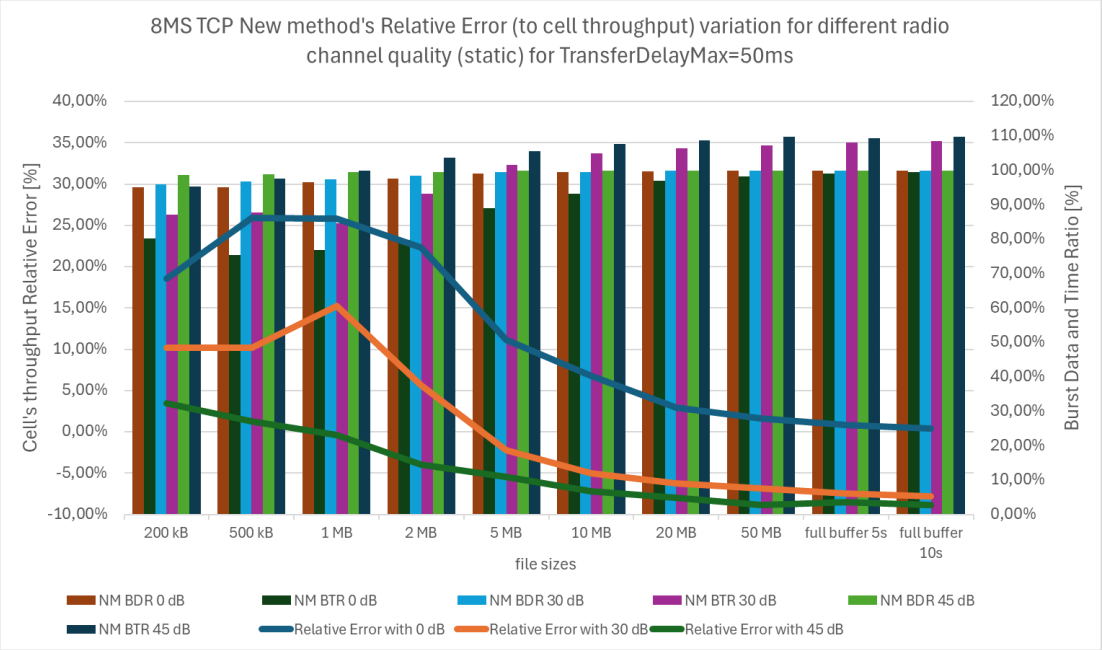

Figure 5.34: TCP/IP 8 multi stream transmission for Inter-site CA with Cell RE for New method with transferDelayMax=50ms value and varying radio channel quality conditions.

Figures 5.34-5.36 present the relative error analysis of a new data transmission method for transferDelayMax values, while varying the radio channel quality conditions (excellent, medium, and poor, respectively). This analysis also incorporates data volume and time components ratios to understand the correlation between relative error and file size.

In Figure 5.34 for a 200kB file size, the time component calculation increases from 80.09% to 87.15% as the attenuation increases from 0 dB to 30 dB, and further to 95.37% for 45 dB. This observation suggests that the single TTIs that occur at the beginning of transmission are segmented into consecutive TBs, fulfilling the 3GPP burst calculation requirement. This segmentation is likely due to the scheduling of TBs with lower MCS values in response to the challenging radio channel quality. In ideal channel conditions, a single TTI would be sufficient to transmit the data, but under degraded conditions, multiple consecutive TTIs are required to carry the same amount of user data but with robust decoding of the signal.

The data volume component also exhibits an increase from 94.99% to 96.01% for attenuation values between 0 dB and 30 dB, and further to 98.71% for 45 dB. This difference highlights that the data volume within individual TTIs is significantly smaller than the overall duration of these TTIs.

For a 50 MB file size, the time component ratio calculation increases from 98.27% to 107.30% for attenuation between 0 dB and 30 dB, and further to 109.69% for 45 dB. The data volume component increases from 99.89% to 99.92% for attenuation between 0 dB and 30 dB, and further to 99.98% for 45 dB. The overestimation of time ratio is attributed to the retransmission mechanism, which leads to an extended burst duration compared to the number of scheduled

TTIs. Additionally, the time between scheduled TTIs is also accounted for, particularly when the PCell is awaiting the completion of transmission by the SCell.

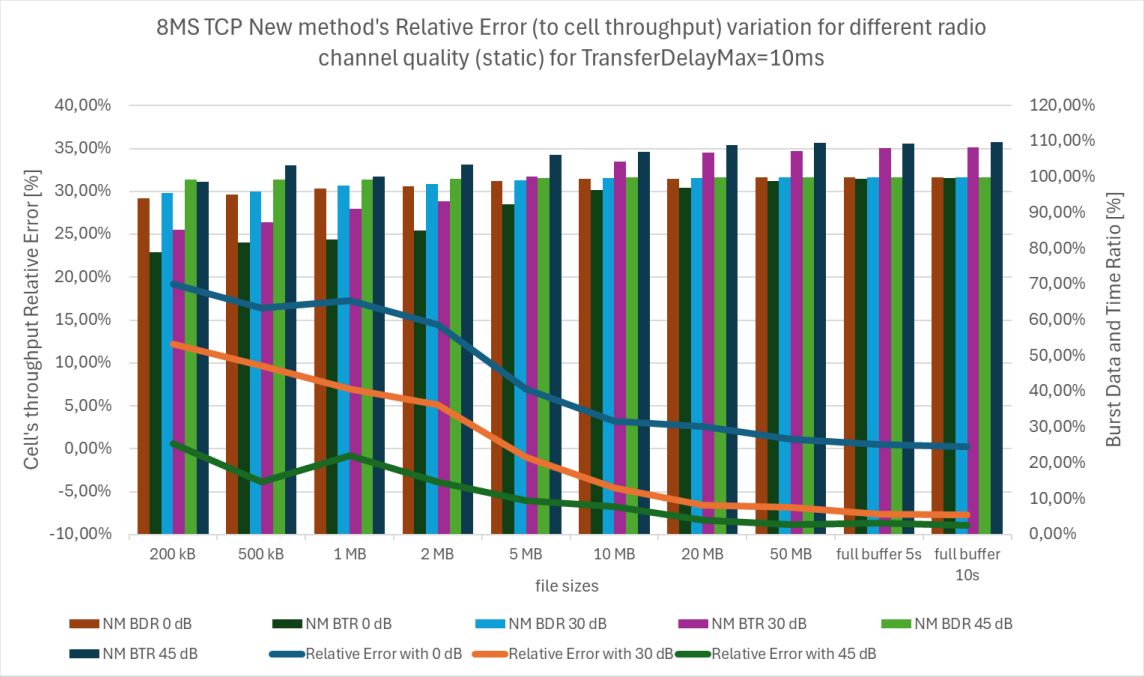

Figure 5.35: TCP/IP 8 multi stream transmission for Inter-site CA with Cell RE for New method with transferDelayMax=10ms value and varying radio channel quality conditions.

In Figure 5.35 the results for transferDelayMax = 10ms demonstrate slightly improved accuracy compared to transferDelayMax = 50ms, likely due to the measured time component with higher frequency. For a 200kB file size, the time component calculation increases from 78.91% to 85.18% for attenuation between 0 dB and 30 dB, and further to 98.75% for 45 dB. The data volume component increases from 94.07% to 95.61% for attenuation between 0 dB and 30 dB, and further to 99.30% for 45 dB.

For a 50 MB file size, the time component calculation increases from 98.81% to 107.23% for attenuation between 0 dB and 30 dB, and further to 109.63% for 45 dB. The data volume component increases from 99.90% to 99.93% for attenuation between 0 dB and 30 dB, and further to 99.97% for 45 dB. The improved time calculation accuracy is attributed to three factors: concatenation of single TTI transmissions, successful retransmission mechanism (unsuccessful retransmissions would result in re-sending the same data from the iperf server), and accounting for the time when the SCell is scheduling while the PCell is inactive.

In Figure 5.36 the results for transferDelayMax = 200ms exhibit the lowest accuracy compared to the other two parameter values. This is expected, as a lower frequency of *eTh* exchange leads to a higher degree of inaccuracy. For a 200kB file size, the time component calculation increases from 70.57% to 76.99% for attenuation between 0 dB and 30 dB, and further to 93.27% for 45 dB. The data volume component increases from 94.18% to 95.84% for attenuation between 0 dB and 30 dB, and further to 99.03% for 45 dB.

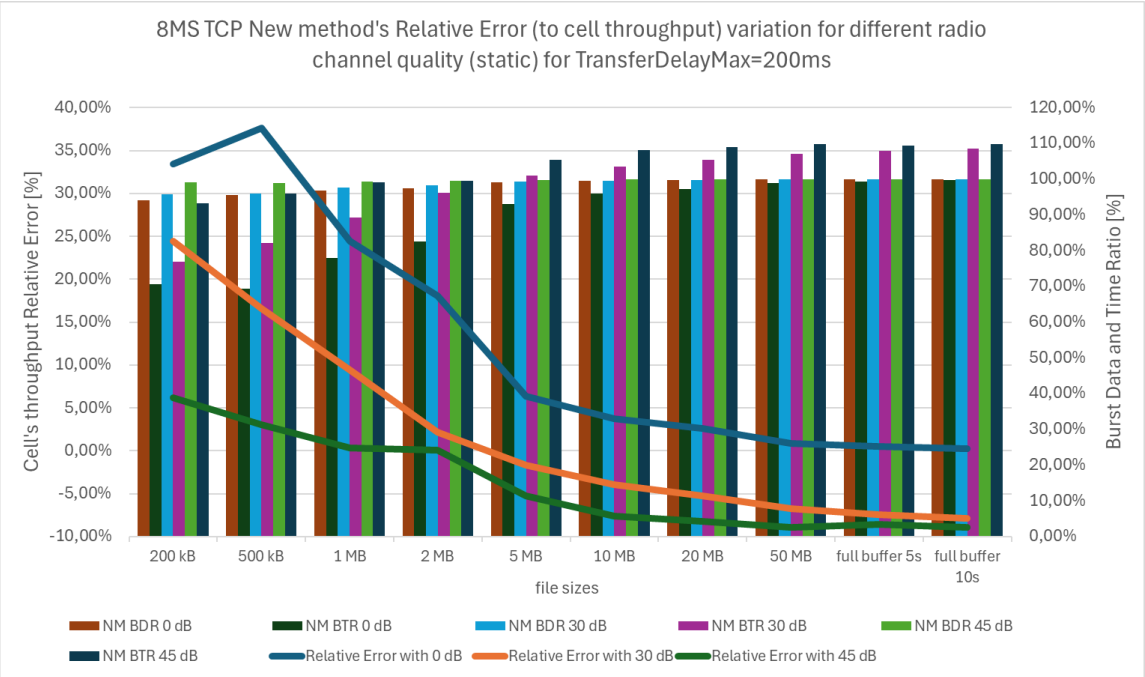

Figure 5.36: TCP/IP 8 multi stream transmission for Inter-site CA with Cell RE for the novel method with transferDelayMax=200ms value and varying radio channel quality conditions.

For a 50 MB file size, the time component calculation increases from 98.99% to 107.09% for attenuation between 0 dB and 30 dB, and further to 109.73% for 45 dB. The data volume component increases from 99.89% to 99.92% for attenuation between 0 dB and 30 dB, and further to 99.98% for 45 dB. The improved time calculation accuracy is attributed to the same three factors mentioned for Figure 5.35.

The analysis demonstrates that the relative error of the new data transmission method is influenced by the transferDelayMax value and the radio channel quality. While the method exhibits improved accuracy with lower transferDelayMax values (the lower the value, the higher the eTh exchange rate) and better channel conditions, it is important to note that perfect radio channel quality is highly improbable in real-world networks. Therefore, the results for 0 dB attenuation should be considered as a theoretical baseline.

For comparison of the measured Cell RE values for different transferDelayMax Table 5.34 is presented. Furthermore, Table 5.35 contains BDR and BTR values for the same test cases.

Table 5.34 – Cell RE with differentiation between transferDelayMax parameter and radio channel quality conditions.

Attenuation	Cell RE with 0dB [%]			Cell RE with 30dB [%]			Cell RE with 45dB [%]		
transferDelayMax	10ms	50ms	200ms	10ms	50ms	200ms	10ms	50ms	200ms
200 kB	19.22	18.60	33.45	12.25	10.17	24.48	0.56	3.50	6.18
500 kB	16.40	25.86	37.63	9.72	10.20	16.59	-3.84	1.25	3.04
1 MB	17.31	25.78	24.45	6.98	15.24	9.42	-0.84	-0.39	0.33
2 MB	14.49	22.31	18.05	5.16	5.60	2.15	-3.87	-4.00	0.07
5 MB	6.96	11.18	6.37	-0.95	-2.23	-1.65	-6.07	-5.41	-5.29
10 MB	3.22	6.79	3.75	-4.53	-5.06	-3.90	-6.72	-7.22	-7.59
20 MB	2.64	2.97	2.59	-6.57	-6.24	-5.25	-8.33	-8.02	-8.26
50 MB	1.11	1.64	0.91	-6.81	-6.88	-6.69	-8.81	-8.85	-8.88
5s	0.49	0.87	0.54	-7.59	-7.45	-7.40	-8.66	-8.48	-8.56
10s	0.29	0.41	0.22	-7.72	-7.84	-7.90	-8.94	-8.84	-8.95

Table 5.35 – Data volume and time component ratios with differentiation between transferDelayMax parameter and radio channel quality conditions.

	0dB attenuation						30dB attenuation						45dB attenuation					
Ratio	BDR [%] and BTR [%]						BDR [%] and BTR [%]						BDR [%] and BTR [%]					
tDelMax	10ms		50ms		200ms		10ms		50ms		200ms		10ms		50ms		200ms	
200 kB	94.1	78.9	95	80.1	94.2	70.6	95.6	85.2	96	87.2	95.8	77	99.3	98.8	98.7	95.4	99	93.3
500 kB	95.2	81.8	95	75.5	95.5	69.4	95.9	87.4	96.7	87.8	95.9	82.2	99.4	103	98.8	97.6	98.9	96
1 MB	96.9	82.6	96.6	76.8	96.9	77.9	97.6	91.2	97.4	84.5	97.7	89.3	99.3	100	99.4	99.8	99.4	99.1
2 MB	97.5	85.1	97.6	79.8	97.5	82.6	98.1	93.3	98.4	93.2	98.2	96.1	99.5	104	99.6	104	99.6	99.5
5 MB	98.8	92.4	99	89.1	99	93.1	99.2	100	99.4	102	99.3	101	99.8	106	99.8	106	99.8	105
10 MB	99.4	96.3	99.5	93.1	99.5	95.9	99.6	104	99.6	105	99.6	104	99.9	107	99.9	108	99.9	108
20 MB	99.5	97	99.8	96.9	99.7	97.2	99.8	107	99.8	107	99.8	105	100	109	100	109	100	109
50 MB	99.9	98.8	99.9	98.3	99.9	99	99.9	107	99.9	107	99.9	107	100	110	100	110	100	110
5s	100	99.5	99.9	99.1	100	99.4	100	108	100	108	100	108	100	110	100	109	100	109
10s	100	99.7	100	99.6	100	99.8	100	108	100	109	100	109	100	110	100	110	100	110

5.4.2.4. eTputFilterConfig related tests

The below test cases aim to evaluate the accuracy of the *eTh* function under adverse radio channel quality conditions. The focus is on validating the function's robustness and precision by conducting tests with both minimum and maximum *eTputFilterConfig* parameter values, representing boundary scenarios. Additionally, the investigation seeks to identify specific radio channel conditions for the SCell that may negatively impact the accuracy of the new method. The goal is to quantify the magnitude of any degradation observed under these conditions, providing a comprehensive assessment of the *eTh* function's performance in challenging network environments.

Two distinct test case scenarios were implemented to evaluate the *eTh* function's performance. The first scenario establishes SINR value equal to 30 dB, serving as a baseline for comparison. The second scenario introduces dynamic SINR changes, simulating realistic network fluctuations. This dynamic scenario involves a loop that alters the user's attenuation every 30 milliseconds with a 10 dB step, ranging from 10 to 60 dB. This manipulation introduces periodic shifts in the SCell's throughput capabilities, transitioning from maximum SINR value (30dB) to challenging conditions every 180 milliseconds, with the transferDelayMax parameter set to 200 milliseconds. This configuration creates a scenario where the SCell's throughput fluctuates at a rate faster than the $\overline{eTh}(t)$ exchange rate, potentially leading to challenges in maintaining accurate throughput estimations and scheduling decisions. This approach emphasizes the impact of these dynamic changes on the current $eTh(t)$ value, as defined by Equation 4.1. By appropriately modifying the forgetfulness factor $T_{eTh}(t)$, it is possible to assess the novel method's responsiveness to these extreme network conditions. This involves evaluating how effectively the method adapts to the fluctuating throughput capabilities of the SCell, considering the interplay between the rate of change in network conditions and the time constant associated with the forgetfulness factor.

The rationale behind this dynamic scenario is to investigate whether the $\overline{eTh}(t)$ calculation performed on the SeNB side might inadvertently force the MeNB to schedule data volumes that exceed the SCell's actual transmission capacity that could lead to inaccurate throughput measurements on the MeNB side due to the inability of the SCell to effectively transmit

the allocated data. By simulating these dynamic conditions, the study aims to assess the $\overline{eTh}(t)$ function's ability to handle such scenarios and ensure accurate throughput management in the presence of fluctuating network conditions.

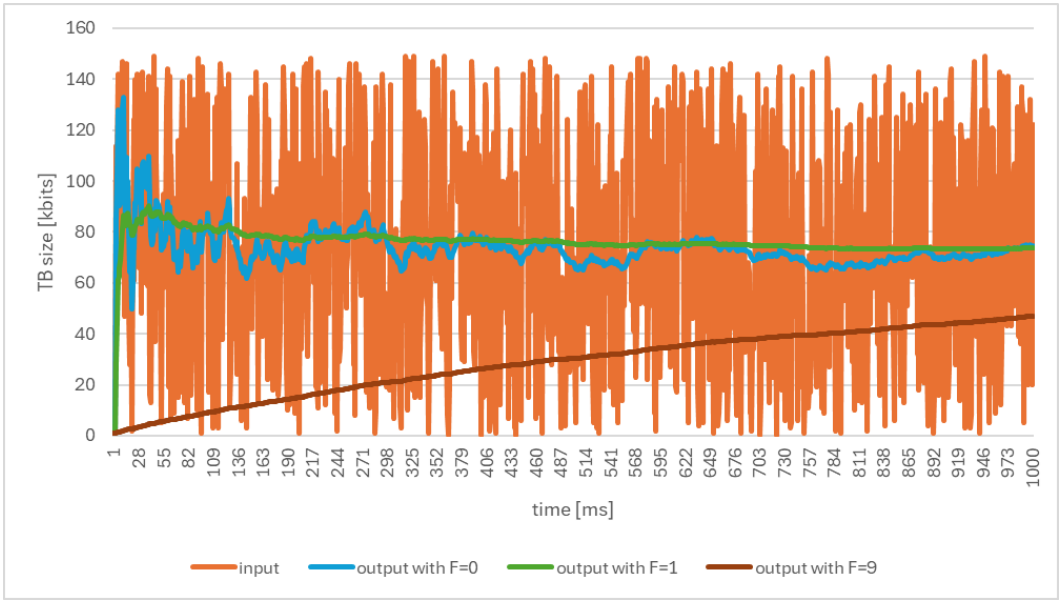

Figure 5.37: *eTh* function example for 1s test case with various forgetfulness factor values and with V set to 990.

Figure 5.38: *eTh* function example for 1s test case with various forgetfulness factor values and with V set to 50.

Figures 5.37 and 5.38 depict the temporal evolution of the *eTh* value, calculated at the SeNB and transmitted to the MeNB, over a 1-second interval. The input value is denoted by $eTh(t)$, while the output value is denoted by $\overline{eTh}(t)$. The output value, expressed as a volume in both figures, represents throughput, specifically the TBS per TTI. For instance, a value of 100 kbits on the y-axis corresponds to an $\overline{eTh}(t)$ of 100kbps. These figures showcase the impact of varying *eTputFilterConfig* parameter values, with the *V* variable set to either 50 or 990. The primary objective of these examples is to illustrate the *eTh* calculation process. Subsequent test cases will further evaluate the precision of the novel method in estimating throughput, regardless

of the specific parameter values employed. This comprehensive analysis aims to validate the robustness and accuracy of the novel method across a range of *eTputFilterConfig* values.

Figure 5.39 presents a visualization of the dynamic SINR fluctuations observed during the test cases. This figure depicts the SINR and RSSI values measured from multiple antenna ports for both the PCell and SCell, captured using the QXDM application from the user's perspective. The PCell radio channel exhibits stable conditions throughout the test cases, maintaining a consistent SINR of 30 dB. In contrast, the SCell experiences significant SINR variations, ranging from 30 dB to -20 dB. This dynamic behavior highlights the challenging network conditions encountered by the SCell, which necessitate robust throughput estimation and traffic flow control strategies due to high BLER value in SCell.

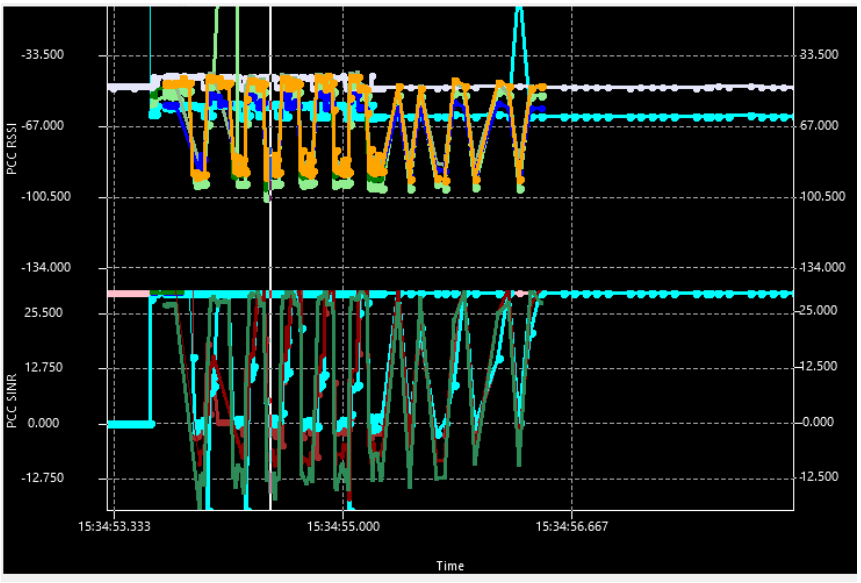

Figure 5.39: Example of SINR and RSSI fluctuations during the test cases measured using the QXDM application.

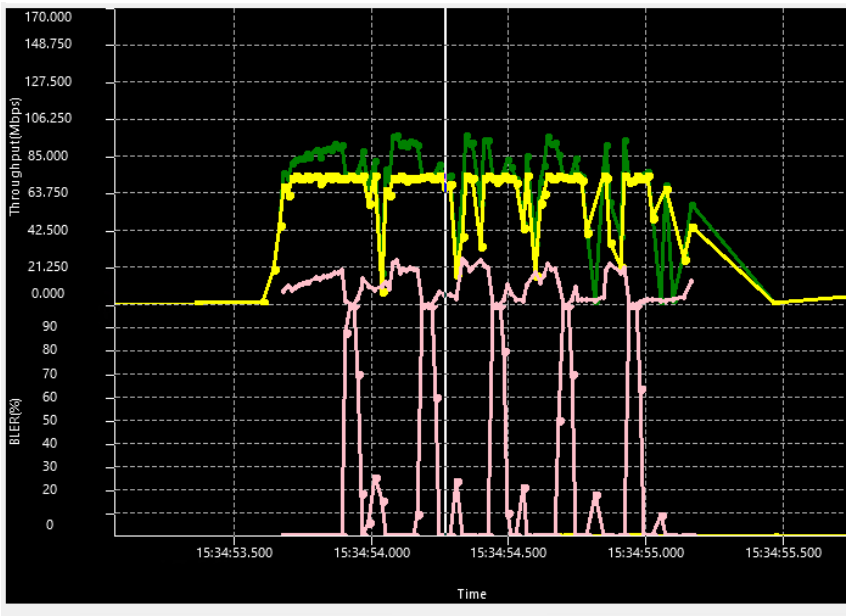

Figure 5.40: Example of application layer throughput and BLER fluctuations during the test cases measured using the QXDM application.

Figure 5.40 complements the analysis by presenting the throughput data obtained from the QXDM application. This figure aims to establish a correlation between the dynamic nature of the radio channel quality conditions and the achieved throughput values, incorporating the Block Error Rate (BLER) metric. The green curve represents the aggregated throughput from both the PCell and SCell, while the yellow curve corresponds to the PCell throughput and the pink curve to the SCell throughput. Notably, the BLER metric is only visible for the SCell, which experiences challenging radio channel quality conditions. This visualization provides valuable insights into the impact of fluctuating SINR on the overall throughput performance, particularly for the SCell, where the BLER metric serves as an indicator of the reliability and efficiency of data transmission.

Tables 5.36 and 5.37 present a comprehensive analysis of various test variations, encompassing different input parameters and scenario conditions. The accuracy of the novel method is evaluated using two metrics: NM TP Cell RE and NM TP App RE. The results demonstrate that despite variations in the $T_{eTh}(t)$ forgetfulness factor, the method consistently maintains a satisfactory level of throughput accuracy. However, a notable exception is observed in test D, where the Cell RE reaches 8.14%, significantly exceeding the typical values observed under similar conditions, such as test F, which exhibits an accuracy of 1.31%.

Table 5.36 – Test case parameter input and precision output values.

	Test	eTput FilterConfig	SINR [dB]	initial MCS	Transfer DelayMax	file size	TCP streams	NM TP Cell RE [%]	NM TP App RE [%]
83	A	990	30	5	200	1s	8	0.54	4.24
84	B	990	dynamic	5	200	1s	8	2.55	43.51
87	C	10	30	5	200	1s	8	1.49	3.74
86	D	10	dynamic	5	200	1s	8	8.14	53.93
81	E	999	dynamic	20	200	5s	8	2.64	12.50
221	F	10	dynamic	20	200	5s	8	1.31	14.13
222	G	51	dynamic	20	200	5s	8	1.74	8.61
77	H	999	dynamic	20	200	5s	8	0.39	2.56
78	I	10	dynamic	20	200	5s	8	1.75	4.92

Table 5.37 – Test case results with differentiation between data volume and time component ratios, and throughput values for test cases defined in Table 5.36.

Test	SM TP [Mbps]	NM TP [Mbps]	App TP [Mbps]	Cell TP [Mbps]	SM BDR [%]	SM BTR [%]	SM TP Cell RE [%]	SM TP App RE [%]	NM BDR [%]	NM BTR [%]	NM TP Cell RE [%]	NM TP App RE [%]
A	49.77	96.74	92.80	96.22	50.66	97.94	-48.28	-46.37	99.94	99.41	0.54	4.24
B	42.70	75.06	52.30	73.19	61.29	105.04	-41.65	-18.35	99.19	96.73	2.55	43.51
C	51.21	98.14	94.60	96.70	51.81	97.83	-47.04	-45.87	99.97	98.51	1.49	3.74
D	44.28	75.58	49.10	69.89	63.42	100.09	-36.64	-9.81	98.72	91.28	8.14	53.93
E	48.57	77.18	68.60	75.19	63.64	98.52	-35.40	-29.20	99.60	97.04	2.64	12.50
F	47.29	77.56	67.96	76.56	61.83	100.10	-38.23	-30.41	99.59	98.31	1.31	14.13
G	47.39	78.31	72.10	76.97	61.35	99.64	-38.43	-34.27	99.67	97.97	1.74	8.61
H	48.66	78.46	76.50	78.16	61.60	98.95	-37.74	-36.39	99.81	99.42	0.39	2.56
I	48.59	80.16	76.40	78.78	60.75	98.50	-38.32	-36.40	99.56	97.84	1.75	4.92

When the eTputFilterConfig parameter is set to 990, the previous historical value of $\overline{eTh}\,(t_{previous})$, as defined in Equation 4.1, exerts a greater influence on the final $\overline{eTh}\,(t)$ value. This implies that a longer time period is required for $\overline{eTh}\,(t)$ to converge to the current $eTh(t)$ value. Conversely, when eTputFilterConfig is set to 10, the convergence time is significantly

reduced, allowing $\overline{eTh}\ (t)$ to rapidly approach the current $eTh(t)$ value. This behavior highlights the impact of the eTputFilterConfig parameter on the time constant associated with the exponential smoothing process, effectively controlling the rate at which the historical data influences the estimated throughput.

The results suggest that putting a high importance for the final *eTh* value on current *eTh* value may lead to an increased relative error given by NM TP Cell RE. However, the significance of such overestimation does not exceed 10%.

The findings indicate that prioritizing the current $eTh(t)$ value in the calculation of the final $\overline{eTh}\ (t)$ value can lead to an elevated overestimation of relative error, as measured by the NM TP Cell RE. However, the magnitude of this overestimation remains within a relatively modest range, not exceeding 10%. This suggests that while a strong emphasis on the current $eTh(t)$ value may introduce a slight bias towards overestimation, the overall impact on the accuracy of the method remains within acceptable limits.

5.4.3. Radio channel quality degradation at distinct cells

This summary aims to evaluate the accuracy discrepancies between the standard and the novel method for data volume and time component burst calculation under varying radio channel quality conditions based on the test cases from Chapter 5.4. The focus is on scenarios where radio channel quality is significantly degraded in the SCell(s) while the PCell(s) maintains acceptable conditions, and scenarios where radio channel quality is degraded in both the PCell and SCell(s). The objective is to analyze the performance of the burst calculation mechanisms in these scenarios, specifically examining how the perceived transmission bottleneck manifests when degradation occurs in both cells and when it occurs in only one cell.

The test cases involve eight multi-stream TCP transmissions with full buffer utilization, each lasting for one second. The application layer and cell throughput for each test case are expected to vary depending on the degradation of the radio channel quality in the associated cell. The parameters *transferDelayMax*, *eTputFilterConfig* and *eTputInitMcs* were held constant at 200, 10 and 5, respectively, across all test cases. This configuration, intentionally set to reduce the accuracy of IP-scheduled throughput method, allowed for the evaluation of Cell RE under adverse radio channel conditions. The novel flow control algorithm enhancement is enabled for both the standard and novel methods, meaning that the accounting of the time component shall differ between the methods as outlined in Chapter 4.5.

5.4.3.1. SCell radio channel quality degradation

Table 5.38: Test case of SCell radio channel quality degradation results with differentiation between data volume, time and throughput values.

SM TP [Mbps]	NM TP [Mbps]	App TP [Mbps]	Cell TP [Mbps]	SM BDR [%]	SM BTR [%]	SM TP Cell RE [%]	SM TP App RE [%]	NM BDR [%]	NM BTR [%]	NM TP Cell RE [%]	NM TP App RE [%]
39.22	72.77	46.00	69.83	63.62	113.27	-43.84	-14.75	98.21	94.25	4.21	58.19

Table 5.38 presents the results of a test case conducted under conditions of SCell-specific radio channel quality degradation, characterized by a 45 dB attenuation. Figures 5.41

and 5.42 depict the temporal evolution of key transmission metrics, including throughput, BLER, RSSI and SINR.

The novel method demonstrates high resilience in accurately accounting for both data volume and time components, achieving 98.21% and 94.25% accuracy, respectively. These results validate the concept outlined in Chapters 4.3 and 4.4.2, particularly the diagram in Figure 4.11, which showcases precise accuracy with a Cell RE below 4.21%. However, the App RE exhibits a significant degradation of 58.19%, indicating that the user's perception of achieved throughput is less accurately estimated compared to the Cell throughput. This discrepancy arises from the omission of time intervals between transmission failure, successful retransmission, and subsequent data transmission, where no data scheduling occurs. The observed discrepancy in throughput estimation can be attributed to two factors. Firstly, the tRlcPduDiscard parameter, which restarts data flow upon SCell transmission failure, contributes to reduced overall throughput. This occurs because data originally intended for SCell is rerouted to PCell, leading to transmission stalling and a decrease in throughput. Secondly, the difference in accounting for retransmission mechanisms, as illustrated in Figure 4.15, also plays a role in the observed discrepancies.

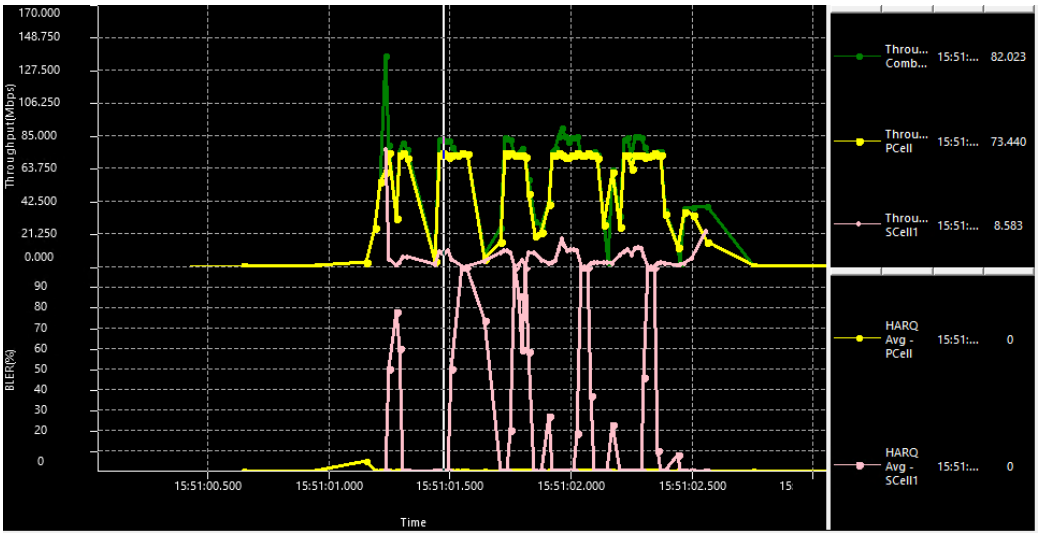

Figure 5.41: TCP/IP 8 multi stream transmission for Inter-site CA with an example of application layer throughput and BLER fluctuations for SCell only during the test cases measured using the QXDM application.

Figures 5.41 and 5.42 present real-time QoS characteristic measurements captured from the Qualcomm QXDM application on the UE side. These figures specifically depict the end-user throughput, BLER, and radio channel quality metrics, including RSSI and SINR, for the specified test case.

Conversely, the standard method overestimates retransmission time, leading to a time component ratio of 113.27% and data volume ratio of 63.62%. This results in an underestimation of Cell RE by -43.84%. However, App RE estimation is more accurate than the novel method, achieving -14.75%. The standard method simply accounts for time between consecutive retransmissions, as depicted in Figure 4.15.

Analysis of SCell transmission issues reveals that the novel method accurately measures IP scheduled throughput compared to the standard method. However, regarding application layer throughput, the standard method's accounting of time between consecutive retransmissions yields better results.

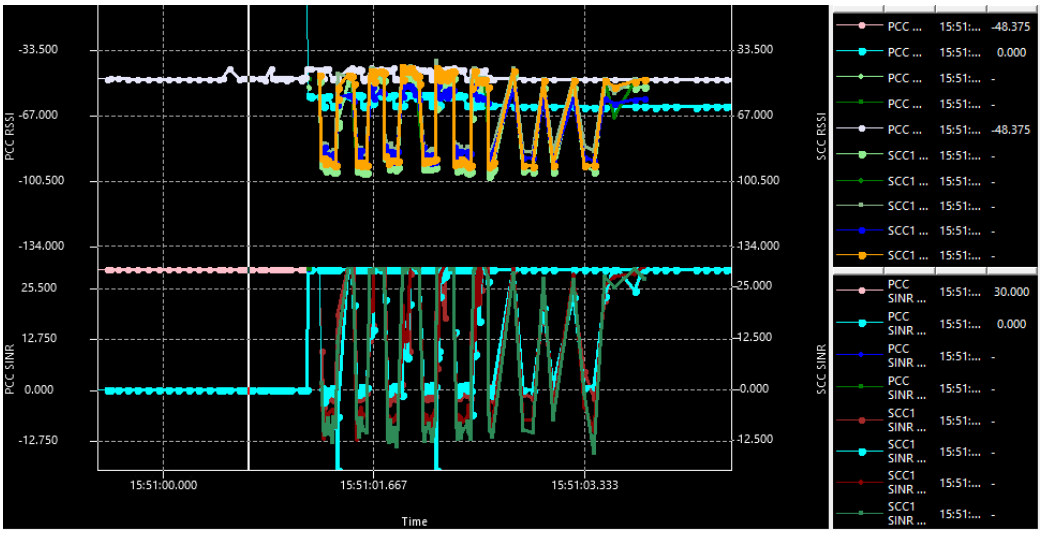

Figure 5.42: TCP/IP 8 multi stream transmission for Inter-site CA with an example of SINR and RSSI fluctuations for SCell only during the test cases measured using the QXDM application.

5.4.3.2. PCell and SCell radio channel quality degradation

Table 5.39 presents the results of a test case conducted under conditions of PCell and SCell specific radio channel quality degradation, characterized by a 45 dB attenuation. Figures 5.43 and 5.44 depict the temporal evolution of key transmission metrics, including throughput, BLER, RSSI and SINR.

Table 5.39: Test case of PCell and SCell radio channel quality degradation results with differentiation between data volume, time and throughput values.

SM TP [Mbps]	NM TP [Mbps]	App TP [Mbps]	Cell TP [Mbps]	SM BDR [%]	SM BTR [%]	SM TP Cell RE [%]	SM TP App RE [%]	NM BDR [%]	NM BTR [%]	NM TP Cell RE [%]	NM TP App RE [%]
11.30	46.14	47.98	48.71	24.32	104.88	-76.81	-76.46	99.76	105.33	-5.29	-3.84

The novel method demonstrates high resilience in accurately accounting for both data volume and time components, achieving 99.76% accuracy and 105.33% overestimated value (5.33% error), respectively. These results validate the concept outlined in Chapters 4.3 and 4.4.2, particularly the diagram in Figure 4.11, which showcases precise accuracy with a Cell RE with a small underestimation of -5.29%. The App RE exhibits a significant improvement of -3.84%, in comparison to SCell quality issue test case. This is related to the fact that PCell also experiences challenging radio channel quality conditions resulting in a situation where the time intervals between transmission failure, successful retransmission, and subsequent data transmission is also counted. This happens because in PCell the flow control algorithm relies on HARQ reception, whereas for SCell it relies on the new estimation concept as outlined in Equation 4.6.

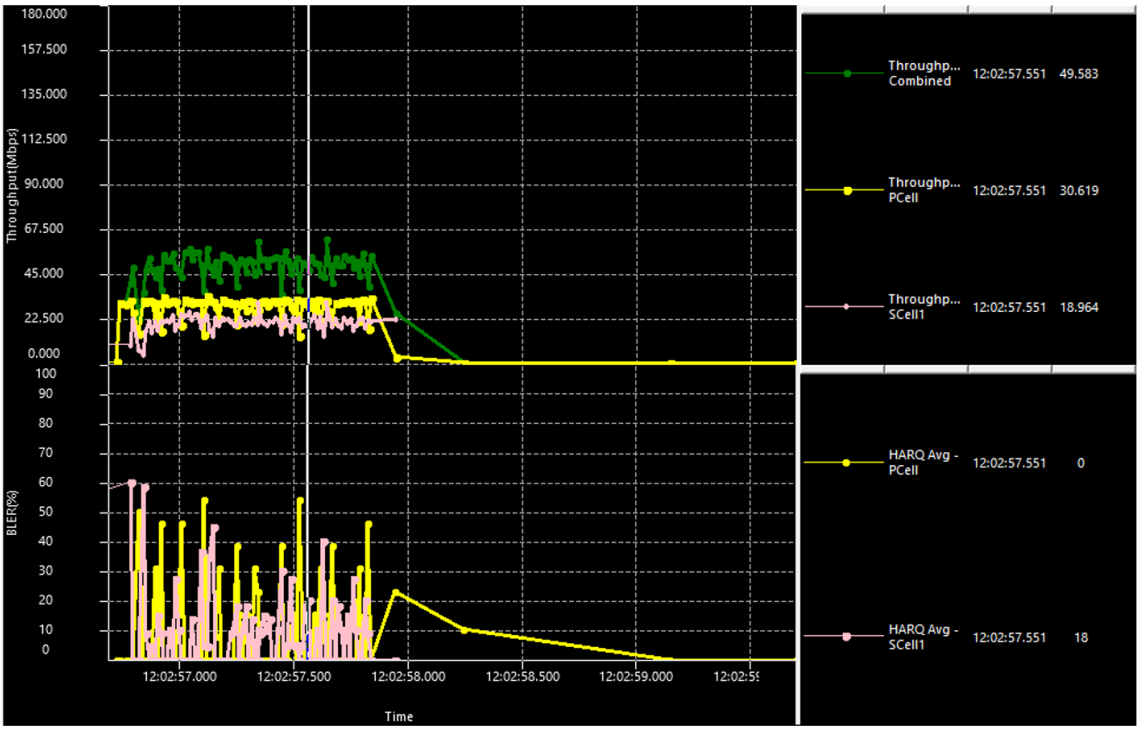

Figure 5.43: TCP/IP 8 multi stream transmission for Inter-site CA with an example of application layer throughput and BLER fluctuations for both PCell and SCell during the test cases measured using the QXDM application.

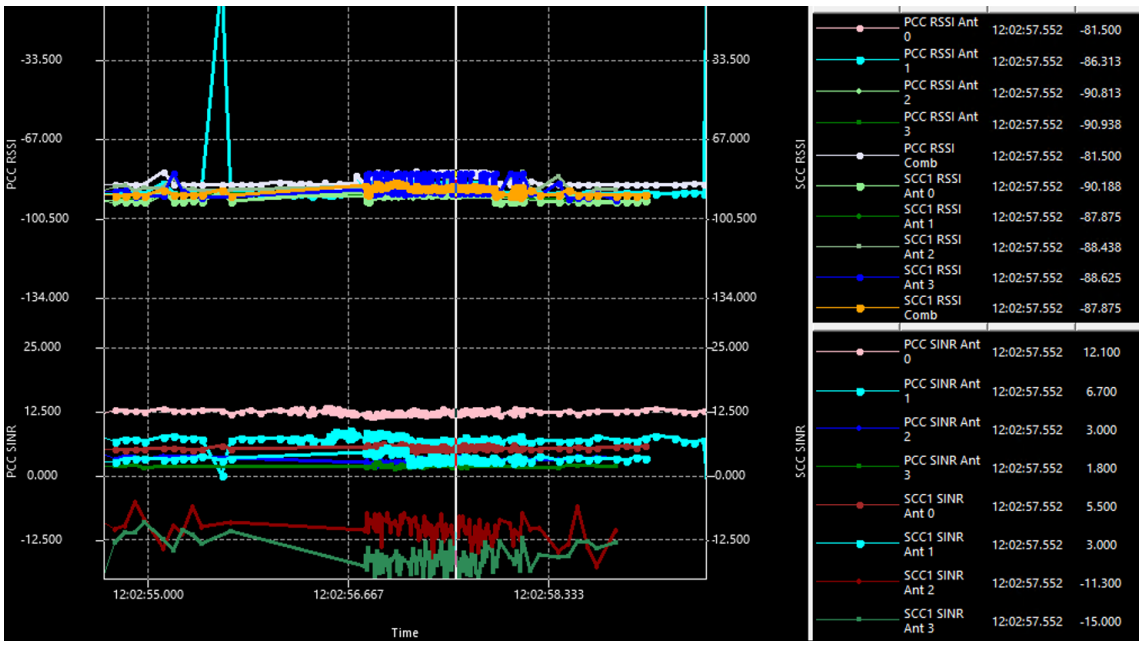

Figure 5.44: TCP/IP 8 multi stream transmission for Inter-site CA with an example of SINR and RSSI fluctuations for PCell and SCell only during the test cases measured using the QXDM application.

The standard method demonstrates an overestimation of retransmission time, leading to a time component ratio of 104.88% (4.88% error). Conversely, a significant underestimation of the data volume component ratio is observed, reaching 24.32%. This reduced data volume accuracy, approximately 2.6 times lower than the previous test case, is attributed to the transmission of a larger data volume over the SCell. Consequently, the Cell RE and App RE achieved -76.81% and -76.46% values, respectively. However, the time component ratio

difference between the standard and novel methods in this test case is negligible, less than 0.5%, with a slightly higher value for the standard method.

Analysis of transmission issues in both the PCell and SCell indicates that the novel method accurately measures IP scheduled throughput compared to the standard method for both Cell RE and App RE.

5.4.4. Dynamic RSRP and SINR

This study investigates the impact of dynamic attenuation changes on the relative error of both the standard and the new method for measuring throughput in both PCell and SCell cells to simulate high interference or fading scenarios. The analysis will examine the distribution of volume and time component ratios in relation to the relative error of cell throughput and application layer throughput.

The study will also explore the relevance of cell throughput in high retransmission scenarios for both the PCell and SCell. In such scenarios, the increased burst time required for retransmissions diminishes the direct comparability of cell throughput to IP-scheduled throughput for a single user connection. Moreover, 4CC connection shall be used to evaluate a more complex connection type during fading or high interference phenomena. The test shall be performed only for inter-site CA connection type, where every distinct SCell belongs to a different SeNB.

To mitigate the influence of TCP slow start and minimize the number of single TTI transmissions, TCP 16 multi-stream transmission is employed. This approach allows for a direct assessment of the impact of challenging radio channel conditions that necessitate link adaptation mechanisms for signal decoding and successful data delivery to the user. The amount of transmitted data volume has been set to 50 MB for each test case.

To evaluate the accuracy of the new throughput measurement method in realistic network conditions characterized by variable radio channel quality, an attenuator was employed to simulate degraded radio signal reception between the radio module and the user. The attenuator details have been described in Chapter 5.4.1.

To evaluate the performance of both methods, a time-varying radio channel models were employed. The radio channel fading model utilizes linear attenuation profiles with a rate of 1 dB per 5, 10 and 20 milliseconds, depending on the test case. This attenuation continues until the signal experiences a cumulative loss of 58 dB, at which point communication becomes unreliable due to the signal-to-noise ratio falling below the threshold for reliable reception. Subsequently, the fading process reverses at the same linear rate. The link adaptation algorithm dynamically adjusts the MCS parameters in response to variations in the radio channel quality. The objective is to verify the accuracy of throughput measurement while ensuring reliable data transmission, without a loss of connection. As the channel quality improves during the fading retreat, the MCS values are incrementally increased, ultimately reaching the maximum achievable value for the given channel conditions.

This resulted in dynamically varying antenna signal attenuation for which the maximum and minimum points have been selected and presented in Table 5.40, using RSSI and SINR the metrics captured with QXDM application at the UE side.

Table 5.40: Inter-site CA antenna signal power and quality level details with SINR values.

Attenuation	Cell type	SINR combined [dB]	SINR Ant 1 [dB]	SINR Ant 2 [dB]	SINR Ant 3 [dB]	RSSI combined [dBm]
0 dB	PCell	30	30	-	-	-37.4
	SCell1	24.2	30	-	-	-50
	SCell2	30	25.8	-	-	-39.5
	SCell3	30	30	-	-	-50.4
58 dB	PCell	-4.3	-1.8	-	-	-85.8
	SCell1	-13.7	-10	-9	-10.6	-92.1
	SCell2	-1.7	-11.4	-5.7	-5.2	-85.8
	SCell3	-5.6	-12.8	-9.5	-12.5	-92.8

The difference between the peak SINR value and the minimum SINR value during a fading event represents the fading depth. This metric quantifies the severity of the signal attenuation caused by fading. The example of SINR variations has been illustrated upon Figure 5.45, 5.46 and 5.47. For Figure 5.46 and 5.47 the transmission has ended upon 2nd and 6th fading depth respectively, meaning that the next 3rd and 7th fading depth had no impact on the transmission scenario.

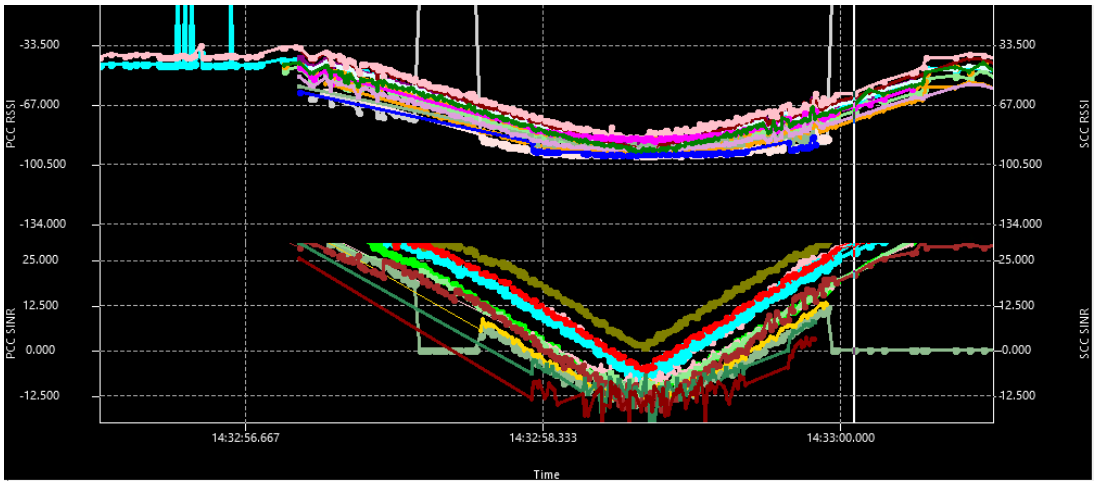

Figure 5.45: Dynamic SINR changes with 1 fading depth with a rate of 1 dB per 20 milliseconds.

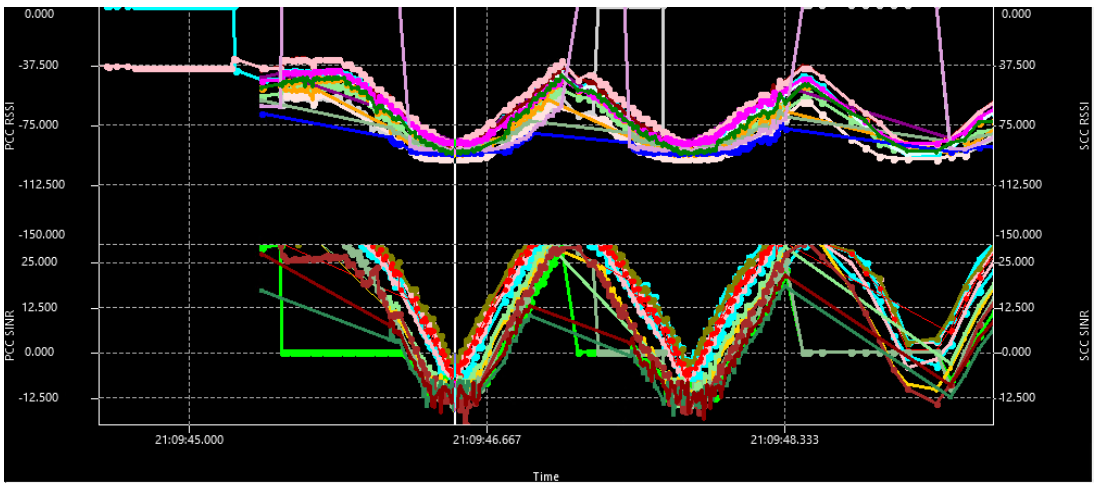

Figure 5.46: Dynamic SINR changes with 2 fading depths with a rate of 1 dB per 10 milliseconds.

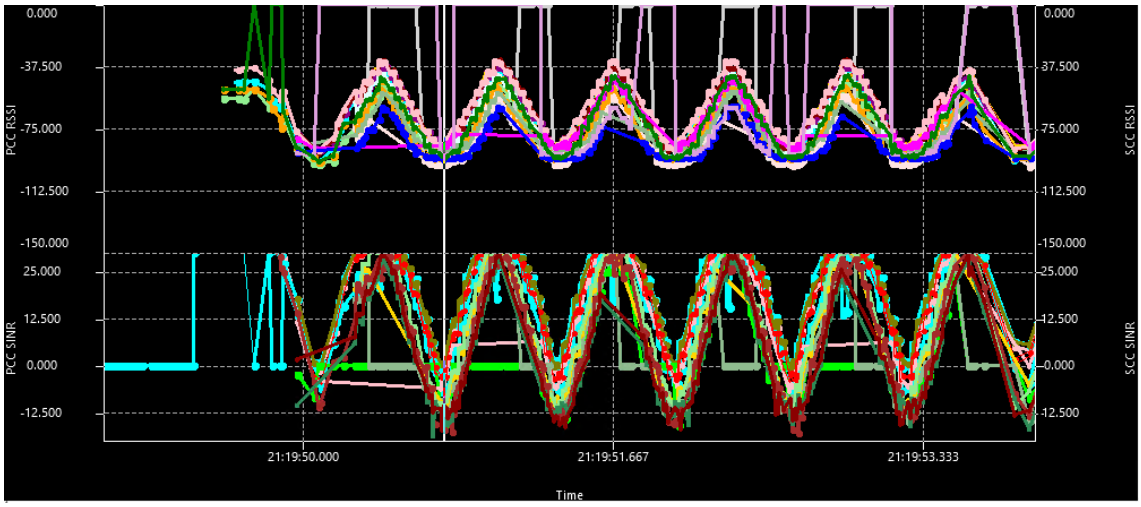

Figure 5.47: Dynamic SINR changes with 6 fading depths with a rate of 1 dB per 5 milliseconds.

Three distinct test scenarios were conducted to evaluate the accuracy of two methods under varying fading event frequencies, as presented in Table 5.41. A comparative analysis of measurement accuracy between the standard and the novel method reveals substantial discrepancies in the context of Inter-site CA scenario.

Table 5.41: 4CC Inter-site CA test scenario accuracy results with different number of fading depths.

Fading Depths	SM TP App RE [%]	SM TP Cell RE [%]	SM BDR [%]	SM BTR [%]	NM TP App RE [%]	NM TP Cell RE [%]	NM BDR [%]	NM BTR [%]
1	-78.28	-80.71	19.6	101.4	10.68	-1.73	99.7	101.4
2	-73.97	-78.34	24.1	111.2	11.54	-7.20	99.9	107.6
6	-73.11	-80.61	24.1	124.5	18.12	-14.82	99.9	117.3

The novel method demonstrates significantly higher accuracy in measuring cell throughput (NM TP Cell RE) compared to the standard method (SM TP Cell RE). This discrepancy arises from the standard method's incompatibility with the burst calculation logic employed in Inter-site CA scenarios, resulting in inaccurate measurement of the transmission data volume component.

The accuracy of the novel method (NM TP Cell RE) decreases with an increasing number of fading events during transmission. However, it exhibits superior resilience to fading compared to the standard method. For instance, the novel method achieves a data volume component ratio of up to 99.9% (NM BDR) even with increased fading depths. Conversely, the time component ratio (NM BTR) increases up to 117.3% for six fading depths due to the increased number of retransmissions in the PCell. This increase in retransmissions extends the burst time length when retransmission events for a specific RLC PDU are successful.

These findings indicate that the novel method effectively addresses the limitations of the standard method in Inter-site CA environments, particularly under dynamic and challenging radio channel conditions. The superior accuracy of the novel method stems from its adaptation to the specific requirements of Inter-site CA, particularly in terms of burst calculation, as detailed in

Chapter 4.4.2. This adaptation ensures accurate measurement of transmission components, leading to a more reliable assessment of performance metrics.

5.5. User Density and Component Carriers Quantity on Measurement Accuracy

This chapter presents a comprehensive evaluation of the novel throughput estimation method, focusing on its accuracy under high-capacity load conditions. The evaluation considers the impact of both increased component carriers and multiple users, comparing the proposed method to the standard approach. Recognizing the inherent interdependence of these factors, the investigation integrates elements from several research objectives:

- Impact of CC Configuration: The number and distribution of SCells and their interaction with the PCell scheduler significantly influence data distribution during transmission and measurement accuracy. The proposed method's adaptability to the PCell scheduler's data distribution algorithm is evaluated using various SCell configurations. The accuracy of the resulting burst-based throughput is assessed, particularly in comparison to the standard method. This analysis aims to quantify the impact of increasing eTh values received from multiple SeNBs on the accuracy of throughput estimation.
- Influence of User Density: The number of active users in the network directly affects the performance of the flow control algorithm, which in turn influences system capacity and the precision of throughput measurement. Testing with high user densities will reveal how the flow control mechanism influences measurement accuracy. This investigation aims to understand the impact of simultaneous high number of scheduled users on the proposed method's ability to accurately estimate throughput in a congested network environment.

5.5.1. Number of Component Carriers

This research investigates the accuracy of IP scheduled throughput measurements in a multi-carrier (nCC) environment for TCP 8 multi-stream transmission across inter-site CA (DC) connections. The utilization of 8 multi-streams aims to mitigate the influence of TCP slow start, thereby enhancing the precision of the measurements and enabling the derivation of meaningful results based on the disparity in the number of carriers employed during the experiment. Each carrier is managed by a distinct eNB, resulting in a proportional non-linear increase in relative error with the escalating number of carriers utilized. It is noteworthy that each SeNB communicates its unique estimated *eTh* value for a specific user to the MeNB.

Figure 5.48 presents a comparative analysis of the relative error exhibited by the new method for different file size transmissions, employing varying numbers of CCs in an inter-site CA configuration. The analysis was conducted under controlled conditions, utilizing 8 TCP streams for data transmission.

Results indicate a consistent trend of decreasing relative error with an increasing number of CCs. While for small file sizes (≤ 500 kB), data transmission variability is observed, a clear pattern emerges for file sizes exceeding 1 MB, demonstrating a diminishing relative error with increased CCs. For a 2 MB file transfer, the data volume component exhibited a reduction with increasing CCs, registering 97.50%, 96.33%, and 96.05% for 2CC, 3CC, and 4CC configurations,

respectively. Conversely, the time component displayed an increasing trend, reaching 82.45%, 86.59%, and 88.66% for the same configurations. This contrasting behavior resulted in a consistent decrease in relative error, measured at 18.26%, 11.25%, and 8.35% for 2CC, 3CC, and 4CC configurations, respectively. For high data volume transfers, the rate of improvement in relative error diminishes, suggesting that the transmission becomes sufficiently stable for any CA configuration to accurately account for the data. The findings suggest that increasing the number of CCs in inter-site CA configurations can effectively reduce relative error, particularly for larger file transfers.

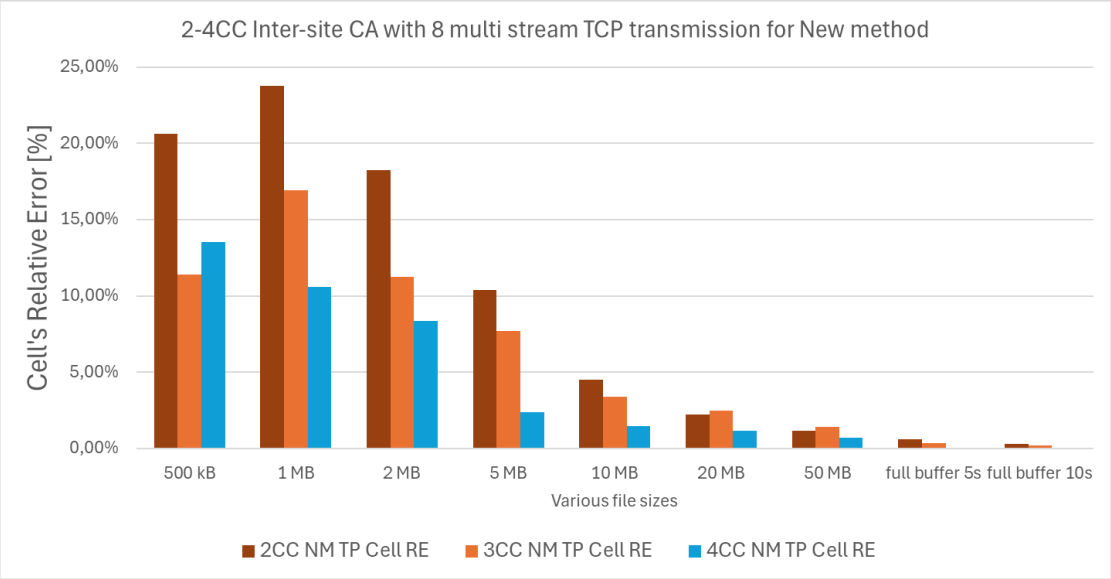

Figure 5.48: Cell's Relative Error in comparison between different CC configuration for inter-site CA for the new method with 8 TCP streams.

Figure 5.49 presents a comparative analysis of the relative error exhibited by the standard method during data transmission in an inter-site CA configuration. The analysis considers varying numbers of CCs.

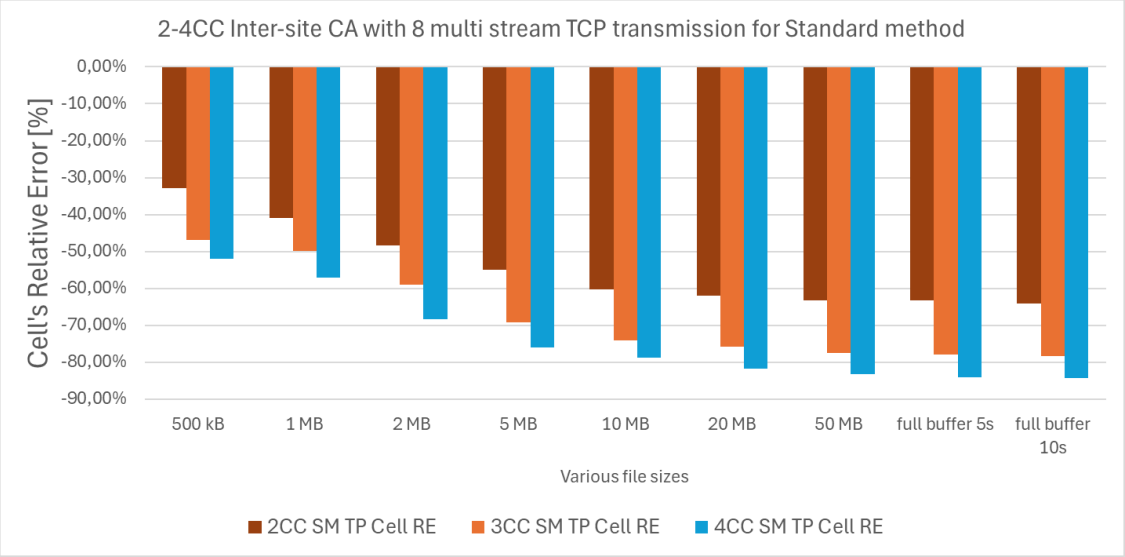

Figure 5.49: Cell's Relative Error in comparison between different CC configuration for inter-site CA for the standard method with 8 TCP streams.

The results indicate a consistent trend of increasing relative error for throughput estimation with an increasing number of CCs. However, this trend is negative compared to the new method, as the standard method consistently underestimates the actual error throughout the test. Furthermore, the continued decrease in relative error with increasing CCs renders the standard method increasingly inaccurate.

For a 2 MB file transfer, the data volume component exhibits a reduction with increasing CCs, registering 43.30%, 35.16%, and 29.81% for 2CC, 3CC, and 4CC configurations, respectively. Conversely, the time component displays an increasing trend, reaching 83.76%, 85.71%, and 94.46% for the same configurations. This contrasting behavior results in a consistent increase in relative error, measured at -48.44%, -58.98%, and -68.44% for 2CC, 3CC, and 4CC configurations, respectively.

For high data volume transfers, the rate of degradation in relative error continues. This is attributed to the increasing distribution of data volume among SCells compared to the PCell transmission.

Figures 5.50 and 5.51 present a comparative analysis of the application layer relative error exhibited by the new method and the standard method during file transmission. The analysis considers varying file sizes and different numbers of CCs within an inter-site CA configuration.

For the new method the results demonstrate a consistent trend across various CC configurations. The relative error reaches its maximum for smaller file sizes (2CC: 5 MB, 3CC: 2 MB, 4CC: 2 MB) and gradually decreases with increasing file size, ultimately stabilizing at the 10-second test scenario. At this point, the relative error values stabilize at 2.52% for 2 CC, 3.08% for 3 CC, and 4.72% for 4 CC. This indicates that for sufficiently large file sizes, the novel method exhibits high precision and reliability.

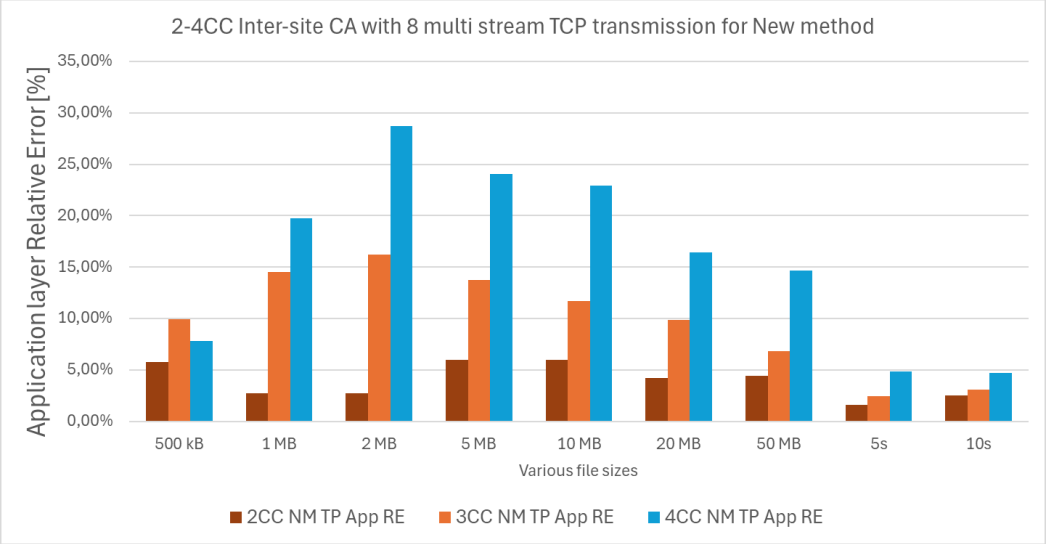

Figure 5.50: Application layer Relative Error in comparison between different CC configuration for inter-site CA for the new method with 8 TCP streams.

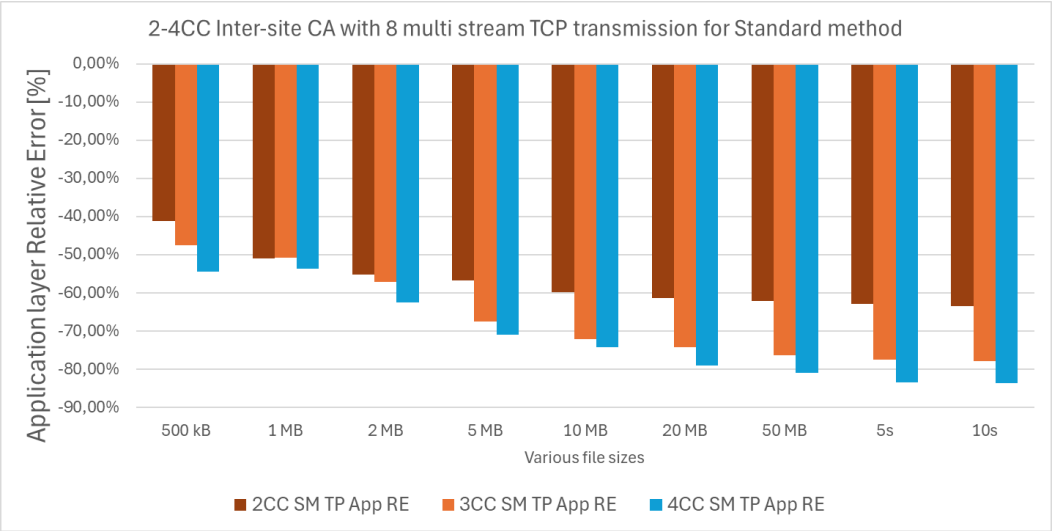

Figure 5.51: Application layer Relative Error in comparison between different CC configuration for inter-site CA for the standard method with 8 TCP streams.

The standard method exhibits a similar trend to that observed in Figure 5.49. With each incremental increase in file size, the negative value of application layer relative error further increases, indicating a reduction in estimation accuracy. This trend suggests that the standard method's performance degrades with increasing numbers of CCs in inter-site CA environments.

Table 5.42 – Inter-site CA traffic details for the new method.

File size	NM BDR [%]			NM BTR [%]			NM Cell RE [%]			NM App RE [%]		
	2CC	3CC	4CC	2CC	3CC	4CC	2CC	3CC	4CC	2CC	3CC	4CC
500 kB	95.15	94.51	93.94	78.90	84.82	82.74	20.60	11.42	13.55	5.76	9.90	7.79
1 MB	96.94	95.19	95.46	78.33	81.41	86.31	23.76	16.93	10.60	2.72	14.50	19.77
2 MB	97.50	96.33	96.05	82.45	86.59	88.66	18.26	11.25	8.35	2.73	16.19	28.71
5 MB	98.96	98.08	97.86	89.65	91.06	95.58	10.38	7.71	2.39	5.99	13.76	24.08
10 MB	99.67	99.01	98.33	95.37	95.74	96.93	4.51	3.42	1.45	5.98	11.69	22.91
20 MB	99.77	99.38	99.09	97.57	96.99	97.96	2.25	2.47	1.15	4.18	9.83	16.42
50 MB	99.90	99.77	99.56	98.77	98.35	98.83	1.14	1.44	0.73	4.44	6.82	14.66
5s	99.95	99.93	99.88	99.34	99.56	99.88	0.62	0.37	0.00	1.59	2.41	4.82
10s	99.97	99.95	99.94	99.66	99.77	100.00	0.31	0.18	-0.06	2.52	3.08	4.72

Table 5.43 – Inter-site CA traffic details for the standard method.

File size	SM BDR [%]			SM BTR [%]			SM Cell RE [%]			SM App RE [%]		
	2CC	3CC	4CC	2CC	3CC	4CC	2CC	3CC	4CC	2CC	3CC	4CC
500 kB	49.91	44.53	40.60	74.24	83.67	84.55	-32.77	-46.78	-51.98	-41.05	-47.51	-54.42
1 MB	47.27	40.41	36.10	80.09	80.43	84.16	-40.98	-49.75	-57.10	-51.02	-50.79	-53.55
2 MB	43.30	35.16	29.81	83.76	85.71	94.46	-48.30	-58.98	-68.44	-55.09	-57.16	-62.51
5 MB	40.20	27.92	23.73	89.37	90.77	98.73	-55.01	-69.24	-75.96	-56.80	-67.52	-70.87
10 MB	37.71	25.21	21.16	94.89	97.64	99.43	-60.25	-74.18	-78.71	-59.69	-72.12	-74.21
20 MB	36.81	23.70	18.39	96.86	98.12	100.94	-61.99	-75.85	-81.78	-61.27	-74.11	-79.03
50 MB	36.01	22.33	16.85	98.22	98.88	100.63	-63.33	-77.42	-83.26	-62.14	-76.22	-80.95
5s	36.27	21.85	15.88	98.58	99.28	100.16	-63.20	-78.00	-84.15	-62.85	-77.55	-83.38
10s	35.56	21.51	15.67	99.23	99.48	99.83	-64.16	-78.38	-84.31	-63.38	-77.75	-83.56

Tables 5.42 and 5.43 present a comprehensive overview of the aforementioned details. Color-coding facilitates the association of tabular data with corresponding chart results displayed in Figures 5.50 and 5.51. The analysis reveals that the new method demonstrates superior performance compared to the standard method in inter-site CA configurations. The new method exhibits high precision and reliability for larger file sizes, while the standard method suffers from

decreasing accuracy with increasing CCs. These findings highlight the potential benefits of the novel method for improving data transmission efficiency and reliability in inter-site CA environments.

5.5.2. Number of Users – based on entity testing with simulated users

This study aims to validate the accuracy of IP scheduled throughput measurement for calculation of time and data volume component in high user density scenarios, where the user data scheduling must be spread to non-adherent Transmission Blocks (TBs) which in result may lead to an erroneous value if the single transmission cycle is divided into multiple bursts rather than one. This test case provides valuable insights into the precision of the novel method when multiple users concurrently utilize the same cell resources, a scenario commonly encountered in cellular networks. To facilitate research, the standard and the novel method were evaluated using high number of users, which serve as a representative model for non-consecutive user data scheduling across TBs.

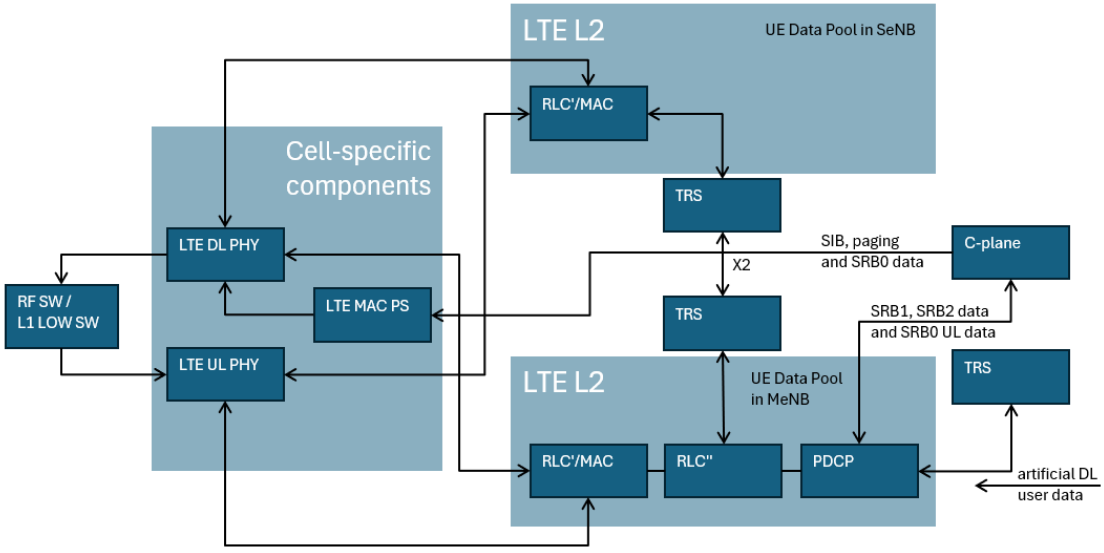

Figure 5.52: Illustrative user data paths in internal traffic simulation for inter-site CA configuration testing in LTE.

This test case deviates from the test line design outlined in Chapter 5.1, necessitating a modified approach to evaluate the impact of multiple simultaneous users on both the standard and novel methods. Due to the complexity of conducting system-level tests with a high number of users concurrently utilizing CA, entity testing within SW was performed using simulated user traffic for an eNB cluster configuration with up to 5CC. A traffic simulation is conducted using artificial data streams, as shown in Figure 5.52, originating from the Transport (TRS) component and entering the LTE L2 component. The IP scheduled throughput measurement is calculated within the L2 component. Upon receiving the artificial data stream, the LTE L2 component executes its software code and initiates flow control procedures to direct the data through the PDCP, RLC (including RLC'' and RLC'), MAC layers. Once all of L2 procedures are completed, the L2 component forwards the data streams to the LTE DL PHY component. This simulation eliminates radio channel degradation issues and relies solely on ideal scheduling principles. Consequently, the results obtained from these tests do not reflect the diverse results observed in

real-world networks serving a high number of users with varying priorities and data transmission needs.

To facilitate a clear evaluation of the obtained results, specific principles were established for this test case. The first constraint limits the maximum number of scheduled UEs per TTI to 10. This ensures that every 1 ms, the available PRBs are evenly distributed among these 10 users. To maximize throughput, UDP full buffer traffic was generated. The simulation involved 50 users, each with a 5CC connection with every cell bandwidth set to 20 MHz. Modulation was set to 256QAM with 2x2 MIMO layers per user. These parameters aim to achieve a cell throughput of up to 1 Gbps. However, in this test case, the equal scheduling strategy should result in 19.5 Mbps per user. Figure 5.53 illustrates an example of this equal PRB resource allocation per user per TTI scheduling time. This tight scheduling, employing a round-robin logic, provides each user with a scheduling opportunity every 5 ms.

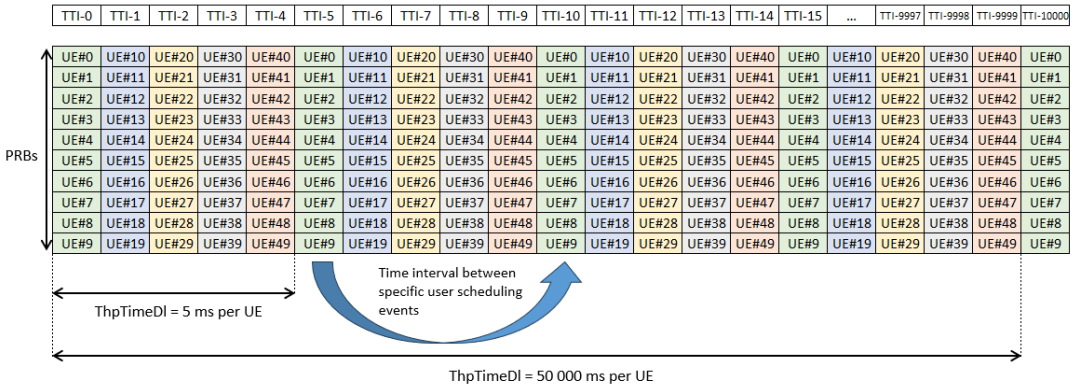

Figure 5.53: An example of equal PRB resource allocation per user per TTI scheduling time.

The performance of both the novel and standard methods for measuring IP scheduled throughput is presented in Tables 5.45 and 5.46. The novel method demonstrates exceptional accuracy in a simplified high user density scenario characterized by equalized PRB allocation across frequency and time domains. The measured throughput values closely align with the simulated 19.5 Mbps per user, exhibiting a minor underestimation of approximately -4.63% for the 5CC Inter-site CA configuration and -1.78% for the 5CC Intra-site CA configuration. Notably, the accuracy of the novel method slightly improves when transitioning from Inter-site to Intra-site with the number of SCells.

Table 5.45: The novel method measurement results for high user density.

number of intra-site SCells	number of inter-site SCells	Flow Control	NM VL [bits]	NM TM [ms]	NM TP [Mbps]	App TP [Mbps]	NM TP RE [%]
0	4	ON	1000587784	52459	19.07	19.5	-4.63
1	3	ON	1000792904	52483	19.07		-4.66
2	2	ON	1000226752	52133	19.19		-4.07
3	1	ON	998694584	51293	19.47		-2.65
4	0	ON	999421784	50876	19.64		-1.78

The standard method exhibits a deficiency in accurately measuring IP-scheduled throughput when employing an Inter-site CA SCell configuration. This inaccuracy arises from the omission of data volume transmitted to the Inter-site CA SCells. Upon transitioning to an Intra-site CA configuration, the standard method demonstrates a significant improvement in accuracy, correctly accounting for both data volume and time components with a precision of 0.34%.

Table 5.46: The standard method measurement results for high user density.

number of intra-site SCells	number of inter-site SCells	Flow Control	SM VL [bits]	SM TM [ms]	SM TP [Mbps]	App TP [Mbps]	SM TP RE [%]
0	4	OFF	7536768	48296	0.16	19.5	-99.22
1	3	OFF	104217216	50414	2.07		-89.66
2	2	OFF	230689000	51525	4.48		-77.61
3	1	OFF	272740656	45342	6.02		-69.92
4	0	OFF	998321320	49748	20.07		0.34

6. SUMMARY

According to dissertation thesis defined in Chapter 1.2 the novel method for capturing traffic parameters exchanged between multiple base stations and user terminals within 4G and 5G cellular networks utilizing DC functionality has been considered. This modified approach significantly improves the accuracy of throughput estimation in comparison with the standardized solution in 3GPP documentation for currently used mobile networks, enabling comprehensive network performance monitoring and evaluation of data transmission service quality. The novel method has been thoroughly tested via multiple different criteria to properly assess the accuracy of IP scheduled throughput measurement calculation in both DC and non-DC systems to determine its versatility over different network configuration types.

The evaluation criteria that are strictly aligned with the novel method's estimation principles, focusing on implementation specifics and improvements compared to the standard method, are the following:

- Impact of key parameters of novel estimation method (Chapter 5.4), in line with thesis T1 and algorithm characteristic T2.
- Impact of time component calculation improvement (Chapter 5.4), in line with algorithm characteristic T2.

Laboratory experiments were conducted to assess the accuracy of the novel IP scheduled throughput measurement estimation for various entry criteria that are widely used in real cellular networks and in the context of thesis defined in Chapter 1.2, such as:

- Impact of TCP slow start mechanism on IP scheduled throughput measurement accuracy (Chapter 5.3), understood as major influential network phenomena, in line with thesis T1 and algorithm characteristics T2 and T3.
- Impact of usage of full buffer UDP and multi-stream TCP protocols (Chapter 5.3), understood as major influential network phenomena, in line with thesis T1 and algorithm characteristics T2 and T3.
- Impact of different packet sizes for a singular transmission per specific user (Chapter 5.3), understood as major influential network phenomena, in line with thesis T1 and algorithm characteristics T2 and T3.
- Impact of non-DC, DC and mixed system environments (Chapter 5.3), in line with thesis T1 and algorithm characteristic T3.
- Impact of short and long transmission durations on stability of the measurement (Chapter 5.3), in line with thesis T1 and algorithm characteristics T2 and T3.
- Impact of static and dynamic radio channel quality variations (Chapter 5.4), in line with thesis T1 and algorithm characteristic T4.
- Impact of retransmission mechanism (Chapter 5.4), understood as major influential network phenomena, in line with thesis T1 and algorithm characteristics T2 and T4.
- Impact of radio channel quality degradation in SCell only and in both PCell and SCell (Chapter 5.4), in line with thesis T1 and algorithm characteristics T2 and T4.

- Impact of the CA connection complexity with different quantities of SCells belonging to different SeNBs (Chapter 5.5), in line with thesis T1 and algorithm characteristics T2 and T5.
- Impact of user density (Chapter 5.5), in line with thesis T1 and algorithm characteristics T2, T3 and T6.

Chapter 5.3 comprehensively evaluated the novel throughput estimation method against the standard method, assessing accuracy and stability. The novel method showed promising accuracy across diverse network configurations and transmission protocols. Notably, superior performance was observed in DC scenarios compared to non-DC environments, with no significant degradation in throughput measurement estimation for non-DC configurations, and in mixed configurations using both intra-site and inter-site SCells. Furthermore, the novel method maintained stable, superior accuracy across TCP and UDP, unlike the standard method. Stability testing of the novel method confirms its accurate throughput measurement estimation, yielding precise results.

The empirical investigation conducted in Chapters 5.3.1–5.3.5 provides evidence supporting the validity of thesis T1. The novel method demonstrably enhances the precision of IP scheduled throughput estimation in DC environments.

Furthermore, the demonstrated improvement in the accuracy of data volume and transmission time estimation provides evidence for the validity of thesis T2, which was positively validated for both intra-site CA (non-DC) and inter-site CA (DC) scenarios. However, in single-cell transmission scenarios, the novel method exhibits slightly lower BDR and BTR values compared to the standard method. This difference becomes negligible for file sizes exceeding 10 MB. Improved accuracy is also observed with parallel transmissions of multiple TCP streams.

Moreover, the findings presented in Chapters 5.3.1-5.3.4 validate thesis T3. Comparable results are observed for non-DC scenarios, while a significant improvement in measurement accuracy is demonstrated for mixed network scenarios (comprising both DC and non-DC) and DC scenarios, characterized by lower relative error values.

Finally, the novel method's characteristic T3 was also empirically validated in Chapter 5.3.5. The results demonstrate accurate relative error values for the novel method under both long (e.g., 800 seconds) and short (e.g., 1 second) transmission durations.

According to Chapter 5.3, the following conclusion arguments were established:

- The TCP slow start mechanism significantly compromises the accuracy of throughput measurements for file sizes below 1 MB, resulting in inaccuracies as high as 60%. However, for file sizes exceeding 50 MB, the accuracy improves significantly, with cell throughput relative error approaching less than 2%.
- Increased burst duration directly correlates with enhanced precision in throughput measurement estimation.
- Employing a minimum of eight multi-stream TCP transmissions effectively mitigates the impact of the TCP slow start mechanism for both of the methods. For the novel method this approach yields cell’s throughput relative error of 18-25% overestimation for file sizes ranging from 100 kB to 2 MB, a 10% relative error for 5 MB files, and less than 5% relative error for

files exceeding 10 MB. Furthermore, for 8MS TCP transmissions, the application layer throughput relative error remains exceptionally low, below 6%, for file sizes exceeding 500 kB and falls below 3% for full buffer TCP transmissions.

- Standard methods exhibit significant inaccuracies in DC and mixed environment scenarios, with cell throughput relative error values higher than -50% for 5MB file size transfers for 2CC connection. These inaccuracies are influenced by the number of component carriers and data volume distribution between PCell and SCells during transmission, and can even reach greater values, such as -80% for 4CC connections.
- Standard methods exhibit significant inaccuracies in throughput measurement assessment for non-DC scenarios employing UDP protocol and a high number of CCs. These inaccuracies are influenced by the number of component carriers and data volume distribution between PCell and SCells during transmission, resulting in highly inaccurate measurements with values below -80%.
- In contrast, the novel method demonstrates remarkable accuracy in all environment scenarios (non-DC, DC, and mixed) for UDP transmission, with application layer relative errors below several percent.

Chapter 5.4 presents an extensive evaluation of the novel throughput estimation method, assessing its accuracy for both internal and external parameters. This method is designed for flexible configuration in network environments demanding optimized performance under challenging radio channel conditions. The evaluation encompasses both dynamic and static radio channel quality changes, which impact the retransmission mechanism and, consequently, the burst duration of the method. Results for DC scenarios demonstrate remarkable accuracy in throughput measurement estimation under perfect radio channel conditions in the PCell and simultaneously demanding conditions in SCell, requiring retransmission only in the SCell, not in PCell. However, challenging radio channel quality in both the PCell and SCell(s) leads to slightly degraded results compared to scenarios involving only the SCell retransmissions.

The empirical investigation conducted in Chapters 5.4.1–5.4.4 provides evidence supporting the validity of thesis T1, as the novel method demonstrably enhances the precision of IP scheduled throughput estimation in DC environments for varying radio channel quality levels.

Furthermore, in Chapter 5.4.1 the novel method's characteristic T2 was positively validated for both intra-site CA (non-DC) and inter-site CA (DC) scenarios, exhibiting comparable BDR and BTR values for non-DC and significantly improved values for DC scenarios. The novel method's characteristic T3 was also empirically validated in Chapters 5.4.1, exhibiting a marginal decrease in Cell RE values relative to the standard method for non-DC environments.

Finally, the empirical validation of the novel method's characteristic T4, conducted in Chapters 5.4.1–5.4.4, demonstrates accurate relative error values under demanding radio channel conditions. Notably, in Chapter 5.4.3, the novel method exhibits enhanced resilience in DC scenarios to retransmission mechanisms, mitigating the impact of SCell signal attenuation and preventing prolonged burst durations.

According to Chapter 5.4, the following conclusion arguments were established:

- Radio channel quality issues at the SCell lead to an overestimation of IP scheduled throughput measurement by several percent, while similar issues at the PCell or both PCell and SCell result in an underestimation of throughput measurement by up to -10%.
- Under conditions of high SCell signal attenuation, the novel method achieved a BTR of 94.25%, whereas the standard method reached 113.27%. This demonstrates the novel method's robustness in handling high attenuation scenarios in SCell only, preventing BTR values exceeding 100%.
- The implementation of a new time component calculation enables more effective interpretation of file transfers as a single burst, increasing the calculated burst length by up to 80% from 34% of the total scheduling time, depending on the transmission flow and IP packet arrival rate.
- An increased frequency of fading occurrences during transmission cycle negatively impacts the accuracy of throughput measurement estimation. Application layer throughput relative error exhibits an increase of up to 18.12% for six one-second fading depths, from 10.68% for a single one-second fading depth. While cell throughput relative error increases up to -14.82%, from -1.73%.
- The novel method, when subjected to dynamic fading and suboptimal parameter configuration in DC scenarios, exhibited maximum unfavorable relative errors of less than 10% for cell relative error and 54% for application layer relative error. However, these inaccuracies were significantly lower in the majority of test cases, ranging from 0.4% to 3% for cell relative error and 3% to 14% for application layer relative error. The combined implementation of the novel flow control algorithm and measurement method demonstrates a highly accurate throughput estimation capability across diverse radio channel conditions.

Chapter 5.5 presents a detailed evaluation of the novel throughput estimation method, assessing its accuracy under high-capacity load conditions and comparing it to the standard approach. The evaluation, conducted in DC scenarios, reveals high accuracy when utilizing a large number of CCs for connections originating from distinct SeNBs.

Empirical investigations presented in Chapters 5.5.1 and 5.5.2 confirm the validity of thesis T1, demonstrating the novel method's effectiveness in enhancing IP scheduled throughput estimation accuracy within DC environments across varying numbers of SCells and users. Chapter 5.5.1 further validates characteristics T3 and T5 of the novel method for inter-site CA (DC) scenarios under distinct number of activated SCells for a single user. Additionally, characteristics T3 and T6 of the novel method are empirically validated in Chapter 5.5.2, exhibiting a substantial improvement in Cell RE values compared to the standard method for mixed and DC environments under a high-load network scenario.

The following conclusion arguments according to Chapter 5.5 were established:

- Each additional CC from distinct SeNB introduces a proportional increase in the application layer relative error for the novel method. This is attributed to the inherent error associated with each $\overline{eTh}(t)$ value transmitted from SeNB to MeNB, which accumulates

linearly as more carriers are involved. Full buffer TCP transmission over a 10-second duration yielded relative errors of 2.52%, 3.08%, and 4.72% for 2CC, 3CC, and 4CC configurations, respectively.

- The inclusion of each additional CC from distinct SeNBs proportionally reduces the cell's relative error for the novel method, transitioning the results for full buffer TCP transmission over 10 seconds from an overestimation of 0.31% for 2CC and 0.18% for 3CC to an underestimation of -0.06% for 4CC.
- The standard method exhibits inaccurate results across all transmission file sizes, with both cell and application layer relative errors demonstrating a further decrease in underestimation as the number of CCs increases. Full buffer TCP transmission over a 10-second duration resulted in cell relative errors of -64.16%, -78.38%, and -84.31% for 2CC, 3CC, and 4CC configurations, respectively, while application layer relative errors were -63.38%, -77.75%, and -83.56% for the same configurations.
- With the high user load of 50 UEs for varying intra-site and inter-site CA configurations the application layer relative error shows highly accurate results for the novel method - less than -5% for UDP transmission. The error decreases to less than -2% with the increase of intra-site SCells from inter-site CA configuration.
- Under a high user load of 50 UEs in inter-site CA configurations, the standard method exhibits significant inaccuracy in UDP transmission, reaching -99.22% application layer relative error for 4 inter-site SCell configurations. However, transitioning from inter-site to intra-site CCs incrementally improves accuracy, reaching -89.66%, 77.61%, and 69.92% for mixed configurations with 1, 2, and 3 SCells, respectively. Ultimately, the standard method achieves high accuracy with a relative error value of 0.34% in capturing IP scheduled throughput measurements for non-DC scenarios with 4 intra-site SCells.

This summary identifies seven key challenges that hinder the accurate estimation of IP scheduled throughput measurement for transmissions in cellular networks.

- The TCP slow start mechanism, where the server awaits an acknowledgment from the UE before increasing the next burst size, introduces a delay in throughput measurement, particularly during the initial burst, potentially underestimating the actual throughput. Both the standard and novel methods are susceptible to the negative effects of TCP slow start, which divides the transmission into multiple bursts. However, the increasing demand for data transmission will necessitate the use of faster protocols than single-stream TCP by IP network operators and application owners.
- The initial MCS (eTputInitMcs) used for throughput estimation may not be optimal, leading to inaccurate measurements due to varying channel conditions. While the novel method design is susceptible to this initial suboptimality, the eTh function quickly adapts the transmitted $\overline{eTh}(t)$ value to the current radio channel quality, mitigating the negative impact within milliseconds.

- The filter type employed for initial MCS (eTputInitMcs) selection can influence throughput measurement accuracy. An unsuitable filter type or a non-optimized one may result in an inaccurate estimation of $\overline{eTh}(t)$, contributing to measurement errors. However, Chapter 5.4.2 demonstrates that the double protection mechanism safeguards accurate measurement method and, primarily, the appropriate flow control of CA functionality in the event of fluctuating SCell radio channel quality.
- The rate of data segment arrival in the PDCP buffer and the granularity of burst segmentation significantly influence throughput measurement. A single transmission file can be divided into multiple bursts if the server cannot provide data at a sufficiently high rate, further complicating the measurement process due to the time difference between the arrival of IP packet segments in the PDCP buffer. This resembles the TCP slow start mechanism, however, insequential packet arrival may be caused by packet processing delays in network nodes rather than TCP acknowledgment design.
- Rapid fluctuations in radio channel quality can lead to an overestimation of actual throughput, as the PCell may incorrectly assume that the eTh value represents the true capacity of the SCell, as detailed in Chapter 5.4.2.
- Retransmission mechanism extends transmission duration by incorporating the time spent waiting for confirmation of consecutive retransmission resources between scheduled transmission periods, which results in underestimation of throughput measurement value.
- Concurrent utilization of cellular network resources by GBR and non-GBR users hinders accurate throughput measurement for both the standard and the novel method. This is because prioritizing GBR users over non-GBR users can prolong data transmission due to scarce scheduling and accounting the time between scheduled TBs for non-GBR users.

Due to the complexity of conducting laboratory-controlled tests involving multiple prioritized users, this dissertation did not include such experiments. These tests would have further explored the limits of both the standard and novel methods in terms of throughput measurement accuracy. The precision of these methods can be negatively impacted in non-DC and DC systems by sudden incoming calls that occupy the MeNB or SeNB, as previously sent *eTh* values may become outdated due to GBR or high-priority user resource allocation. Since CA traffic is non-GBR, the *eTh* will fluctuate. This phenomenon, combined with unfavorable radio channel quality and suboptimal configuration of the novel method, could significantly compromise the accuracy of throughput measurement assessments. However, this dissertation focused solely on developing a solution to accurately measure IP scheduled throughput in DC systems, surpassing the accuracy of the standard method used in non-DC systems. This objective was successfully achieved and has been validated.

The research presented in Chapter 5 validates the hypothesis proposed in Chapter 1.2. The novel throughput estimation method detailed in Chapter 4.4 constitutes a significant contribution to the field of cellular network design and operation, particularly in the context of supporting user traffic through multiple base stations simultaneously, utilizing techniques such as dual connectivity and carrier aggregation.

BIBLIOGRAPHY

[1] *5G; System Architecture for the 5G System*, 3GPP TS 23.501 version 15.2.0 Release 15.

[2] Holma H., Toskala A., Nakamura T.: *5G Technology: 3GPP New Radio*, Nokia Bell Labs, Finland, December 2019.

[3] Dahlman E., Parkvall S., Skold J.: *4G: LTE/LTE-Advanced for Mobile Broadband (Second Edition)*, Academic Press, 2013.

[4] *5G; Management and orchestration; 5G performance measurements*, 3GPP TS 28.552 version 17.0.0 Release 17.

[5] Qamar F., Hindia M., Abbas T., Dimyati K., Sadegh Amiri I.: *Investigation of QoS Performance Evaluation over 5G Network for Indoor Environment at millimeter wave Bands*, International Journal of Electronics and Telecommunications. 65. p.95-101, 2019

[6] Sreedevi P., Udaykiran Babu G.S.: *Monitoring QoS in 5G Networks*, International Journal of Scienetific Engineering and Technology Research, July 2017, p.4697-4700.

[7] Kapassa E., Touloupou M., Stavrianos P., Xilouris G., Kyriazis D.: *Managing and Optimizing Quality of Service in 5G Environments Across the Complete SLA Lifecycle*, Advances in Science, Technology and Engineering Systems Journal. 4, 2019

[8] Mohsen N., Hassan K. S.: *C-RAN simulator: A tool for evaluating 5G cloud-based networks system-level performance*, IEEE 11th International Conference on Wireless and Mobile Computing, Networking and Communications (WiMob), Abu Dhabi, 2015, pp. 302-309.

[9] Du L. et al.: *C/U Split Multi-Connectivity in the Next Generation New Radio System*, IEEE 85th Vehicular Technology Conference (VTC Spring), Sydney, NSW, Australia, 2017, pp. 1-5.

[10] Pathak L., Sharma D., Vrind T., Das D.: *Protocol for reduction in network resource wastage for 4G dual SIM dual standby user equipment*, 15th IEEE Annual Consumer Communications & Networking Conference (CCNC), Las Vegas, NV, 2018, pp. 1-4.

[11] *5G; NR; Layer 2 measurements*, 3GPP TS 38.314 version 16.1.0 Release 16.

[12] *Evolved Universal Terrestrial Radio Access E-UTRA; Layer 2 - Measurements*, 3GPP TS 36.314 version 16.0.0 Release 16.

[13] Kollar M., Tomala M., Zięba A.: *Evaluation of DL IP scheduled throughput for inter eNB carrier aggregation*, Patent Application WO2019192716A1, October 10, 2019.

[14] Sinaeepourfard A., Krogstie J., Petersen S. A., Ahlers D.: *F2c2C-DM: A Fog-to-cloudlet-to-Cloud Data Management Architecture in Smart City*, IEEE 5th World Forum on Internet of Things (WF-IoT), Limerick, Ireland, 2019, pp. 590-595.

[15] Sinaeepourfard A., Krogstie J., Petersen S. A.: *A Distributed-to-Centralized Smart Technology Management (D2C-STM) model for Smart Cities: a Use Case in the Zero Emission Neighborhoods*, IEEE International Smart Cities Conference (ISC2), Casablanca, Morocco, 2019, pp. 760-765.

[16] Yang S., Chou C.: *Design dynamic virtualized bandwidth allocation scheme to improve networking performance in cloud platform*, IEEE 9th International Conference on Communication Software and Networks (ICCSN), Guangzhou, 2017, pp. 283-288.

[17] Kollar M., Tomala M., Zięba A.: *Evaluation of DL IP scheduled throughput for inter eNB carrier aggregation*, U.S. Patent 11523407B2, December 12, 2022.

[18] Iperf3, https://software.es.net/iperf/ (date of access May 4, 2021).

[19] Hedlund A., Cotanis I.: *An Introduction to Carrier Aggregation Testing*, An Ascom Network Testing White Paper, 2014.

[20] *Performance Management (PM); Performance measurements; Evolved Universal Terrestrial Radio Access Network (E-UTRAN)*, 3GPP TS 32.425 Version 17.0.0 Release 17.

[21] *Key Performance Indicators (KPI) for Evolved Universal Terrestrial Radio Access Network (E-UTRAN): Definitions*, 3GPP TS 32.450 Version 16.0.0 Release 16.

[22] *Key Performance Indicators (KPI) for Evolved Universal Terrestrial Radio Access Network (E-UTRAN): Requirements*, 3GPP TS 32.451 Version 16.0.0 Release 16.

[23] ur Rehman T., Baig M. A. I., Ahmad A.: *LTE downlink throughput modeling using neural networks*, IEEE 8th Annual Ubiquitous Computing, Electronics and Mobile Communication Conference (UEMCON), New York, NY, USA, 2017, pp. 265-270.

[24] *X2 interface user plane protocol*, 3GPP TS 36.425 Version 17.0.0 Release 17.

[25] Salo J., Zacarías B. E.: *Analysis of LTE Radio Load and User Throughput*, International Journal of Computer Networks & Communications (IJCNC) Vol.9, No. 6, November 2017.

[26] Brik B., Boutiba K., Ksentini A.: *Deep Learning for B5G Open Radio Access Network: Evolution, Survey, Case Studies, and Challenges*, IEEE Open Journal of the Communications Society, January 2022.

[27] Zięba A., Sadowski J., Kollar M., Tatarczyk K.: *Measurement Accuracy Of IP Scheduled Throughput In LTE Network With Dual Connectivity*, Przegląd Telekomunikacyjny + Wiadomości Telekomunikacyjne, 4/2023, str. 260-263, doi: 10.15199/59.2023.4.57.

[28] Liu G., Wang C., Ma X., Yang Y.: *Keep Your Data Locally: Federated-Learning-Based Data Privacy Preservation in Edge Computing*, in IEEE Network, vol. 35, no. 2, pp. 60-66, March/April 2021.

[29] Kodama S., Nakagawa R., Takahashi N.: *TCP Multi-Stream Data Transfer using Multiple Network Interface Cards*, 11th Computer Science and Electronic Engineering (CEEC), Colchester, UK, 2019, pp. 24-28.

[30] Farrugia N., Buttigieg V., Briffa J. A.: *Multi-Stream TCP: Leveraging the Performance of a Per-Packet Multipath Routing Algorithm When Using TCP and SDN*, IEEE 44th Conference on Local Computer Networks (LCN), Osnabrueck, Germany, 2019, pp. 218-221.

[31] Zingirian N.: *Multi-Stream TCP Design*, IEEE 19th International Conference on Intelligent Computer Communication and Processing (ICCP), Cluj-Napoca, Romania, 2023, pp. 123-130.

[32] Hu H., Zhu X., Wang Y., Pan R., Zhu J., Bonomi F.: *Proxy-Based Multi-Stream Scalable Video Adaptation Over Wireless Networks Using Subjective Quality and Rate Models*, in IEEE Transactions on Multimedia, vol. 15, no. 7, pp. 1638-1652, November 2013.

[33] Atxutegi E., Arvidsson Å., Liberal F., Grinnemo K. J., Brunstrom A.: *TCP Performance over Current Cellular Access: A Comprehensive Analysis,* In Lecture Notes in Computer Science

(Including Subseries Lecture Notes in Artificial Intelligence and Lecture Notes in Bioinformatics), LNCS 10768:371–400, Springer Verlag.

[34] Seok SJ., Kim HJ., Jung KM., Kim KH., Kang CH.: *Dynamic Multi-stream Transport Protocol*, In: *Challenges for Next Generation Network Operations and Service Management*, APNOMS 2008, Lecture Notes in Computer Science, vol 5297. Springer, Berlin, Heidelberg.

[35] Allman M.: *On the generation and use of TCP acknowledgments*, SIGCOMM Comput. Commun. Rev. 28, 5 (October 1998), 4–21.

[36] W. Richard Stevens.: *TCP Slow Start, Congestion Avoidance, Fast Retransmit, and Fast Recovery Algorithms*, January 1997. RFC 2001.

[37] J. Postel.: *Transmission Control Protocol*, September 1981. RFC 793.

[38] Van Jacobson and Michael Karels. Congestion Avoidance and Control. In ACM SIGCOMM, 1988.

[39] Wang H., Rosa C., Pedersen K.I.: *Dual connectivity for LTE-advanced heterogeneous networks*, Wireless Netw 22, 1315–1328, May 2016.

[40] Zhao L., Zhong Z., Niu Y., Zhou H.: *Performance Evaluation of Dual Connectivity in Non-standalone 5G IoT Networks*. 2019.

[41] Nguyen T. and Sen-Ching Cheung S.: *Multimedia streaming using multiple TCP connections*, PCCC 2005. 24th IEEE International Performance, Computing, and Communications Conference, 2005., Phoenix, AZ, USA, 2005, pp. 215-223.

[42] Han J., Liu J., Xue K., Sun Q. and Lu J.: *Toward High-Quality Real-Time Video Streaming: An Efficient Multi-Stream and Multi-Path Scheduling Framework*, in IEEE Transactions on Networking, 2025, doi: 10.1109/TON.2025.3547278.

[43] Mobile Data Traffic Outlook, https://www.ericsson.com/en/mobility-report/dataforecasts/mobiletraffic-forecast/ (date of access May, 2025).

[44] Han, Z., Hasegawa G.: *Overcoming Fairness and Latency Challenges in BBR with an Adaptive Delay Detection*, IEEE Access 2025, 13, 37318–37327.

[45] Kihungi Njogu C.; Yang W.; Waita Njogu H.; Bosire A.: *BBR-with enhanced bandwidth estimation (BBR-EBE+): An improved BBR congestion control algorithm based on TCP acknowledgment compression and aggregation*. Telecommun. Syst. 2025, 88, 1–13.

[46] *Key Performance Indicators (KPI) for Evolved Universal Terrestrial Radio Access Network (E-UTRAN): Definitions*, 3GPP TS 36.213 Version 18.0.0 Release 18.

[47] Zięba A., Kollar M., Tatarczyk K., Sadowski J.: *Practical Approach to IP Scheduled Throughput Measurements in Dual Connectivity Systems*, Intl Journal of Electronics and Telecommunications, 2023, vol. 69, no. 4, pp. 645-654, doi: 10.24425/ijet.2023.146518.

[48] *5G end to end Key Performance Indicators (KPI)*, 3GPP TS 28.554 Version 19.0.0 Release 19.

[49] Yusoff N. M., Ali D. M., Idris A., Ismail S. and Noh K. S. S. K. M.*, QEEA algorithm for throughput improvement in the LTE networks,* 2017 7th IEEE International Conference on Control System, Computing and Engineering (ICCSCE), Penang, Malaysia, 2017, pp. 54-58, doi: 10.1109/ICCSCE.2017.8284379.

[50] Hamchaoui I., Jobert S. and Boufelja S., *IP aware radio scheduling: Introducing IP QoS management in LTE networks,* 2013 IEEE International Conference on Communications Workshops (ICC), Budapest, Hungary, 2013, pp. 1238-1242, doi: 10.1109/ICCW.2013.6649426.

[51] Li L. and Ye T., *Research on throughput prediction of 5G network based on LSTM,* in Intelligent and Converged Networks, vol. 3, no. 2, pp. 217-227, June 2022, doi: 10.23919/ICN.2022.0006.

[52] Pan M. -S., Lin T. -M., Chiu C. -Y. and Wang C. -Y., *Downlink Traffic Scheduling for LTE-A Small Cell Networks With Dual Connectivity Enhancement,* in IEEE Communications Letters, vol. 20, no. 4, pp. 796-799, April 2016, doi: 10.1109/LCOMM.2016.2522404.

[53] Kang S.and Bahk S., *Analysis of Dual Connectivity Gain in Terms of Delay and Throughput,* 2018 International Conference on Information and Communication Technology Convergence (ICTC), Jeju, Korea (South), 2018, pp. 1218-1220, doi: 10.1109/ICTC.2018.8539635.

[54] Dubey S. and Meena J., *Improvement of Throughput using Dual Connectivity in Non-Standalone 5G NR Networks,* 2020 Third International Conference on Smart Systems and Inventive Technology (ICSSIT), Tirunelveli, India, 2020, pp. 6-12, doi: 10.1109/ICSSIT48917.2020.9214179.

[55] Wang H., Rosa C. and Pedersen K. I., *Inter-eNB Flow Control for Heterogeneous Networks with Dual Connectivity,* 2015 IEEE 81st Vehicular Technology Conference (VTC Spring), Glasgow, UK, 2015, pp. 1-5, doi: 10.1109/VTCSpring.2015.7145881.

[56] *Small cell enhancements for E-UTRA and E-UTRAN - Higher Layer Aspects*, 3GPP TS 36.842 Version 12.0.0 Release 12, Dec. 2013.

[57] *Physical layer procedures for data,* version 15.9.0, 3GPP TS 38.214 NR, 2020.

[58] *NG-RAN; F1 application protocol (F1AP)*, 3GPP TS 38.473 Version 18.5.0 Release 18.

[59] *NG-RAN; Architecture description*, 3GPP TS 38.401 Version 18.5.0 Release 18.

[60] *Kollar M., Tomala M., Zięba A.: Evaluation of DL IP scheduled throughput for inter eNB carrier aggregation, U.S. Patent 11943799B2, December 12, 2022.*

[61] Shreevastav R. and Carbajo R. S., *Dynamic RLC mode based upon link adaptation to reduce latency and improve throughput in cellular networks,* 2016 IEEE 7th Annual Ubiquitous Computing, Electronics & Mobile Communication Conference (UEMCON), New York, NY, USA, 2016, pp. 1-6, doi: 10.1109/UEMCON.2016.7777932.

[62] Mallik N., Chakrabarti S. and Das S., *Study of throughput based on the impact of propagation effects and traffic patterns in wireless cellular networks,* 2017 2nd IEEE International Conference on Recent Trends in Electronics, Information & Communication Technology (RTEICT), Bangalore, India, 2017, pp. 101-105, doi: 10.1109/RTEICT.2017.8256566.

[63] Wang D., Sattiraju R. R., Qiu A., Partani S. and Schotten H. D., *Effect of Retransmissions on the Performance of C-V2X Communication for 5G*, 2020 IEEE 92nd Vehicular Technology Conference (VTC2020-Fall), Victoria, BC, Canada, 2020, pp. 1-7, doi: 10.1109/VTC2020-Fall49728.2020.9348560.

Appendix 1: Single Stream TCP Transmission details

This chapter presents a comprehensive analysis of test cases conducted under Chapter 5.3.1, focusing on the validation of IP scheduled throughput measurement accuracy in a multi-burst scenario for TCP single-stream transmission across diverse UE-level connection types. The investigation encompasses three distinct connection configurations: single-cell, intra-site CA (non-DC), and inter-site CA (DC). To assess the effectiveness of 2CC CA, an analysis is performed for specific file size transmissions, aiming to identify optimal conditions for bandwidth aggregation by examining the impact of distinct bandwidth combinations on data transfer efficiency across various file sizes.

A1.1. Single Cell Transmission

This study investigates the accuracy of two throughput estimation methods in cellular networks utilizing single cell connection, focusing on the impact of file size and the TCP slow start mechanism. The new flow control algorithm is employed for both the standard and the novel method.

Figure A1.1 depicts the measured throughput performance for both the standard and novel methods, utilizing throughput reference from eNB and end-user perspective, during single-cell data transmission across a range of file sizes.

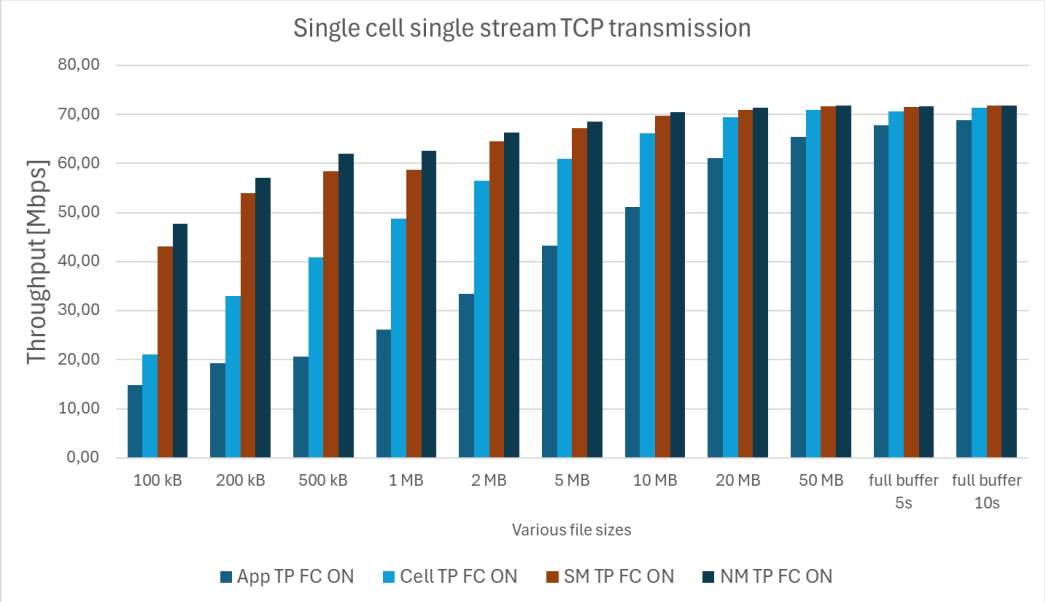

Figure A1.1: TCP/IP single stream transmission for single cell traffic for various file sizes with different throughput types.

Figure A1.2 provides supplementary precision analysis for the data presented in Figure A1.1. The left y-axis displays the data volume and time component ratios, represented by columnar data, while the right y-axis depicts the relative error in estimation of cell throughput, represented by curves. Figure A1.2 demonstrates that both methods achieve an acceptable level of accuracy after transmitting a 10 MB file. Further transmission, exceeding 50 MB, results in enhanced precision. A significant limitation hindering accurate throughput measurement arises from the division of a single file transmission via TCP into multiple burst transmissions. This fragmentation is directly linked to TCP's slow start mechanism, which necessitates constant

confirmation in the reverse direction regarding the success of data transmission. From the eNB's perspective, it becomes challenging to determine whether a transmission fragmented into multiple bursts, separated by a time interval (indicating an empty PDCP buffer after receiving the next data burst), corresponds to a single transmission or not. Only the data-transmitting server and the data receiving end-user possess this information. Increased traffic fragmentation within the eNB's PDCP buffer poses a significant challenge to both methods in accurately determining the time elapsed from the application layer perspective. The list of acronyms is presented in Chapter 5.2.3.

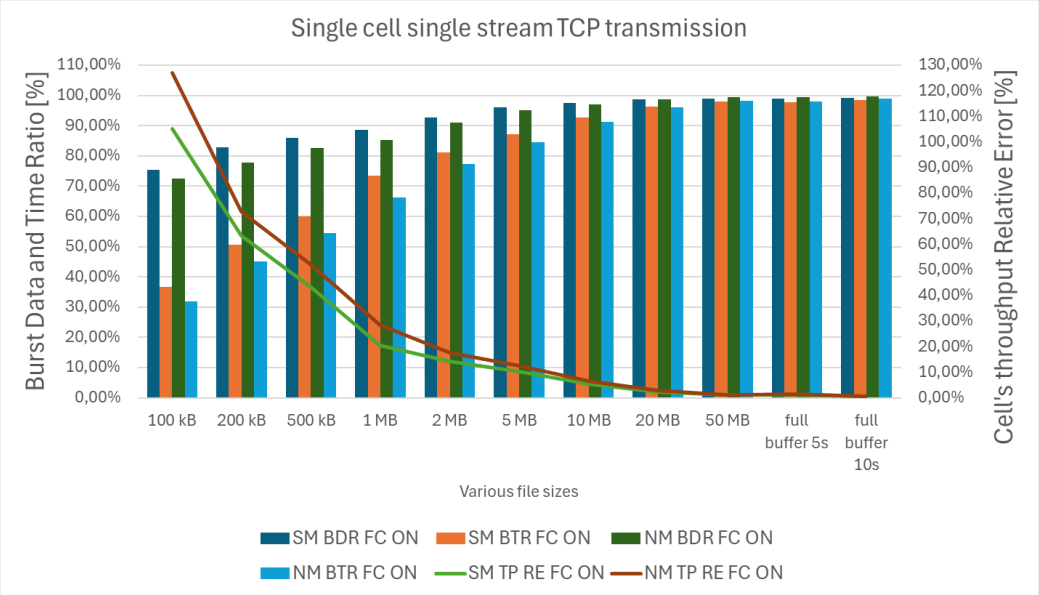

Figure A1.2: TCP/IP single stream transmission for single cell traffic with relative error and volume and time components ratios between Standard and New method.

Table A1.1 presents a comprehensive analysis of the data presented in Figures A1.1 and A1.2, incorporating an additional metric - STTI burst ratio, which quantifies the percentage distribution of single TTIs during the transmission of various file sizes. The influence of TCP slow start decreases with the increase of the file size, resulting in a higher number of single TTIs during the transmission of smaller files. The standard method exhibits a slight advantage in precision accuracy compared to the new method for small file sizes ranging from 100 kB to 1 MB, with a maximum gain of up to 21%. However, this gain progressively diminishes for larger file sizes, reaching a mere 0.2% for 50 MB file transmissions. As file size increases, cell's throughput exhibits a corresponding rise, approaching its maximum capacity. This occurs despite the inherent limitations imposed by the TCP slow start mechanism, which initially restricts data transmission rates.

Table A1.1 – TCP/IP single stream transmission for single cell traffic with various transmission metric details between Standard and New method.

file size	SM TP [Mbps]	NM TP [Mbps]	App TP [Mbps]	Cell TP [Mbps]	SM BDR [%]	SM BTR [%]	SM TP Cell RE [%]	SM TP App RE [%]	NM BDR [%]	NM BTR [%]	NM TP Cell RE [%]	NM TP App RE [%]	STTI burst ratio [%]
100 kB	43.15	47.69	14.90	21.02	75.35	36.71	105.26	189.59	72.45	31.93	126.88	220.10	81.2
200 kB	54.00	57.03	19.33	33.04	82.72	50.60	63.46	179.37	77.71	45.02	72.64	195.05	67.3
500 kB	58.40	61.99	20.63	40.81	85.94	60.06	43.11	183.10	82.55	54.35	51.88	200.46	71.6
1 MB	58.70	62.62	26.12	48.71	88.65	73.56	20.51	124.74	85.29	66.35	28.55	139.74	44.8
2 MB	64.46	66.38	33.45	56.48	92.68	81.19	14.14	92.71	90.93	77.37	17.53	98.43	26.0
5 MB	67.21	68.54	43.20	60.95	96.08	87.13	10.27	55.58	95.02	84.50	12.45	58.66	10.9
10 MB	69.72	70.49	51.08	66.16	97.61	92.62	5.39	36.50	97.11	91.14	6.55	38.01	13.7
20 MB	70.99	71.38	61.13	69.38	98.63	96.39	2.32	16.13	98.80	96.03	2.88	16.76	4.5
50 MB	71.63	71.76	65.35	70.88	98.93	97.90	1.05	9.60	99.46	98.25	1.24	9.81	3.0
5s	71.54	71.70	67.73	70.63	98.92	97.67	1.28	5.62	99.44	97.96	1.51	5.86	0.9
10s	71.78	71.87	68.89	71.37	99.09	98.53	0.57	4.19	99.68	99.00	0.69	4.32	0.9

Based on the acquired values from Table A1.1 the following observations have been noted:

- Throughput Scaling: As file size increases, both cellular and application layer throughput exhibit a proportional increase. This is attributed to the scheduling mechanism reaching its optimal capacity, despite the inherent limitations imposed by the TCP slow start phenomenon.
- Initial SM/NM BTR Behavior: During the initial transmission phase, the high frequency of single TTI bursts results in a low value for SM/NM BTR, as measured by both the standard and the new method.
- SM/NM BTR Increase: With an increase in the IP packet rate originating from the iperf server to the eNB, the SM/NM BTR value demonstrates an upward trend.
- Data Volume vs. Time: The proportion of SM/NM BDR conveyed by single TTIs is significantly less than the corresponding SM/NM BTR duration. For instance, with a 100 kB file size, for the standard method the data volume from the single and last TTIs constitutes approximately 25% of total volume, while the corresponding time represents around 64% of total scheduling duration.
- A newly implemented flow control enhancement, activated during the testing phase, aligns the time calculation principles of both the standard and the new methods. However, the implementation is different.
- The standard method consistently demonstrates slightly smaller cell's throughput relative error results compared to the new method across a range of file sizes. The standard method exhibits a value closer to the cell's throughput, approximately 20% smaller, in each test case.
- This discrepancy in relation to application layer throughput relative error diminishes with increasing file size, decreasing from 15% for a 100 kB file to 3% for a 10-second transmission between the two methods, but still showing an advantage for the standard method.

- Small File Sizes (100 kB - 2 MB): Both methods exhibit significant inaccuracies, characterized by overestimation of throughput. The standard method displayed cell's throughput relative error values ranging from 14.14% to 105.26%, while the new method exhibited even greater values, ranging from 17.53% to 126.88%.
- Large File Size (10 MB): Both methods demonstrate a significant improvement in precision compared to smaller file sizes. The standard method achieved an accuracy of approximately 5.39%, while the new method reached 6.55% in relation to the cell's throughput. This improvement is attributed to the extended transmission time associated with a fully saturated PDCP buffer, which minimizes the influence of TCP slow start. However, the relative error in relation to application layer throughput remained substantial, around 37%.
- 10-Second Transmission: Both methods exhibited excellent precision for 10-second transmissions, with relative errors below 1% for cell's throughput and 5% for application layer throughput.

This analysis reveals that the accuracy of throughput estimation methods is significantly influenced by packet file size and the TCP slow start mechanism. While both methods demonstrate improved accuracy with larger file sizes, the new method consistently exhibits greater inaccuracies compared to the standard method for smaller file sizes.

Furthermore, based on the noted observations, the following IP scheduled throughput method characteristics are concluded:

- The TCP slow start mechanism significantly impacts the accuracy of throughput estimation, particularly for smaller file sizes.
- The standard method generally exhibits slightly better accuracy than the new method, especially for smaller file sizes.
- The accuracy of both methods improves with larger file sizes due to the extended transmission time associated with a fully saturated PDCP buffer.
- Further research is needed to develop more accurate methods for estimating throughput, particularly for scenarios involving smaller file sizes and the TCP slow start mechanism. A critical area for investigation is the optimization of the transition period between data initialization and buffer saturation. This analysis should focus on identifying strategies to minimize the time required to reach a fully saturated buffer state, thereby maximizing the efficiency of data transmission.

A1.2. Intra-site CA Transmission

This study investigates the accuracy of two throughput estimation methods in cellular networks utilizing intra-site CA, focusing on the impact of file size and the TCP slow start mechanism. The analysis compares the standard calculation method with the new method based on different architectural principles. Two distinct flow control algorithms are employed to isolate the influence of the estimation methods from the specific flow control implementation.

Figure A1.3 depicts the measured throughput performance for both the standard and novel methods, utilizing throughput reference from eNB and end-user perspective, during intra-site CA (non-DC) data transmission across a range of file sizes.

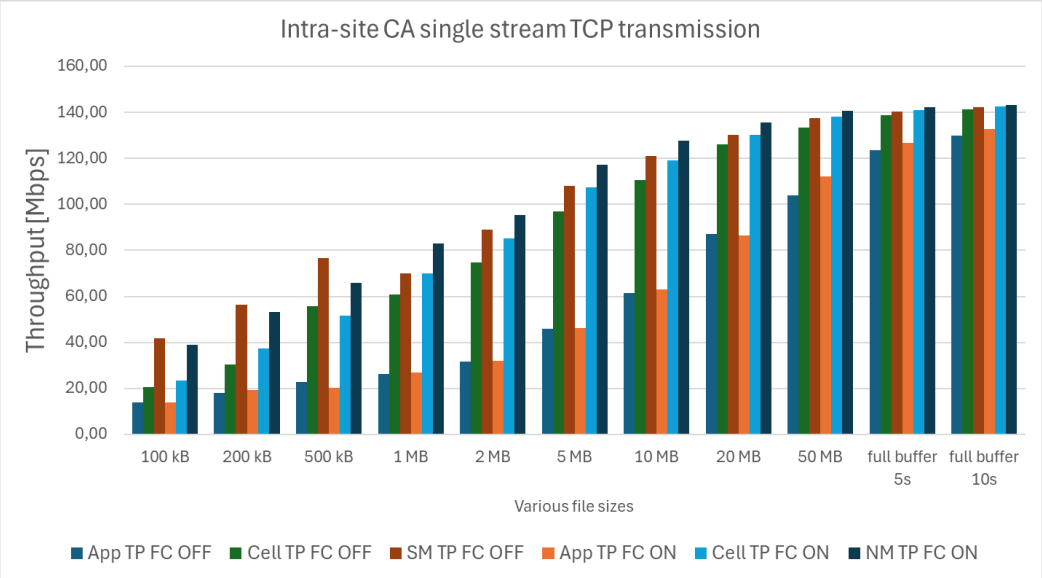

Figure A1.3: TCP/IP single stream transmission for 2CC Intra-site CA traffic with various throughput values.

Figure A1.4 provides supplementary precision analysis for the data presented in Figure A1.3. The left y-axis displays the data volume and time component ratios, represented by columnar data, while the right y-axis depicts the relative error in estimation of cell throughput, represented by curves. Figure A1.4 illustrates the distinct data distribution patterns observed in single-cell and 2CC CA connections. The introduction of data splitting between the primary cell and the secondary cell in 2CC CA connections creates an additional layer of data segmentation. This segmentation can potentially lead to misinterpretations of user throughput, particularly for small packet transmissions.

For a 2CC CA connection, the accuracy of both methods becomes acceptable after transmitting a 50 MB file over TCP using a single stream. Further increases in file size led to improved precision. Similarly, for single cell transmission, a significant limitation hindering accurate throughput measurement arises from the fragmentation of a single file transmission via TCP into multiple burst transmissions. This fragmentation is directly linked to TCP's slow start mechanism, which requires constant acknowledgement of successful data transmission in the reverse direction. From the eNB's perspective, it becomes challenging to distinguish between a single transmission fragmented into multiple bursts, separated by a time interval (indicating an empty PDCP buffer after receiving the next data burst), and multiple independent transmissions. Furthermore, the challenge of accurately determining the time elapsed from the application layer perspective is exacerbated when data volume is split across two separate cells steered by different schedulers but residing on the same eNB. This information is only available to the data-transmitting server and the receiving end-user. For both methods, increased traffic fragmentation within the eNB's PDCP buffer poses a significant challenge to accurately determine the time elapsed from the application layer perspective. Additionally, a threshold of data volume exists

beyond which transmission across multiple cells becomes advantageous. Larger data volumes result in higher precision.

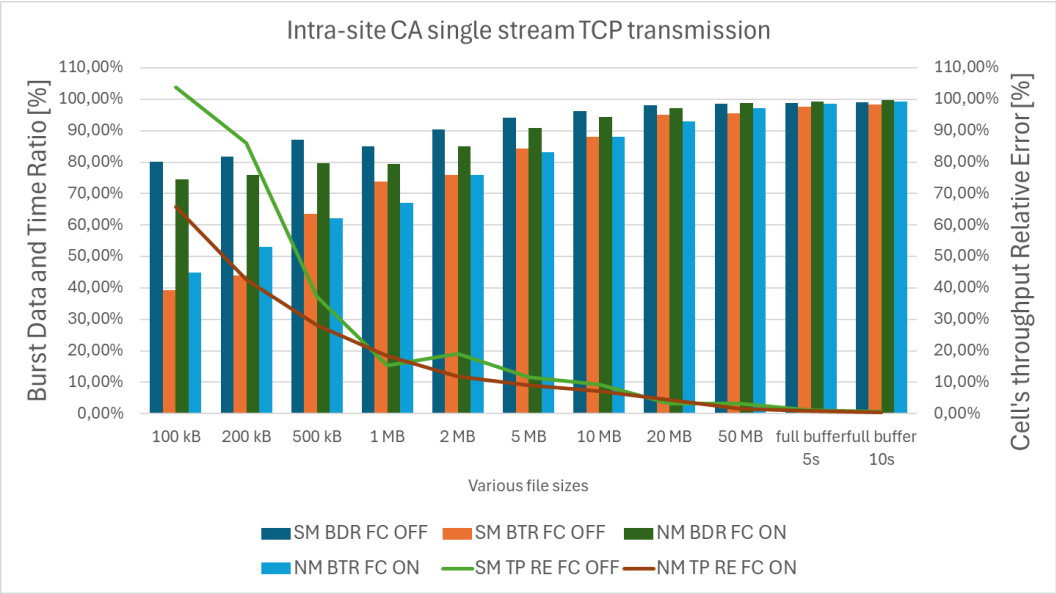

Figure A1.4: TCP/IP single stream transmission for Intra-site CA 2CC traffic with relative error and volume/time ratios between Standard and New method.

Tables A1.2 and A1.3 provide a detailed analysis of the data visualized in Figures A1.3 and A1.4. The analysis incorporates the metric STTI burst ratio, which represents the percentage distribution of single TTIs during the transmission of varying file sizes. The impact of TCP slow start diminishes with increasing file size, leading to a higher frequency of single TTIs during the transmission of smaller files. The traffic data is presented in separate tables due to the use of two distinct flow control algorithms: the legacy algorithm designed for non-DC systems and the novel algorithm specifically developed for DC systems. It is important to note that the distinct flow control algorithms result in different transmission processes, making direct 1:1 comparison challenging. However, the results presented are averaged over multiple iterations, providing the most robust comparison possible.

In contrast to single-cell scenarios, the standard method exhibits a slight decrease in relative error accuracy for file sizes of 100 and 200 kB. This discrepancy is directly attributed to a divergent interpretation of the time component between the two methods. The new method demonstrates a clear advantage by assuming incoming IP packets in the PDCP buffer are received when the buffer is full, whereas the standard method, due to its distinct flow control algorithm, interprets these occurrences as an empty PDCP buffer. Furthermore, as the reception of such IP packet data results in the scheduling of a single TTI, it is disregarded by the standard method and its flow control algorithm requirements. For larger file sizes of 500 kB and 1 MB, the standard method exhibits improved accuracy, achieving a comparable relative error level to the new method. This suggests that the impact of the differing time component interpretation diminishes with increasing file size.

Table A1.2: TCP/IP single stream transmission for Intra-site CA traffic with flow control OFF with various transmission metric details between Standard and New method.

file size	SM TP [Mbps]	NM TP [Mbps]	App TP [Mbps]	Cell TP [Mbps]	SM BDR [%]	SM BTR [%]	SM TP Cell RE [%]	SM TP App RE [%]	NM BDR [%]	NM BTR [%]	NM TP Cell RE [%]	NM TP App RE [%]	STTI burst ratio [%]
100 kB	41.90	43.51	13.90	20.55	80.05	39.25	103.93	201.45	75.21	35.51	111.77	213.04	84.2
200 kB	56.38	57.83	18.11	30.29	81.72	43.91	86.13	211.30	72.46	37.95	90.92	219.33	80.3
500 kB	76.61	75.96	22.72	55.84	87.09	63.48	37.19	237.17	78.81	57.94	36.03	234.33	68.1
1 MB	69.95	71.50	26.21	60.66	85.11	73.81	15.31	166.88	76.95	65.28	17.87	172.79	53.1
2 MB	88.86	87.43	31.60	74.61	90.30	75.82	19.10	181.20	85.71	73.14	17.18	176.66	47.7
5 MB	108.17	106.88	46.00	96.82	94.14	84.27	11.72	135.15	91.86	83.22	10.39	132.35	37.1
10 MB	121.00	119.21	61.49	110.72	96.34	88.16	9.28	96.79	95.23	88.45	7.66	93.87	18.1
20 MB	130.21	131.15	87.03	126.19	98.20	95.17	3.18	49.61	97.56	93.87	3.93	50.70	11.1
50 MB	137.50	136.47	104.00	133.36	98.59	95.62	3.11	32.21	98.95	96.69	2.33	31.22	5.4
5s	140.33	140.30	123.70	138.69	98.87	97.72	1.18	13.44	99.34	98.20	1.16	13.42	1.9
10s	142.28	142.09	130.00	141.23	99.01	98.27	0.75	9.45	99.66	99.06	0.61	9.30	1.8

Table A1.3: TCP/IP single stream transmission for Intra-site CA traffic with flow control ON with various transmission metric details between Standard and New method.

file size	SM TP [Mbps]	NM TP [Mbps]	App TP [Mbps]	Cell TP [Mbps]	SM BDR [%]	SM BTR [%]	SM TP Cell RE [%]	SM TP App RE [%]	NM BDR [%]	NM BTR [%]	NM TP Cell RE [%]	NM TP App RE [%]	STTI burst ratio [%]
100 kB	35.61	38.79	14.01	23.39	59.03	38.77	52.27	154.17	74.49	44.92	65.83	176.82	59.1
200 kB	48.68	53.34	19.42	37.38	63.89	49.06	30.23	150.68	75.85	53.16	42.67	174.64	71.6
500 kB	66.69	65.90	20.09	51.45	49.98	38.56	29.62	231.95	79.76	62.26	28.10	228.04	73.7
1 MB	86.97	82.84	26.92	69.97	49.81	40.07	24.30	223.10	79.42	67.08	18.39	207.74	71.3
2 MB	107.75	95.43	31.94	85.26	70.07	55.45	26.37	237.38	85.02	75.97	11.92	198.81	60.9
5 MB	126.33	117.24	46.28	107.47	81.99	69.75	17.55	172.97	90.82	83.26	9.09	153.32	37.7
10 MB	134.61	127.63	63.17	119.12	86.31	76.38	13.00	113.09	94.40	88.11	7.15	102.05	28.7
20 MB	139.04	135.75	86.48	130.11	92.75	86.79	6.87	60.78	97.12	93.09	4.34	56.97	21.7
50 MB	141.71	140.60	112.00	138.25	97.33	94.96	2.50	26.53	98.84	97.18	1.70	25.54	9.9
5s	143.23	142.33	126.70	141.10	98.05	96.60	1.51	13.04	99.35	98.49	0.87	12.34	4.3
10s	143.66	143.24	132.86	142.63	98.47	97.76	0.73	8.13	99.64	99.21	0.43	7.82	3.5

Based on the acquired values from Tables A1.2 and A1.3 the following observations have been noted:

- Throughput Scaling: As file size increases, both cellular and application layer throughput exhibit a proportional increase, indicating that the scheduling mechanism approaches its optimal capacity. However, the TCP slow start phenomenon limits the initial throughput, and significant throughput gains for intra-site CA are observed only for file sizes exceeding 2 MB compared to single-cell connections.

- Initial SM/NM BTR Behavior: During the initial transmission phase, the high frequency of single TTI bursts results in low SM/NM BTR values for both methods. For a 100 kB file, the standard method with flow control disabled yields a SM BTR of 39.25%, while the new method achieves 44.92%, indicating a slight improvement.
- SM/NM BTR Increase: As the IP packet rate from the iperf server to the eNB increases, SM/NM BTR values demonstrate an upward trend. The standard method exhibits less precise values for 100 and 200 kB file transfers and for large data transfers (50 MB and above). However, for files between 500 kB and 20 MB, the standard method shows slightly better performance.
- Data Volume vs. Time: The proportion of data volume ratio (SM/NM BDR) conveyed by single TTIs is significantly lower than the corresponding time duration. For a 100 kB file, the data volume from the single and last TTIs constitutes approximately 20% of the total volume for the standard method and 25% for the new method, while the corresponding time represents around 60% and 55% of the total scheduling duration, respectively.
- A newly implemented flow control enhancement aligns the time calculation principles of both methods, although the implementation differs. The cell's throughput exhibits slightly increased values compared to the previous algorithm, indicating improved data scheduling. The more precise burst counting in the new method provides a closer representation of the actual scheduled throughput.
- Compared to single-cell transmission, the new method consistently demonstrates slightly superior relative error results across a range of file sizes, with two exceptions for 1 MB and 20 MB files. This may be attributed to stochastic variations in traffic generation. The new method exhibits a value closer to the cell's throughput, almost twice as good for very small file sizes (100 kB and 200 kB), but the difference becomes marginal (0.3-2.6%) for files larger than 5 MB.
- The new method shows improved application layer relative error for 100, 200, and 500 kB file transfers, but degrades for 1 MB to 20 MB files. For files larger than 50 MB, the error improves again. This is due to the significant difference between application layer throughput and cell's throughput, and the new algorithm's ability to schedule data more efficiently, increasing the overall counted IP scheduled throughput while the application layer throughput does not increase proportionally.
- Small File Sizes (100 kB - 2 MB): Both methods exhibit significant inaccuracies, characterized by overestimation of throughput. The standard method overestimates by 15.31% to 103.93%, while the new method shows better results, ranging from 11.92% to 65.83%.
- Large File Size (10 MB): Both methods demonstrate improved precision compared to smaller file sizes. The standard method achieves an accuracy of approximately 9.28%, while the new method reaches 7.15% in relation to the cell's throughput. This improvement is attributed to the extended transmission time associated with a fully saturated PDCP buffer, minimizing the influence of TCP slow start. However, the relative error in relation to application

layer throughput remains substantial, much greater than for single-cell transmission (96.79% for the standard method and 102.05% for the new method).

- 10-Second Transmission: Both methods exhibit excellent precision for 10-second transmissions, with relative errors of 1.18% and 0.87% for cell's throughput and 9.45% and 7.82% for application layer throughput for the standard and the new method, respectively.

This analysis reveals that the accuracy of throughput estimation methods is significantly influenced by packet file size and the TCP slow start mechanism. Compared to single-cell transmission, intra-site CA connection type introduces greater accuracy for IP scheduled throughput measurement. The new flow control algorithm, along with the new method, shows improvement, especially for small file sizes, and a slight improvement for longer transmissions.

Furthermore, based on the noted observations, the following IP scheduled throughput method characteristics are concluded:

- The TCP slow start mechanism significantly impacts the accuracy of throughput estimation, particularly for smaller file sizes. However, for 100 and 200 kB file sizes, the relative error in relation to cell's throughput inaccuracy is twice as small as for single-cell transmission, representing a significant improvement. For files larger than or equal to 10 MB, the relative error difference is insignificant compared to single-cell transmission for the same file size.
- The standard method generally exhibits slightly worse accuracy than the new method, especially for larger file sizes, but the new method exhibits superior results for small file sizes.
- The accuracy of both methods improves with larger file sizes due to the extended transmission time associated with a fully saturated PDCP buffer.
- Further research is needed to develop more accurate methods for estimating throughput, particularly for scenarios involving smaller file sizes and the TCP slow start mechanism. A critical area for investigation is the optimization of the transition period between data initialization and buffer saturation. This analysis should focus on identifying strategies to minimize the time required to reach a fully saturated buffer state, thereby maximizing the efficiency of data transmission.
- The observed inaccuracies stem from the TCP slow start mechanism, which only accounts for data transmitted during the final phase of transmission, neglecting the initial and intermediate stages. Consequently, the measured volume (SM/NM BDR) and time (SM/NM BTR) ratios are underestimated compared to the actual data transfer. The reported user throughput metric exhibits an overestimation due to its exclusive consideration of the most efficient portion of the transmission process, neglecting the transmission time intervals during which TBs are conveyed via single TTIs and the time periods between these single TTIs. The requirement for concurrent scheduling of two cells and coordinated transmission between them introduces an additional source of imprecision. This is because the Intra-site CA scenario shares the same scheduling criteria and calculation method as the Inter-site CA scenario, both relying on the eTh parameter.

- For packet file sizes exceeding 10 MB, both methods demonstrate a continued significant improvement in precision compared to smaller file sizes. This enhancement is primarily attributed to the extended transmission time associated with a fully saturated PDCP buffer, which constitutes the majority of the total time duration. As a result, both the measured volume (SM/NM BDR) and time (SM/NM BTR) ratios closely approximate the actual data transfer, as the influence of slow TCP start diminishes.
- The overall performance of the proposed method exhibits a decline of relative error in relation to application layer throughput compared to a single-cell transmission. This is attributed to the inherent complexity of the multi-cell scenario, where a single scheduler is responsible for determining all necessary constraints, leading to a more straightforward calculation method.

A1.3. Inter-site CA Transmission

This study investigates the accuracy of two throughput estimation methods in cellular networks utilizing inter-site CA, focusing on the impact of file size and the TCP slow start mechanism. The new flow control algorithm is employed for both the standard and the novel method.

Figure A1.5 depicts the measured throughput performance for both the standard and the novel method, utilizing throughput reference from eNB and end-user perspective, during inter-site CA (DC) data transmission across a range of file sizes.

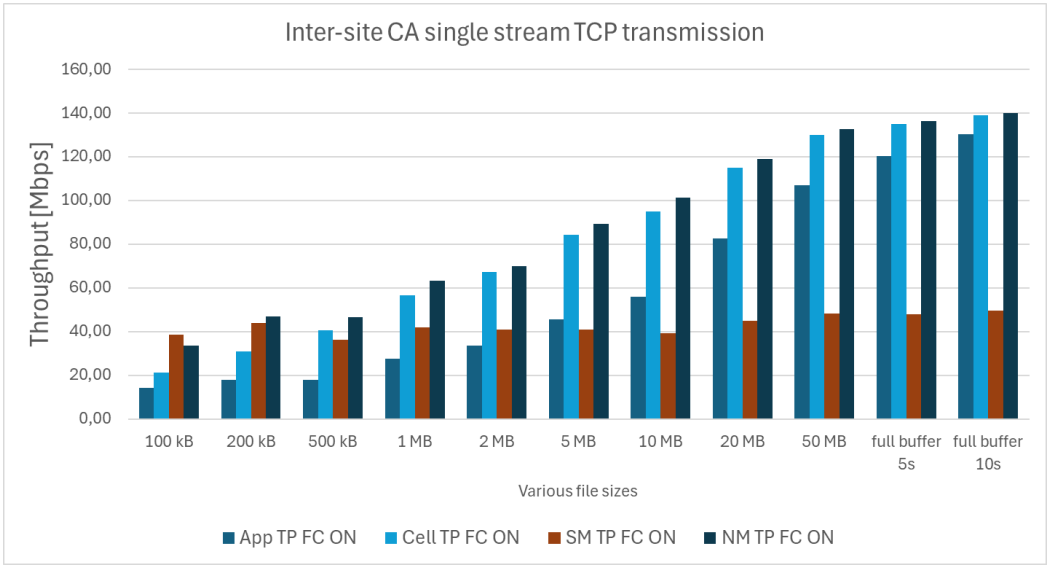

Figure A1.5: TCP/IP single stream transmission for 2CC Inter-site CA traffic with various throughput values.

Figure A1.6 provides supplementary precision analysis for the data presented in Figure A1.5. The left y-axis displays the data volume and time component ratios, represented by columnar data, while the right y-axis depicts the relative error in estimation of cell throughput, represented by curves. Figure A1.6 illustrates the distinct data distribution patterns observed in single-cell and 2CC CA connections. The introduction of data splitting between the primary cell and the secondary cell in 2CC CA connections creates an additional layer of data segmentation. This segmentation can potentially lead to misinterpretations of user throughput, particularly for

small packet transmissions. For inter-site CA with 2CC, the accuracy of the new method becomes acceptable for file sizes exceeding 50 MB when transmitted over TCP using a single stream (-P iperf parameter set to 1, indicating a single parallel stream). The precision further improves for greater file sizes. However, full buffer 5s tests reveal a high degree of erroneous underestimation of throughput value for standard method.

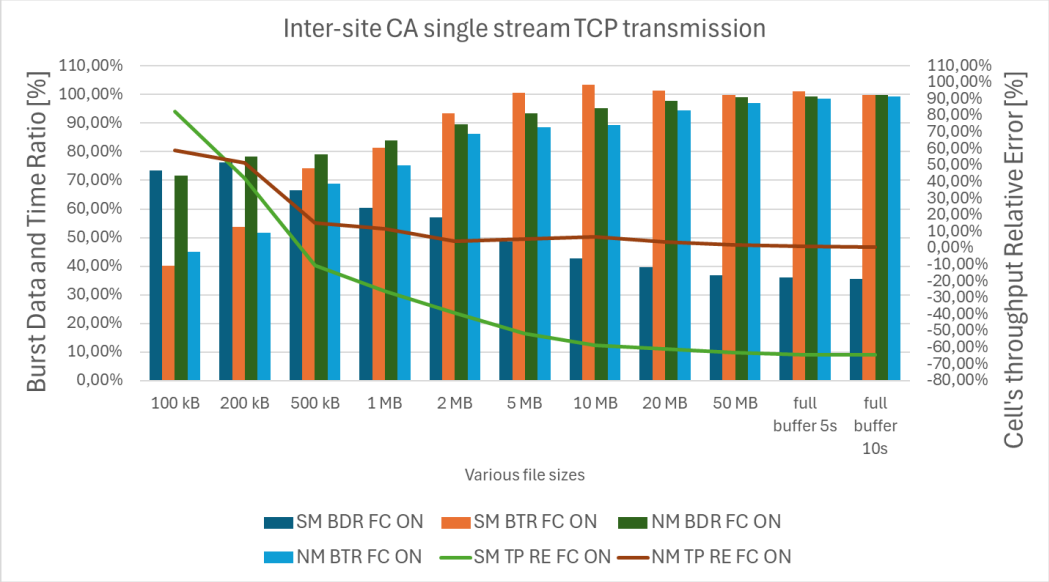

Figure A1.6: TCP/IP single stream transmission for Inter-site CA 2CC traffic with relative error and volume/time ratios between Standard and New method.

The discrepancy in precision between the standard and the new method arises primarily from the underestimation of data volume by the standard method as file size increases. The standard method does not count all of the PCell's data volume and skips the data volume sent to SCell. Also, this underestimation is coupled with an erroneous interpretation of transmission time. The observed high precision of the standard method in approximating application layer throughput for file sizes between 2 and 5 MB is coincidental. This apparent accuracy is attributed to a combination of factors:

- Underestimation of Data Volume: The standard method underestimates the total data volume transmitted over the PCell, failing to account for all data transferred.
- Overestimation of Transmission Time: The standard method overestimates the transmission time compared to the new method.

This combination of underestimation and overestimation leads to a fortuitous cancellation of errors, resulting in a seemingly accurate approximation of application layer throughput for the specified file size range. However, as the file size increases, the underestimation of data volume becomes more pronounced, leading to a diminishing accuracy of the standard method.

In contrast to the single-cell and Intra-site CA scenarios, the standard method exhibits a contrasting behavior. As file size increases, the measured volume decreases due to the transfer of data to the secondary cell. Simultaneously, the time component increases, reflecting the

extended transmission duration. This seemingly paradoxical outcome leads to a more accurate measurement for the standard method in DC environment compared to the new method.

However, for larger file sizes, where the influence of the slow TCP start mechanism diminishes, the accuracy of the standard method is expected to decrease. This is because the underestimation of data volume becomes less pronounced as the initial and intermediate stages contribute a smaller proportion to the overall transmission. The new method demonstrates superior performance compared to the conventional method for file sizes exceeding 20 MB. However, for file sizes below 20 MB, the new method exhibits inferior performance due to the limits in implementing the calculation algorithm of the standard method within this range.

Table A1.4 provides a detailed analysis of the data visualized in Figures A1.5 and A1.6. The analysis incorporates the metric STTI burst ratio, which represents the percentage distribution of single TTIs during the transmission of varying file sizes. The impact of TCP slow start diminishes with increasing file size, leading to a higher frequency of single TTIs during the transmission of smaller files. The traffic data is presented in separate tables due to the use of two distinct flow control algorithms: a legacy algorithm designed for non-DC systems and the novel algorithm specifically developed for DC systems. It is important to note that the distinct flow control algorithms result in different transmission processes, making direct 1:1 comparison challenging. However, the results presented are averaged over multiple iterations, providing the most robust comparison possible.

Table A1.4: TCP/IP single stream transmission for Inter-site CA traffic with various transmission metric details between Standard and New method.

file size	SM TP [Mbps]	NM TP [Mbps]	App TP [Mbps]	Cell TP [Mbps]	SM BDR [%]	SM BTR [%]	SM TP Cell RE [%]	SM TP App RE [%]	NM BDR [%]	NM BTR [%]	NM TP Cell RE [%]	NM TP App RE [%]	STTI burst ratio [%]
100 kB	38.63	33.70	14.31	21.18	73.43	40.27	82.35	169.94	71.73	45.09	59.10	135.52	80.2
200 kB	43.80	46.80	17.88	30.85	76.31	53.74	42.00	144.99	78.32	51.62	51.73	161.77	63.5
500 kB	36.30	46.66	17.89	40.55	66.47	74.26	-10.48	102.91	79.13	68.77	15.06	160.81	64.5
1 MB	41.86	63.13	27.48	56.48	60.39	81.46	-25.87	52.34	84.03	75.18	11.78	129.73	59.9
2 MB	41.00	69.86	33.45	67.20	56.94	93.33	-38.98	22.57	89.64	86.23	3.96	108.85	60.7
5 MB	40.79	89.15	45.54	84.34	48.70	100.70	-51.64	-10.44	93.50	88.45	5.71	95.76	27.5
10 MB	39.29	101.30	56.00	94.87	42.84	103.44	-58.58	-29.84	95.30	89.25	6.78	80.89	17.8
20 MB	44.99	119.07	82.53	114.90	39.64	101.23	-60.84	-45.48	97.80	94.38	3.63	44.28	15.5
50 MB	48.15	132.81	106.93	130.00	36.93	99.70	-62.96	-54.97	99.11	97.01	2.16	24.20	6.4
5s	48.02	136.23	120.30	135.03	35.95	101.06	-64.43	-60.08	99.42	98.54	0.89	13.24	5.4
10s	49.51	139.89	130.30	139.16	35.54	99.90	-64.42	-62.00	99.72	99.21	0.52	7.36	2.4

Based on the acquired values from Table A1.4, the following observations have been noted:

- Throughput Scaling: As file size increases, both cell's and application layer throughput exhibit a proportional increase, indicating that the scheduling mechanism approaches its optimal capacity. However, the TCP slow start phenomenon limits the initial throughput, and

significant throughput gains for inter-site CA are observed only for file sizes exceeding 1 MB compared to single-cell connections.

- Initial SM/NM BTR Behavior: During the initial transmission phase, the high rate of single TTI bursts results in low SM/NM BTR values for both methods. For a 100 kB file, the standard method with flow control enabled yields a SM/NM BTR of 40.27%, while the new method achieves 45.09%, indicating a slight improvement, similarly as for intra-site CA.
- SM/NM BTR Increase: As the IP packet rate from the iperf server to the eNB increases, SM/NM BTR values demonstrate an upward trend. The standard method exhibits more precise values for 100 kB file transfers but for large data transfers (5 MB and above) it exhibits an overestimation of time component. However, for files between 200 kB and 2 MB, the standard method shows slightly better performance than the new method.
- Data Volume vs. Time: The proportion of data volume (ThpVolDl) conveyed by individual TTIs is significantly lower than the corresponding time duration. For a 100 kB file, the data volume from the single and last TTIs constitutes approximately 26.57% of the total volume for the standard method and 28.27% for the new method, while the corresponding time represents around 59.73% and 54.91% of the total scheduling duration, respectively.
- A newly implemented flow control enhancement aligns the time calculation principles of both methods, although the implementation differs, thus the standard method experiences an overestimation. The cell's throughput exhibits slightly decreased values compared to the intra-site CA solution of both the previous and the new algorithm. This is a natural consequence of intra-site CA superiority over inter-site CA. However, despite slightly lesser effectiveness of inter-site CA, the new method alongside with new algorithm provides more precise burst counting which is a closer representation of the actual scheduled throughput.
- Compared to the standard method for single-cell and intra-site CA transmission, the new method consistently demonstrates superior relative error results across a range of file sizes, with a single exception for 200 kB file. This may be attributed to stochastic variations in traffic generation. The new method exhibits a value closer to the cell's throughput, even slightly better than the new method for intra-site CA.
- The new method shows outstanding precision in comparison to the standard method for inter-site CA transmission. The standard method shows only a better result for 500 kB, where the proportion of measured data volume and time components formed coincidentally a better quotient.
- The new method shows improved application layer relative error for 100, 200 and 500 kB file transfers, but degrades for 1 MB to 20 MB files. For files larger than 50 MB, the error improves again. This is due to the significant difference between application layer throughput and cell's throughput, and the new algorithm's ability to schedule data more efficiently, increasing the overall counted IP scheduled throughput while the application layer throughput does not increase proportionally.

- Small File Sizes (100 kB - 200 kB): Both of the methods exhibit significant inaccuracies, characterized by overestimation of throughput. The standard method overestimates by 42% to 82.35%, while the new method shows better results, ranging from 51.73% to 59.1%.
- Medium File Sizes (500 kB – 2 MB): Surprisingly, the new method shows high accuracy ranging from 4% to 15%. While the standard method demonstrates a tendency towards underestimation due to the exclusion of data volume directed to the SCell from the count, while concurrently overestimating the temporal component.
- Large File Size (10 MB): The new method demonstrates slightly worse precision compared to smaller file sizes. But the precision improves for 20 MB files and above. The standard method achieves even worse results than for smaller file sizes, as the data distribution to the SCell increases with the incremental increase of file size, reaching the underestimation of cell's relative error of -58.58%.
- 10-Second Transmission: The new method exhibits excellent precision for 10-second transmissions, with relative errors of 0.89% for cell's throughput and 7.36% for application layer throughput for the new method. The standard method continues to degrade the throughput estimation to -64.42 % of cell's relative error and -62% of application layer relative error.

This analysis reveals that the accuracy of throughput estimation methods is significantly influenced by packet file size and the TCP slow start mechanism. The standard method in inter-site CA environment compared to single-cell transmission and intra-site CA connection type introduces complete inaccuracy for IP scheduled throughput measurement. The lack of accuracy increases with every SCell conveyed into the aggregated connection, as the data volume sent to the SCells is omitted and moreover, the part related to PCell data volume is omitted as well. Furthermore, the standard method seems to overestimate the time component counting which passes the number of total TTIs that are being scheduled. Conversely, the new method with the new flow control algorithm shows its superiority for both cell's and application layer relative error in comparison to the standard method. This proves that the novelty proposed by the new method meets the requirements for inter-site CA environment, where the standard method fails to do so.

Furthermore, based on the noted observations, the following IP scheduled throughput method characteristics are concluded:

- The TCP slow start mechanism significantly impacts the accuracy of throughput estimation, particularly for smaller file sizes. However, for 100, 200 and 500 kB file sizes, the relative error in relation to cell's throughput inaccuracy is twice as small as for single-cell transmission, representing a significant improvement. For files larger than or equal to 10 MB, the relative error difference is insignificant compared to single-cell and intra-site CA transmission for the same file size.
- For inter-site CA solution, the standard method exhibits much worse accuracy than the new method, especially for larger file sizes.

- The accuracy of the new method improves with larger file sizes due to the extended transmission time associated with a fully saturated PDCP buffer.
- Further research is needed to develop more accurate methods for estimating throughput, particularly for scenarios involving smaller file sizes and the TCP slow start mechanism. A critical area for investigation is the optimization of the transition period between data initialization and buffer saturation. This analysis should focus on identifying strategies to minimize the time required to reach a fully saturated buffer state, thereby maximizing the efficiency of data transmission.
- The observed inaccuracies stem from the TCP slow start mechanism, which only accounts for data transmitted during the final phase of transmission, neglecting the initial and intermediate stages. Consequently, the measured volume (SM/NM BDR) and time (SM/NM BTR) ratios are underestimated compared to the actual data transfer. The reported user throughput metric exhibits an overestimation due to its exclusive consideration of the most efficient portion of the transmission process, neglecting the transmission time intervals during which TBs are conveyed via single TTIs and the time periods between these single TTIs. The requirement for concurrent scheduling of two cells and coordinated transmission between them introduces an additional source of imprecision. This is because the Intra-site CA scenario shares the same scheduling criteria and calculation method as the Inter-site CA scenario, both relying on the eTh parameter.
- For packet file sizes exceeding 10 MB, both methods demonstrate a continued significant improvement in precision compared to smaller file sizes. This enhancement is primarily attributed to the extended transmission time associated with a fully saturated PDCP buffer, which constitutes the majority of the total time duration. As a result, both the measured volume (SM/NM BDR) and time (SM/NM BTR) ratios closely approximate the actual data transfer, as the influence of slow TCP start diminishes.
- The overall performance of the proposed method exhibits a decline of relative error in relation to application layer throughput compared to a single-cell transmission. This is attributed to the inherent complexity of the multi-cell scenario, where a single scheduler is responsible for determining all necessary constraints, leading to a more straightforward calculation method.

A1.4. Usefulness of CA 2CC usage per file size for single stream TCP traffic

The efficacy of CA for single-stream TCP traffic is demonstrably advantageous only for file sizes exceeding 10 MB from end-user perspective as shown in Figure A1.7. This observation is attributed to the inherent slow start mechanism of TCP traffic, necessitating extended periods to fully exploit the bandwidth potential of the RAN. For file sizes below 10 MB, single-cell connections exhibit comparable efficiency when employing single-stream TCP traffic, relative to CA. Consequently, no performance gains are realized by utilizing CA for small file transfers, resulting solely in increased energy consumption for the User Equipment (UE). This trend shifts for file sizes equal to or exceeding 20 MB, where the simultaneous transmission of data across

multiple carriers becomes practically advantageous in terms of throughput effectiveness, enabling faster data transfer from the user's perspective.

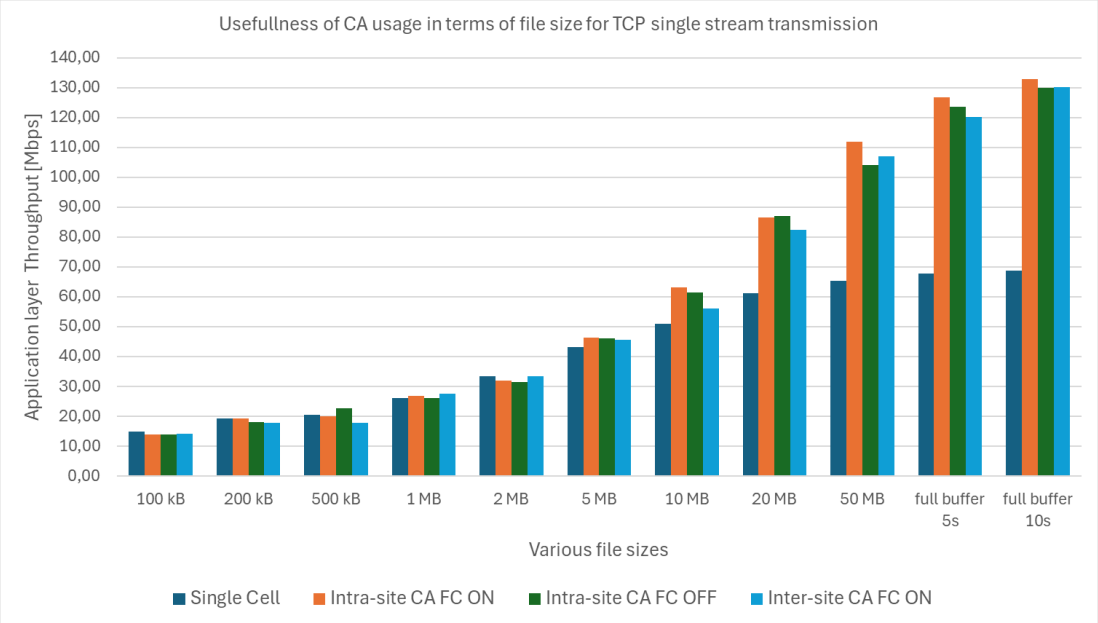

Figure A1.7: Usefulness of CA usage from the end-user perspective.

The observed superior throughput performance of intra-site CA compared to inter-site CA is a direct consequence of the centralized control architecture. With intra-site CA, all component carriers are managed by a single scheduler unit located within a single BTS. This centralized control enables:

- Reduced eNB Retention Delay: The scheduler unit can make rapid handover decisions and resource allocation adjustments, minimizing the delay experienced by UE during handover events.
- Enhanced Resource Synchronization and Utilization: The centralized scheduler optimizes resource allocation across all component carriers, ensuring efficient utilization and minimizing interference.
- Simplified Signal Processing: Signal processing for all carriers is handled by the single BTS, reducing computational overhead and improving overall efficiency.

However, inter-site CA can offer advantage in case of coverage extension scenario, where by combining carriers from geographically dispersed BTSs, inter-site CA can extend network coverage and provide improved connectivity in areas with limited signal power level.

Figure A1.8 provides a comparative analysis of the performance benefits of CA from the eNB perspective. The figure demonstrates that even for small file transfers (e.g., 1 MB), the centralized scheduling of intra-site CA results in faster and more efficient data transmission compared to single-carrier operation in ideal radio channel quality conditions.

In conclusion, while intra-site CA offers superior throughput performance due to its centralized control architecture, inter-site CA can be advantageous in specific scenarios where

coverage extension is a priority. The choice between these two approaches depends on the specific network deployment and performance objectives.

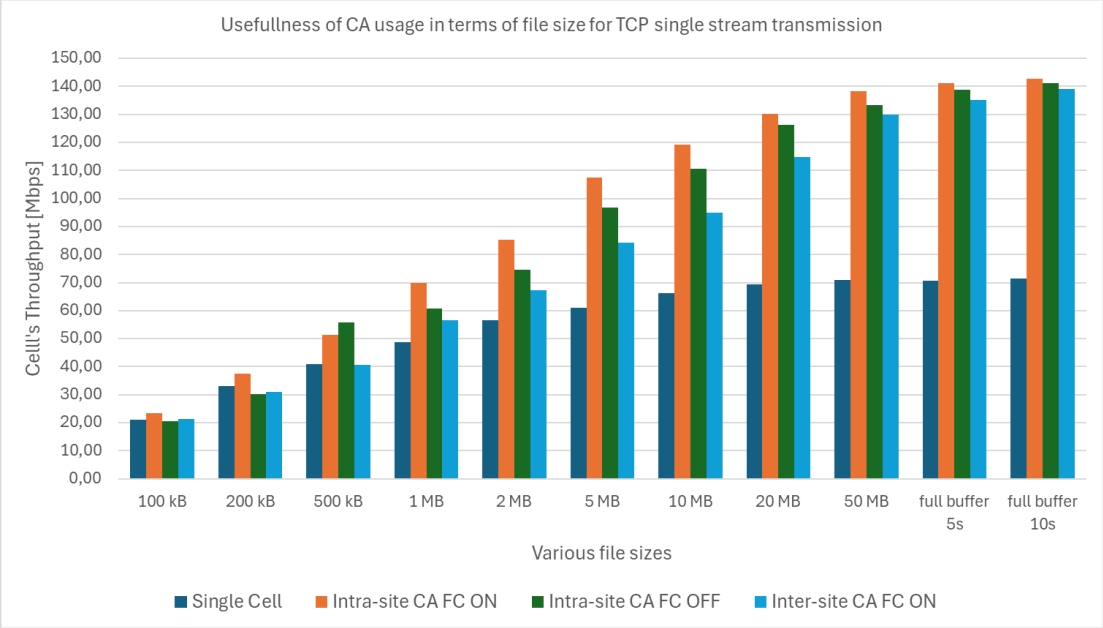

Figure A1.8: Usefulness of CA usage from the eNB's scheduler perspective.

A1.5. Summary – throughput tables

Tables 5.8 and 5.9 present a comprehensive overview of throughput values across diverse connection types for both the standard and novel methods. These tables serve as a reference for the input values utilized in the calculation of relative error.

However, the measured IP scheduled throughput, as indicated in the tabulated data, also represents the peak achievable data rate during a given transmission. When compared to both application layer throughput and cell throughput, it becomes evident that the IP scheduled throughput serves as an upper bound for the observed data rates. This observation suggests that the limited data transmission rate from the iperf server to the eNB acts as a bottleneck, preventing the eNB from reaching its full theoretical throughput capacity.

Table A1.5: Measured throughput comparison between the two methods and two reference points – part 1.

File size	no CA				Inter-CA			
	SM TP [Mbps]	NM TP [Mbps]	App TP [Mbps]	Cell TP [Mbps]	SM TP [Mbps]	NM TP [Mbps]	App TP [Mbps]	Cell TP [Mbps]
100 kB	43.15	47.69	14.90	21.02	38.63	33.70	14.31	21.18
200 kB	54.00	57.03	19.33	33.04	43.80	46.80	17.88	30.85
500 kB	58.40	61.99	20.63	40.81	36.30	46.66	17.89	40.55
1 MB	58.70	62.62	26.12	48.71	41.86	63.13	27.48	56.48
2 MB	64.46	66.38	33.45	56.48	41.00	69.86	33.45	67.20
5 MB	67.21	68.54	43.20	60.95	40.79	89.15	45.54	84.34
10 MB	69.72	70.49	51.08	66.16	39.29	101.30	56.00	94.87
20 MB	70.99	71.38	61.13	69.38	44.99	119.07	82.53	114.90
50 MB	71.63	71.76	65.35	70.88	48.15	132.81	106.93	130.00
5s	71.54	71.70	67.73	70.63	48.02	136.23	120.30	135.03
10s	71.78	71.87	68.89	71.37	49.51	139.89	130.30	139.16

Table A1.6: Measured throughput comparison between the two methods and two reference points – part 2.

File size	Intra-site CA with FC OFF				Intra-site CA with FC ON			
	SM TP [Mbps]	NM TP [Mbps]	App TP [Mbps]	Cell TP [Mbps]	SM TP [Mbps]	NM TP [Mbps]	App TP [Mbps]	Cell TP [Mbps]
100 kB	41.90	43.51	13.90	20.55	35.61	38.79	14.01	23.39
200 kB	56.38	57.83	18.11	30.29	48.68	53.34	19.42	37.38
500 kB	76.61	75.96	22.72	55.84	66.69	65.90	20.09	51.45
1 MB	69.95	71.50	26.21	60.66	86.97	82.84	26.92	69.97
2 MB	88.86	87.43	31.60	74.61	107.75	95.43	31.94	85.26
5 MB	108.17	106.88	46.00	96.82	126.33	117.24	46.28	107.47
10 MB	121.00	119.21	61.49	110.72	134.61	127.63	63.17	119.12
20 MB	130.21	131.15	87.03	126.19	139.04	135.75	86.48	130.11
50 MB	137.50	136.47	104.00	133.36	141.71	140.60	112.00	138.25
5s	140.33	140.30	123.70	138.69	143.23	142.33	126.70	141.10
10s	142.28	142.09	130.00	141.23	143.66	143.24	132.86	142.63

Appendix 2: Multi Stream TCP Transmission details

This chapter presents a comprehensive analysis of test cases conducted under Chapter 5.3.2, focusing on the validation of IP scheduled throughput measurement accuracy in a multi-burst scenario for TCP multi-stream transmission across diverse UE-level connection types. The investigation encompasses three distinct connection configurations: single-cell, intra-site CA (non-DC), and inter-site CA (DC). To assess the effectiveness of 2CC CA, an analysis is performed for specific file size transmissions, aiming to identify optimal conditions for bandwidth aggregation by examining the impact of distinct bandwidth combinations on data transfer efficiency across various file sizes.

A2.1. Non-DC Single-cell connection, 2 streams

This study investigates the accuracy of two throughput estimation methods in cellular networks utilizing single cell connection for 2 TCP streams, focusing on the impact of file size and the TCP slow start mechanism. The new flow control algorithm is employed for both the standard and the novel method.

Figure A2.1 depicts the measured throughput performance for both the standard and novel methods, utilizing throughput reference from eNB and end-user perspective, during single-cell data transmission across a range of file sizes.

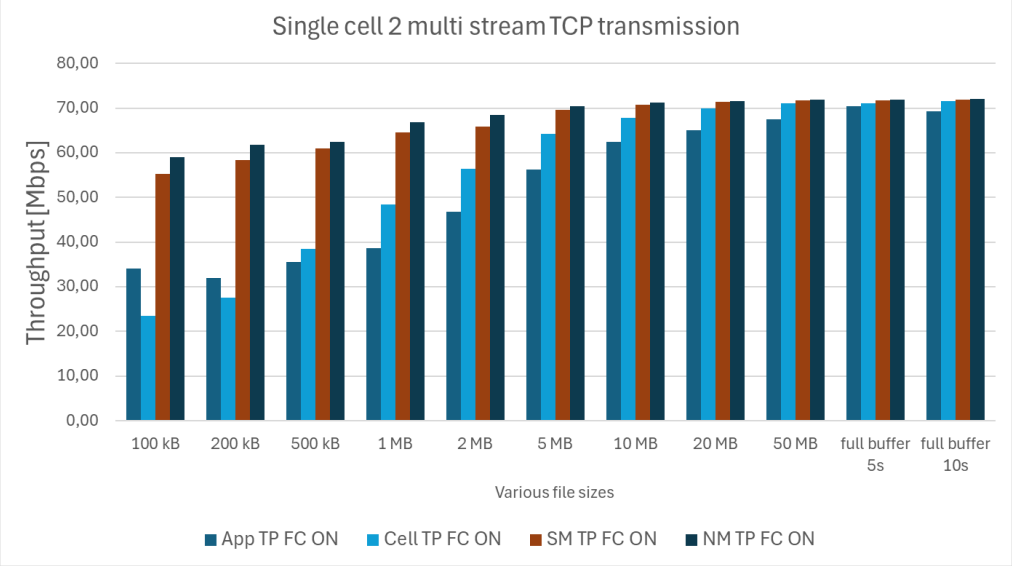

Figure A2.1: TCP/IP 2 multi stream transmission for single cell traffic with various throughput values.

Figure A2.2 provides supplementary precision analysis for the data presented in Figure A2.1. The left y-axis displays the data volume and time component ratios, represented by columnar data, while the right y-axis depicts the relative error in estimation of cell throughput, represented by curves. Figure A2.2 presents results for a single-cell connection, where the accuracy of both methods becomes acceptable after transmitting a 10 MB file over TCP using a 2 multi stream (-P iperf parameter set to 2, indicating a 2 parallel streams). The precision further improves after transmitting a 50 MB file. Similarly, as in Chapter 5.3.1 tests, the significant limitation hindering accurate throughput measurement arises from the division of a single file

transmission via TCP into multiple burst transmissions. This fragmentation is directly linked to TCP's slow start mechanism, which necessitates constant confirmation in the reverse direction regarding the success of data transmission. From the eNB's perspective, it becomes challenging to determine whether a transmission fragmented into multiple bursts, separated by a time interval (indicating an empty PDCP buffer after receiving the next data burst), corresponds to a single transmission or not. Only the data-transmitting server and the data receiving end-user possess this information. Increased traffic fragmentation within the eNB's PDCP buffer poses a significant challenge to both methods to accurately determine the time elapsed from the application layer perspective. An increase in the number of streams results in a marginal enhancement of the application layer throughput growth rate as file size increases.

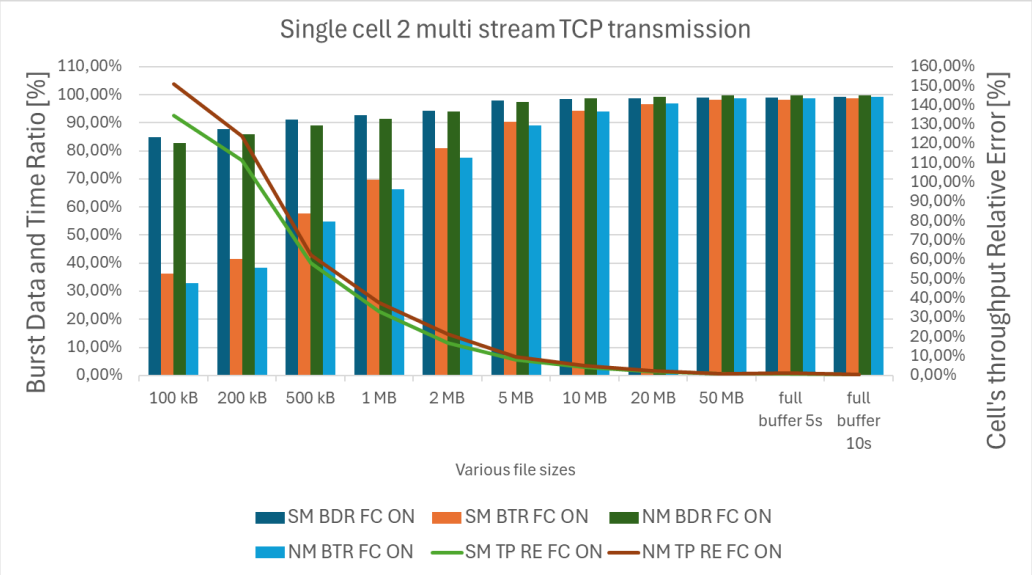

Figure A2.2: TCP/IP 2 multi stream transmission for single cell traffic with relative error and volume/time ratios between Standard and New method.

Table A2.1 presents a comprehensive analysis of the data presented in Figures A2.1 and A2.2, incorporating an additional metric, STTI burst ratio, which quantifies the percentage distribution of single TTIs during the transmission of various file sizes. The impact of TCP slow start diminishes with increasing file size and number of TCP streams. The standard method demonstrates a significant advantage in precision accuracy relative to the new method for diminutive file sizes of 100 and 200 kB, achieving a maximum gain of up to 16%. For file sizes ranging from 500 kB to 2 MB, the advantage in terms of relative error is approximately 4%, while for 5 MB file sizes, it fluctuates around 1%. Moreover, this gain progressively diminishes for larger file sizes, reaching a mere 0.14% for 50 MB file transmissions. As file size increases, the cell's throughput also escalates, as it attains its full capacity despite the TCP slow start phenomenon.

Table A2.1: TCP/IP 2 multi stream transmission details for single cell traffic with relative error and volume/time ratios between Standard and New method.

file size	SM TP [Mbps]	NM TP [Mbps]	App TP [Mbps]	Cell TP [Mbps]	SM BDR [%]	SM BTR [%]	SM TP Cell RE [%]	SM TP App RE [%]	NM BDR [%]	NM BTR [%]	NM TP Cell RE [%]	NM TP App RE [%]	STTI burst ratio [%]
100 kB	55.23	59.05	34.11	23.53	84.98	36.20	134.76	61.91	82.78	32.98	151.03	73.13	72
200 kB	58.39	61.82	31.96	27.62	87.64	41.45	111.43	82.69	86.00	38.42	123.86	93.43	70
500 kB	60.97	62.50	35.48	38.51	91.24	57.63	58.32	71.85	89.05	54.87	62.29	76.16	57
1 MB	64.51	66.78	38.67	48.44	92.71	69.61	33.17	66.83	91.40	66.30	37.85	72.69	47
2 MB	65.85	68.44	46.85	56.45	94.41	80.92	16.67	40.56	94.02	77.54	21.25	46.09	24
5 MB	69.58	70.35	56.23	64.28	97.92	90.46	8.24	23.73	97.42	89.01	9.44	25.11	13
10 MB	70.83	71.29	62.41	67.88	98.43	94.33	4.35	13.49	98.80	94.08	5.02	14.22	4
20 MB	71.36	71.60	65.07	69.85	98.76	96.67	2.16	9.67	99.28	96.87	2.49	10.03	3
50 MB	71.77	71.88	67.49	71.14	99.08	98.21	0.89	6.35	99.71	98.69	1.03	6.50	1.4
5s	71.80	71.90	70.34	71.14	99.04	98.13	0.93	2.08	99.73	98.67	1.07	2.22	1.1
10s	71.92	71.98	69.24	71.63	99.14	98.74	0.40	3.87	99.83	99.36	0.48	3.95	1.8

A2.2. Non-DC Single-cell connection, 8 streams

This study investigates the accuracy of two throughput estimation methods in cellular networks utilizing single cell connection for 8 TCP streams, focusing on the impact of file size and the TCP slow start mechanism. The new flow control algorithm is employed for both the standard and the novel method.

Figure A2.3 depicts the measured throughput performance for both the standard and the novel method, utilizing throughput reference from eNB and end-user perspective, during single-cell data transmission across a range of file sizes.

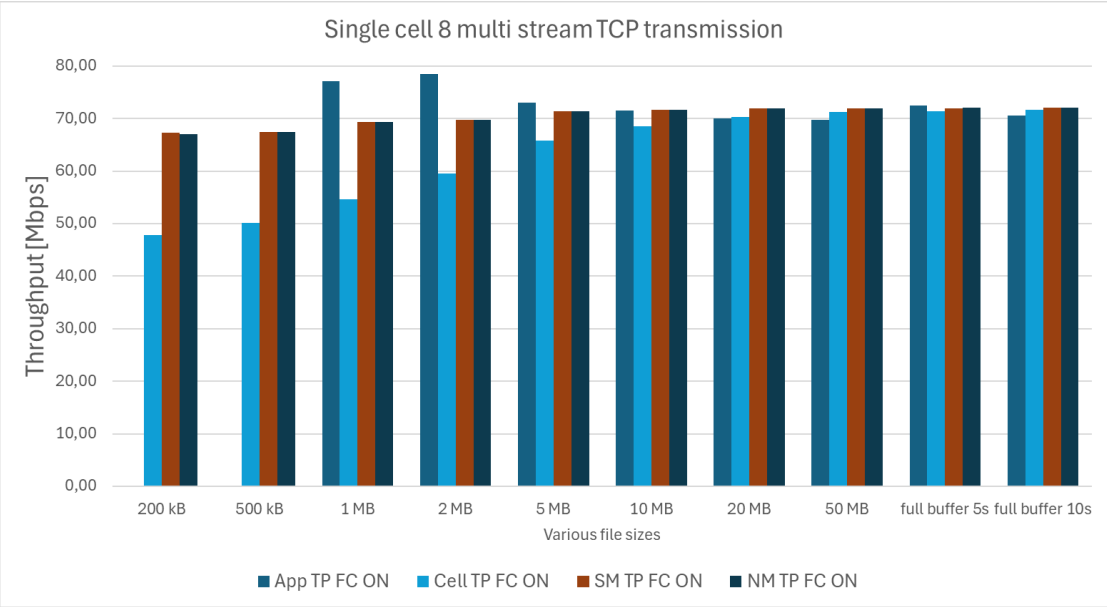

Figure A2.3: TCP/IP 8 multi stream transmission for single cell traffic with various throughput values.

Figure A2.4 presents results for a single-cell connection, where the accuracy of both methods becomes acceptable after transmitting a 10 MB file over TCP using an 8 multi streams (-P iperf parameter set to 8, indicating a 8 parallel streams). The precision further improves after transmitting a 5 MB file. Similarly to Chapter 5.3.1, the significant limitation hindering accurate throughput measurement arises from the division of a single file transmission via TCP into multiple burst transmissions, however, this effect is only visible during this test case for file sizes up to 2 MB. This fragmentation is directly linked to TCP's slow start mechanism. Furthermore, the indistinguishable SM and NM TP RE results in Figure A2.4 demonstrate comparable accuracy between the two methods.

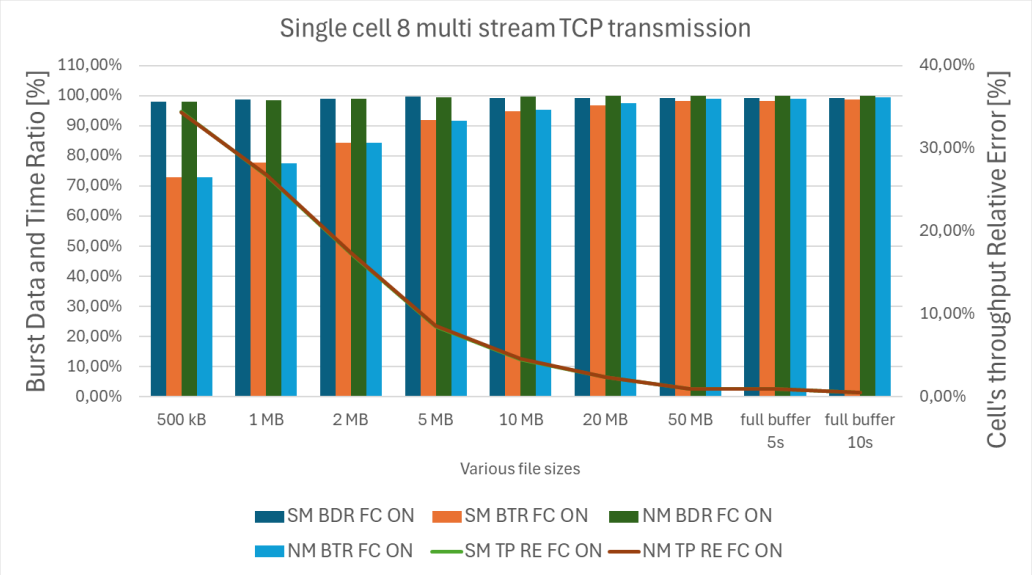

Figure A2.4: TCP/IP 8MS transmission for single cell traffic with Cell RE and BDR/BTR for both method.

Table A2.2 provides a comprehensive analysis of the data presented in Figures A2.3 and A2.4, incorporating the STTI burst ratio as an additional metric. The impact of TCP slow start diminishes with increasing file size and number of TCP streams. Increasing the number of TCP streams from 2 to 8 results in a 2.5-fold decrease in the STTI burst ratio, leading to improved BDR and BTR accounting. The application layer throughput is slightly overestimated for file sizes ranging from 1 MB to 5 MB, based on the maximum cell throughput, which is around 72 Mbps.

Table A2.2: TCP/IP 8MS transmission for single cell traffic with Cell RE and BDR/BTR for both methods.

file size	SM TP [Mbps]	NM TP [Mbps]	App TP [Mbps]	Cell TP [Mbps]	SM BDR [%]	SM BTR [%]	SM TP Cell RE [%]	SM TP App RE [%]	NM BDR [%]	NM BTR [%]	NM TP Cell RE [%]	NM TP App RE [%]	STTI burst ratio [%]
200 kB	67.23	67.07	N/A	47.82	97.26	69.18	40.59	N/A	97.03	69.18	40.26	N/A	22.6
500 kB	67.47	67.43	N/A	50.18	98.14	72.98	34.47	N/A	97.90	72.86	34.38	N/A	12.2
1 MB	69.28	69.34	77.05	54.66	98.69	77.87	26.74	-10.09	98.44	77.60	26.85	-10.01	9.3
2 MB	69.76	69.78	78.44	59.48	98.96	84.38	17.28	-11.07	98.91	84.31	17.32	-11.04	10.2
5 MB	71.34	71.37	73.03	65.74	99.63	91.82	8.52	-2.32	99.58	91.73	8.56	-2.27	2.6
10 MB	71.64	71.69	71.45	68.56	99.15	94.88	4.50	0.27	99.72	95.37	4.57	0.33	1.8
20 MB	71.91	71.92	70.05	70.23	99.25	96.92	2.40	2.66	99.88	97.53	2.41	2.67	0.127
50 MB	71.98	71.98	69.75	71.30	99.31	98.36	0.96	3.20	99.96	99.01	0.96	3.20	0.171
5s	71.99	72.00	72.41	71.33	99.26	98.35	0.93	-0.59	99.95	99.01	0.95	-0.56	0.009
10s	72.02	72.03	70.61	71.65	99.26	98.74	0.52	2.00	99.98	99.44	0.54	2.01	0.008

A2.3. Non-DC Single-cell connection, 16 streams

This study investigates the accuracy of two throughput estimation methods in cellular networks utilizing single cell connection for 16 TCP streams, focusing on the impact of file size and the TCP slow start mechanism. The new flow control algorithm is employed for both the standard and the novel method. Application layer throughput measurements for 200 kB, 500 kB, 1 MB, 2 MB, and 5 MB file sizes exhibited an overestimation. This discrepancy arises from limitations within the iperf tool, which inaccurately interprets throughput when multiple TCP streams are employed.

Figure A2.5 depicts the measured throughput performance for both the standard and the novel method, utilizing throughput reference from eNB and end-user perspective, during single-cell data transmission across a range of file sizes.

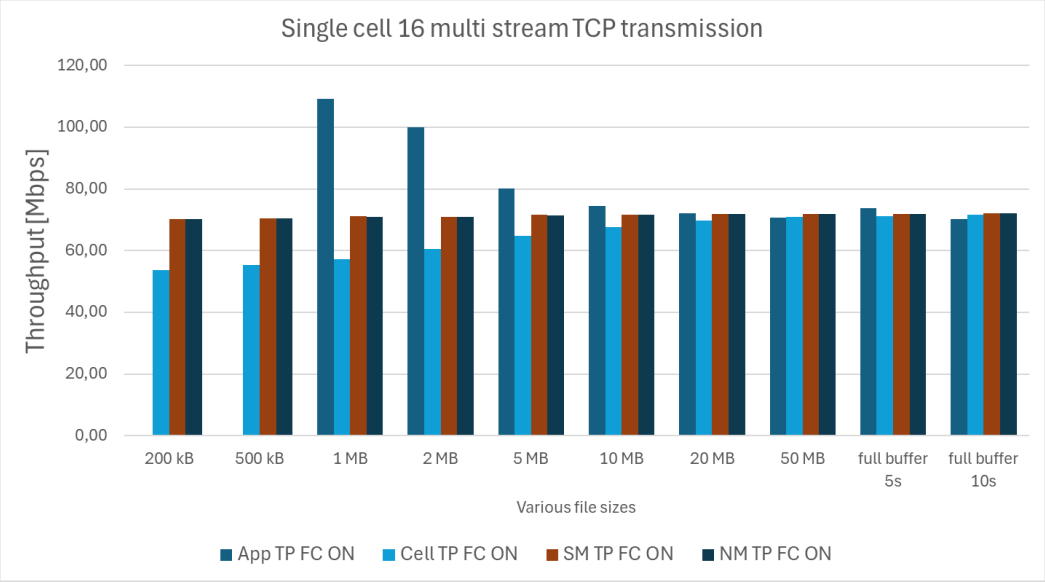

Figure A2.5: TCP/IP 16 multi stream transmission for single cell traffic with various throughput values.

Figure A2.6 presents results for a single-cell connection, where the accuracy of both methods becomes acceptable after transmitting a 10 MB file over TCP using 16 multi streams (-P iperf parameter set to 16, indicating 16 parallel streams). The precision further improves after transmitting a 50 MB file. Similarly to Chapter 5.3.1, the significant limitation hindering accurate throughput measurement arises from the division of a single file transmission via TCP into multiple burst transmissions. This fragmentation is directly linked to TCP's slow start mechanism, which necessitates constant confirmation in the reverse direction regarding the success of data transmission. From the eNB's perspective, it becomes challenging to determine whether a transmission fragmented into multiple bursts, separated by a time interval (indicating an empty PDCP buffer after receiving the next data burst), corresponds to a single transmission or not. Only the data-transmitting server and the data receiving end-user possess this information. Increased traffic fragmentation within the eNB's PDCP buffer poses a significant challenge to both methods in accurately determining the time elapsed from the application layer perspective. An increase in the number of streams results in a marginal enhancement of the application layer throughput

growth rate as file size increases. Moreover, Figure A2.6 reveals no discernible difference between the SM and NM TP RE results, showing similar accuracy level between the two methods.

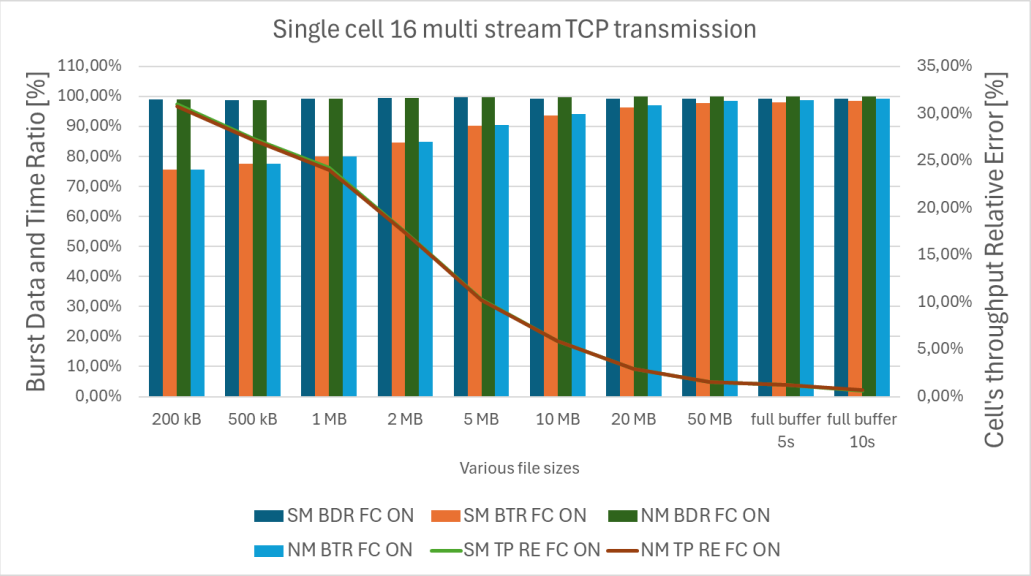

Figure A2.6: TCP/IP 16 multi stream transmission for single cell traffic with relative error and volume/time ratios between Standard and New method.

Table A2.3 provides a comprehensive analysis of the data presented in Figures A2.5 and A2.6, incorporating the STTI burst ratio as an additional metric. The impact of TCP slow start diminishes with increasing file size and number of TCP streams. Increasing the number of TCP streams from 2 to 16 results in a 6-fold decrease in the STTI burst ratio, leading to improved BDR and BTR accounting. The application layer throughput is slightly overestimated for file sizes ranging from 1 MB to 10 MB, based on the maximum cell throughput, which is around 72 Mbps.

Table A2.3: TCP/IP 16 multi stream transmission details for single cell traffic with relative error and volume/time ratios between Standard and New method.

file size	SM TP [Mbps]	NM TP [Mbps]	App TP [Mbps]	Cell TP [Mbps]	SM BDR [%]	SM BTR [%]	SM TP Cell RE [%]	SM TP App RE [%]	NM BDR [%]	NM BTR [%]	NM TP Cell RE [%]	NM TP App RE [%]	STTI burst ratio [%]
200 kB	70.29	70.18	N/A	53.66	99.11	75.67	30.99	NA	99.00	75.69	30.79	N/A	11.596
500 kB	70.47	70.39	N/A	55.32	98.83	77.58	27.39	NA	98.68	77.55	27.25	N/A	15.744
1 MB	71.19	71.06	109.15	57.29	99.34	79.94	24.26	-34.78	99.22	79.99	24.05	-34.89	6.143
2 MB	71.06	70.99	100.08	60.50	99.54	84.74	17.47	-28.99	99.51	84.79	17.35	-29.06	6.852
5 MB	71.55	71.51	80.23	64.86	99.69	90.36	10.32	-10.82	99.67	90.39	10.26	-10.87	4.279
10 MB	71.74	71.74	74.56	67.75	99.28	93.76	5.89	-3.79	99.82	94.27	5.89	-3.79	2.396
20 MB	71.96	71.93	72.15	69.88	99.31	96.45	2.97	-0.27	99.90	97.05	2.94	-0.30	0.512
50 MB	72.00	72.01	70.69	70.93	99.20	97.73	1.51	1.86	99.97	98.48	1.52	1.86	0.350
5s	71.99	72.01	73.74	71.13	99.30	98.11	1.21	-2.37	99.97	98.75	1.23	-2.35	0.048
10s	72.02	72.03	70.25	71.56	99.22	98.58	0.65	2.52	99.98	99.32	0.66	2.53	0.009

A2.4. Non-DC Intra-site CA connection, 2 streams

This study investigates the accuracy of two throughput estimation methods in cellular networks utilizing intra-site CA for 2 TCP streams, focusing on the impact of file size and the TCP slow start mechanism. The analysis compares the standard calculation method with the new method based on different architectural principles. Two distinct flow control algorithms are employed to isolate the influence of the estimation methods from the specific flow control implementation.

Figure A2.7 depicts the measured throughput performance for both the standard and the novel method, utilizing throughput reference from eNB and end-user perspective, during intra-site CA (non-DC) data transmission across a range of file sizes.

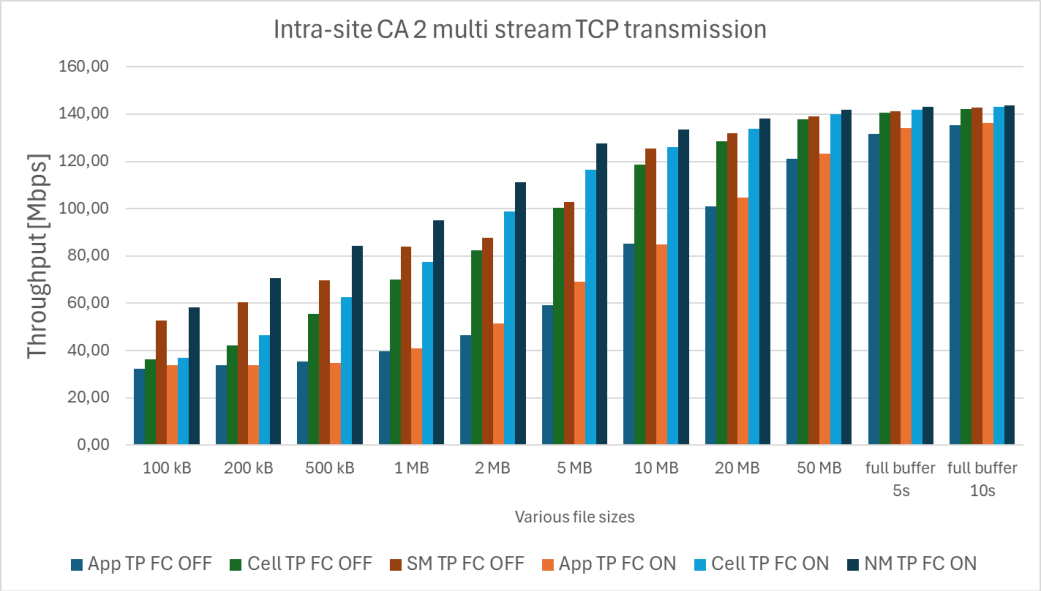

Figure A2.7: TCP/IP 2 multi stream transmission for 2CC Intra-site CA traffic with various throughput values.

Figure A2.8 illustrates the distinct data distribution patterns observed in single-cell and 2CC CA connections. The introduction of data splitting between the primary cell and the secondary cell in 2CC CA connections creates an additional layer of data segmentation. This segmentation can potentially lead to misinterpretations of user throughput, particularly for small packet transmissions.

For a 2CC CA connection, the accuracy of both methods becomes acceptable after transmitting a 10 MB file over TCP using 2 multi streams. Further increases in file size led to improved precision. Similarly, for single cell transmission, a significant limitation hindering accurate throughput measurement arises from the fragmentation of a single file transmission via TCP into multiple burst transmissions. This fragmentation is directly linked to TCP's slow start mechanism, which requires constant acknowledgement of successful data transmission in the reverse direction. From the eNB's perspective, it becomes challenging to distinguish between a single transmission fragmented into multiple bursts, separated by a time interval (indicating an empty PDCP buffer after receiving the next data burst), and multiple independent transmissions. Furthermore, the challenge of accurately determining the time elapsed from the application layer perspective is exacerbated when data volume is split across two separate cells steered by

different schedulers but residing on the same eNB. This information is only available to the data-transmitting server and the receiving end-user. For both methods, increased traffic fragmentation within the eNB's PDCP buffer poses a significant challenge to accurately determine the time elapsed from the application layer perspective. The utilization of two concurrent TCP streams results in a general enhancement of throughput, effectively bridging the discrepancy between the application layer and the cell's perspective. The accelerated rate at which data streams enter the PDCP buffer, compared to single-stream transmission, enables the eNB to execute data scheduling at a significantly faster pace. Furthermore, both throughput measurements exhibit a closer alignment with the IP-scheduled throughput, as determined by both methods. Additionally, a threshold of data volume exists beyond which transmission across multiple cells becomes advantageous. Larger data volumes result in higher precision.

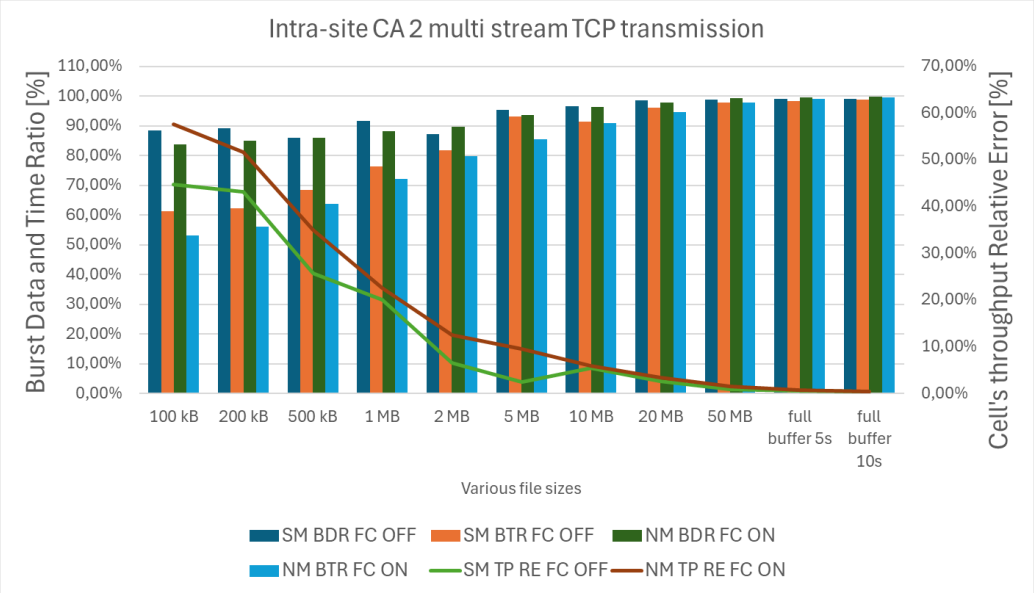

Figure A2.8: TCP/IP 2 multi stream transmission for Intra-site CA 2CC traffic with relative error and volume/time ratios between Standard and New method.

Tables A2.10 and A2.11 provide a detailed analysis of the data visualized in Figures A2.7 and A2.8. The analysis incorporates the metric STTI burst ratio. The impact of TCP slow start diminishes with increasing file size and number of TCP streams. The traffic data is presented in separate tables due to the use of two distinct flow control algorithms: the legacy algorithm designed for non-DC systems and the novel algorithm specifically developed for DC systems. It is important to note that the distinct flow control algorithms result in different transmission processes, making direct 1:1 comparison challenging. However, the results presented are averaged over multiple iterations, providing the most robust comparison possible.

In contrast to single-cell transmission scenarios, the standard method demonstrates a significant improvement in relative error accuracy compared to the new method for file sizes ranging from 100 kB to 5 MB. This discrepancy is directly attributed to the divergent flow control algorithm behavior, where the standard method exhibits greater precision in managing data flow compared to the novel method's adaptation. Furthermore, in multi-stream transmission scenarios, where the data inflow rate is higher compared to single-stream transmission, the advantage of

the novel method in accurately accounting for buffer fullness, as observed in Chapter 5.3.1, diminishes. For file sizes exceeding 10 MB, the new method demonstrates comparable relative error to the standard method, with a difference ranging from 0.07% to 0.67%. This convergence suggests that the influence of differing time component interpretations diminishes with increasing file size. The rapid saturation of the PDCP buffer, driven by continuous IP packet inflow, renders the initial transmission phase with a limited number of packets negligible in the overall data transfer.

Table A2.4: TCP/IP 2 multi stream transmission for Intra-site CA 2CC with flow control OFF traffic details with relative error and volume/time ratios between Standard and New method.

file size	SM TP [Mbps]	NM TP [Mbps]	App TP [Mbps]	Cell TP [Mbps]	SM BDR [%]	SM BTR [%]	SM TP Cell RE [%]	SM TP App RE [%]	NM BDR [%]	NM BTR [%]	NM TP Cell RE [%]	NM TP App RE [%]	STTI BR [%]
100 kB	52.74	58.70	32.17	36.45	88.52	61.17	44.72	63.94	84.22	52.29	61.06	82.46	76.8
200 kB	60.38	61.96	33.91	42.18	89.18	62.29	43.16	78.07	83.95	57.14	46.91	82.72	44.8
500 kB	69.75	74.96	35.25	55.49	85.92	68.36	25.69	97.84	85.85	63.55	35.08	112.62	68.9
1 MB	83.93	89.70	39.66	69.90	91.59	76.28	20.07	111.60	88.99	69.35	28.33	126.16	77.5
2 MB	87.80	97.53	46.59	82.38	87.17	81.79	6.58	88.46	90.04	76.06	18.39	109.33	65.3
5 MB	102.81	110.27	59.17	100.39	95.23	92.99	2.41	73.75	93.54	85.15	9.85	86.37	36.0
10 MB	125.28	126.06	85.11	118.73	96.51	91.47	5.52	47.20	96.75	91.13	6.17	48.11	32.7
20 MB	131.99	132.90	101.09	128.67	98.48	96.00	2.58	30.56	98.09	94.96	3.29	31.47	8.1
50 MB	139.01	139.65	121.00	137.73	98.81	97.90	0.93	14.89	99.27	97.90	1.39	15.42	3.1
5s	141.32	141.54	131.70	140.43	98.98	98.35	0.63	7.31	99.58	98.80	0.79	7.47	3.8
10s	142.63	142.76	135.33	142.12	99.14	98.79	0.35	5.39	99.79	99.34	0.45	5.49	0.9

Table A2.5: TCP/IP 2 multi stream transmission for Intra-site CA 2CC with flow control ON traffic details with relative error and volume/time ratios between Standard and New method.

file size	SM TP [Mbps]	NM TP [Mbps]	App TP [Mbps]	Cell TP [Mbps]	SM BDR [%]	SM BTR [%]	SM TP Cell RE [%]	SM TP App RE [%]	NM BDR [%]	NM BTR [%]	NM TP Cell RE [%]	NM TP App RE [%]	STTI BR [%]
100 kB	43.25	58.42	33.77	37.06	38.71	33.16	16.73	28.09	83.76	53.13	57.64	72.99	67.2
200 kB	56.60	70.77	33.80	46.68	46.29	38.18	21.24	67.46	85.08	56.13	51.59	109.38	70.2
500 kB	63.77	84.41	34.79	62.54	47.95	47.02	1.97	83.31	85.91	63.65	34.98	142.64	67.0
1 MB	89.32	95.03	40.85	77.54	51.09	44.36	15.19	118.67	88.28	72.03	22.55	132.65	65.0
2 MB	108.58	111.07	51.60	98.78	37.40	34.03	9.92	110.43	89.75	79.82	12.44	115.26	64.4
5 MB	134.25	127.64	69.27	116.58	70.32	61.06	15.15	93.81	93.49	85.40	9.48	84.26	53.5
10 MB	136.10	133.58	84.95	126.13	84.59	78.39	7.91	60.22	96.35	90.98	5.90	57.24	24.6
20 MB	140.38	138.19	104.83	133.68	93.91	89.43	5.01	33.91	97.89	94.70	3.37	31.82	18.7
50 MB	142.83	141.93	123.11	139.85	96.96	94.93	2.13	16.02	99.19	97.74	1.49	15.29	7.6
5s	143.63	142.93	134.11	141.96	98.14	96.99	1.18	7.10	99.61	98.93	0.68	6.57	2.5
10s	144.06	143.55	136.11	143.07	97.55	96.87	0.69	5.84	99.76	99.43	0.33	5.46	3.3

The implementation of the standard method with flow control enhancement exhibits unexpectedly low relative error in relation to cell throughput. This phenomenon is attributed to the close proportionality between the quotient of data volume and time components. For instance,

with 200 kB traffic, 46.68% of data volume corresponds to 38.18% of the time component, resulting in a mere 21.24% relative error, which is considered as rather low value. However, despite these favorable results, the standard method fails to accurately account for the total volume and time of user transmission. The novel method demonstrates improved accuracy in incorporating BDR and BTR values compared to the standard method. However, the resulting quotient exhibits unfavorable outcomes. For instance, during a 200 kB file transmission, the Cell RE attains a value of 51.59%, with corresponding BDR and BTR values of 85.08% and 56.13%, respectively.

A2.5. Non-DC Intra-site CA connection, 8 streams

This study investigates the accuracy of two throughput estimation methods in cellular networks utilizing intra-site CA for 8 TCP streams, focusing on the impact of file size and the TCP slow start mechanism. The analysis compares the standard calculation method with the new method based on different architectural principles. Two distinct flow control algorithms are employed to isolate the influence of the estimation methods from the specific flow control implementation.

Figure A2.9 depicts the measured throughput performance for both the standard and novel methods, utilizing throughput reference from eNB and end-user perspective, during intra-site CA (non-DC) data transmission across a range of file sizes.

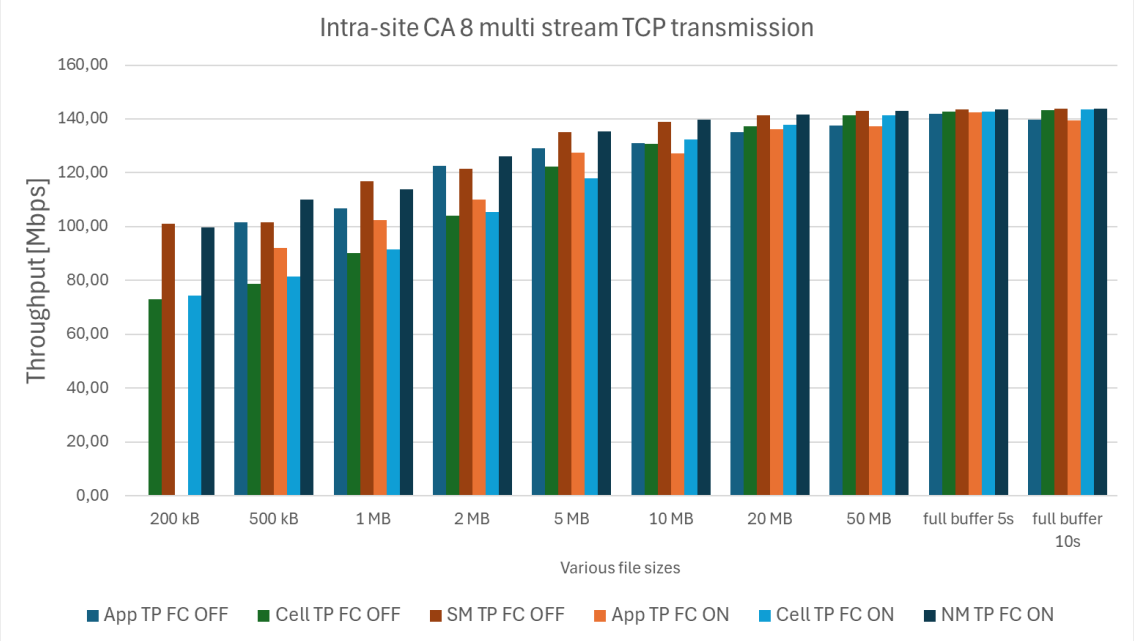

Figure A2.9: TCP/IP 8 multi stream transmission for 2CC Intra-site CA traffic with various throughput values.

Figure A2.10 illustrates the distinct data distribution patterns observed in single-cell and 2CC CA connections. The introduction of data splitting between the primary cell and the secondary cell in 2CC CA connections creates an additional layer of data segmentation. This segmentation can potentially lead to misinterpretations of user throughput, particularly for small packet transmissions.

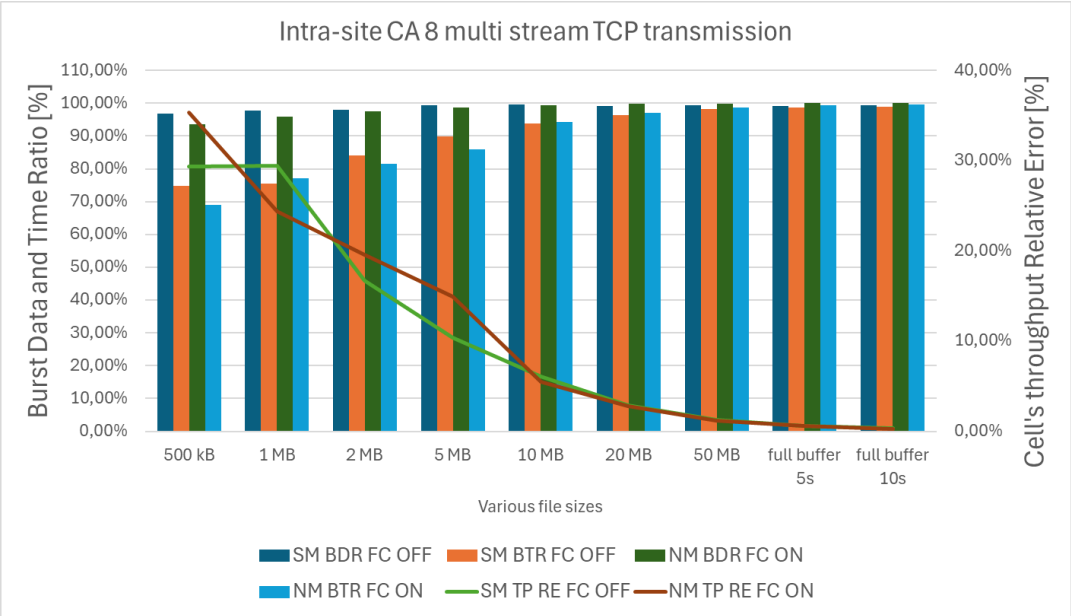

Figure A2.10: TCP/IP 8 multi stream transmission for Intra-site CA 2CC traffic with relative error and volume/time ratios between Standard and New method.

Table A2.6 and A2.7 provide a comprehensive analysis of the data presented in Figures A2.9 and A2.10, incorporating the STTI burst ratio as an additional metric. The impact of TCP slow start diminishes with increasing file size and number of TCP streams. Increasing the number of TCP streams from 2 to 8, for Table A2.6 results for standard method, does not yield in expected decrease of the STTI burst ratio, which in consequence also does not decrease SM TP Cell RE. However, results from Table A2.7 for the standard method due to the change of flow control algorithm are improved, for example SM TP Cell RE diminishes, along with STTI BR metric, reaching more closely to NM TP Cell RE value.

Table A2.6: TCP/IP 8 multi stream transmission for Intra-site CA 2CC with flow control OFF traffic details with relative error and volume/time ratios between Standard and New method.

file size	SM TP [Mbps]	NM TP [Mbps]	App TP [Mbps]	Cell TP [Mbps]	SM BDR [%]	SM BTR [%]	SM TP Cell RE [%]	SM TP App RE [%]	NM BDR [%]	NM BTR [%]	NM TP Cell RE [%]	NM TP App RE [%]	STTI BR [%]
200 kB	101.16	100.19	N/A	73.18	89.00	64.38	38.24	N/A	94.17	68.78	36.92	N/A	78.54
500 kB	101.76	103.14	101.71	78.67	96.78	74.82	29.35	0.05	95.51	72.85	31.11	1.40	77.19
1 MB	116.94	114.11	106.83	90.32	97.71	75.47	29.47	9.46	96.74	76.57	26.33	6.81	74.40
2 MB	121.49	123.00	122.55	104.08	98.00	83.96	16.72	-0.87	97.51	82.51	18.18	0.37	48.59
5 MB	135.15	133.65	129.10	122.41	99.32	89.96	10.40	4.68	99.10	90.77	9.18	3.53	45.22
10 MB	138.85	137.92	131.10	130.87	99.62	93.89	6.10	5.91	99.51	94.42	5.39	5.21	23.35
20 MB	141.39	141.04	135.00	137.40	99.21	96.41	2.90	4.73	99.73	97.16	2.64	4.47	8.62
50 MB	143.11	142.94	137.50	141.35	99.32	98.10	1.24	4.08	99.91	98.79	1.13	3.96	4.27
5s	143.47	143.45	142.00	142.63	99.24	98.65	0.59	1.04	99.95	99.38	0.57	1.02	1.73
10s	143.75	143.75	139.60	143.27	99.26	98.93	0.34	2.98	99.98	99.64	0.33	2.97	0.76

Table A2.7: TCP/IP 8 multi stream transmission for Intra-site CA 2CC with flow control ON traffic details with relative error and volume/time ratios between Standard and New method.

file size	SM TP [Mbps]	NM TP [Mbps]	App TP [Mbps]	Cell TP [Mbps]	SM BDR [%]	SM BTR [%]	SM TP Cell RE [%]	SM TP App RE [%]	NM BDR [%]	NM BTR [%]	NM TP Cell RE [%]	NM TP App RE [%]	STTI BR [%]
200 kB	88.27	99.67	N/A	74.51	50.64	42.75	18.46	N/A	93.95	70.24	33.76	N/A	48.64
500 kB	105.62	110.11	92.22	81.38	52.84	40.72	29.78	14.52	93.46	69.08	35.30	19.39	45.04
1 MB	105.19	113.83	102.53	91.53	49.90	43.42	14.92	2.59	95.89	77.11	24.36	11.02	34.41
2 MB	119.21	126.08	109.96	105.42	56.39	49.87	13.08	8.41	97.56	81.57	19.60	14.66	23.25
5 MB	132.25	135.50	127.40	117.91	51.03	45.50	12.16	3.81	98.77	85.95	14.92	6.36	11.00
10 MB	139.00	139.69	127.30	132.46	79.59	75.85	4.93	9.19	99.30	94.16	5.46	9.74	4.71
20 MB	142.06	141.71	136.30	137.88	98.97	96.06	3.03	4.23	99.72	97.03	2.78	3.97	2.57
50 MB	143.29	143.09	137.30	141.45	99.19	97.92	1.30	4.36	99.89	98.74	1.16	4.22	0.38
5s	143.61	143.59	142.38	142.74	99.15	98.55	0.61	0.87	99.95	99.36	0.59	0.85	0.37
10s	143.88	143.85	139.50	143.43	99.25	98.94	0.31	3.14	99.97	99.68	0.29	3.12	0.04

The implementation of the standard method with flow control enhancement exhibits unexpectedly low relative error in relation to cell throughput. This phenomenon is attributed to the close proportionality between the quotient of data volume and time components. For instance, with 200 kB traffic, 50.64% of data volume corresponds to 42.75% of the time component, resulting in a mere 18.46% relative error, which is considered as rather low value and slightly better than for two TCP streams. However, despite these favorable results, the standard method fails to accurately account for the BDR and BTR of user transmission. The novel method exhibits enhanced precision in integrating BDR and BTR values relative to both the standard method and the utilization of eight TCP streams. Consequently, the resulting quotient demonstrates improved outcomes compared to the use of two TCP streams. For example, during a 200 kB file transmission, the Cell RE achieves a value of 33.76%, with corresponding BDR and BTR values of 93.95% and 70.24%, respectively.

A2.6. Non-DC Intra-site CA connection, 16 streams

This study investigates the accuracy of two throughput estimation methods in cellular networks utilizing intra-site CA for 16 TCP streams, focusing on the impact of file size and the TCP slow start mechanism. The analysis compares the standard calculation method with the new method based on different architectural principles. Two distinct flow control algorithms are employed to isolate the influence of the estimation methods from the specific flow control implementation.

Figure A2.11 depicts the measured throughput performance for both the standard and the novel method, utilizing throughput reference from eNB and end-user perspective, during intra-site CA (non-DC) data transmission across a range of file sizes.

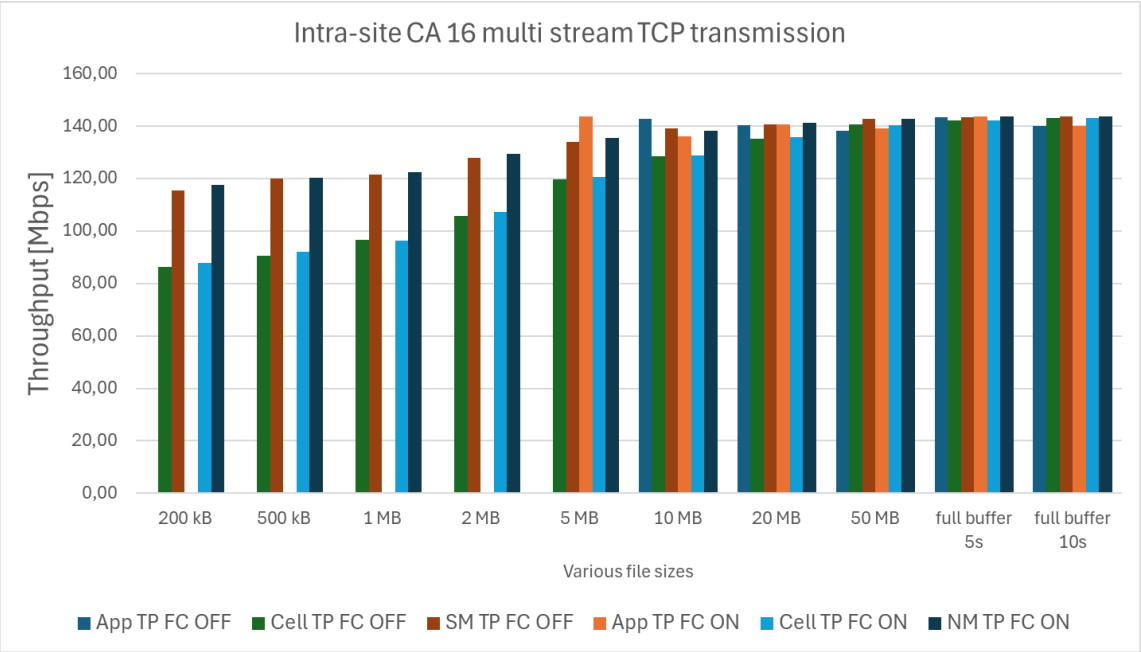

Figure A2.11: TCP/IP 16 multi stream transmission for 2CC Intra-site CA traffic with various throughput values.

Figure A2.12 illustrates the distinct data distribution patterns observed in single-cell and 2CC CA connections. The introduction of data splitting between the primary cell and the secondary cell in 2CC CA connections creates an additional layer of data segmentation. This segmentation can potentially lead to misinterpretations of user throughput, particularly for small packet transmissions.

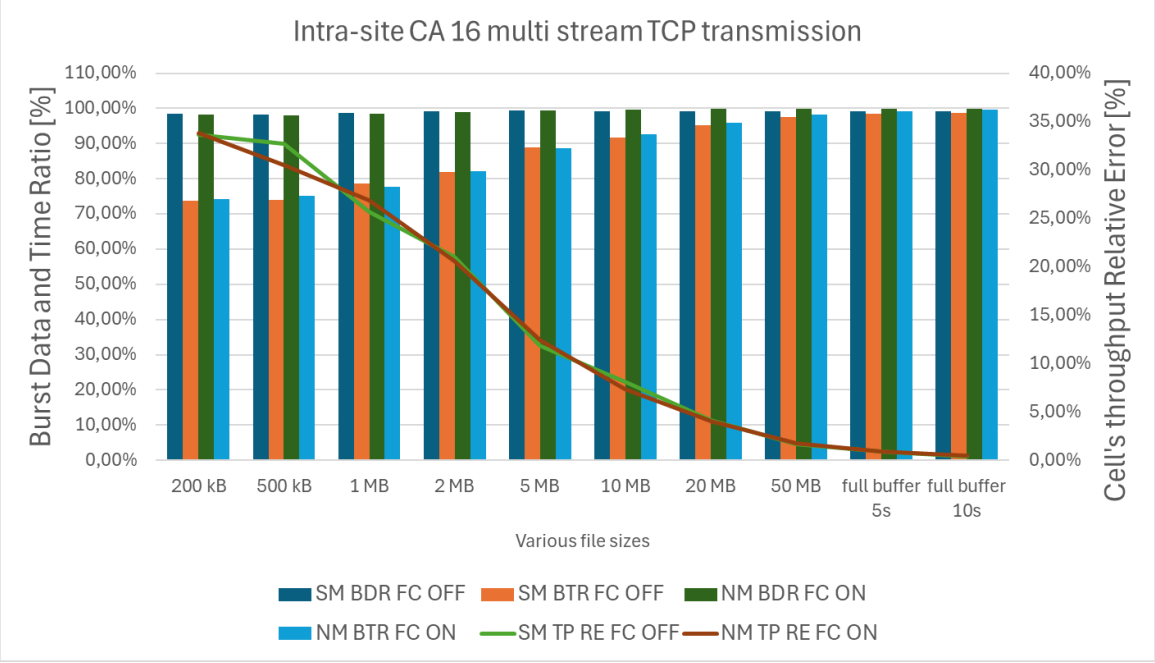

Figure A2.12: TCP/IP 16 multi stream transmission for Intra-site CA 2CC traffic with relative error and volume/time ratios between Standard and New method.

Table A2.8 and A2.9 provide a comprehensive analysis of the data presented in Figures A2.11 and A2.12, incorporating the STTI burst ratio as an additional metric. The impact of TCP slow start diminishes with increasing file size, leading to a reduction in the number of single TTIs. Increasing the number of TCP streams from 2 to 16, for Table A2.8 results for standard method, does not yield in expected decrease of the STTI burst ratio. However, SM TP Cell RE value is decreased with more accurate accounting of BDR and BTR. The results from Table A2.9 for the standard method are slightly improved due to the change of flow control algorithm, for example SM TP Cell RE diminishes, along with STTI BR metric, reaching more closely to NM TP Cell RE value.

Table A2.8: TCP/IP 16 multi stream transmission for Intra-site CA 2CC with flow control OFF traffic details with relative error and volume/time ratios between Standard and New method.

file size	SM TP [Mbps]	NM TP [Mbps]	App TP [Mbps]	Cell TP [Mbps]	SM BDR [%]	SM BTR [%]	SM TP Cell RE [%]	SM TP App RE [%]	NM BDR [%]	NM BTR [%]	NM TP Cell RE [%]	NM TP App RE [%]	STTI BR [%]
200 kB	115.43	114.41	N/A	86.37	98.54	73.73	33.64	N/A	98.28	74.20	32.46	N/A	74.09
500 kB	120.07	118.10	N/A	90.45	98.25	74.01	32.75	N/A	98.00	75.05	30.57	N/A	78.99
1 MB	121.49	122.33	N/A	96.70	98.70	78.56	25.63	N/A	98.40	77.79	26.51	N/A	74.30
2 MB	127.90	127.23	N/A	105.68	99.14	81.91	21.03	N/A	98.96	82.20	20.39	N/A	77.00
5 MB	134.06	134.06	N/A	119.85	99.40	88.85	11.86	N/A	99.31	88.77	11.86	N/A	65.24
10 MB	138.99	138.38	142.70	128.55	99.09	91.65	8.12	-2.60	99.67	92.59	7.65	-3.03	39.82
20 MB	140.78	140.65	140.30	135.21	99.23	95.30	4.12	0.34	99.82	95.96	4.03	0.25	24.71
50 MB	142.89	142.89	138.20	140.53	99.18	97.54	1.68	3.39	99.94	98.29	1.68	3.39	6.46
5s	143.51	143.49	143.50	142.25	99.28	98.41	0.89	0.01	99.98	99.11	0.87	-0.01	3.83
10s	143.81	143.80	139.90	143.19	99.25	98.82	0.43	2.79	99.98	99.56	0.43	2.79	1.35

Table A2.9: TCP/IP 16 multi stream transmission for Intra-site CA 2CC with flow control ON traffic details with relative error and volume/time ratios between Standard and New method.

file size	SM TP [Mbps]	NM TP [Mbps]	App TP [Mbps]	Cell TP [Mbps]	SM BDR [%]	SM BTR [%]	SM TP Cell RE [%]	SM TP App RE [%]	NM BDR [%]	NM BTR [%]	NM TP Cell RE [%]	NM TP App RE [%]	STTI BR [%]
200 kB	115.50	117.58	N/A	87.85	61.10	46.47	31.48	N/A	97.64	72.95	33.85	N/A	36.23
500 kB	104.18	120.26	N/A	92.14	36.35	32.15	13.07	N/A	97.62	74.79	30.52	N/A	34.93
1 MB	120.00	122.34	N/A	96.43	71.02	57.07	24.44	N/A	98.44	77.59	26.86	N/A	21.62
2 MB	129.68	129.28	N/A	107.19	70.53	58.30	20.98	N/A	98.72	81.85	20.61	N/A	11.22
5 MB	134.08	135.45	143.60	120.47	59.85	53.77	11.30	-6.63	99.27	88.29	12.44	-5.67	16.59
10 MB	138.19	138.36	136.12	128.87	69.45	64.77	7.23	1.52	99.61	92.78	7.36	1.65	6.47
20 MB	141.60	141.40	140.60	135.91	96.49	92.61	4.19	0.71	99.80	95.93	4.04	0.57	3.11
50 MB	142.74	142.70	139.20	140.26	99.19	97.47	1.77	2.55	99.94	98.24	1.73	2.51	0.75
5s	143.54	143.55	143.70	142.29	99.24	98.38	0.88	-0.11	99.97	99.09	0.88	-0.11	0.33
10s	143.79	143.79	140.10	143.15	99.26	98.81	0.45	2.63	99.98	99.53	0.45	2.64	0.03

The implementation of the standard method with flow control enhancement exhibits an unexpectedly low relative error in relation to cell throughput. This phenomenon can be attributed to the close proportionality between the quotient of data volume and time components. For

instance, with 200 kB traffic, 61.10% of the data volume corresponds to 46.47% of the time component, resulting in a 31.48% relative error. This represents a less favorable outcome for Cell RE compared to the two and eight TCP stream use cases. The novel method demonstrates improved accuracy in incorporating BDR and BTR values compared to the standard method. Consequently, the resulting quotient exhibits improved outcomes compared to the use of two TCP streams. For example, during a 200 kB file transmission, the Cell RE achieves a value of 33.85%, with corresponding BDR and BTR values of 97.64% and 72.95%, respectively. However, these results for the novel method are comparable to those obtained with eight TCP streams.

A2.7. DC Inter-site CA connection, 2 streams

This study investigates the accuracy of two throughput estimation methods in cellular networks utilizing inter-site CA for 2 TCP streams, focusing on the impact of file size and the TCP slow start mechanism. The new flow control algorithm is employed for both the standard and the novel method.

Figure A2.13 depicts the measured throughput performance for both the standard and the novel method, utilizing throughput reference from eNB and end-user perspective, during inter-site CA data transmission across a range of file sizes.

Figure A2.14 illustrates the distinct data distribution patterns observed in single-cell and 2CC CA connections. The introduction of data splitting between the primary cell and the secondary cell in 2CC CA connections creates an additional layer of data segmentation. This segmentation can potentially lead to misinterpretations of user throughput, particularly for small packet transmissions.

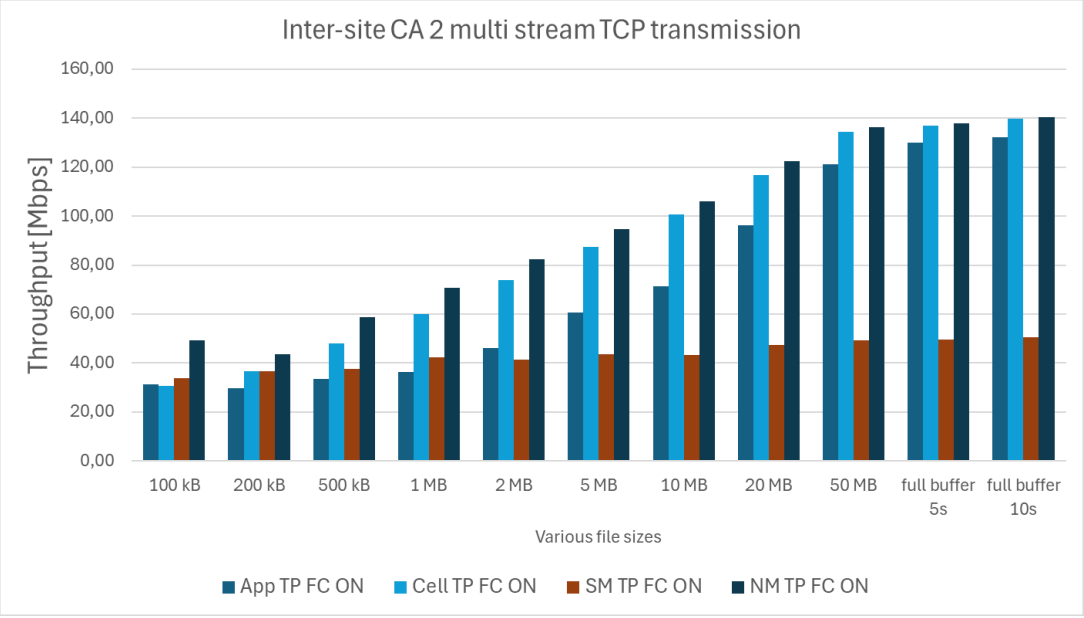

Figure A2.13: TCP/IP 2 multi stream transmission for 2CC Inter-site CA traffic with various throughput values.

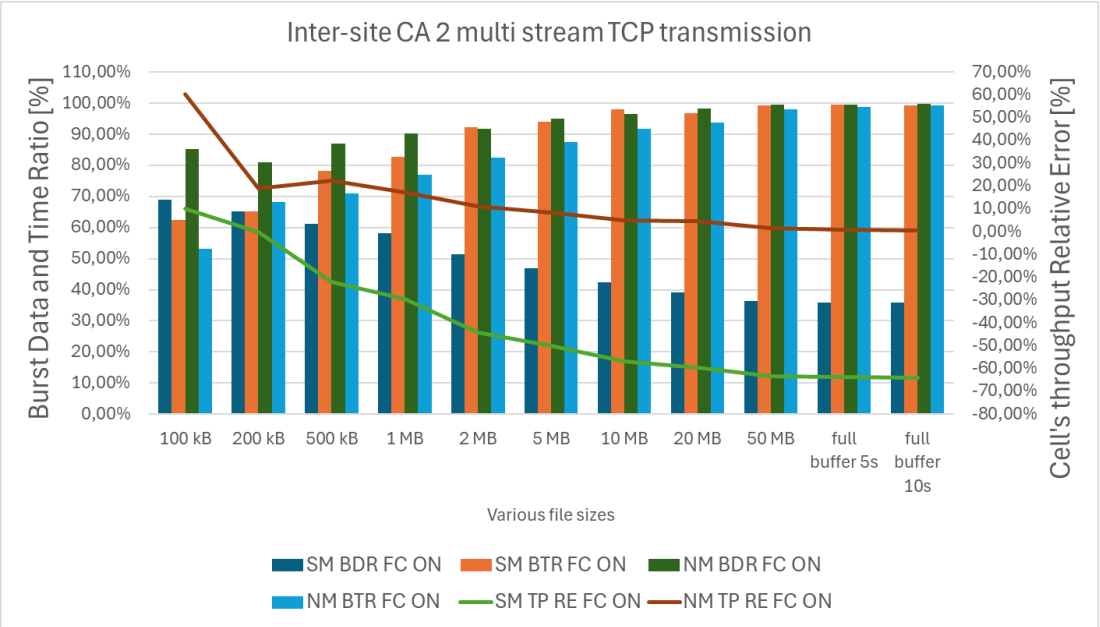

Figure A2.14: TCP/IP 2 multi stream transmission for Inter-site CA 2CC traffic with relative error and volume/time ratios between Standard and New method.

For inter-site CA with 2CC, the accuracy of the new method becomes acceptable for file sizes exceeding 10 MB when transmitted over TCP using 2 multi streams (-P iperf parameter set to 2, indicating 2 parallel streams). The precision further improves with greater file sizes. However, starting from 1 MB file size and above the tests reveal a high degree of erroneous underestimation of throughput value for the standard method.

The discrepancy in precision between the standard and the new method arises primarily from the underestimation of data volume by the standard method as file size increases. The standard method does not count all the PCell's data volume and skips the data volume sent to SCell. This is even more clearly visible for small file sizes when the PDCP buffer is saturated with new data inflow due to 2 simultaneous streams. Also, this underestimation is coupled with an erroneous interpretation of transmission time. The observed precision of the standard method between -10% and 20% of relative error in approximating application layer throughput for file sizes between 100 kB and 2 MB is coincidental. This apparent accuracy is attributed to a combination of factors:

- Underestimation of Data Volume: The standard method underestimates the total data volume transmitted over the PCell, failing to account for all data transferred.
- Overestimation of Transmission Time: The standard method overestimates the transmission time compared to the novel method.

This combination of underestimation and overestimation leads to a fortuitous cancellation of errors, resulting in a seemingly accurate approximation of application layer throughput for the specified file size range. However, as the file size increases, the underestimation of data volume becomes more pronounced, leading to a diminishing accuracy of the standard method.

Table A2.10: TCP/IP 2 multi stream transmission for Inter-site CA 2CC traffic details with relative error and volume/time ratios between Standard and New method.

file size	SM TP [Mbps]	NM TP [Mbps]	App TP [Mbps]	Cell TP [Mbps]	SM BDR [%]	SM BTR [%]	SM TP Cell RE [%]	SM TP App RE [%]	NM BDR [%]	NM BTR [%]	NM TP Cell RE [%]	NM TP App RE [%]	STTI BR [%]
100 kB	33.75	49.16	31.35	30.63	68.90	62.52	10.20	7.67	85.30	53.15	60.50	56.81	60.9
200 kB	36.76	43.73	29.88	36.78	65.28	65.32	-0.06	23.02	81.00	68.13	18.90	46.35	73.1
500 kB	37.47	58.85	33.44	48.01	61.15	78.35	-21.95	12.05	87.09	71.04	22.60	76.00	61.1
1 MB	42.32	70.59	36.50	60.16	58.18	82.70	-29.65	15.94	90.27	76.93	17.34	93.39	51.4
2 MB	41.30	82.27	46.10	73.92	51.49	92.17	-44.13	-10.42	91.79	82.48	11.29	78.45	36.6
5 MB	43.58	94.78	60.65	87.45	46.85	93.99	-50.16	-28.14	94.94	87.60	8.39	56.28	24.9
10 MB	43.42	105.96	71.24	100.76	42.28	98.13	-56.91	-39.05	96.48	91.74	5.16	48.73	14.4
20 MB	47.27	122.28	96.40	116.70	39.21	96.79	-59.49	-50.96	98.29	93.80	4.78	26.85	9.2
50 MB	49.23	136.41	121.30	134.42	36.35	99.27	-63.38	-59.42	99.46	98.01	1.48	12.46	2.4
5s	49.59	138.03	130.00	136.99	36.01	99.47	-63.80	-61.85	99.65	98.89	0.76	6.18	2.6
10s	50.42	140.53	132.20	139.80	35.78	99.22	-63.93	-61.86	99.81	99.29	0.52	6.30	2.1

Table A2.10 presents a comprehensive analysis of the data depicted in Figure A2.14, incorporating the STTI burst ratio metric. The influence of TCP slow start diminishes with increasing file size and number of TCP streams. The novel method exhibits a substantial improvement in the Cell RE metric, starting from 1 MB file transfers, demonstrating a value of 17.34% compared to -29.65% for the standard method. As the file size increases, for instance, during a full buffer 10 s transmission, the Cell RE displays 0.52% for the novel method and -63.93% for the standard method, highlighting a significant improvement for the novel method. However, for very small files, such as 200 kB, the advantage diminishes, as the novel method exhibits a Cell RE value of 18.90%, compared to -0.06% for the standard method. This phenomenon can be attributed to the close proportionality between the quotient of data volume and time components for the standard method, where for 200 kB file transfers, the BDR exhibits a value of 65.28% and BTR a value of 65.32%. Conversely, the novel method, for the same file size transmission, displays a BDR of 81.00% and a BTR of 68.13%, which is a direct reason for showing worse Cell RE values than for the standard method.

A2.8. DC Inter-site CA connection, 8 streams

This study investigates the accuracy of two throughput estimation methods in cellular networks utilizing inter-site CA for 8 TCP streams, focusing on the impact of file size and the TCP slow start mechanism. The new flow control algorithm is employed for both the standard and the novel method.

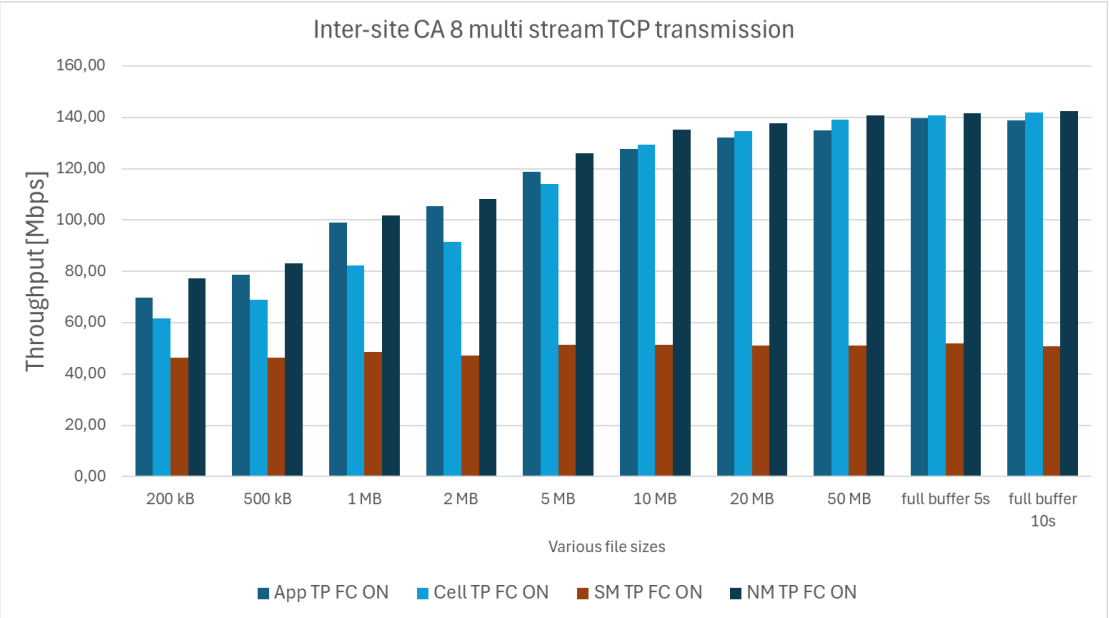

Figure A2.15: TCP/IP 8 multi stream transmission for 2CC Inter-site CA traffic with various throughput values.

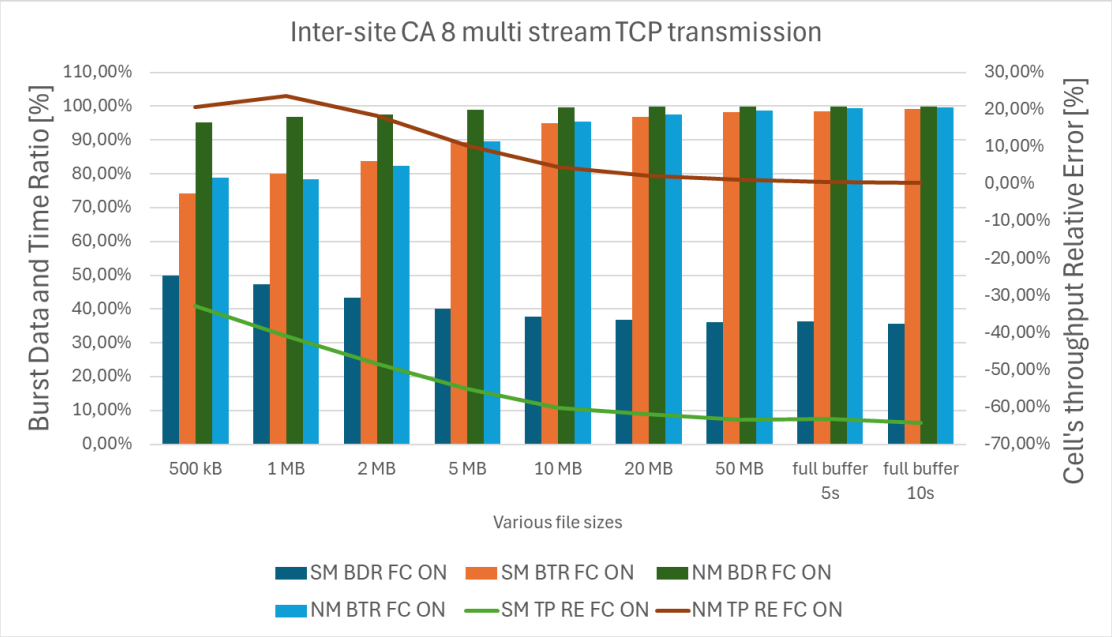

Figure A2.16: TCP/IP 8 multi stream transmission for Inter-site CA 2CC traffic with relative error and volume/time ratios between Standard and New method.

Figure A2.15 depicts the measured throughput performance for both the standard and the novel method, utilizing throughput reference from eNB and end-user perspective, during inter-site CA data transmission across a range of file sizes.

Figure A2.16 illustrates the distinct data distribution patterns observed in single-cell and 2CC CA connections. The introduction of data splitting between the primary cell and the secondary cell in 2CC CA connections creates an additional layer of data segmentation. This segmentation can potentially lead to misinterpretations of user throughput, particularly for small packet transmissions.

Table A2.11 presents a comprehensive analysis of the data depicted in Figure A2.16, incorporating the STTI burst ratio metric. The influence of TCP slow start diminishes with increasing file size and number of TCP streams. The novel method exhibits a substantial improvement in the Cell RE metric, starting from 1 MB file transfers, demonstrating a value of 23.76% compared to -40.98% for the standard method. As the file size increases, for instance, during a full buffer 10 s transmission, the Cell RE displays 0.31% for the novel method and -64.16% for the standard method, highlighting a significant improvement for the novel method. However, for very small files, such as 200 kB, the advantage diminishes, as the novel method exhibits a Cell RE value of 25.47%, compared to -24.64% for the standard method. This phenomenon can be attributed to the close proportionality between the quotient of data volume and time components for the standard method, where for 200 kB file transfers, the BDR exhibits a value of 54,63% and BTR a value of 72,49%. The advantage of precise throughput values observed for very small file transfers using eight TCP streams, compared to two TCP streams, is no longer present. Conversely, the novel method, for the same file size transmission, displays a BDR of 94,57% and a BTR of 75,38%, which is a direct reason for showing worse Cell RE values than for the standard method. Moreover, the novel method shows an improvement in accurate BDR and BTR calculation when compared to two TCP stream transmissions.

Table A2.11: TCP/IP 8 multi stream transmission for Inter-site CA 2CC traffic details with relative error and volume/time ratios between Standard and New method.

file size	SM TP [Mbps]	NM TP [Mbps]	App TP [Mbps]	Cell TP [Mbps]	SM BDR [%]	SM BTR [%]	SM TP Cell RE [%]	SM TP App RE [%]	NM BDR [%]	NM BTR [%]	NM TP Cell RE [%]	NM TP App RE [%]	STTI BR [%]
200 kB	46.37	77.19	69.66	61.52	54.63	72.49	-24.64	-33.44	94.57	75.38	25.47	10.81	40.79
500 kB	46.38	83.20	78.67	68.99	49.91	74.24	-32.77	-41.05	95.15	78.90	20.60	5.76	32.73
1 MB	48.51	101.72	99.03	82.19	47.27	80.09	-40.98	-51.02	96.94	78.33	23.76	2.72	24.54
2 MB	47.27	108.13	105.25	91.43	43.30	83.76	-48.30	-55.09	97.50	82.45	18.26	2.73	16.82
5 MB	51.32	125.92	118.80	114.08	40.20	89.37	-55.01	-56.80	98.96	89.65	10.38	5.99	13.58
10 MB	51.43	135.23	127.60	129.39	37.71	94.89	-60.25	-59.69	99.67	95.37	4.51	5.98	4.26
20 MB	51.20	137.73	132.20	134.70	36.81	96.86	-61.99	-61.27	99.77	97.57	2.25	4.18	2.25
50 MB	51.04	140.78	134.80	139.19	36.01	98.22	-63.33	-62.14	99.90	98.77	1.14	4.44	0.31
5s	51.83	141.72	139.50	140.85	36.27	98.58	-63.20	-62.85	99.95	99.34	0.62	1.59	0.42
10s	50.83	142.30	138.80	141.85	35.56	99.23	-64.16	-63.38	99.97	99.66	0.31	2.52	0.64

A2.9. DC Inter-site CA connection, 16 streams

This study investigates the accuracy of two throughput estimation methods in cellular networks utilizing inter-site CA for 16 TCP streams, focusing on the impact of file size and the TCP slow start mechanism. The new flow control algorithm is employed for both the standard and the novel method.

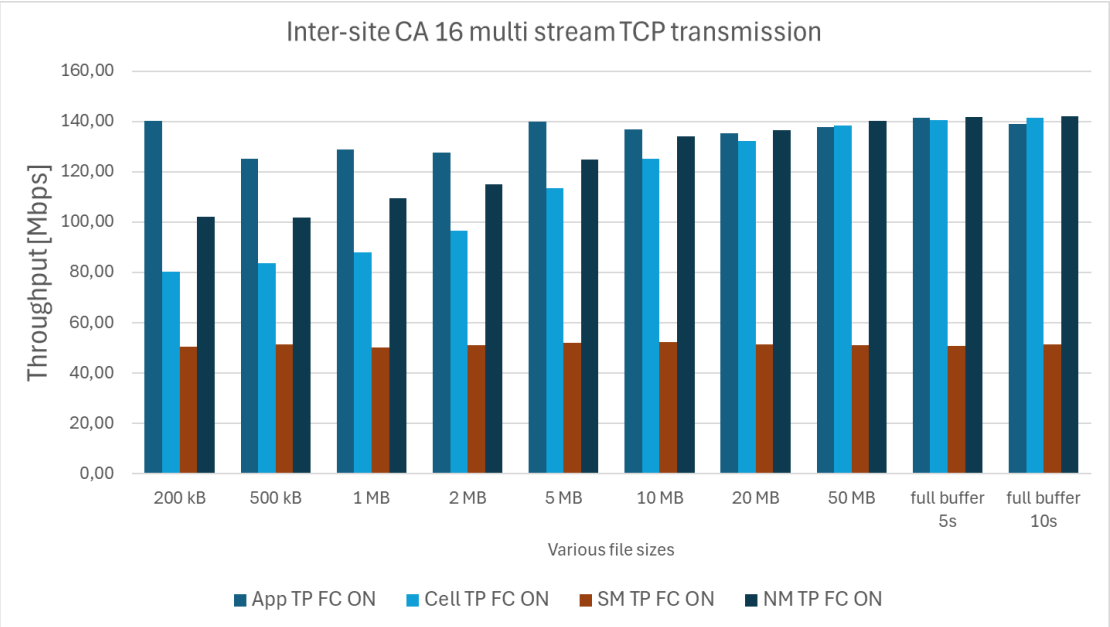

Figure A2.17: TCP/IP 16 multi stream transmission for 2CC Inter-site CA traffic with various throughput values.

Figure A2.17 depicts the measured throughput performance for both the standard and the novel method, utilizing throughput reference from eNB and end-user perspective, during inter-site CA data transmission across a range of file sizes.

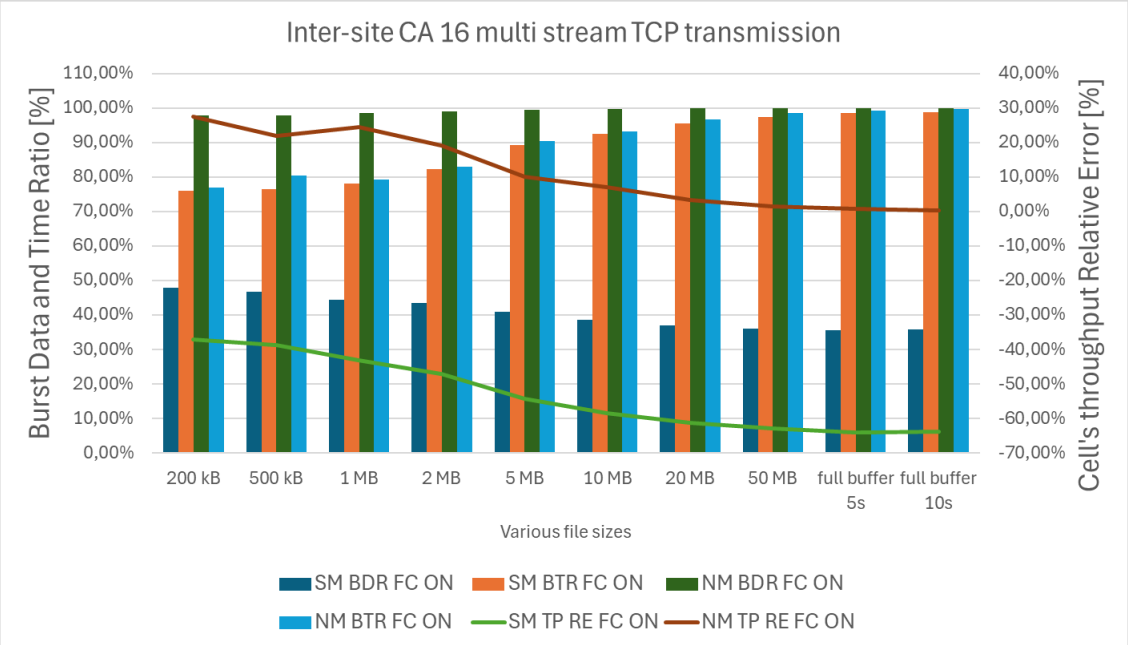

Figure A2.18: TCP/IP 16 multi stream transmission for Inter-site CA 2CC traffic with relative error and volume/time ratios between Standard and New method.

Figure A2.18 illustrates the distinct data distribution patterns observed in single-cell and 2CC CA connections. The introduction of data splitting between the primary cell and the secondary cell in 2CC CA connections creates an additional layer of data segmentation. This segmentation can potentially lead to misinterpretations of user throughput, particularly for small packet transmissions.

Table A2.12 presents a comprehensive analysis of the data depicted in Figure A2.18, incorporating the STTI burst ratio metric. The impact of TCP slow start diminishes with increasing file size and number of TCP streams. The novel method demonstrates a significant improvement in the Cell RE metric, starting from 1 MB file transfers, showing a value of 24.47% compared to -43.18% for the standard method. This represents a slight improvement over the eight TCP stream transmission as well. As the file size increases, for example, during a full buffer 10 s transmission, the Cell RE shows 0.34% for the novel method and -63.80% for the standard method, demonstrating a significant improvement for the novel method. However, for large file transfers there is no improvement observed compared to the eight TCP stream scenario. For very small files, such as 200 kB, the advantage of the standard method for 2 or 8 TCP streams diminishes, as the novel method exhibits a Cell RE value of 27.42%, compared to -37.06% for the standard method. For the standard method, and for 200 kB file transfers, the BDR exhibits a value of 47.84%, showing a downward trend, and BTR a value of 76.01%, showing an upward trend in comparison to two and eight TCP streams. Conversely, the novel method, for the same file size transmission, displays a BDR of 97.89% and a BTR of 76.83%, showing an upward trend in comparison to two and eight TCP streams.

Table A2.12: TCP/IP 16 multi stream transmission for Inter-site CA 2CC traffic details with relative error and volume/time ratios between Standard and New method.

file size	SM TP [Mbps]	NM TP [Mbps]	App TP [Mbps]	Cell TP [Mbps]	SM BDR [%]	SM BTR [%]	SM TP Cell RE [%]	SM TP App RE [%]	NM BDR [%]	NM BTR [%]	NM TP Cell RE [%]	NM TP App RE [%]	STTI BR [%]
200 kB	50,54	102,31	140,25	80,30	47,84	76,01	-37,06	-63,97	97,89	76,83	27,42	-27,05	22.00
500 kB	51,28	101,85	125,27	83,59	46,85	76,36	-38,65	-59,06	97,91	80,35	21,85	-18,70	26.54
1 MB	50,07	109,70	128,84	88,13	44,33	78,03	-43,18	-61,14	98,61	79,23	24,47	-14,86	27.97
2 MB	51,23	115,21	127,60	96,78	43,59	82,35	-47,06	-59,85	98,89	83,07	19,04	-9,71	15.32
5 MB	52,03	125,06	140,10	113,64	40,91	89,35	-54,21	-62,86	99,48	90,40	10,05	-10,74	14.32
10 MB	52,20	134,28	137,00	125,35	38,52	92,49	-58,35	-61,90	99,73	93,09	7,13	-1,98	3.70
20 MB	51,42	136,71	135,40	132,39	37,12	95,58	-61,16	-62,02	99,85	96,70	3,26	0,97	1.67
50 MB	51,27	140,42	137,90	138,31	36,10	97,37	-62,93	-62,82	99,95	98,44	1,53	1,83	1.26
5s	50,75	141,68	141,40	140,59	35,53	98,42	-63,90	-64,11	99,97	99,21	0,78	0,20	0.06
10s	51,28	142,15	139,00	141,67	35,78	98,86	-63,80	-63,11	99,98	99,65	0,34	2,26	0.20

A2.10. Usefulness of CA 2CC usage per file size for multi stream TCP traffic

The utilization of CA for multi-stream TCP traffic demonstrates significant performance enhancements, even for relatively small file sizes. Empirical observations indicate that CA outperforms single-cell connections for files exceeding 500 kB with 8 and 16 multi-streams and 5 MB with 2 multi streams, as perceived by the end-user. Figures A2.19, A2.20 and A2.21 visually represent the benefits of CA for the mentioned traffic types.

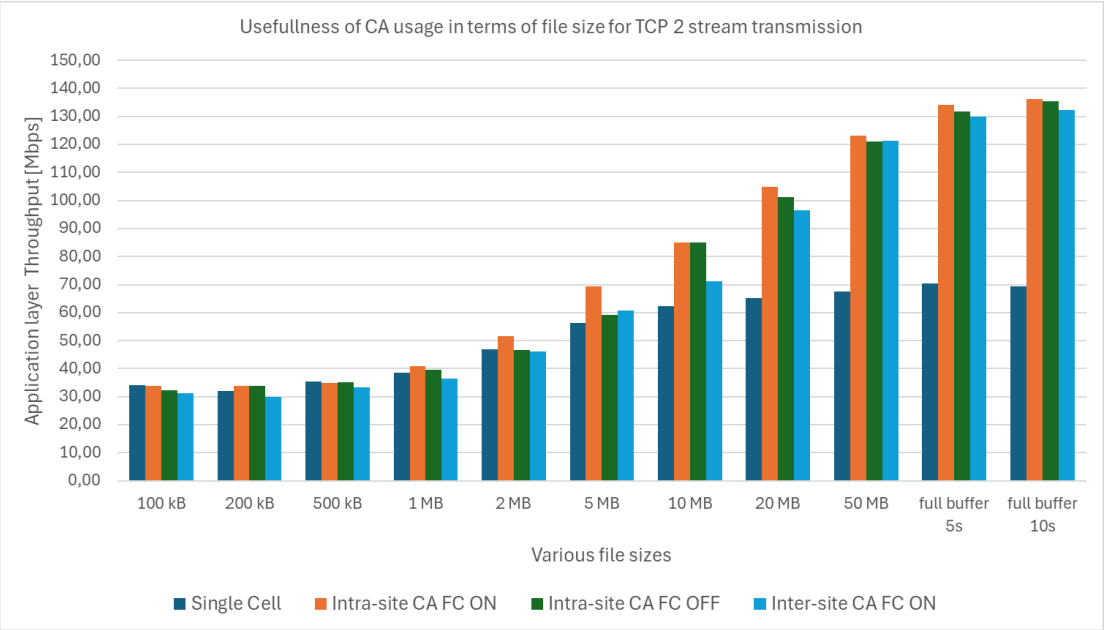

Figure A2.19: Usefulness of CA usage from the end-user perspective for 2 TCP streams.

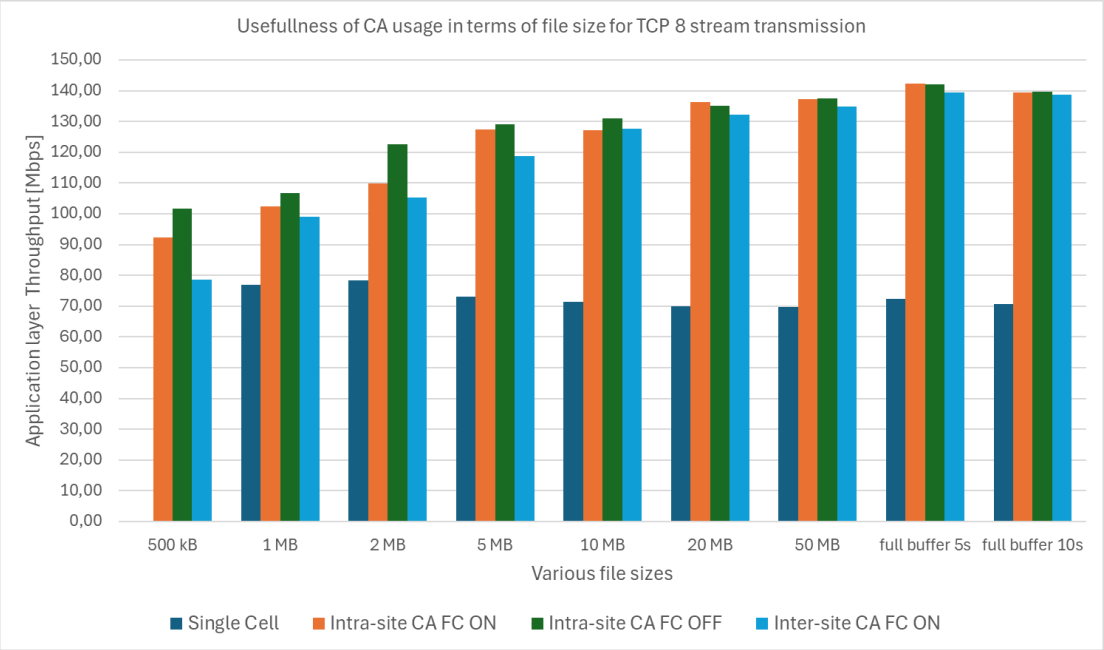

Figure A2.20: Usefulness of CA usage from the end-user perspective for 8 TCP streams.

This observed advantage can be attributed to the inherent slow-start mechanism of TCP, which necessitates a prolonged period to fully leverage the available bandwidth within the RAN. As the number of TCP streams increases, the benefits of CA become more pronounced, enabling faster file transfer even for smaller file sizes compared to single-cell or single stream connections. This trend is further amplified when employing a greater number of CCs for CA, resulting in a more substantial performance gain. However, for 8 and 16 TCP stream transmissions the application layer throughput could not always be measured correctly, as it showed erroneous values exceeding maximum theoretical value, thus not all file sizes are present within below test cases.

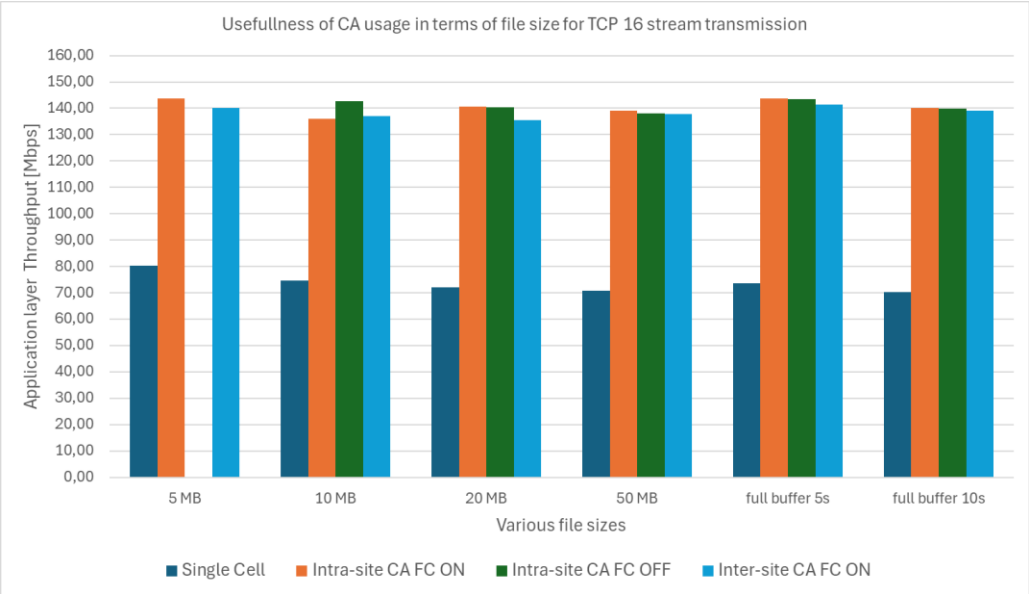

Figure A2.21: Usefulness of CA usage from the end-user perspective for 16 TCP streams.

Figures A2.22, A2.23, and A2.24 present a comparative analysis of the performance gains achieved by CA from the eNB perspective, considering varying numbers of TCP streams. The figures illustrate that even for small file transfers (e.g., 1 MB), centralized scheduling of intra-site CA with two TCP streams yields faster and more efficient data transmission compared to single-carrier operation under ideal radio channel conditions. Notably, for scenarios involving eight and sixteen TCP streams, intra-site CA with flow control enhancement demonstrates advantages even for small file transfers, such as 100 kB, when operating under perfect SINR conditions.

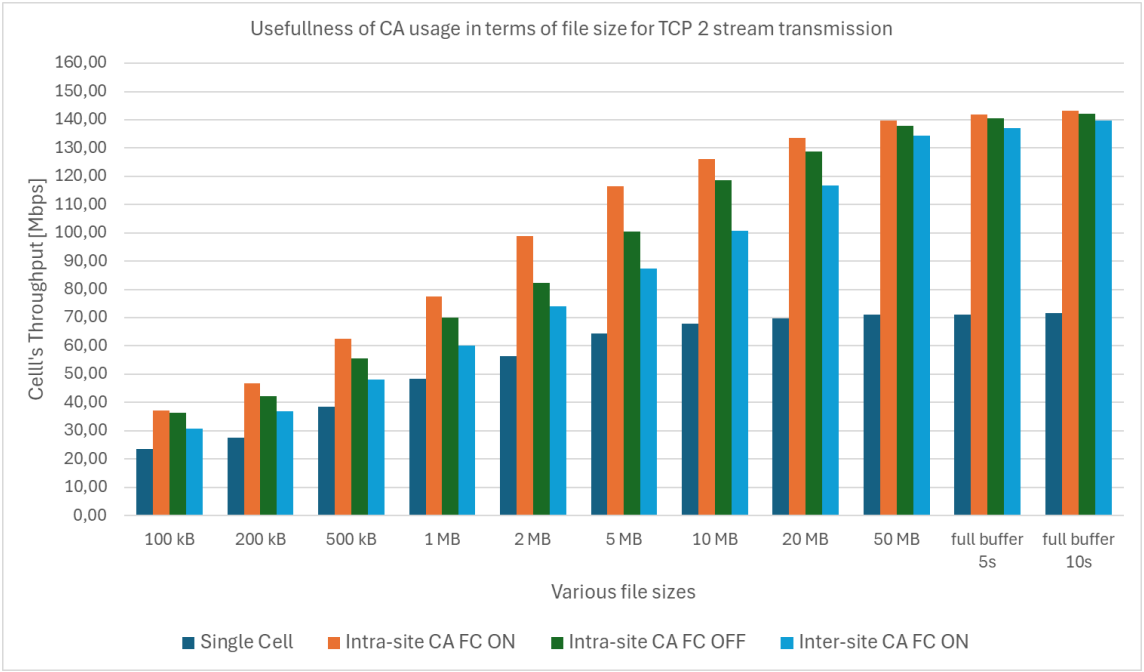

Figure A2.22: Usefulness of CA usage from the eNB's scheduler perspective for 2 TCP streams.

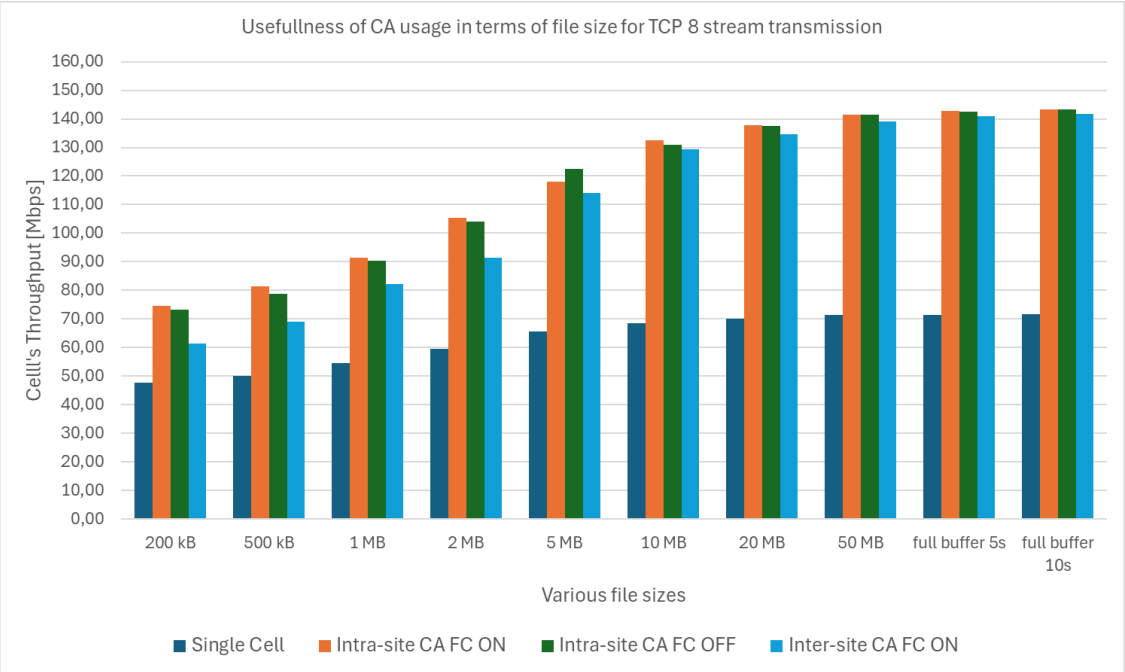

Figure A2.23: Usefulness of CA usage from the eNB's scheduler perspective for 8 TCP streams.

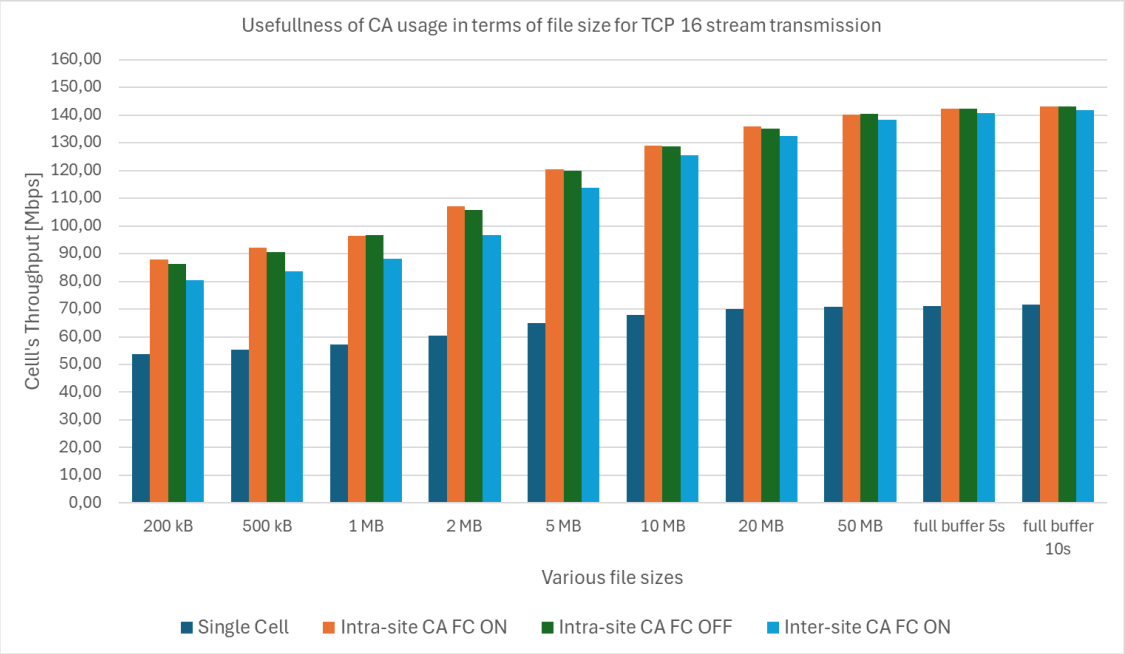

Figure A2.24: Usefulness of CA usage from the eNB's scheduler perspective for 16 TCP streams.

A2.11. Summary – throughput tables

Tables A2.13-A2.18 provide a comprehensive summary of throughput values across various connection types for both the standard and novel methods. These tables serve as a reference for the input values used in the calculation of relative errors.

Table A2.13: Measured throughput comparison for 2MS TCP for the two methods and two reference points – part 1.

File size	no CA				Inter-site CA			
	SM TP [Mbps]	NM TP [Mbps]	App TP [Mbps]	Cell TP [Mbps]	SM TP [Mbps]	NM TP [Mbps]	App TP [Mbps]	Cell TP [Mbps]
100 kB	55.23	59.05	34.11	23.53	33.75	49.16	31.35	30.63
200 kB	58.39	61.82	31.96	27.62	36.76	43.73	29.88	36.78
500 kB	60.97	62.50	35.48	38.51	37.47	58.85	33.44	48.01
1 MB	64.51	66.78	38.67	48.44	42.32	70.59	36.50	60.16
2 MB	65.85	68.44	46.85	56.45	41.30	82.27	46.10	73.92
5 MB	69.58	70.35	56.23	64.28	43.58	94.78	60.65	87.45
10 MB	70.83	71.29	62.41	67.88	43.42	105.96	71.24	100.76
20 MB	71.36	71.60	65.07	69.85	47.27	122.28	96.40	116.70
50 MB	71.77	71.88	67.49	71.14	49.23	136.41	121.30	134.42
5s	71.80	71.90	70.34	71.14	49.59	138.03	130.00	136.99
10s	71.92	71.98	69.24	71.63	50.42	140.53	132.20	139.80

Table A2.14: Measured throughput comparison for 2MS TCP for the two methods and two reference points – part 2.

File size	Intra-site CA with FC OFF				Intra-site CA with FC ON			
	SM TP [Mbps]	NM TP [Mbps]	App TP [Mbps]	Cell TP [Mbps]	SM TP [Mbps]	NM TP [Mbps]	App TP [Mbps]	Cell TP [Mbps]
100 kB	52.74	58.70	32.17	36.45	43.25	58.42	33.77	37.06
200 kB	60.38	61.96	33.91	42.18	56.60	70.77	33.80	46.68
500 kB	69.75	74.96	35.25	55.49	63.77	84.41	34.79	62.54
1 MB	83.93	89.70	39.66	69.90	89.32	95.03	40.85	77.54
2 MB	87.80	97.53	46.59	82.38	108.58	111.07	51.60	98.78
5 MB	102.81	110.27	59.17	100.39	134.25	127.64	69.27	116.58
10 MB	125.28	126.06	85.11	118.73	136.10	133.58	84.95	126.13
20 MB	131.99	132.90	101.09	128.67	140.38	138.19	104.83	133.68
50 MB	139.01	139.65	121.00	137.73	142.83	141.93	123.11	139.85
5s	141.32	141.54	131.70	140.43	143.63	142.93	134.11	141.96
10s	142.63	142.76	135.33	142.12	144.06	143.55	136.11	143.07

Table A2.15: Measured throughput comparison for 8MS TCP for the two methods and two reference points – part 1.

File size	no CA				Inter-site CA			
	SM TP [Mbps]	NM TP [Mbps]	App TP [Mbps]	Cell TP [Mbps]	SM TP [Mbps]	NM TP [Mbps]	App TP [Mbps]	Cell TP [Mbps]
100 kB	N/A	N/A	N/A	N/A	N/A	N/A	N/A	N/A
200 kB	67.23	67.07	N/A	47.82	46.37	77.19	69.66	61.52
500 kB	67.47	67.43	N/A	50.18	46.38	83.20	78.67	68.99
1 MB	69.28	69.34	77.05	54.66	48.51	101.72	99.03	82.19
2 MB	69.76	69.78	78.44	59.48	47.27	108.13	105.25	91.43
5 MB	71.34	71.37	73.03	65.74	51.32	125.92	118.80	114.08
10 MB	71.64	71.69	71.45	68.56	51.43	135.23	127.60	129.39
20 MB	71.91	71.92	70.05	70.23	51.20	137.73	132.20	134.70
50 MB	71.98	71.98	69.75	71.30	51.04	140.78	134.80	139.19
5s	71.99	72.00	72.41	71.33	51.83	141.72	139.50	140.85
10s	72.02	72.03	70.61	71.65	50.83	142.30	138.80	141.85

Table A2.16: Measured throughput comparison for 8MS TCP for the two methods and two reference points – part 2.

File size	Intra-site CA with FC OFF				Intra-site CA with FC ON			
	SM TP [Mbps]	NM TP [Mbps]	App TP [Mbps]	Cell TP [Mbps]	SM TP [Mbps]	NM TP [Mbps]	App TP [Mbps]	Cell TP [Mbps]
100 kB	N/A	N/A	N/A	N/A	N/A	N/A	N/A	N/A
200 kB	101.16	100.19	N/A	73.18	88.27	99.67	N/A	74.51
500 kB	101.76	103.14	101.71	78.67	105.62	110.11	92.22	81.38
1 MB	116.94	114.11	106.83	90.32	105.19	113.83	102.53	91.53
2 MB	121.49	123.00	122.55	104.08	119.21	126.08	109.96	105.42
5 MB	135.15	133.65	129.10	122.41	132.25	135.50	127.40	117.91
10 MB	138.85	137.92	131.10	130.87	139.00	139.69	127.30	132.46
20 MB	141.39	141.04	135.00	137.40	142.06	141.71	136.30	137.88
50 MB	143.11	142.94	137.50	141.35	143.29	143.09	137.30	141.45
5s	143.47	143.45	142.00	142.63	143.61	143.59	142.38	142.74
10s	143.75	143.75	139.60	143.27	143.88	143.85	139.50	143.43

Table A2.17: Measured throughput comparison for 16MS TCP for the two methods and two reference points – part 1.

File size	no CA				Inter-site CA			
	SM TP [Mbps]	NM TP [Mbps]	App TP [Mbps]	Cell TP [Mbps]	SM TP [Mbps]	NM TP [Mbps]	App TP [Mbps]	Cell TP [Mbps]
100 kB	N/A	N/A	N/A	N/A	N/A	N/A	N/A	N/A
200 kB	70.29	70.18	N/A	53.66	50.54	102.31	140.25	80.30
500 kB	70.47	70.39	NA	55.32	51.28	101.85	125.27	83.59
1 MB	71.19	71.06	109.15	57.29	50.07	109.70	128.84	88.13
2 MB	71.06	70.99	100.08	60.50	51.23	115.21	127.60	96.78
5 MB	71.55	71.51	80.23	64.86	52.03	125.06	140.10	113.64
10 MB	71.74	71.74	74.56	67.75	52.20	134.28	137.00	125.35
20 MB	71.96	71.93	72.15	69.88	51.42	136.71	135.40	132.39
50 MB	72.00	72.01	70.69	70.93	51.27	140.42	137.90	138.31
5s	71.99	72.01	73.74	71.13	50.75	141.68	141.40	140.59
10s	72.02	72.03	70.25	71.56	51.28	142.15	139.00	141.67

Table A2.18: Measured throughput comparison for 16MS TCP for the two methods and two reference points – part 2.

File size	Intra-site CA with FC OFF				Intra-site CA with FC ON			
	SM TP [Mbps]	NM TP [Mbps]	App TP [Mbps]	Cell TP [Mbps]	SM TP [Mbps]	NM TP [Mbps]	App TP [Mbps]	Cell TP [Mbps]
100 kB	N/A	N/A	N/A	N/A	N/A	N/A	N/A	N/A
200 kB	115.43	114.41	N/A	86.37	115.50	117.58	N/A	87.85
500 kB	120.07	118.10	N/A	90.45	104.18	120.26	N/A	92.14
1 MB	121.49	122.33	N/A	96.70	120.00	122.34	N/A	96.43
2 MB	127.90	127.23	N/A	105.68	129.68	129.28	N/A	107.19
5 MB	134.06	134.06	N/A	119.85	134.08	135.45	143.60	120.47
10 MB	138.99	138.38	142.70	128.55	138.19	138.36	136.12	128.87
20 MB	140.78	140.65	140.30	135.21	141.60	141.40	140.60	135.91
50 MB	142.89	142.89	138.20	140.53	142.74	142.70	139.20	140.26
5s	143.51	143.49	143.50	142.25	143.54	143.55	143.70	142.29
10s	143.81	143.80	139.90	143.19	143.79	143.79	140.10	143.15

Appendix 3: Static Radio Channel Quality variations

A3.1. Intra-site-CA connection (non-DC)

Figures A3.1 and A3.2 depict the relative error of both the novel and the standard method in measuring cell throughput for an eight-stream transmission scenario under three distinct radio channel quality conditions: 0 dB, 30 dB, and 45 dB of attenuation. Furthermore, the distribution of relative errors for data volume and time components is categorized based on specific file sizes.

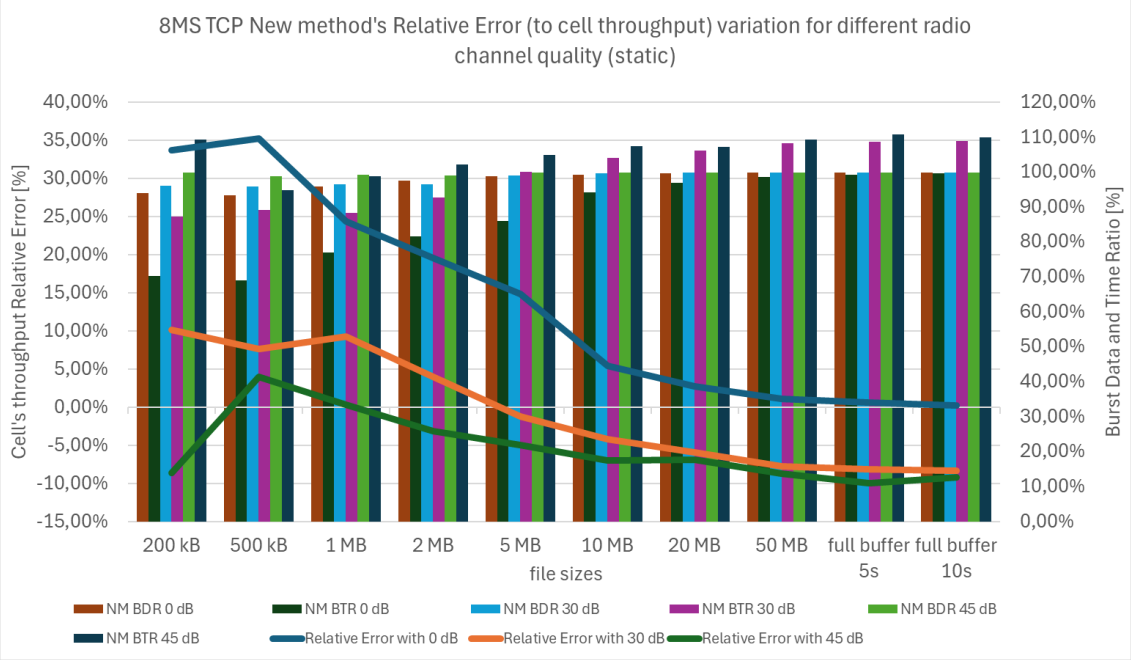

Figure A3.1: TCP/IP 8 multi stream transmission for Intra-site CA with Relative Error to cell throughput for New method.

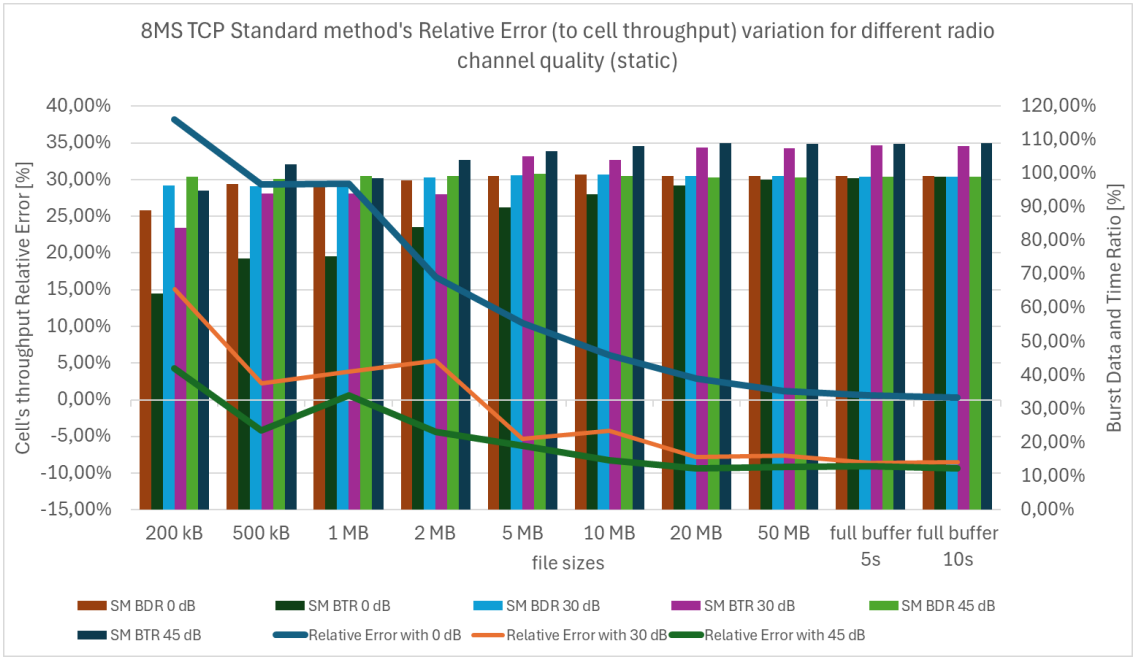

Figure A3.2: TCP/IP 8 multi stream transmission for Intra-site CA with Relative Error to cell throughput for Standard method.

Increased attenuation of radio signals results in degraded radio channel quality, quantifiable through RSSI and SINR metrics. Optimal channel quality, defined by the RSSI and SINR values in Table 5.22, is observed with 0 dB attenuation from the programmable attenuator. Increasing attenuation to 30 dB and 45 dB degrades channel conditions, resulted in the activation of cellular network link adaptation mechanisms. Initially, the coding rate of the radio signal is adjusted based on CQI feedback. If this fails, retransmission of unacknowledged data with a more robust coding rate is initiated. Consequently, significant attenuation can lead to a high retransmission ratio utilizing the HARQ mechanism at the MAC layer. Retransmissions prolong the burst time component calculation, potentially exceeding the total number of scheduled TTIs with user data, which serves as a reference for relative error. This results in an underestimation of throughputs relative error when referenced against the total PDCP SDU volume and scheduled TTIs. However, in high-retransmission scenarios, the relative error referenced against application layer throughput exhibits high precision, closely aligning with the end-user perceived value, typically below 1%.

Figures A3.1 and A3.2 demonstrate that 30 dB and 45 dB attenuation result in a significant increase in retransmissions within both PCell and SCell, extending the calculated burst time. This extended duration surpasses the number of scheduled TTIs with user data, indicating the limitations of this reference point. For larger file sizes and a 0 dB attenuation scenario, the relative error approaches 0%, proving high accuracy. Conversely, for 30 dB and 45 dB attenuations, the relative error approximates -9% and -10%, respectively. This observation highlights a strong correlation between burst duration and the HARQ retransmission ratio, exhibiting average BLER of 11.06% for high attenuation and 7.93% for moderate attenuation during the test cases with FC ON.

While a direct comparison of two methods under identical test constraints is conducted, inherent variations exist between traffic simulations. Consequently, the processing of the same file size in the MeNB and SeNB, during transmission in DL direction, may exhibit differing patterns, leading to variations in throughput values and relative errors. To mitigate this variability, multiple test repetitions are performed to obtain an average value, providing a reliable basis for comparison, as presented in Table A3.1.

Under ideal radio channel conditions, the relative error consistently remains non-negative for both the standard and the novel method. This is attributed to the absence of re-transmission mechanisms, which typically occur during strong interference when user data cannot be successfully decoded. For attenuation of 0 dB, the relative error for both methods demonstrates close proximity, rarely exceeding a 5% difference for small file sizes and remaining below 0.2% for files larger than 20 MB.

In moderate attenuation scenarios, the relative error for small file sizes exhibits a reduction to an acceptable level, typically below 10% for most tests. However, for larger file sizes, both methods exhibit underestimation exceeding -9%. Similarly, under 45 dB attenuation, underestimation is observed even for 200 kB file sizes. This phenomenon is attributed to re-

transmission mechanisms, which extend the duration of the time component. Detailed information regarding data volume and time component values is presented in Table A3.2.

Furthermore, challenging radio channel conditions necessitate the scheduler to segment incoming PDCP SDU packets into smaller TB sizes. This segmentation results in burst extension with enhanced coding robustness, leading to a reduction in overall throughput and increasing the probability of a burst to be counted according to 3GPP requirements.

Table A3.1: Throughput relative error results for both the standard and new method for Intra-site CA.

File size	0 dB		30 dB		45 dB	
	SM TP Cell RE [%]	NM TP Cell RE [%]	SM TP Cell RE [%]	NM TP Cell RE [%]	SM TP Cell RE [%]	NM TP Cell RE [%]
200 kB	38.24	33.76	15.09	10.11	4.29	-8.61
500 kB	29.35	35.30	2.21	7.68	-4.22	4.04
1 MB	29.47	24.36	3.82	9.29	0.61	0.37
2 MB	16.72	19.60	5.32	4.04	-4.41	-3.09
5 MB	10.40	14.92	-5.33	-1.15	-6.29	-4.90
10 MB	6.10	5.46	-4.21	-4.17	-8.20	-6.95
20 MB	2.90	2.78	-7.81	-5.90	-9.34	-6.83
50 MB	1.24	1.16	-7.59	-7.70	-9.16	-8.68
5s	0.59	0.59	-8.57	-8.10	-9.00	-9.90
10s	0.34	0.29	-8.50	-8.30	-9.32	-9.20

Table A3.2: Data volume and time components relative error results for both the standard and new method for Intra-site CA.

File size	0 dB SM		0 dB NM		30 dB SM		30 dB NM		45 dB SM		45 dB NM	
	BDR [%]	BTR [%]	BDR [%]	BTR [%]	BDR [%]	BTR [%]	BDR [%]	BTR [%]	BDR [%]	BTR [%]	BDR [%]	BTR [%]
200 kB	89.00	64.38	93.95	70.24	96.43	83.78	96.10	87.27	99.06	94.98	99.88	109.29
500 kB	96.78	74.82	93.46	69.08	96.17	94.09	95.97	89.12	98.39	102.72	98.80	94.96
1 MB	97.71	75.47	95.89	77.11	97.66	94.06	96.58	88.37	99.18	98.58	99.25	98.89
2 MB	98.00	83.96	97.56	81.57	98.74	93.75	96.54	92.79	99.35	103.94	99.04	102.20
5 MB	99.32	89.96	98.77	85.95	99.53	105.13	99.04	100.19	99.83	106.53	99.85	105.00
10 MB	99.62	93.89	99.30	94.16	99.69	104.07	99.79	104.13	99.21	108.07	99.95	107.42
20 MB	99.21	96.41	99.72	97.03	99.24	107.65	99.86	106.12	98.79	108.97	99.97	107.29
50 MB	99.32	98.10	99.89	98.74	99.26	107.42	99.94	108.28	98.87	108.84	99.91	109.41
5s	99.24	98.65	99.95	99.36	99.05	108.34	99.95	108.76	99.09	108.89	99.89	110.88
10s	99.26	98.93	99.97	99.68	98.98	108.18	99.98	109.03	98.92	109.08	99.92	110.05

A comparative analysis of measurement accuracy between the standard and the new method reveals that for Intra-site CA scenarios involving file sizes exceeding 2 MB and utilizing 8-stream TCP transmission, both methods exhibit high accuracy from the eNB perspective, resulting in negligible differences. This proves that the new method doesn't experience any degradation in comparison to the standard method.

A3.2. Inter-site-CA connection (DC)

Figures A3.3 and A3.4 depict the relative error of both the novel and the standard method in measuring cell throughput for an eight-stream transmission scenario under three distinct radio

channel quality conditions: 0 dB, 30 dB, and 45 dB of attenuation. Furthermore, the distribution of relative error for data volume and time components is categorized based on specific file sizes.

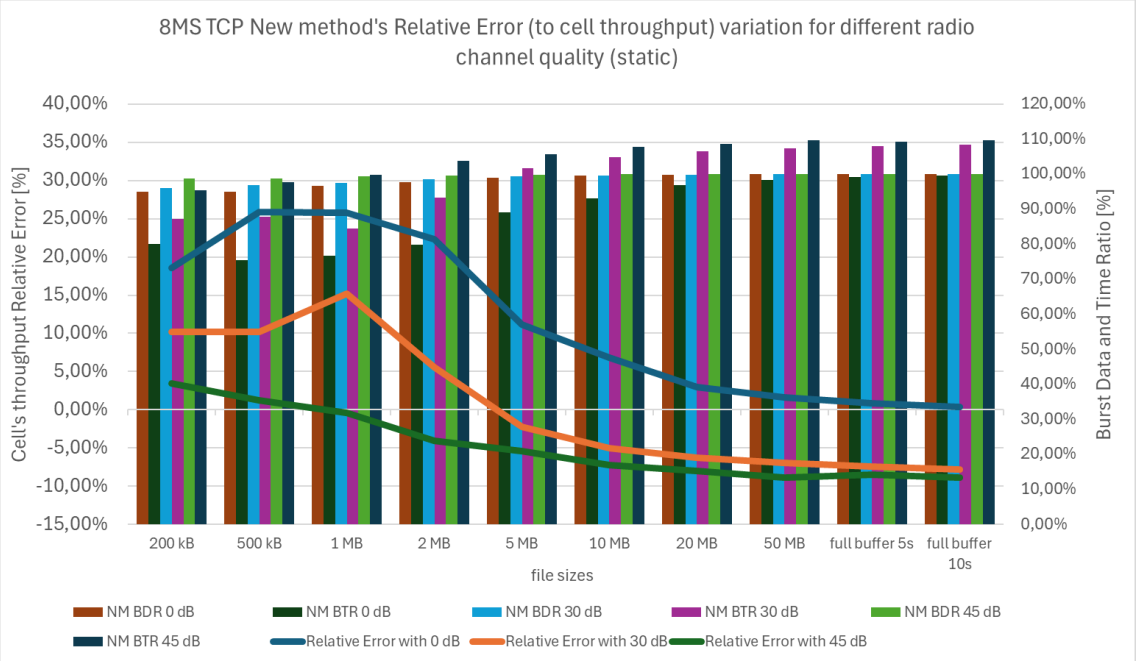

Figure A3.3: TCP/IP 8 multi stream transmission for Inter-site CA with Relative Error to cell throughput for New method.

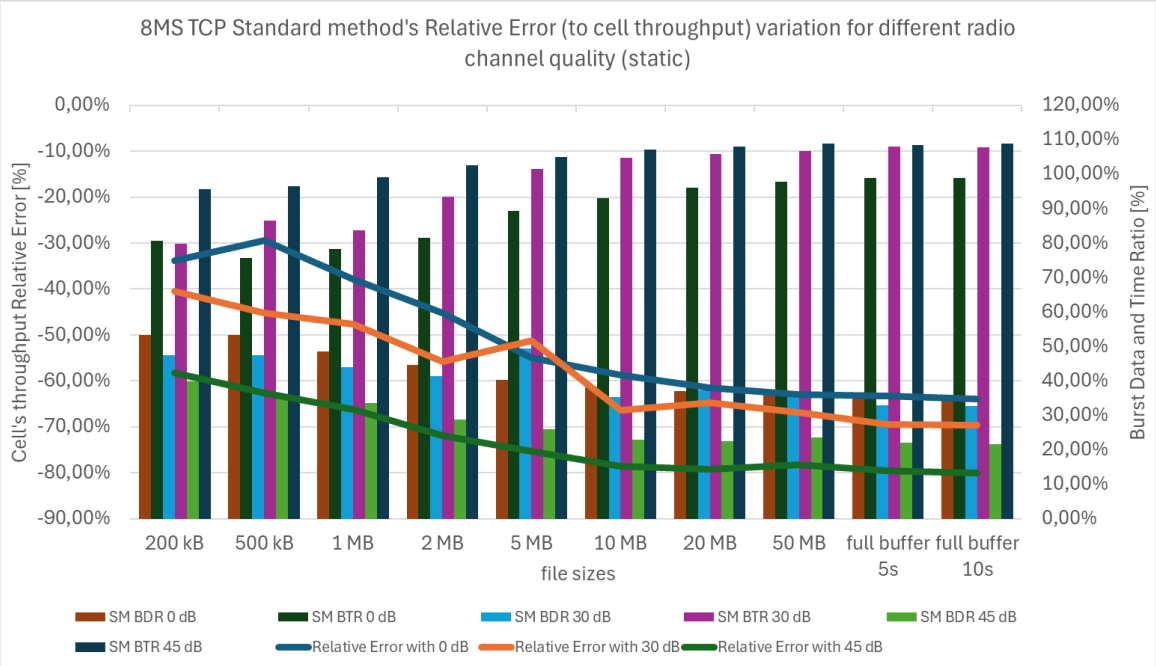

Figure A3.4: TCP/IP 8 multi stream transmission for Inter-site CA with Relative Error to cell throughput for Standard method.

Figures A3.3 and A3.4 demonstrate that 30 dB and 45 dB attenuation result in a significant increase in retransmissions within both PCell and SCell, extending the calculated burst time. This extended duration surpasses the number of scheduled TTIs with user data, indicating the limitations of this reference point. For larger file sizes and a 0 dB attenuation scenario, the relative error approaches 0%, proving high accuracy. Conversely, for 30 dB and 45 dB

attenuations, the relative error approximates -8% and -9%, respectively, close to the results for intra-site CA configuration. This observation highlights a strong correlation between burst duration and the HARQ retransmission ratio, exhibiting average BLER of 8.89% for high attenuation and 7.95% for moderate attenuation.

Under ideal channel conditions (0 dB attenuation), the novel method exhibits consistently non-negative relative error due to the absence of retransmission mechanisms. In contrast, the standard method displays consistently negative relative error, attributed to inaccurate burst data volume and time accounting. Specifically, at 0 dB attenuation, the standard method shows a -61.52% relative error for 20 MB files, while the novel method exhibits a relative error equal or less than 2.97% for files greater or equal to 20 MB.

Consistent with moderate attenuation intra-site CA scenarios, the novel method demonstrates reduced relative error for small files (around 10% for 200 kB and 500 kB). However, the novel method exhibits underestimation exceeding -7% for larger files. This underestimation extends to files greater than 1 MB under 45 dB attenuation, attributed to the increased time component resulting from retransmission mechanisms. Nevertheless, the novel method shows improved accuracy (between 200 kB and 1 MB) compared to intra-site CA scenarios. Detailed relative error, data volume and time component values are provided in Tables A3.3 and A3.4.

Table A3.3: Relative error results for both the standard and new method for Inter-site CA.

File size	0 dB		30 dB		45 dB	
	SM TP Cell RE [%]	NM TP Cell RE [%]	SM TP Cell RE [%]	NM TP Cell RE [%]	SM TP Cell RE [%]	NM TP Cell RE [%]
200 kB	-33.85	18.60	-40.54	10.17	-58.20	3.50
500 kB	-29.46	25.86	-45.17	10.20	-62.58	1.25
1 MB	-37.92	25.78	-47.59	15.24	-66.21	-0.39
2 MB	-45.20	22.31	-55.79	5.60	-71.86	-4.00
5 MB	-55.00	11.18	-51.29	-2.23	-75.30	-5.41
10 MB	-58.77	6.79	-66.30	-5.06	-78.59	-7.22
20 MB	-61.52	2.97	-64.80	-6.24	-79.22	-8.02
50 MB	-63.02	1.64	-66.92	-6.88	-78.25	-8.85
5s	-63.22	0.87	-69.52	-7.45	-79.61	-8.48
10s	-63.94	0.41	-69.64	-7.84	-80.05	-8.84

Table A3.4: Data volume and time component ratios results for both the standard and new method for Inter-site CA.

File size	0 dB SM		0 dB NM		30 dB SM		30 dB NM		45 dB SM		45 dB NM	
	BDR [%]	BTR [%]	BDR [%]	BTR [%]	BDR [%]	BTR [%]	BDR [%]	BTR [%]	BDR [%]	BTR [%]	BDR [%]	BTR [%]
200 kB	53.38	80.69	94.99	80.09	47.50	79.88	96.01	87.15	39.96	95.62	98.71	95.37
500 kB	53.35	75.63	94.99	75.47	47.48	86.59	96.73	87.78	36.08	96.42	98.83	97.60
1 MB	48.60	78.28	96.56	76.76	43.88	83.72	97.40	84.52	33.51	99.15	99.41	99.80
2 MB	44.63	81.44	97.63	79.82	41.32	93.44	98.44	93.22	28.84	102.48	99.55	103.70
5 MB	40.23	89.40	99.02	89.06	49.46	101.54	99.37	101.64	25.91	104.88	99.83	105.55
10 MB	38.38	93.10	99.46	93.14	35.30	104.75	99.55	104.85	22.91	107.04	99.90	107.68
20 MB	36.97	96.07	99.75	96.88	37.24	105.80	99.82	106.46	22.44	108.01	99.96	108.67
50 MB	36.17	97.82	99.89	98.27	35.32	106.78	99.92	107.30	23.69	108.93	99.98	109.69
5s	36.33	98.79	99.94	99.08	32.91	107.99	99.96	108.01	22.11	108.48	99.98	109.24
10s	35.67	98.91	99.96	99.55	32.70	107.71	99.97	108.47	21.72	108.86	99.99	109.69

A comparative analysis of measurement accuracy between the standard and the new method reveals significant discrepancies in the context of Inter-site CA scenarios. The analysis considers various file sizes and utilizes 8-stream TCP transmission.

The new method demonstrates high accuracy from the eNB perspective, regardless of the file size. Conversely, the standard method exhibits extremely low accuracy due to its incompatibility with the new burst calculation logic employed in Inter-site CA scenarios. This incompatibility results in inaccurate measurement of transmission data volume component.

These findings indicate that the new method effectively addresses the limitations of the standard method in Inter-site CA environments. Furthermore, the new method exhibits no degradation in accuracy compared to Intra-site CA configurations, suggesting its applicability across diverse CA scenarios.

The superior accuracy of the new method stems from its adaptation to the specific requirements of Inter-site CA, particularly in terms of burst calculation. This adaptation ensures accurate measurement of transmission components, leading to a more reliable assessment of performance metrics.

In conclusion, the new method provides a significant improvement in measurement accuracy for Inter-site CA scenarios, addressing the shortcomings of the standard method and demonstrating its robustness across different CA configurations.

Appendix 4: Laboratory equipment

Figure A4.1 depicts an electromagnetically shielded enclosure housing the UE to minimize extraneous interference. This enclosure was employed during system testing, as also illustrated schematically in Figure 5.26.

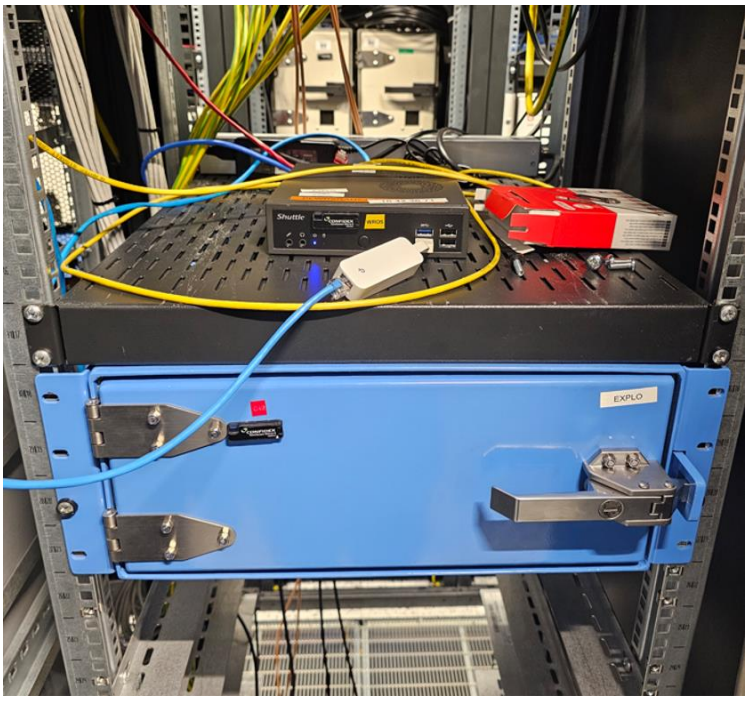

Figure A4.1: Shieldbox used during test scenarios.

Figure A4.2 illustrates a Qualcomm SM8150-based UE with its printed circuit board (PCB) with an open shieldbox in the background, utilized in controlled system testing. The UE is interfaced with the BTS via permanently affixed, low-loss coaxial cables (referred to as "pigtails") to mitigate radio frequency leakage, thereby minimizing potential inter-cell interference and ensuring stable signal power level measurements.

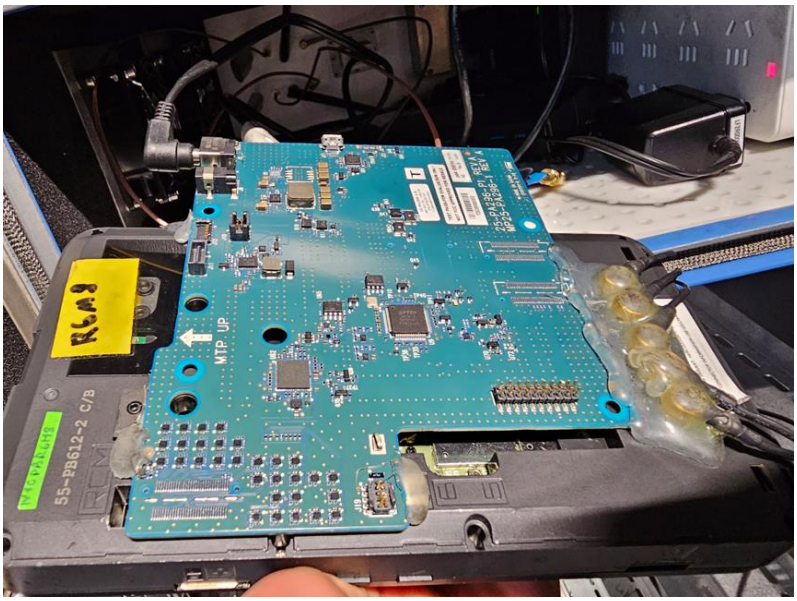

Figure A4.2: User equipment, Qualcomm SM8150.

Figure A4.3 shows a JWF Industries programmable attenuator integrated into the radio frequency signal path between the RF ports of the eNBs and a shielded enclosure to facilitate the controlled simulation of diverse radio channel propagation characteristics. This configuration is depicted in the testbed schematic of Figure 5.26.

Figure A4.3: Programmable attenuator JWF Industries model 50PA-574.

Figure A4.4 depicts the power splitter used for the FDD eNBs within testbed schematic in Figure 5.26. Figures A4.5 and A4.6 present the Radio Unit hardware devices and RACKs with system modules comprising the network cluster.

Figure A4.4: Mini-Circuits ZN2PD2-63-S+ (350-6000 MHz) power splitter.

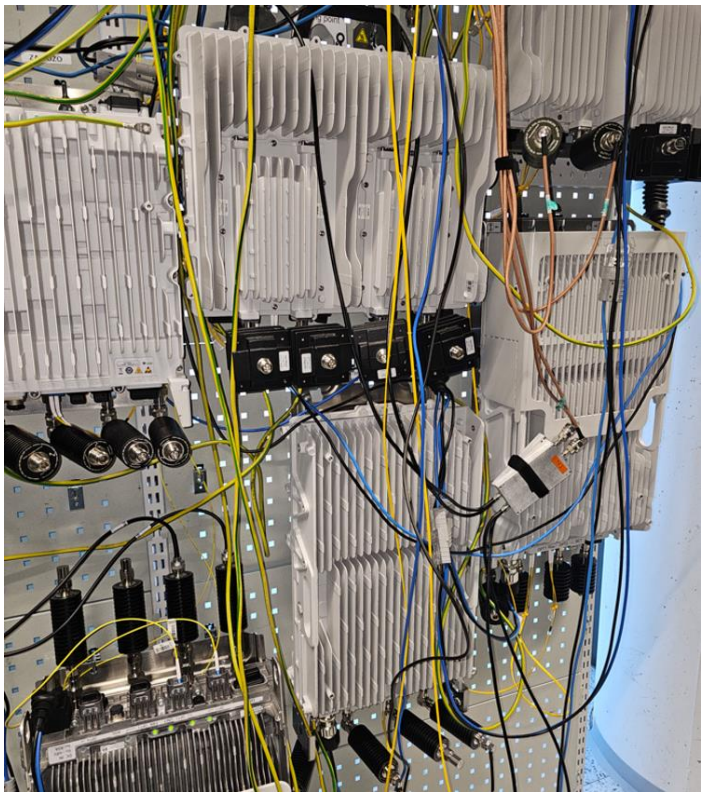

Figure A4.5: Radio Units with Omnitek fixed attenuators (AT-RD-4G-50-50-NM-NF).

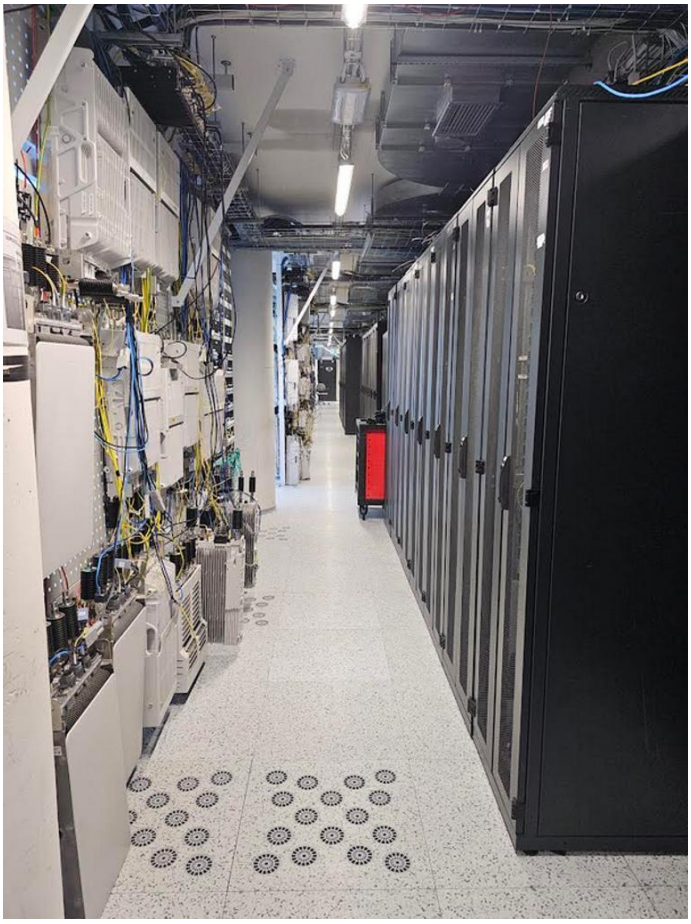

Figure A4.6: RACKs and radio units in a laboratory alley.

Appendix 5: Acknowledgement of Implementation

Figure A5.1 depicts the verification of implementation of the novel solution described in the dissertation.

NOKIA

Wroclaw, 16.06.2025

Acknowledgment of Implementation

We, the undersigned, hereby acknowledge that the computational method described in the PhD dissertation "Evaluation method of IP Scheduled Throughput for Inter-eNB Carrier Aggregation and Cloud based environment" by Mr. Arkadiusz Zieba, has been implemented in functionalities LTE5077 IP Throughput Counter Extension for CA scenarios for 4G technology, and 5GC002637 Throughput counters for 5G technology of the Nokia BTS software. All the results presented in the dissertation have been produced using Nokia commercial software.

Sincerely,

Tomasz Wierzbowski
A&D Director

Krzysztof Tatarczyk
BTS SW Performance Monitoring Lead

General Office:

Nokia Solutions and Networks
Rodziny Hiszpanskich 8
02-685 Warszawa, Poland

Office Address:

Nokia Solutions and Networks
West Link, ul. Szybowcowa 2
54-130 Wrocław, Poland

Figure A5.1: Acknowledgment of Implementation in Nokia commercial software.